

# Investigating Conformance Monitoring Issues in Air Traffic Control Using Fault Detection Approaches

by

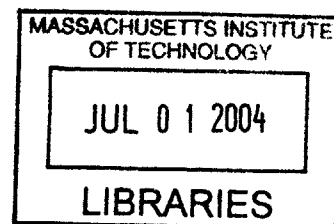
**Tom George Reynolds**

B. Eng. (Hons), Aeronautical Engineering, University of Bristol, UK, 1995  
S. M., Aeronautics and Astronautics, Massachusetts Institute of Technology, USA, 1998

Submitted to the Department of Aeronautics and Astronautics  
in partial fulfillment of the requirements for the degree of

Doctor of Philosophy in the field of Aerospace Systems  
at the  
Massachusetts Institute of Technology

February 2004  
degree list



© 2003 Massachusetts Institute of Technology. All rights reserved.

**AERO**

Signature of Author: \_\_\_\_\_

\_\_\_\_\_  
Tom G. Reynolds  
Department of Aeronautics and Astronautics  
October 31, 2003

Certified by: \_\_\_\_\_

\_\_\_\_\_  
R. John Hansman  
Professor of Aeronautics and Astronautics  
Thesis Committee Chair

Certified by: \_\_\_\_\_

\_\_\_\_\_  
John-Paul B. Clarke  
Associate Professor of Aeronautics and Astronautics  
Thesis Committee Member

Certified by: \_\_\_\_\_

\_\_\_\_\_  
James K. Kuchar  
Ph. D., MIT Lincoln Laboratory  
Thesis Committee Member

Certified by: \_\_\_\_\_

\_\_\_\_\_  
Daniel E. Hastings  
Professor of Aeronautics and Astronautics, Professor of Engineering Systems  
Thesis Committee Member

Accepted by: \_\_\_\_\_

\_\_\_\_\_  
Edward M. Greitzer  
H. N. Slater Professor of Aeronautics and Astronautics  
Chair, Committee on Graduate Students

[This page intentionally left blank]

# **Investigating Conformance Monitoring Issues in Air Traffic Control Using Fault Detection Approaches**

by

**Tom George Reynolds**

Submitted to the Department of Aeronautics and Astronautics  
on October 31, 2003, in partial fulfillment of the requirements for the degree of  
Doctor of Philosophy in the field of Aerospace Systems

## **Abstract**

In order to maintain Air Traffic Control (ATC) system safety, security and efficiency, conformance monitoring must be performed to ensure that aircraft adhere to their assigned clearances. New Decision Support Tools (DSTs), coupled to advanced communication, navigation and surveillance technologies are being developed which may enable more effective conformance monitoring to be undertaken relative to today. However, there are currently no general analysis techniques to help identify fundamental conformance monitoring issues and more effective approaches that new DSTs should employ.

An approach to address this need is presented in this work that draws parallels between ATC conformance monitoring and general system fault detection, allowing fault detection methods developed for other domains to be employed for this new application. The resulting Conformance Monitoring Analysis Framework provides a structure to research conformance monitoring issues and approaches. Detailed discussions are presented for each of the elements of the framework, including the Conformance Basis, Actual System Representation, Conformance Monitoring Model, Conformance Residual Generation and Decision-Making components. Flight test data during a simple lateral non-conformance maneuver was used to demonstrate various implementation options of the framework.

Application of the framework for ATC conformance monitoring research was demonstrated using flight test and simulator data in various operational and surveillance environments. Key findings in the lateral, vertical and longitudinal domains during non-transitioning and transitioning flight regimes are presented. In general, it was found that more effective conformance monitoring can be conducted relative to existing systems in the non-transitioning environments when advanced surveillance systems provide higher accuracy, higher update rate and higher order dynamic state information for use in more sophisticated DST algorithms. This is contrasted to the significantly greater conformance monitoring challenges that exist in the transitioning regimes due to Conformance Basis and modeling uncertainties. These challenges can be handled through the use of procedural design, higher fidelity modeling techniques or the surveillance of intent states. Two extended applications of the framework are also presented: a method for intent inferencing to determine what alternative trajectory a non-conforming aircraft may be following and a technique for environmental parameter estimation.

Thesis Committee Chair: R. John Hansman  
Title: Professor of Aeronautics and Astronautics

[This page intentionally left blank]

---

# Acknowledgements

---

The document you now hold before you would not have been possible without the guidance, support and friendship of many people. This is my humble attempt at acknowledging their contributions.

Firstly, sincerest thanks to Prof. John Hansman for giving me the opportunity to work with and learn from him over the last five years, as well as the all-important financial support. Thanks to my other committee members: Prof. John-Paul Clarke for giving me the first hope of working in ICAT and all of the guidance thereafter; and to Dr. Jim Kuchar for the friendly prods of the research in better directions and the amazing lectures. Thanks to Prof. Daniel Hastings for being my minor advisor in Space Systems Engineering and for my very first class experiences at MIT. Thanks to Prof. Amedeo Odoni for all of his help over the years and to my thesis readers, Dr. Lee Yang and Prof. Kristina Lundqvist. This work would also not have been possible without the financial and technical support of many other people. Top of that list are Richard Barhydt and Mark Ballin at NASA Langley Research Center who have provided unwavering support for this research. Mike Paglione at the FAA Technical Center, as well as Robert Oxborrow and Bob Struth of the Boeing ATM group, provided invaluable operational data and support that added significantly to the results of this work. Thanks to Alan Midkiff for providing operational insights on my work over the years, and to Frank Billarant and Josh Pollock for their work on the simulation capability. Finally, thanks to the Aero/Astro staff who have put up with me over the years, particularly Ping Lee for making sure I got paid and Marie Stuppard for the friendly encouragement.

On a more personal level, there have been too many people who have offered friendship, advice and/or moral support over the years to possibly thank you all. Instead I send a sincere thank you to all of my friends in ICAT and the wider MIT community: it has been an honour to have you as colleagues. But special appreciation goes to the “old-timers” with whom I’ve shared the trials and tribulations of the MIT Aero/Astro Ph.D. process: Yiannis Anagnostakis, Cyrus Jilla, Thomas Jones, Paulo Lozano, Natasha Neogi, Laurence Vigeant-Langlois and Lee Winder.

Greatest thanks of all go to the people who have kept me sane over the years: my family. To Mum and Dad: thanks for always supporting and believing in me. You made it all possible. To my siblings, Jim and Kate: thanks for being great role models. We’ve completed the Dr. Reynolds set. Finally, thanks to the newest member of my family. To Hayley: you made it all worthwhile.

[This page intentionally left blank]

---

# Table of Contents

---

<b>Acknowledgements .....</b>	<b>5</b>
<b>List of Figures .....</b>	<b>11</b>
<b>List of Tables .....</b>	<b>17</b>
<b>Acronyms .....</b>	<b>19</b>
<b>CHAPTER 1: Introduction to Conformance Monitoring in Air Traffic Control.....</b>	<b>23</b>
1.1 Motivation for Conformance Monitoring Research in ATC.....	23
1.2 Detecting Deviant Behavior in General Engineering Systems .....	25
1.2.1 Signal-Based Fault Detection Techniques.....	25
1.2.2 Knowledge-Based Fault Detection Techniques.....	26
1.2.3 Model-Based Fault Detection Techniques.....	26
1.3 Factors Affecting Conformance Monitoring in ATC.....	28
1.3.1 Representation of Conformance Monitoring Functions .....	28
1.3.2 Autoflight Tracking Function .....	29
1.3.3 Pilot Tracking Function.....	31
1.3.4 Conformance Monitoring Function.....	32
1.4 General Controller Functions in ATC.....	34
1.5 Need for Development of Conformance Monitoring Analysis Tools.....	36
1.6 Thesis Overview .....	37
<b>CHAPTER 2: Review of Existing ATC Conformance Monitoring Decision Support Tools .....</b>	<b>39</b>
2.1 Introduction.....	39
2.2 Review of Operational Tools.....	39
2.2.1 Precision Runway Monitor (PRM).....	39
2.2.2 Host Computer System (HCS) .....	43
2.2.3 User Request Evaluation Tool (URET).....	47
2.2.4 Canadian Automated Air Traffic System (CAATS) .....	52
2.2.5 Other Operational Systems.....	53

2.3	Review of Developmental Tools.....	55
2.3.1	Flight Progress Monitor (FPM).....	55
2.3.2	NarSim.....	58
2.3.3	Tactical Separation Assisted Flight Environment (TSAFE) .....	59
2.4	Summary .....	67
<b>CHAPTER 3: Development of the Conformance Monitoring Analysis Framework .....</b>		<b>71</b>
3.1	Introduction.....	71
3.2	Conformance Monitoring as Fault Detection.....	71
3.3	The Conformance Monitoring Analysis Framework (CMAF).....	73
3.3.1	Conformance Basis.....	74
3.3.2	Actual System Representation.....	75
3.3.3	Conformance Monitoring Model (CMM) .....	78
3.3.4	Conformance Residual Generation Scheme .....	82
3.3.5	Decision-Making Scheme.....	87
3.4	Designing CMAF Elements to Meet Conformance Monitoring Requirements in ATC.....	89
3.4.1	False Alarm & Time-To-Detection Figures of Merit .....	91
3.4.2	Maximum Conformance Residual Figure of Merit .....	92
3.5	Summary .....	94
<b>CHAPTER 4: Investigating Implementation Issues of the Conformance Monitoring Analysis Framework Elements.....</b>		<b>95</b>
4.1	Introduction.....	95
4.2	Flight Test Non-Conformance Scenario .....	95
4.2.1	Flight Test Data Collection.....	95
4.2.2	Non-Conformance Scenario .....	97
4.3	Investigating Conformance Monitoring Model Fidelity Issues .....	99
4.4	Investigating Conformance Residual Generation Issues.....	104
4.4.1	Absolute Linear vs. Quadratic Scalar Functions Example .....	104
4.4.2	Scalar vs. Vector Forms Example .....	106
4.5	Investigating Decision-Making & Figure of Merit Issues .....	111
4.5.1	False Alarm/Time-To-Detection Figure of Merit Example.....	111
4.5.2	Maximum Conformance Residual Figure of Merit Example .....	114
4.6	Summary .....	116



<b>CHAPTER 5: Investigating Conformance Monitoring Issues Using the Analysis Framework &amp; Operational ATC Data .....</b>	<b>119</b>
5.1 Introduction.....	119
5.2 Operational ATC Data Collection.....	120
5.3 Operational Conformance Monitoring Issues in Key Flight Regimes.....	122
5.3.1 Lateral Conformance Monitoring: Straight Flight.....	123
5.3.2 Lateral Conformance Monitoring: Transitioning Flight.....	130
5.3.3 Vertical Conformance Monitoring: Level Flight.....	138
5.3.4 Vertical Conformance Monitoring: Transitioning Flight .....	143
5.3.5 Longitudinal Conformance Monitoring: Constant Speed Flight.....	144
5.3.6 Longitudinal Conformance Monitoring: Transitioning Flight.....	146
5.3.7 Implications of Conformance Monitoring Issues for Future ATC System Design .....	147
5.4 Conformance Basis Observability Issues in Key Flight Phases.....	148
5.4.1 Conformance Basis Observability Issues: Departure Phase.....	149
5.4.2 Conformance Basis Observability Issues: En-Route Phase.....	154
5.4.3 Conformance Basis Observability Issues: Descent Phase .....	158
5.4.4 Conformance Basis Observability Issues: Approach Phase .....	159
5.4.5 Implications of Conformance Basis Observability for Future ATC System Design.....	164
5.5 Summary.....	165
 <b>CHAPTER 6: Investigating Conformance Monitoring Issues Using the Analysis Framework &amp; Simulated ATC Data.....</b>	 <b>169</b>
6.1 Introduction.....	169
6.2 Simulated ATC Data Collection .....	170
6.3 Simulated Conformance Monitoring Issues in Key Flight Regimes .....	172
6.3.1 Lateral Conformance Monitoring: Straight Flight.....	172
6.3.2 Lateral Conformance Monitoring: Flight Plan Transitions .....	177
6.3.3 Lateral Conformance Monitoring: ATC Heading Vector Transitions.....	179
6.3.4 Vertical Conformance Monitoring: Level Flight.....	183
6.3.5 Vertical Conformance Monitoring: Transitioning Flight .....	185
6.3.6 Longitudinal Conformance Monitoring: Constant Speed Flight.....	188
6.3.7 Longitudinal Conformance Monitoring: Transitioning Flight.....	189
6.4 Summary.....	190

<b>CHAPTER 7: Extended Applications of the Conformance Monitoring Analysis Framework .....</b>	<b>193</b>
7.1 Introduction.....	193
7.2 Intent Inferencing.....	193
7.3 Environmental Parameter Estimation .....	199
7.4 Summary.....	205
<b>CHAPTER 8: Conclusions, Contributions &amp; Future Work .....</b>	<b>207</b>
8.1 Conclusions.....	207
8.2 Contributions.....	211
8.3 Future Work.....	213
<b>References .....</b>	<b>215</b>
<b>Appendix A: Aircraft Navigation Issues.....</b>	<b>223</b>

---

# List of Figures

---

## Chapter 1

Figure 1.1: General Signal-Based Fault Detection Concept.....	26
Figure 1.2: General Model-Based Fault Detection Concept.....	27
Figure 1.3: Notional Representation of a Conformance Monitoring Function.....	28
Figure 1.4: ATC Control Loops Affecting Conformance Monitoring .....	29
Figure 1.5: Lateral Actual Navigation Performance (ANP) Characteristics .....	30
Figure 1.6: Example Aircraft Tracking Characteristics.....	31
Figure 1.7: Cockpit Displays for Pilot Path Tracking .....	32
Figure 1.8: Lateral Flight Technical Error (FTE) Characteristics .....	32
Figure 1.9: Required Navigational Performance (RNP) Concept .....	33
Figure 1.10: Generalized Controller Cognitive Process Model.....	35
Figure 1.11: Example En-Route Non-Conformance Scenarios.....	36

## Chapter 2

Figure 2.1: Precision Runway Monitor Schematic.....	40
Figure 2.2: PRM Blunder Risk Model.....	43
Figure 2.3: HCS Processing Elements.....	44
Figure 2.4: Sample En-Route Center Flight Progress Strip.....	44
Figure 2.5: HCS Lateral Association Checking.....	45
Figure 2.6: AERA Lateral Conformance Bound Concept.....	48
Figure 2.7: URET Horizontal and Vertical Conformance Bounds.....	49
Figure 2.8: CAATS Display Symbology for Conforming & Non-Conforming Aircraft .....	52
Figure 2.9: PHARE 4D Contract Concept.....	55
Figure 2.10: PHARE Tube Definitions .....	56
Figure 2.11: NarSim Conformance Monitoring Scenarios .....	58
Figure 2.12: TSAFE Architecture.....	60
Figure 2.13: Simplified TSAFE Functionality .....	61
Figure 2.14: TSAFE Non-Transitioning Horizontal Tracking Error Categories .....	62
Figure 2.15: TSAFE Non-Transitioning Vertical Tracking Error Categories .....	63

Figure 2.16: TSAFE Transitioning Horizontal Tracking Error Categories .....	64
Figure 2.17: TSAFE Transitioning Vertical Tracking Error Categories .....	65
Figure 2.18: Example Horizontal and Vertical Critical Maneuvers .....	66

### Chapter 3

Figure 3.1: General Fault Detection Framework .....	72
Figure 3.2: Conformance Monitoring in General Fault Detection Framework .....	72
Figure 3.3: The Conformance Monitoring Analysis Framework (CMAF) .....	73
Figure 3.4: Simplified Actual System Representation.....	75
Figure 3.5: Intent & Dynamic State Relationships in the Actual System Representation.....	76
Figure 3.6: Visualization of Surveillance Environments using the Actual System Representation .....	77
Figure 3.7: Conformance Monitoring Model as a Mental Model in the Controller .....	81
Figure 3.8: Comparison of Absolute Linear & Quadratic Functions in Residual Generation.....	85
Figure 3.9: Example Non-Conformance Scenarios .....	86
Figure 3.10: Example Vector Conformance Residuals .....	87
Figure 3.11: Scalar & Vector Decision Thresholds.....	89
Figure 3.12: Multiple Alert Stages Enabled by Nested Thresholds.....	89
Figure 3.13: Example Use of Figures of Merit to Determine Appropriate CMAF Implementations.....	91
Figure 3.14: False Alarm/Time-To-Detection Trade-Off Schematic .....	92
Figure 3.15: Standard Operating Characteristic (SOC) Curve Schematic.....	92
Figure 3.16: Maximum Conformance Residual Figure of Merit Definition .....	93

### Chapter 4

Figure 4.1: Experimental Boeing 737-400 Flight Test Aircraft .....	95
Figure 4.2: Flight Test Lateral Non-Conformance Scenario .....	97
Figure 4.3: Lateral Non-Conformance Scenario Dynamic States .....	98
Figure 4.4: High Fidelity CMM Representation of Trajectory-Following Autopilot.....	100
Figure 4.5: Medium Fidelity CMM Heading and Roll State Behaviors.....	101
Figure 4.6: Observed Relationship Between Heading Correction and Cross-Track Error During Recovery Flight Segment.....	101
Figure 4.7: Heading and Roll State Errors for Low & Medium Fidelity CMMs .....	103
Figure 4.8: Dynamic State Variations During Nominal Flight Segment.....	105
Figure 4.9: Absolute Linear vs. Quadratic Scalar Function During Nominal Flight Segment.....	105
Figure 4.10: Absolute Linear vs. Quadratic Scalar Function for Entire Non-Conformance Scenario .....	106

Figure 4.11: Example Scalar Conformance Residual.....	107
Figure 4.12: Example 3D Vector Conformance Residual .....	109
Figure 4.13: Combined & Parallel Conformance Residuals Using Derivative and Integral Functions ...	110
Figure 4.14: Lateral Non-Conformance Scenario Conformance Residuals .....	112
Figure 4.15: Generic Threshold-Based Decision-Making Strategy.....	112
Figure 4.16: Lateral Non-Conformance False Alarm/Time-To-Detection Metrics.....	113
Figure 4.17: Recovery Trajectory in Maximum Conformance Residual Figure of Merit.....	114
Figure 4.18: Lateral Non-Conformance Maximum Conformance Residual Figure of Merit.....	116

## Chapter 5

Figure 5.1: Implementation of Analysis Framework Using Operational Data.....	119
Figure 5.2: Flight Test Profiles.....	120
Figure 5.3: Seattle Center (ZSE) Airspace & En-Route Radar Locations.....	122
Figure 5.4: Lateral Non-Conformance Scenario.....	124
Figure 5.5: Lateral Non-Conformance Scenario Dynamic States .....	124
Figure 5.6: Lateral Non-Conformance Scenario Weighting Factor Determination.....	125
Figure 5.7: Lateral Non-Conformance Scenario Conformance Residuals with Aircraft & Radar Data...	126
Figure 5.8: Lateral Non-Conformance Scenario False Alarm/Time-To-Detection Metrics.....	127
Figure 5.9: Effect of Non-Conformance Angles on Position-Based Time to Detection .....	128
Figure 5.10: Analysis of Heading Non-Conformance Detection in Existing Systems.....	128
Figure 5.12: Time-To-Detection of 10° Heading Non-Conformance in Existing Systems .....	129
Figure 5.13: Lateral Transition Scenario .....	130
Figure 5.14: Circular Arc Fillet Definition.....	131
Figure 5.15: Lateral Transition Scenario Dynamic States .....	131
Figure 5.16: Lateral Transition Scenario Error States .....	132
Figure 5.17: Lateral Transition Scenario Conformance Residuals.....	133
Figure 5.18: Comparison Between Lateral Transition Trajectories for Flight Tests 1 & 2.....	134
Figure 5.19: Relative Non-Transition/Transition Threshold Values for Example Scenario .....	134
Figure 5.20: Transition Non-Conformance Scenario .....	136
Figure 5.21: Transition Non-Conformance False Alarm/Time-To-Detection Metrics .....	136
Figure 5.22: Reduced Benefit of Higher Order States During Transitions.....	137
Figure 5.23: Intent State Usage During Transition Non-Conformance Scenario.....	138
Figure 5.24: Barometric Altitude Deviations Recorded During Cruise Phase .....	139
Figure 5.25: Barometric & GPS Altitude Comparison During Cruise.....	140

Figure 5.26: Vertical Deviation Dynamic States .....	141
Figure 5.27: Vertical Deviation Conformance Residuals with Aircraft & Radar Data .....	142
Figure 5.28: Vertical Deviation False Alarm/Time-To-Detection Metrics .....	142
Figure 5.29: Vertical Deviations at Detection .....	143
Figure 5.30: Calibrated Airspeed During Cruise Flight .....	145
Figure 5.31: Calibrated Airspeed Deviation Scenario .....	145
Figure 5.32: Speed Surveillance Limitations .....	147
Figure 5.33: Importance of Consistency of Conformance Basis Among ATC Agents .....	148
Figure 5.34: Standard Instrument Departure (SID) for BFI Runway 13R .....	149
Figure 5.35: Trajectory Uncertainty During Departure .....	150
Figure 5.36: Flight Test Departure Tracks Relative to HCS Flight Plan Route .....	151
Figure 5.37: Three-Dimensional Departure Flight Tracks .....	152
Figure 5.38: Vertical Profile Relative to Assigned Altitude During Flight Test Departure .....	153
Figure 5.39: Evolution of Lateral HCS Flight Plan and Actual Flight Path Flown .....	154
Figure 5.40: Lateral Deviations from HCS Route After Direct-To SZT Amendment .....	155
Figure 5.41: High Altitude Sectors Involved in the Direct-To GLASR Route Amendment .....	156
Figure 5.42: Evolution of Assigned Altitudes and Actual Altitude Profile .....	158
Figure 5.43: Vertical Conformance Basis and Surveillance Issues on Descent .....	158
Figure 5.44: Standard Terminal Arrival Route (STAR) to BFI .....	160
Figure 5.45: Flight Test Arrival Tracks Relative to HCS Flight Plan Route .....	160
Figure 5.46: Instrument Landing System (ILS) Schematic .....	161
Figure 5.47: ILS Approach Procedure into BFI Used During Test Flights .....	162
Figure 5.48: Flight Test Arrival Tracks Relative to ILS Path .....	162
Figure 5.49: Flight Test ILS Localizer and Glide Slope Deviations .....	163
Figure 5.50: Conformance Basis Updating in Current ATC System .....	164
Figure 5.51: Potential Conformance Basis Updating Enhancements in Future ATC System .....	165

## **Chapter 6**

Figure 6.1: Implementation of the Analysis Framework Using Simulated ATC Data .....	169
Figure 6.2: Flight Simulator Cockpit Screenshot .....	170
Figure 6.3: Flight Simulator/MATLAB Integration Capability .....	171
Figure 6.4: Simulated Lateral Non-Conformance Dynamic States with Environmental Disturbances (Autopilot Guidance) .....	173

Figure 6.5: Effect of Environmental Disturbances on FA/TTD Metrics During Lateral Non-Conformance (Autopilot Guidance).....	174
Figure 6.6: Simulated Lateral Non-Conformance Dynamic States with Different Guidance Modes (Zero Turbulence).....	175
Figure 6.7: Effect of Guidance Mode on FA/TTD Metrics During Lateral Non-Conformance (Zero Turbulence).....	176
Figure 6.8: Simulated Flight Tracks Under Various Flight Plan Transition Modes.....	177
Figure 6.9: Simulated Lateral Transition Non-Conformance Scenarios .....	178
Figure 6.10: Simulated Lateral Transition Non-Conformance Scenario Dynamic States.....	179
Figure 6.11: Heading Vector Transition Scenario.....	180
Figure 6.12: Heading Vector Scenario State Behaviors .....	180
Figure 6.13: Heading Vector Scenario Conformance Residuals .....	181
Figure 6.14: Using Cross-Correlation Functions to Detect Timing Issues in Heading Vector Scenario .	182
Figure 6.15: Simulated Vertical Non-Conformance Dynamic States with Environmental Disturbance and with Different Guidance Modes .....	184
Figure 6.16: Effect of Environmental Disturbance and Guidance Mode on FA/TTD Metrics During Vertical Non-Conformance .....	185
Figure 6.17: Simulated Vertical Transition Dynamic States .....	186
Figure 6.18: Vertical Transition Thresholds Schematic .....	187
Figure 6.19: Simulated Speed Non-Conformance with Environmental Disturbances .....	188
Figure 6.20: Simulated Speed Transition States.....	189

## **Chapter 7**

Figure 7.1: Fault Isolation Using a Bank of System Models.....	194
Figure 7.2: Intent Inferencing Using a Bank of Conformance Bases.....	195
Figure 7.3: Intent Inferencing Late Turn Scenario.....	196
Figure 7.4: Hypothesized Alternate Trajectories for Intent Inferencing Scenario.....	196
Figure 7.5: Conformance Residuals for Alternate Trajectories .....	197
Figure 7.6: Relative Likelihood of Alternate Trajectories.....	198
Figure 7.7: Environmental Parameter Estimation Using the Conformance Monitoring Analysis Framework.....	199
Figure 7.8: Wind Effects in a Lateral ATC Scenario .....	200
Figure 7.9: Wind Field Estimation Example (1 Aircraft).....	201
Figure 7.10: Wind Field Estimation Example (3 Aircraft).....	202

Figure 7.11: Wind Field Estimation Using Filter Equations ..... 204

**Appendix A**

Figure A.1: Rhumb Line Navigation ..... 223

Figure A.2: Comparison of Great Circle and Rhumb Line Routes Between BOS and LHR ..... 224

Figure A.3: Approximating Great Circle Route With Rhumb Line Segments ..... 225



---

# List of Tables

---

## Chapter 2

Table 2.1: HCS Lateral Association Checking Thresholds .....	45
Table 2.2: HCS Vertical Association Checking Thresholds .....	46
Table 2.3: URET Nominal Conformance Bound Values .....	49
Table 2.4: URET Lateral Reconformance Scenarios.....	51
Table 2.5: TSAFE Non-Transitioning Horizontal Conflict Detection Trajectories.....	62
Table 2.6: TSAFE Non-Transitioning Vertical Conflict Detection Trajectories.....	63
Table 2.7: TSAFE Transitioning Horizontal Conflict Detection Trajectories.....	64
Table 2.8: TSAFE Transitioning Vertical Tracking Error Conflict Detection Trajectories .....	65
Table 2.9: Fault Detection Categorizations & State Usage of Conformance Monitoring Tools .....	68

## Chapter 3

Table 3.1: Example Forms of Conformance Basis .....	74
Table 3.2: Example Conformance Monitoring Model Fidelities.....	79

## Chapter 4

Table 4.1: ARINC 429 Databus Parameters Archived During Flight Test .....	96
Table 4.2: GPS Parameters Archived During Flight Test .....	97
Table 4.3: Non-Conformance Scenario Weighting Factors.....	104
Table 4.4: Evolution of Vector Residuals During Lateral Non-Conformance Scenario .....	108

## Chapter 5

Table 5.1: HCS Parameters Archived During Test Flights .....	121
Table 5.2: Lateral Non-Conformance Scenario Weighting Factors .....	126
Table 5.3: Time-To-Detection of 10° Non-Conformance with Existing System Thresholds under Nominal Operating Conditions.....	129
Table 5.4: Relative Non-Transition/Transition Threshold Values for Existing Tools .....	135

**Chapter 6**

Table 6.1: Weighting Factors in Heading Vector Scenario ..... 181

**Chapter 7**

Table 7.1: Wind Field Parameter Estimation Results ..... 202

---

# Acronyms

---

AACS	Automated Airspace Computer System
ADS	Automatic Dependent Surveillance
ADS-A	Automatic Dependent Surveillance-Address
ADS-B	Automatic Dependent Surveillance-Broadcast
ADS-C	Automatic Dependent Surveillance-Contract
AERA	Automated En-Route Air Traffic Control
AIAA	American Institute of Aeronautics and Astronautics
ANP	Actual Navigation Performance
ARINC	Aeronautical Radio Incorporated
ARSR	Air Route Surveillance Radar
ARTCC	Air Route Traffic Control Center
ARTS	Automated Radar Terminal System
ASR	Airport Surveillance Radar
ATC	Air Traffic Control
ATM	Air Traffic Management
ATP	Airspace To Protect
BFI	Boeing Field/King County International Airport
BOS	Boston Logan Airport
CAATS	Canadian Automated Air Traffic System
CALT	Caution-Alert Lead Time
CAS	Calibrated Airspeed
CB	Conformance Basis
CD&R	Conflict Detection & Resolution
CDU	Control Display Unit
CMAF	Conformance Monitoring Analysis Framework
CMM	Conformance Monitoring Model
CNS	Communication, Navigation & Surveillance
CPDLC	Controller Pilot Data Link Communication
CR	Conformance Residual

CTAS	Center-TRACON Automation System
DAG-TM	Distributed Air Ground Traffic Management
DART	Data Analysis and Reduction Tool
DDM	Difference in Depth of Modulation
DME	Distance Measuring Equipment
DST	Decision Support Technology
EPE	Estimated Position Error
EPU	Estimate of Position Uncertainty
ETA	Estimated Time of Arrival
ETMS	Enhanced Traffic Management System
ETOPS	Extended Range Twin Operations
FA	False Alarm
FAA	Federal Aviation Administration
FANS	Future Air Navigation System
FCU	Flight Control Unit
FDI	Fault Detection and Isolation
FDP	Flight Data Processor
FDPS	Flight Data Processing System
FL	Flight Level
FLCH	Flight Level Change Mode
FMA	Final Monitor Aid
FMC	Flight Management Computer
FMS	Flight Management System
FPM	Flight Position Monitor
FPS	Flight Progress Strip
FS2002	Microsoft® Flight Simulator 2002
FTE	Flight Technical Error
GAATS	Gander Automated Air Traffic System
GNSS	Global Navigation Satellite System
GPS	Global Positioning System
GS	Glide Slope
HCS	Host Computer System
HF	High Frequency
HFDL	High Frequency Datalink

HMI	Human Machine Interface
HSI	Horizontal Situation Indicator
IAS	Indicated Airspeed
ICAO	International Civil Aviation Organisation
IFR	Instrument Flight Rules
ILS	Instrument Landing System
IMC	Instrument Meteorological Conditions
IRS	Inertial Reference System
IRU	Inertial Reference Unit
LHR	London Heathrow Airport
LNAV	Lateral Navigation
LOA	Letter Of Agreement
LRU	Line Replaceable Unit
MASPS	Minimum Aviation System Performance Standards
MCP	Mode Control Panel
MEM	Memphis International Airport
MINIT	Minutes In Trail
MIT	Massachusetts Institute of Technology, Miles In Trail
MOA	Military Operations Area
MSAW	Minimum Safe Altitude Warning
NASA	National Aeronautics and Space Administration
NAVAID	Navigational Aid
NLR	Nationaal Lucht- en Ruimtevaartlaboratorium / National Aerospace Lab., Netherlands
NOAA	National Oceanic and Atmospheric Administration
NPS	Navigation Performance Scales
NTAP	National Track Analysis Program
NTZ	No Transgression Zone
OACC	Oceanic Area Control Center
PFD	Primary Flight Display
PHARE	Programme for Harmonised Air Traffic Management Research in Eurocontrol
PID	Proportional, Integral, Derivative
PRM	Precision Runway Monitor
PVD	Plan View Display
RDP	Radar Data Processor

RNAV	Area Navigation
RNP	Required Navigation Performance
RTA	Required Time of Arrival
RTCA	formerly the Radio Technical Committee on Aeronautics
RVSM	Reduced Vertical Separation Minima
SAATS	Shanwick Automated Air Traffic System
SAR	System Analysis Recording
SATCOM	Satellite Communication
SEA	Seattle-Tacoma International Airport
SID	Standard Instrument Departure
SOC	System Operating Characteristic
SOP	Standard Operating Procedure
STAR	Standard Terminal Arrival Route
SUA	Special Use Airspace
TAS	True Airspeed
TF	Transfer Function
TFR	Temporary Flight Restriction
TOD	Top Of Descent
TRACON	Terminal Radar Approach Control
TSAFE	Tactical Separation Assisted Flight Environment
TTD	Time-To-Detection
URET	User Request Evaluation Tool
TAAATS	The Australian Automated Air Traffic System
VDL3	VHF Datalink Mode 3
VDOP	Vertical Dilution of Precision
VFR	Visual Flight Rules
VHF	Very High Frequency
VNAV	Vertical Navigation
VOR	VHF Omni-Directional Range
V/S	Vertical Speed
VSI	Vertical Speed Indicator
ZSE	Seattle ARTCC

---

# CHAPTER 1: Introduction to Conformance Monitoring in Air Traffic Control

---

## 1.1 Motivation for Conformance Monitoring Research in ATC

The primary goals of Air Traffic Control (ATC) are to ensure the safety, security and efficiency of air traffic operations. In order to achieve these aims, clearances are issued to each aircraft that have been determined to be conflict-free, secure and efficient over a certain period of time. In today's system, these clearances are created and issued by air traffic controllers given the constraints of the ATC system design. In future ATC concepts such as Free Flight [Post & Knorr (2003)] and Distributed Air-Ground Traffic Management (DAG-TM) [Green *et al.* (2000)], the clearances may be based on aircraft-preferred trajectories that are authorized by a centralized ground element so long as they do not produce conflicts. In either case, an ATC function is required to ensure that aircraft adhere to their assigned clearances by detecting any excessive deviations that could compromise system operation, enabling corrective action to be initiated when required. This function is termed conformance monitoring in this document, although other terms such as flight path monitoring, flight plan monitoring, route adherence monitoring, association checking, deviation detection and blunder detection are also found in the literature to describe the same general process in ATC.

There is currently much interest in improving conformance monitoring capability in ATC as it influences many of the areas where future ATC system performance improvements are desired. For example, conformance monitoring is crucial to ensuring the validity of conflict detection and resolution algorithms that are being widely developed to allow increased capacity (through reduced separation minima) and more efficient routings in future ATC environments [FAA (1999)]. In addition, the specific heightened awareness of the threat that deviant aircraft could pose to the security of the air transport system [ACARE (2002), Walker *et al.* (2002)] reinforces the need for more effective conformance monitoring than is possible in today's ATC system.

Improvements to conformance monitoring in future ATC systems may be enabled through the application of advanced technologies, particularly Decision Support Tools (DSTs) and improved communication, navigation and surveillance (CNS) systems. The potential benefits associated with the introduction of these technologies are listed below:

- The wider introduction of decision-support tools provides an opportunity to develop more sophisticated and automated conformance monitoring algorithms that can provide assistance to air traffic controllers and pilots for conformance monitoring during high workload or high criticality operations.
- Improved communications enabled by satellite communications (SATCOM) and digital datalinks such as High-Frequency Datalinks (HFDL) will allow for more detailed and unambiguous clearance delivery from the ground to pilots, or even directly to the aircraft automation systems.
- Navigational improvements of modern aircraft equipped with advanced Flight Management Systems (FMS), autopilots, area navigational capability and Global Navigation Satellite System (GNSS) sensors increase aircraft capability to track clearances more accurately and hence allow easier detection of abnormal behaviors.
- Surveillance enhancements provided by more sophisticated ground-based digital radar systems and Automatic Dependent Surveillance-Address/Broadcast/Contract (ADS-A/B/C) systems where aircraft broadcast certain states to other users provide the capability to provide higher accuracy, higher update rate and higher content state information for conformance monitoring.

In the past, the conformance monitoring task was typically performed by air traffic controllers comparing radar data with the assigned flight path. Significant deviations often existed before an aircraft non-conformance could be detected due to surveillance and workload limitations, as well as the requirement to account for numerous different aircraft tracking capabilities. The potential application of automation for improved conformance monitoring is being recognized as new decision support tools are being deployed and developed for ATC. However, most still use relatively simple algorithms where non-conformance is flagged when the observed position deviation of an aircraft from its assigned trajectory exceeds some pre-determined threshold value. There is often little or no indication as to the rationale for how these threshold values were assigned and whether they are appropriate in the context of the conformance monitoring needs of current and future operating environments. Hence, there is a need for general analysis techniques to identify fundamental conformance monitoring issues in ATC, to assist in the development of future approaches that take greater advantage of new technologies and which better support the requirements of ATC operations. This is the focus of the research presented in this document.



## 1.2 Detecting Deviant Behavior in General Engineering Systems

The detection of deviant behavior is a widespread problem in engineering systems. For example, automated systems are routinely used in hospitals to monitor a patient's vital signs for any deviation from a nominal range, alerting medical staff when parameters such as blood pressure, heart and respiration rate or blood oxygen saturation levels rise above or fall below certain acceptable thresholds [Hoyhtya (1996)]. Analogous systems monitoring the health of processes in nuclear power generation [Sheridan (1992)], automobile collision warning systems [Najm *et al.* (2001)], computer network integrity and financial indicators all use this same general approach. In the aerospace domain, operating parameters and vibration levels are monitored in commercial and military aircraft engines to determine when maintenance is required [Boeing (1999), Abbott (1996)], to detect failures in spacecraft propulsion systems like the Space Shuttle main engines [Lozano (1998)] and to check the integrity of outputs of avionics such as Global Positioning System (GPS) navigation systems [Brown (1996)].

These examples, as well as the many others that could be cited, illustrate the pervasiveness of the general deviation detection problem. General analysis approaches termed “fault detection techniques” have been developed for this class of problem. While a wide range of fault detection techniques that have been developed over the last few decades, they can be broadly classified into one of three main categories [Frank (1996)]:

- Signal-based fault detection techniques
- Knowledge-based fault detection techniques
- Model-based fault detection techniques

The concepts underlying each of these techniques developed for detecting faults in general systems will prove to be fundamental to the conformance monitoring analysis approaches developed throughout the rest of this document. Hence, background information to each of the fault detection technique categories is briefly discussed in the following subsections.

### 1.2.1 Signal-Based Fault Detection Techniques

The signal-based fault detection technique involves the monitoring of a measured or synthesized variable relative to a threshold, as illustrated in Figure 1.1. Types of variables used in such approaches include simple measurements of the system outputs or synthesized metrics such as means, limit values, trends, power spectral densities and correlation coefficients. The main advantage of a signal-based

technique is its simplicity, both in implementation and comprehension by an operator and this helps to explain why it is the most pervasive technique employed by general monitoring schemes today [Isermann (2000)]. Signal-based techniques are most effective at detecting relatively large changes in an observable state, such as would occur after a large sudden fault. They are generally less effective at detecting more slowly-evolving faults unless they exist for an extended period of time.

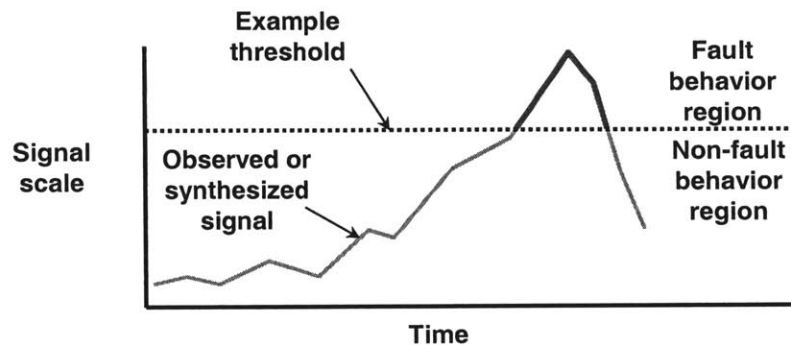


**Figure 1.1: General Signal-Based Fault Detection Concept**

### 1.2.2 Knowledge-Based Fault Detection Techniques

Knowledge-based fault detection techniques capture the expected dynamic behavior of the system in which faults are to be detected in terms of heuristic symptoms or qualitative descriptions [Jain (1998)]. These expectations are then compared to the observed behaviors. Often the expectations are based on rules, standard operating procedures and facts of nominal system operation elicited by expert operators. As engineering systems increase in complexity such that analytical models of system operation become harder to develop, more attention is being given to these knowledge-based approaches. They do not require any explicit analytical modeling (although expert operator “mental models” of the system operation may be critical to forming their own knowledge basis) and allow empirical process knowledge to be taken into account. However, their lack of quantitative metrics can be also be a significant restriction when these techniques are applied in numerical cost:benefit analyses that are often required in system design. In addition, expert elicitation techniques may not provide a complete representation of the key processes. Hence, these knowledge-based techniques are often used to support more traditional quantitative approaches rather than to replace them completely.

### 1.2.3 Model-Based Fault Detection Techniques

In model-based fault detection, a model of the system being monitored is used in parallel with the operation of the actual system as illustrated in Figure 1.2. This is used to develop an expectation of the

nominal, fault-free behavior of the states of interest at any given time or location, given the same command input as the actual system. These expectations are compared to the observed value of the states output from sensors or surveillance systems that are monitoring the actual system.

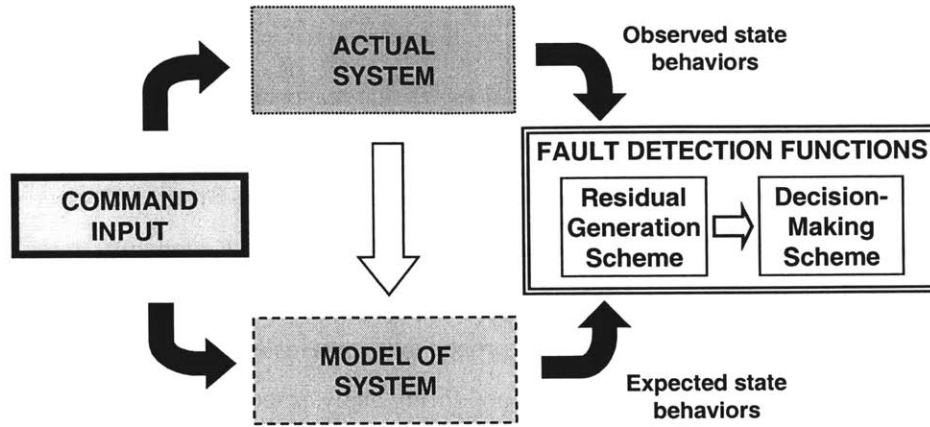


**Figure 1.2: General Model-Based Fault Detection Concept**

To perform this comparison, the observed and expected behaviors at any given time are input to the general fault detection processes of:

- **Residual generation:** the difference between the observed and expected state behaviors is quantified by a “residual”. The residual is generated in such a way that the larger the difference between the observed and expected behaviors, the larger are the characteristics of the residual (e.g. in terms of the value of a scalar residual or the magnitude of a vector residual).
- **Decision-making:** once a residual has been generated, a decision-making function determines whether it indicates a fault exists in the system or not. Often a fault is declared if a residual property exceeds a pre-determined threshold. Signal detection theory can be used to set thresholds based on metrics of interest, such as false alarm rate or time-to-detection targets.

Typically, the most challenging elements in the implementation of a model-based fault detection approach are the development of the system model and the associated scheme that generates the residual from its outputs. There are numerous closely-related methods that can be employed that are generally divided into parity space, parameter estimation and observer-based approaches [Frank (1996)]. Much of the theoretical fault detection research literature concentrates on the conception and optimal design of these various approaches [e.g. Chen & Patton (1996), Gertler (1998), Patton *et al.* (2000)], detailed

discussions of which are beyond the scope or need of this thesis. However, they generally involve mathematical (e.g. parity, state space) or simulation models of the key elements of the system dynamics.

Although a certain degree of modeling uncertainty always exists due to unmodeled disturbances and limited fidelity, model-based fault detection methods are generally considered superior to the pure signal and knowledge-based approaches under circumstances when a reasonable model can be developed. Note that a residual in the form of a scalar is just the same as a synthesized signal and a decision-making scheme can be defined in the form of a threshold, just as in the signal-based fault detection approach. Similarly, a model of the system can incorporate knowledge-based elements into its definition. Therefore, signal and knowledge-based fault detection approaches can be integrated into a model-based framework to develop a unified fault detection approach that contains elements of each technique. These facts will be utilized in the general conformance monitoring analysis techniques developed in this thesis.

### 1.3 Factors Affecting Conformance Monitoring in ATC

#### 1.3.1 Representation of Conformance Monitoring Functions

In this thesis, conformance monitoring in ATC will be limited to the specific function that determines whether an aircraft is deviating from its assigned clearance. A notional representation of this conformance monitoring function about a generic trajectory-based clearance is given in Figure 1.3.

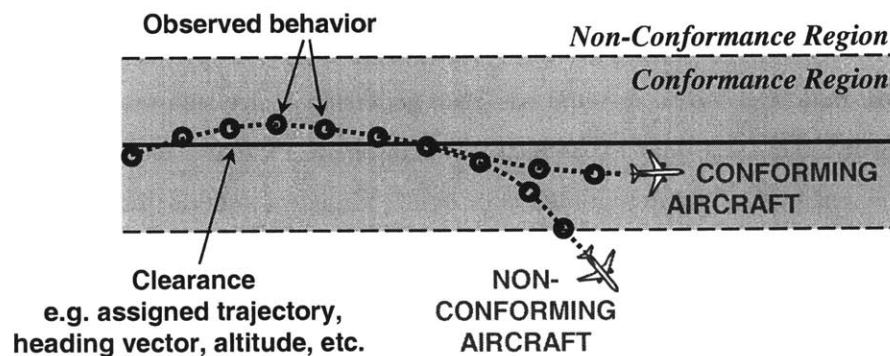


**Figure 1.3: Notional Representation of a Conformance Monitoring Function**

Examples of trajectory-based clearances include an assigned flight plan route, an ATC-assigned heading, speed or altitude, and a standard procedure route. Around the trajectory is a conformance region that is large enough to account for nominal variations in the observed trajectory of a conforming aircraft, (due to the surveillance and aircraft tracking limitations) but small enough for timely detection of deviant

aircraft. Although the generic conformance region in Figure 1.3 only bounds the aircraft’s cross-track deviation from the assigned trajectory, the general concept should be considered as existing in wider state space. In addition, the boundary between the conformance and non-conformance regions does not have to be the sharp boundary illustrated, but could be defined probabilistically using, for example, fuzzy logic approaches.

In order to understand the factors that influence the nominal variations in the observed trajectory of a conforming aircraft, Figure 1.4 presents relevant control loops in the current ATC system. The general conformance monitoring function is shown in the outermost control loop, with pilot and autoflight tracking functions as inner loops. Each of these control loops and their relevance to conformance monitoring research will be discussed in more detail in the following subsections.

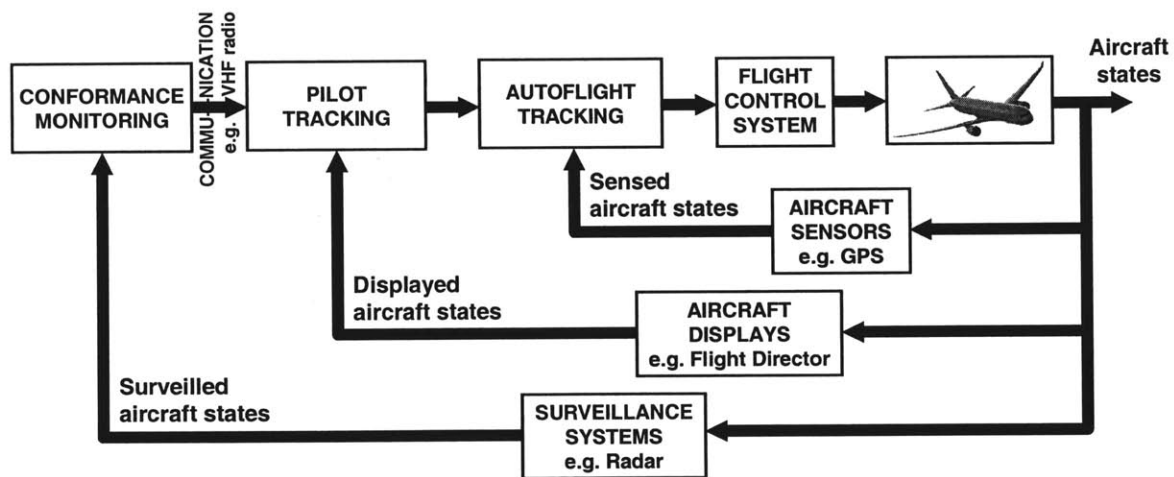


Figure 1.4: ATC Control Loops Affecting Conformance Monitoring

### 1.3.2 Autoflight Tracking Function

Autoflight systems typically monitor the sensed aircraft states relative to targets derived from the programmed trajectory in the Flight Management System (FMS) or some simpler autopilot target state such as commanded heading. Corrective inputs are made to the flight control system in response to any deviations from the target value. Deviations could be caused by a variety of factors, including navigational sensor errors, environmental disturbances and autoflight system control law design. Navigational sensor errors are measured by an “Actual Navigation Performance” (ANP) metric in Boeing aircraft and “Estimated Position Error” (EPE) in Airbus aircraft<sup>†</sup>. Both describe the computed navigation

<sup>†</sup> The general term “Estimated Position Uncertainty” (EPU) is used by the RTCA [RTCA (2000)]

system accuracy for the aircraft's position at any given time. For example, lateral ANP is expressed as a value in nautical miles (nm) representing a circle of that radius which is centered at the estimated position such that the probability of the true position of the aircraft residing inside the circle equals 95%. Vertical ANP is expressed in feet and represents a symmetric band centered on the baro-corrected altitude where the probability of the aircraft being inside that band equals 95% [Boeing (2003)]. Figure 1.5 illustrates how the lateral ANP performance of a selection of Boeing aircraft types varies as a function of navigational equipment on the aircraft. It can be seen that better aircraft navigational performance is associated with the most advanced GPS-updated Inertial Reference Systems (IRS) compared to those updated by VHF Omni-directional Range (VOR) and/or Distance Measuring Equipment (DME) radio navigation aids on the ground. Worst performance is associated with the standalone IRS since they suffer from uncorrected drift over time.

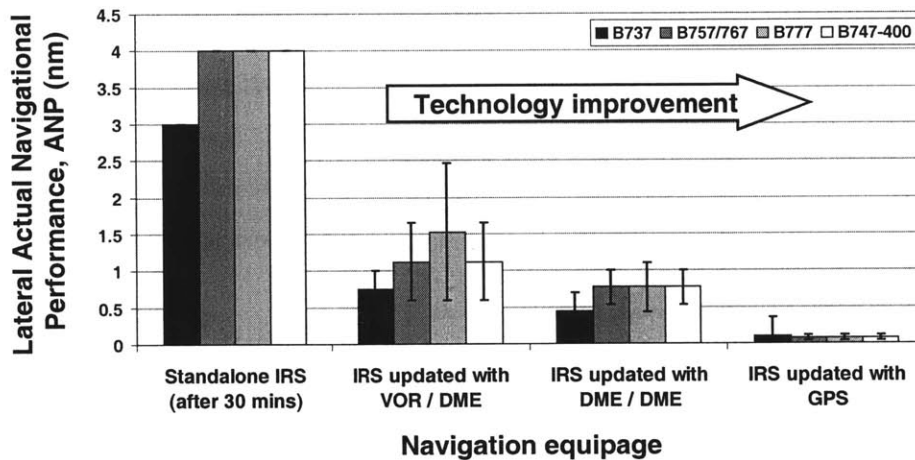


**Figure 1.5: Lateral Actual Navigation Performance (ANP) Characteristics [adapted from Boeing (2000)]**

In addition to these navigational sensor performance capabilities, the level of autoflight system technology also has a significant effect on the tracking performance. This is illustrated in Figure 1.6, which shows the cross-track deviation from the same trajectory for a 1960s-era Boeing B737-200 and a 1990s-era Airbus A320<sup>†</sup>. The A320 aircraft has an advanced FMS system coupled to GPS navigational sensors that allow for lateral navigational guidance along a programmed trajectory. Cross track deviations of less than 0.4 nm are evident. The B737-200 has a less advanced lateral guidance autopilot capability that tracks VOR radial signals whose accuracy decreases with range from the ground station.

<sup>†</sup> The cross-track deviations were calculated for two commercial flights on the same flight plan leg at similar times from FAA radar data supplied by Mike Paglione, FAA Technical Center, Atlantic City, NJ in January 2000.

Much larger cross-track deviations of over 2.5 nm are observed in this case. From a conformance monitoring perspective, the path tracking variability of an advanced FMS/GPS-equipped aircraft can be expected to be much less than that of an older generation aircraft, so the former could theoretically be held to tighter conformance standards.

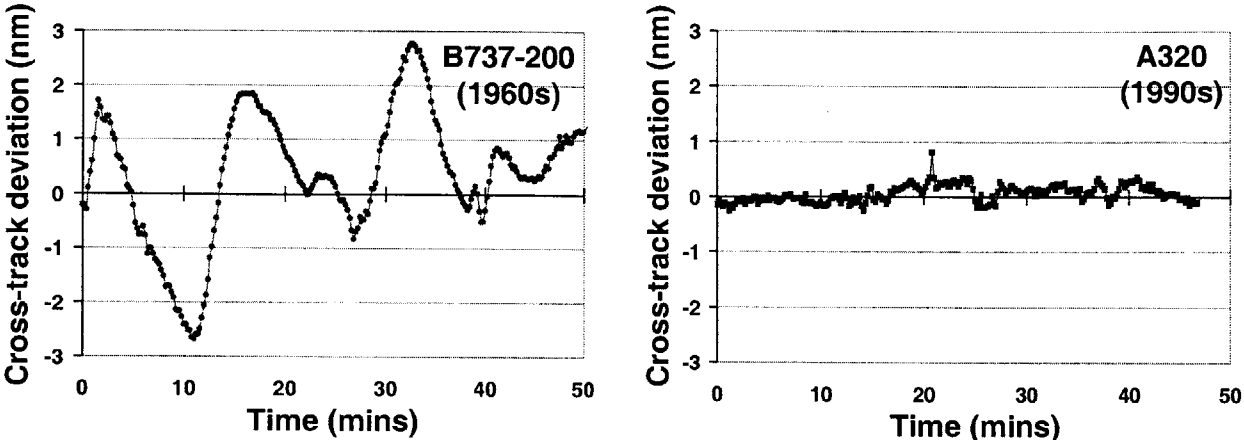


Figure 1.6: Example Aircraft Tracking Characteristics

1.3.3 Pilot Tracking Function

In addition to the aircraft autoflight tracking capability, the flight crew are also involved in the overall aircraft control loop, either directly if they are flying manually, or indirectly if they are monitoring an autopilot’s performance. In order to define the tracking performance of a pilot or a pilot/autopilot combination, a concept known as “Flight Technical Error” (FTE) has been defined. It is a measure of the position errors induced by the tracking dynamics of the guidance, control system and/or pilot combination when following a specified path under various environmental conditions [Boeing (2003)].

In the lateral domain, the pilot can monitor the aircraft’s behavior relative to the specified path via cockpit displays, such as the Flight Director on the Primary Flight Display (PFD) or the map display of the programmed FMS route on the Horizontal Situation Indicator (HSI). These are shown in Figure 1.7. Studies have been conducted to define the FTE under various manual guidance scenarios with the pilot using these displays. An example for Boeing aircraft tracking a leg of a flight plan is presented in Figure 1.8. It is seen that the FTE is larger for the cases where the pilot is involved in the tracking task compared to the autopilot alone. As a result, much more aircraft tracking variability would be expected under conditions where the aircraft is being (or may be) flown manually relative to the autopilot guidance case.

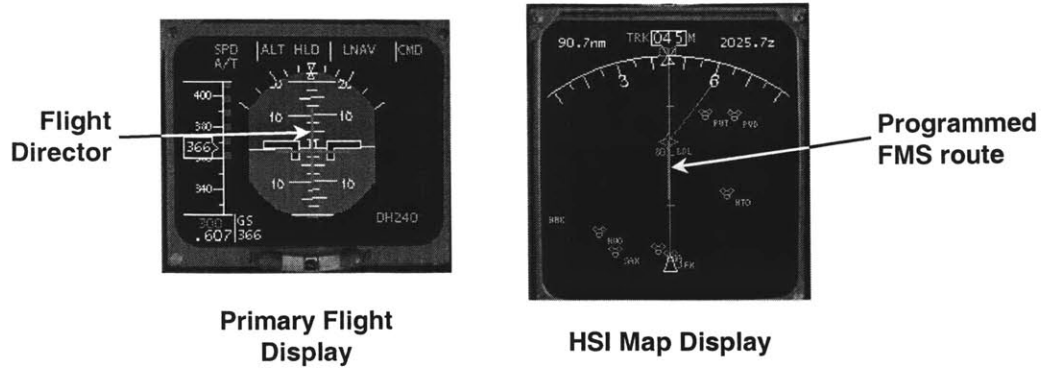


Figure 1.7: Cockpit Displays for Pilot Path Tracking

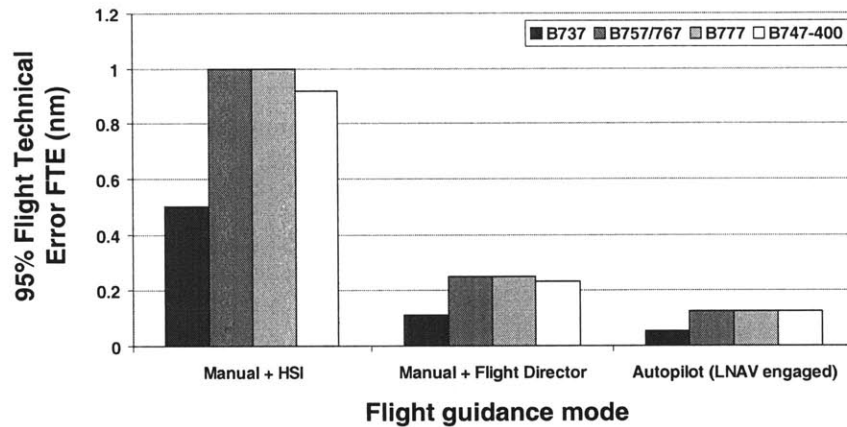


Figure 1.8: Lateral Flight Technical Error (FTE) Characteristics [adapted from Boeing (2000)]

### 1.3.4 Conformance Monitoring Function

The final loop in Figure 1.4 represents the conformance monitoring function. Controllers perform this function using feedback from surveillance systems (such as radars) to determine whether the aircraft is behaving in a manner consistent with their knowledge of the clearance. Note that although ground-based controller conformance monitoring is the baseline case considered in this thesis, future ATC may also require conformance monitoring functions to be undertaken by flight crew of one aircraft monitoring another, such as in pairwise self separation. The issues discussed are generalisable for both cases.

Since the conformance monitoring function is the outermost control loop, it is influenced by the autoflight and pilot tracking functions just described, as well as limitations in the surveillance system being used (e.g. finite accuracy and update rate) and the communications systems used for the



transmission of new clearances (e.g. VHF radio). The expected variability that makes up the Conformance Region in the conformance monitoring representation of Figure 1.3 must therefore account for each of these factors. However, it is challenging to account for the expected variability in the autoflight and pilot tracking since they are functions of navigation equipage, autoflight capability and current flight guidance mode of each aircraft being monitored. These are factors that generally have poor observability and over which the controller has limited (if any) control. This issue has traditionally been dealt with by assuming that the expected aircraft and pilot variability follows some “worst case” scenario. However, for the large majority of aircraft within the system that are capable of better performance than this worst case, this leads to unnecessarily conservative assumptions of aircraft and pilot tracking performance variability. This limits both the effectiveness with which conformance monitoring can be conducted and also wider operational procedural design such as required widths of route structures.

In order to begin taking advantage of the superior capability of modern aircraft within the system, the Required Navigation Performance (RNP) concept was introduced in the 1990s, defined by ICAO as “a statement of the navigation performance accuracy necessary for operation within a defined airspace” [ICAO (1996)]. An RNP-X airspace specification implies that the aircraft must have navigational capability to stay within  $\pm X$  nm laterally or  $\pm X$  ft vertically for at least 95% of the flight time within that region [RTCA (2000)]. Figure 1.9 illustrates this concept in the lateral domain.

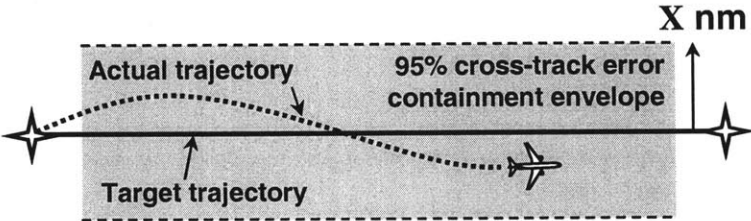


**Figure 1.9: Required Navigational Performance (RNP) Concept**

Note that RNP defines the ultimate performance of the tracking required of an aircraft if it is to operate in specific airspace and not the means by which that performance is achieved. This effectively removes concerns over specific navigational equipment and flight mode of any given aircraft so long as the specified performance is met. Although not all airspace currently has RNP-specifications, its use is expected to become widespread in the future. Typical lateral RNP requirements in different environments can be summarized as [Moir & Seabridge (2003)]:

- RNP-12 for oceanic operations
- RNP-2 for en-route operations
- RNP-1 for terminal area operations
- RNP-0.3 for approach operations

Note how the RNP specifications call for improved performance nearer to airports as traffic density increases. This specification of navigational performance requirements can be used to bound the pilot and aircraft tracking performance elements in the conformance monitoring task in each of these environments. Other important advances to the conformance monitoring function will be brought about by the introduction of advanced surveillance equipment (e.g. Automatic Dependent Surveillance (ADS) systems) that have higher accuracy, update rate and content than existing systems, and new communication systems (e.g. Controller-Pilot Datalink (CPDLC)) that will allow for more flexible and unambiguous clearances to be sent to the aircraft being monitored.

## 1.4 General Controller Functions in ATC

In order to understand the context of the conformance monitoring task relative to all the others required of a controller in the current system, studies have been undertaken to elucidate the main controller cognitive tasks. They have been identified as [Pawlak *et al.* (1996), Reynolds *et al.* (2002)]:

- Monitoring
- Planning
- Implementing
- Evaluating
- Maintenance of Situation Awareness.

The relationship of these processes in ATC is illustrated in the cognitive process model of Figure 1.10. The “Current Plan” is the controller’s internal representation of the schedule of events and commands to be implemented as well as the resulting aircraft trajectories planned to ensure that the air traffic situation evolves in an efficient and conflict-free manner. The Current Plan, along with the results of the Decision Processes, is used to Implement a set of Commands that act on the Air Traffic Situation. The impact of those commands on the Air Traffic Situation is fed back to the controller’s Situation Awareness [Endsley & Rogers (1994)] through a Surveillance Path. The Monitoring process then observes the overall air traffic situation to ensure that the traffic flows conform to the Current Plan.

Conformance monitoring of individual aircraft to their clearances (the definition used in this thesis) can be viewed as the sub-tasks that make up this overall Monitoring task. The Current Plan is constantly evaluated to ensure its effectiveness in producing conflict-free, efficient and secure trajectories. The outputs from both the Monitoring and Evaluation functions can trigger a re-plan process if required.

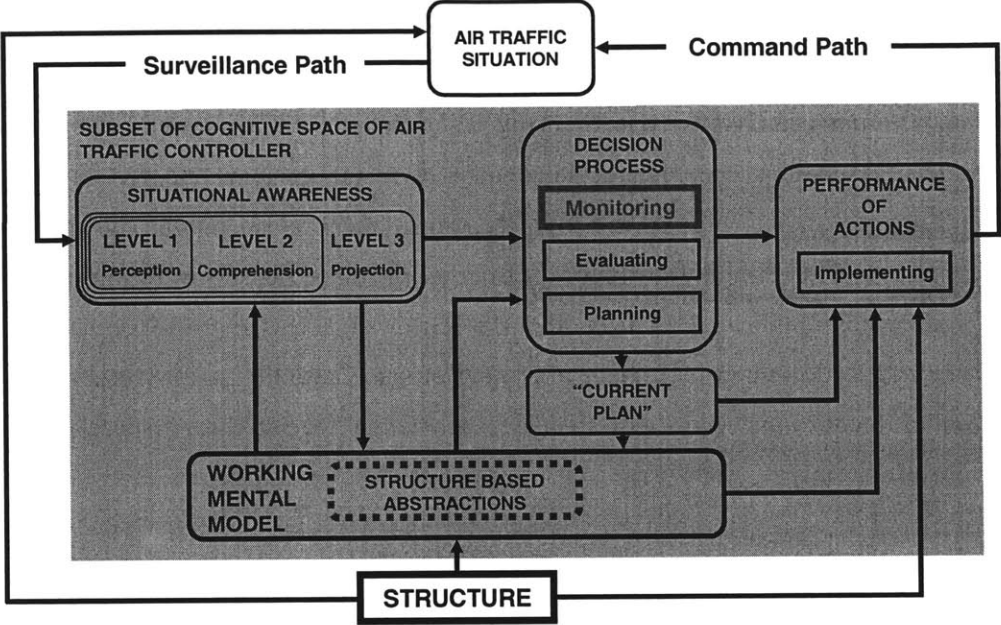
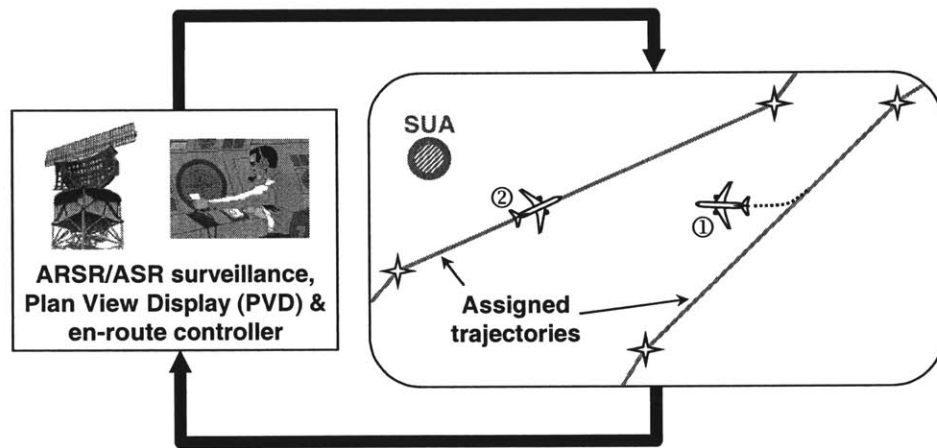


Figure 1.10: Generalized Controller Cognitive Process Model [Reynolds et al. (2002)]

The relative importance of each of the five tasks identified above is dependent upon the ATC environment. The consequences of non-conformance of an individual aircraft and the ability to detect it through ground-based conformance monitoring also depend on the ATC environment in which the deviation occurs. For example, an aircraft on an Instrument Landing System (ILS) final approach that deviates excessively from its path can quickly cause a conflict with an aircraft on an independent approach to a parallel runway. The ability to undertake ground-based conformance monitoring to rapidly detect aircraft deviations was therefore a fundamental driver in the design of close-spaced independent parallel approach procedures in the US [Shank & Hollister (1994)]. For these operations, a dedicated final approach controller is employed to monitor a high resolution display and initiate an evasive maneuver if one of the aircraft deviates excessively into a pre-determined region. Of the five key cognitive tasks identified above, Monitoring overrides all the other tasks for this controller. There is little in the way of Planning or Evaluating required as the controller accepts traffic from the upstream terminal area controller at a pre-agreed rate. Maintenance of Situation Awareness is limited to those aircraft on a

well-established approach path, while an Implementation task is only required when Monitoring indicates the need for an emergency maneuver of a threatened aircraft.

However, in more general ATC environments, such as in the en-route domain, the relative workload across the five key cognitive tasks is much more evenly distributed. The controller needs to develop a Plan for the traffic within the sector, then Implement and Monitor behavior to the Plan, while all the time Evaluating the validity of the Plan and Maintaining Situation Awareness. It is apparent that the conformance monitoring task is only one of many being undertaken by the en-route controller, and therefore workload limitations can dictate the amount of resources available for any one of them. However, conformance monitoring is still of vital importance to operations in this wider ATC environment. For example, if an aircraft blunders from its clearance (as shown for aircraft ① in Figure 1.11) it may produce conflicts with aircraft in other traffic flows (such as aircraft ②), thereby requiring a re-plan of all the traffic flows and inefficient re-routing of some aircraft. A deviant aircraft could also become a potential threat to the security of airspace, such as the Special Use Airspace (SUA) region in Figure 1.11.



**Figure 1.11: Example En-Route Non-Conformance Scenarios**

## **1.5 Need for Development of Conformance Monitoring Analysis Tools**

New CNS technologies hold the potential for improvements to ATC conformance monitoring. The application of decision support tools for the conformance monitoring task may enable these improvements to be realized, for example through the use of more surveilled states and more sophisticated conformance monitoring algorithms to assist in the task during high workload or high

criticality ATC environments. Existing decision support tools, however, use very simple conformance monitoring algorithms that do not take full advantage of all the new capabilities within the system. This is partly because of a lack of analysis capability to determine what set and accuracy of states would be most useful from a surveillance system and why; what conformance monitoring approaches should be adopted by the decision support systems with these states and what benefits may be seen by their introduction. The primary objectives for the research presented here are to deal with these limitations through:

- Development of a methodology that allows investigation of ATC conformance monitoring issues.
- Implementation of the resulting methodology to investigate fundamental conformance monitoring issues.
- Use of results to identify conformance monitoring approaches in current & future technological and operational ATC environments.

## **1.6 Thesis Overview**

This chapter has served as an introduction to conformance monitoring, its importance in ATC, as well as the need for and objectives of the research presented in this document. Chapter 2 contains a detailed discussion of the conformance monitoring functions of some existing ATC decision support tools in order to establish the current state of the art in this field and to provide a context for the research. Chapter 3 contains a description of the Conformance Monitoring Analysis Framework that has been developed to allow the investigation of conformance monitoring issues and analysis of conformance monitoring approaches. A variety of fundamental techniques that can be employed in the implementation of the elements of the proposed framework are described in Chapter 4. One example implementation for each element is then used for detailed analyses of conformance monitoring issues in realistic ATC environments using operational data in Chapter 5. The findings are expanded upon by using simulation techniques in Chapter 6. Extended applications of the analysis framework for intent inferencing and environmental parameter estimation are discussed in Chapter 7. Chapter 8 contains the key conclusions and contributions of the research, as well as a discussion of potential future research directions.

[This page intentionally left blank]

---

# **CHAPTER 2: Review of Existing ATC Conformance Monitoring Decision Support Tools**

---

## **2.1 Introduction**

This chapter contains a detailed discussion of the conformance monitoring elements of a selection of existing decision support tools that are documented in open literature. The discussion highlights the conformance monitoring approach employed by each to establish the current state of the art in this field. The standard fault detection classifications described in the previous chapter are used as a convenient method for categorizing the conformance monitoring approaches being employed by each tool. Section 2.2 includes those tools that are currently operational or undergoing widespread field trials in ATC, while Section 2.3 includes tools that are undergoing serious development. Summary characteristics of the various systems and the implications for the current research are summarized in the final section.

## **2.2 Review of Operational Tools**

This section contains a detailed review of several tools currently employed in ATC operations. The Precision Runway Monitor (PRM) is discussed first. It employs a simple threshold-based conformance monitoring criterion and the development of this criterion was well documented. The other tools discussed in detail involve elements of the Host Computer System (HCS), User Request Evaluation Tool (URET) and the Canadian Automated Air Traffic System (CAATS). These generally employ similar threshold-based conformance monitoring criteria, but the rationale for the threshold settings is less clear. A brief discussion is also included of several other tools that are operational but for which extensive details were not available.

### **2.2.1 Precision Runway Monitor (PRM)**

The ability to use independent approaches at major airports with parallel runways helps to improve capacity and reduce delay during Instrument Meteorological Conditions (IMC) by removing the spacing requirements between aircraft on the different parallel approach paths. In the past, regulations have

limited the use of independent approaches to airports with parallel runways separated by more than 4300 ft [FAA (2000)]. However, many major airports such as Memphis, Raleigh-Durham, Houston and Detroit have parallel runways separated by less than this 4300 ft minimum. Hence there has been much effort expended over the last decade to determine the requirements that may allow independent parallel approach operations to be conducted to airports with more closely-spaced runways.

One of the systems developed for this application is the Precision Runway Monitor (PRM), illustrated schematically in Figure 2.1. It integrates an advanced high azimuthal accuracy (minimum 1 mrad) / high update rate (maximum 2.4 seconds) radar, a high resolution display called the Final Monitor Aid (FMA) and a computer system for automatic alerting functions. The FMA display explicitly identifies the cleared (ILS) path, a non-conformance region (the “No Transgression Zone” (NTZ)) and the aircraft location from the advanced surveillance system relative to these elements. A dedicated final approach controller monitors this display and initiates a break-out maneuver of the threatened aircraft via voice communication if a deviation into the NTZ is detected visually or an alert is issued by the alerting logic [LaFrey (1989)]. When this system is used, independent closely-spaced parallel approaches are approved by the FAA to runways separated by a minimum of 3400 ft [FAA (2000)].

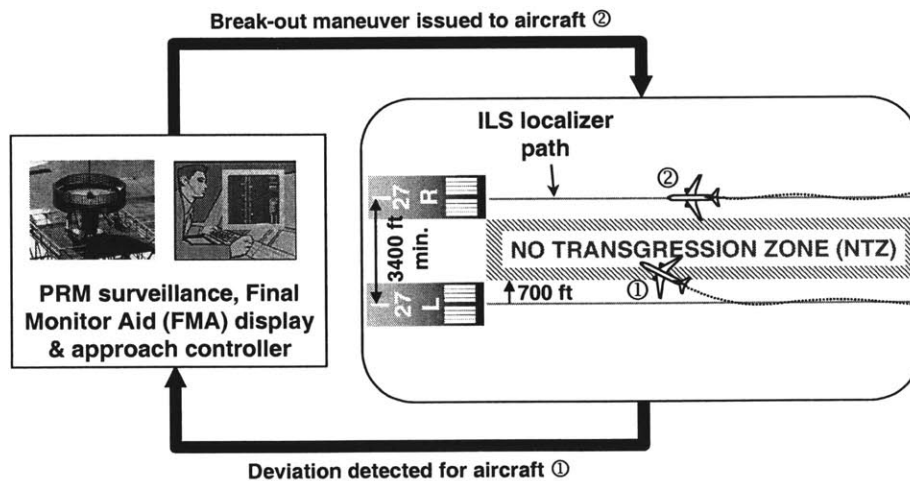


**Figure 2.1: Precision Runway Monitor Schematic**

Using the fault detection classifications described in the previous chapter, the PRM conformance monitoring approach can be classified as a simple signal-based strategy. The signal is the observed cross-track position of the aircraft relative to the ILS localizer path. This is compared to the threshold defined by the applicable boundary of the NTZ, generally 700 ft from the approach path.



The ability to undertake ground-based conformance monitoring to rapidly detect aircraft deviations was a fundamental driver in the design of this system. PRM is also one of the few systems for which there is detailed documentation in the open literature of the analysis undertaken to establish system parameters, specifically threshold settings and minimum surveillance performance requirements. No documentation of equivalent analysis could be found with respect to the design of system parameters in the other systems described in this Chapter. Since this is a significant difference between the systems, abbreviated details of the PRM analysis are described below.

The design of the PRM system involved extensive data collection and analysis by MIT Lincoln Laboratory and the Federal Aviation Administration (FAA) [Shank & Hollister (1994)]. The analysis began with an assessment of the sequence of events involved in a typical deviation detection and resolution. These were categorized as:

1. Deviation (“blunder”) begins.
2. Alerting system (“caution alert”) triggered.
3. Break-out decision by FMA controller.
4. Break-out command communicated to endangered aircraft.
5. Endangered aircraft break-out maneuver initiated.
6. Increasing separation achieved.

This sequence of events was characterized in terms of a set of time parameters involved in each step. These included the time used by the sensor to detect the deviation and generate an alert; the time used by the controller to recognize the alarm and determine the proper response; the time used to communicate the break-out maneuver to the endangered aircraft; the time used by the flight crew to comprehend and initiate the break-out command; the aircraft response time and the time required until separation between the two aircraft started increasing. For each deviation scenario, this set of time parameters could be equated to an equivalent set of distance parameters. Analysis was conducted to understand the values that each of these time-distance parameters could take during realistic blunder scenarios, as described next.

Firstly, combined PRM sensor/alerting system performance to support the application was characterized in terms of a “Caution-Alert Lead Time” (CALT) metric defined by the time between the issuance of a caution alert (triggered when the alerting algorithm predicts the aircraft to enter the NTZ within 10 seconds) and a second warning alert when the penetration of the NTZ is detected to have

occurred. Analysis was subsequently conducted with measured and simulated aircraft tracks to determine average CALT performance for various sensor accuracies (1, 2 & 3 mrad), update rates (0.5, 1.0, 2.4 & 4.8 seconds) and runway separations (3000, 3400 & 4300 ft) for a “standard” 30° blunder scenario.

Secondly, analysis of appropriate NTZ dimensions required knowledge of the nominal distribution of aircraft positions around the final approach course, i.e. the Flight Technical Error. This parameter affects the CALT (since it depends, in part, on where the aircraft is located relative to the NTZ boundary at the start of the deviation) and the false alarm rate of the alerting system (if the NTZ is too large, entry to the region could occur from natural aircraft deviations along the approach path rather than because of a potentially hazardous blunder). Therefore, a large data collection exercise was undertaken where over 4000 ILS approaches to Memphis International Airport (MEM) were recorded and center-line deviations characterized at 15, 10, 5 and 2 nm from touchdown [Owen (1993)] to characterize the “nominal” deviations during this procedure. This was then used to determine the probability of an aircraft entering the NTZ of various dimensions due to flight technical error.

Thirdly, controller response and communication delay studies were conducted. Controller response times as functions of sensor update rate, runway separation, blunder angle and experience level were measured through studies at the Memphis PRM site. Radio communication analyses were used to determine distribution curves for the length of time required to transmit a break-out command and the length of time the tower control frequency was likely to be blocked by other communications.

Fourthly, studies to determine pilot response times to break-out maneuver commands were conducted using commercial flight simulators and airline pilots flying simulated approaches to MEM under IMC with decision heights of 100 and 200 ft.

These analyses were used in the development of the PRM Blunder Risk Model which employed a Monte Carlo simulation to determine the distribution of the minimum separation between aircraft for a given sensor, NTZ dimension and runway separation. For each simulation run, a value was taken from each distribution discussed above and summed to determine the total response time. This was then used with distributions of the likely relative locations of the two aircraft on parallel final approaches and standard turn rate aircraft dynamics (heading acceleration of 1°/sec<sup>2</sup> until 3°/sec was reached) to determine the minimum separation achieved for that trial. This process was repeated a large number of times to construct the minimum separation distribution for that configuration. These results were then used to determine minimum sensor requirements, runway separation and NTZ dimensions which set the

limits on PRM operations in order to remain below a certain collision risk target, as shown in Figure 2.2. This target was chosen to be no worse than the collision risk during operational non-PRM ILS approaches, calculated to be  $4.0 \times 10^{-8}$  per approach pair.

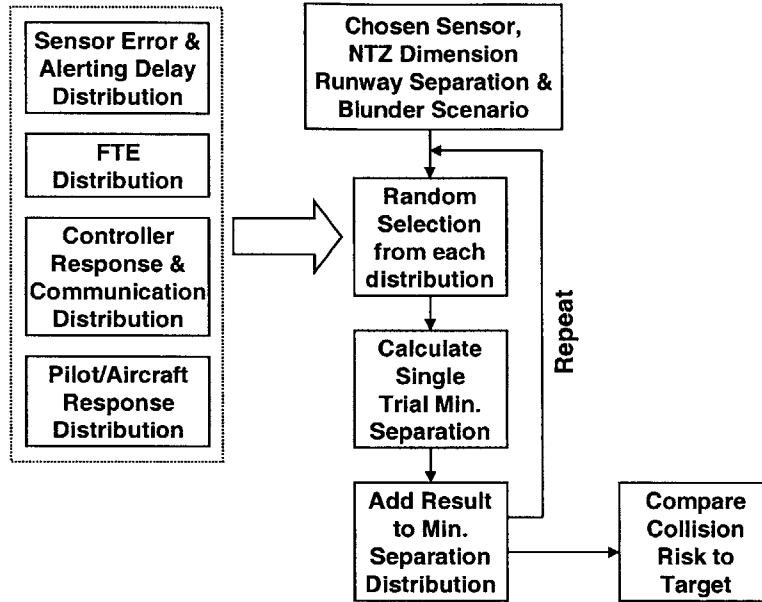


Figure 2.2: PRM Blunder Risk Model [adapted from Shank & Hollister (1994)]

### 2.2.2 Host Computer System (HCS)

The FAA Host Computer System (HCS) processes the flight information and radar data for both en-route and terminal area air traffic control in the US (i.e. the Air Route Traffic Control Centers (ARTCCs) and Terminal Radar Approach Controls (TRACONs) respectively) as illustrated in Figure 2.3. Note that some additional processing is undertaken in the TRACON environment by the Automated Radar Terminal System (ARTS), some of which falls into the category of conformance monitoring, for example determining when to trigger the Minimum Safe Altitude Warning (MSAW) if an aircraft descends too fast near the ground. However, details of the ARTS processing was not readily available and so will not be considered further here.

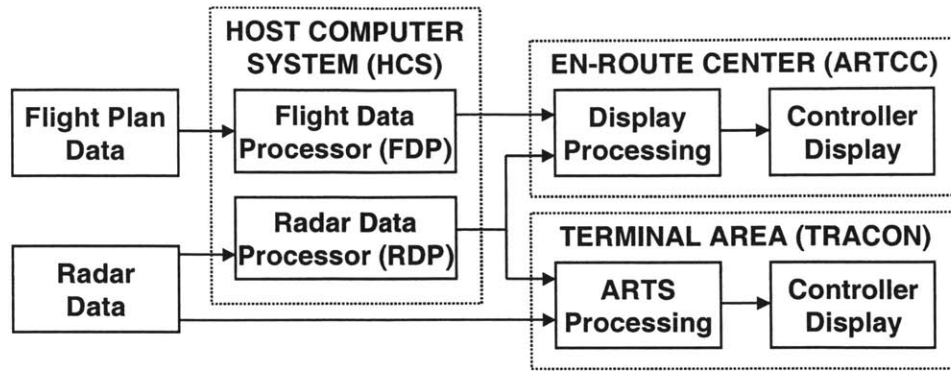


Figure 2.3: HCS Processing Elements [adapted from NRC(1998)]

The Flight Data Processor (FDP) component in the HCS takes flight plan inputs prior to departure and amendments from the controllers while the aircraft are en-route. From this it calculates a 4D route and time of flight for the flight plan identifying fixes along the route and estimated arrival times at those fixes. This information is transmitted at the appropriate time to the controlling en-route sectors and via the Automated Radar Terminal System (ARTS) to TRACONs and towers to be printed out on Flight Progress Strips (FPSs) for use by the controllers in these facilities. A sample en-route flight progress strip showing the FDP-derived route of flight and estimated time over a given fix on the route is presented in Figure 2.4.

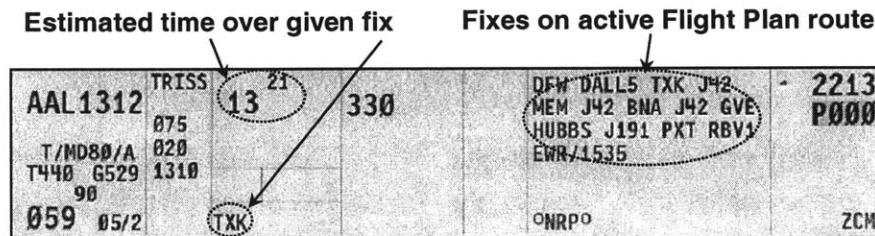


Figure 2.4: Sample En-Route Center Flight Progress Strip

The Radar Data Processor (RDP) element of the HCS receives data from the radars within the system, transforms it into a format suitable for display and uses filtering techniques to infer the heading and speed of the aircraft being tracked. In order to improve the accuracy of these filtering processes, the RDP attempts to “associate” a given radar return with previous returns and flight plan routes output from the FDP [Lincoln (1998)]. This is achieved through “association checking” algorithms in the lateral, longitudinal and vertical domains relative to the 4D prediction of the aircraft locations from the FDP

[FAA (1992), FAA (1993)]. Thus, association checking can be considered a simple form of conformance monitoring. The processes employed in these HCS algorithms are described below.

A rectangular “association area” is defined for lateral and longitudinal checking that is centered on the extrapolated flight plan position and aligned with the flight plan velocity vector as shown in Figure 2.5. The dimensions of the association area are defined as the thresholds on allowable lateral and longitudinal deviations from the expected position. The threshold values are functions of the assigned altitude and whether the current position is in a flight plan leg region or a transition region (defined as being within 15 nm of a lateral transition point greater than 30°). The pre-determined threshold values used by the HCS for lateral association checking are presented in Table 2.1. Note that there is no longitudinal adherence checking in the turn region.

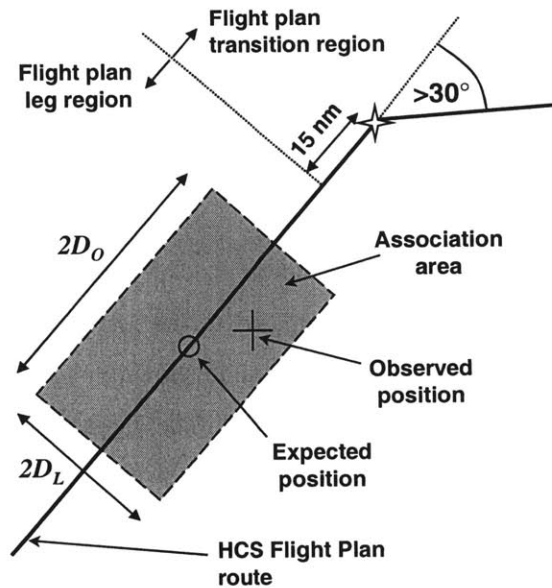


Figure 2.5: HCS Lateral Association Checking [adapted from FAA (1992)]

Table 2.1: HCS Lateral Association Checking Thresholds [adapted from FAA (1995)]

Assigned Altitude	Flight Plan Leg Region		Flight Plan Transition Region	
	Lateral Threshold ( $D_L$ )	Longitudinal Threshold ( $D_O$ )	Lateral Threshold ( $D_L$ )	Longitudinal Threshold ( $D_O$ )
≤ 10,000 ft	4 nm	4 nm	8 nm	N/A
10,001 – 18,000 ft	6 nm	6 nm	10 nm	N/A
18,001 – 33,000 ft	8 nm	8 nm	12 nm	N/A
> 33,000 ft	10 nm	10 nm	14 nm	N/A

The observed positions of the aircraft from the radar input are separated into lateral and longitudinal deviations and compared to the appropriate threshold value. When the observed deviations are within the prescribed lateral and longitudinal thresholds, the aircraft are considered to be “flat-tracked” and the HCS utilizes the Flight Plan to improve its estimates of heading and future position. These estimates are then used to update the predicted flight progress for use in future longitudinal conformance monitoring algorithms. However, if the observed lateral or longitudinal deviations exceed the threshold, then the aircraft is flagged as being out of adherence in that dimension, the aircraft switches to a “free-tracked” status and the graphical indication for that flight on the radar screen changes from a diamond (◇) in “flat-tracked” mode to a triangle (△) in “free-tracked” mode. This subtle change in the flight indicator on the radar screen is the primary alert to the controller of a non-conforming aircraft in the lateral or longitudinal domain. The controller must then manually enter flight progress information for “free-tracked” aircraft or else the time dimension of the 4D predicted flight plan diverges from the actual flight behavior. If the longitudinal deviation becomes excessive, either the flight plan will “time-out” requiring the entire flight plan to be re-entered manually, or the flight could arrive at a facility boundary before its flight plan has been transmitted to the relevant sector by the FDP [Lincoln (1998)].

A similar approach is taken to vertical association checking when the aircraft is at a level altitude: the reported Mode C transponder altitude is compared to the assigned altitude, and non-adherence is declared when the deviation exceeds the appropriate value shown in Table 2.2. Vertical deviations that exceed the prescribed limits are alerted by flashing the altitude element of the datablock associated with the flight on the controller’s display. Vertical *transitions*, however, are handled differently than in the lateral domain. No association checking is attempted during a vertical maneuver, presumably due to the larger uncertainty in the vertical trajectory to be flown. All aircraft are assumed to be in adherence during a vertical transition [Paglione *et al.* (2000)], although it is unclear at what point the switch back to level altitude association checking is resumed after a level-off should have occurred.

**Table 2.2: HCS Vertical Association Checking Thresholds [Paglione *et al.* (2000)]**

Assigned Altitude	Vertical Non-Transition (Level Altitude)
< FL290	± 200 ft
> FL290	± 500 ft

This description of the conformance monitoring processes in the HCS highlights several important issues. Firstly, the conformance monitoring in the HCS can be classified as a signal-based fault detection approach where the observed positional deviation from the expected position on the flight plan route is the signal that is compared to a pre-determined threshold appropriate for the axis and flight regime being considered. These thresholds are generally large because of the need for simplicity across many ATC environments, the limited surveillance capability in the en-route domain and the wide range of tracking capabilities of aircraft with different navigational equipages using the airspace. This is illustrated by the fact that at typical cruise altitudes of commercial aircraft, lateral deviations of up to 8 nm either side of the expected position in the lateral and longitudinal dimensions are considered conforming by the HCS algorithms. This is twice the 4 nm width of a typical airway.

Secondly, the notion of requiring wider conformance bounds at flight plan transition points is important and one that is seen carried through many of the other systems to be discussed.

Thirdly, the different threshold values used in the horizontal and vertical axes demonstrates the fact that tracking performance and expectation of the trajectory to be flown is different in the two domains. For example, deviations in excess of 500 ft during level flight are sufficient to trigger a non-conformance alert, as compared to 8 nm (i.e. over 48,000 ft) in the horizontal domain. This is due to the fact that commercial aircraft have much better altitude tracking performance to a specified barometric altitude target than they do to a lateral path target and can thus be held to a much stricter standard. In addition, the altitude is much more observable than the lateral position state. This has the associated impact on operations that lower vertical separation minima of 1000 or 2000 ft are allowable in the vertical axis compared to 3 or 5 nm in the horizontal. Vertical transitions are a very different story, however. Here, the vertical trajectory to be flown is so uncertain that no conformance monitoring is even attempted in the HCS under these conditions.

### **2.2.3 User Request Evaluation Tool (URET)**

The User Request Evaluation Tool (URET) is a decision support tool that uses HCS data at its input but provides a Conflict Detection and Resolution (CD&R) capability for en-route air traffic controllers. It has been implemented in several ATC en-route centers beginning in 1996 as part of Free Flight Phase 1 studies [Love *et al.* (2002)]. Flight plan data is used to construct a 4D trajectory of an aircraft's route of flight and alerts are generated for any conflicts that exist between other aircraft. A conformance monitoring function is therefore required to ensure the validity of the conflict detection algorithms based on the assumed 4D trajectories.

Much of the URET functionality is based on an earlier prototype called the Automated En-Route Air traffic control (AERA) system, which was developed in the early 1990s [Wetherby *et al.* (1993)]. The conformance monitoring function in AERA was based on the definition of a region of conformance which used bounds that reflected the aircraft's ability to fly the expected trajectory. The shape and size of these bounds were considered to be functions of the ground and aircraft navigational equipment, wind prediction accuracies and characteristics of the route itself, as illustrated for the lateral domain in Figure 2.6. For example, the conformance bounds were designed to be wider at points farther from a navigational aid (NAVAID) to account for the loss of accuracy with range inherent in a system with an angular guidance signal, such as a VOR. Allowance for a range of transition behaviors due to different aircraft dynamics and autoflight settings was also included. However, specifics of how these issues quantitatively affected the bounds did not appear to have been developed.

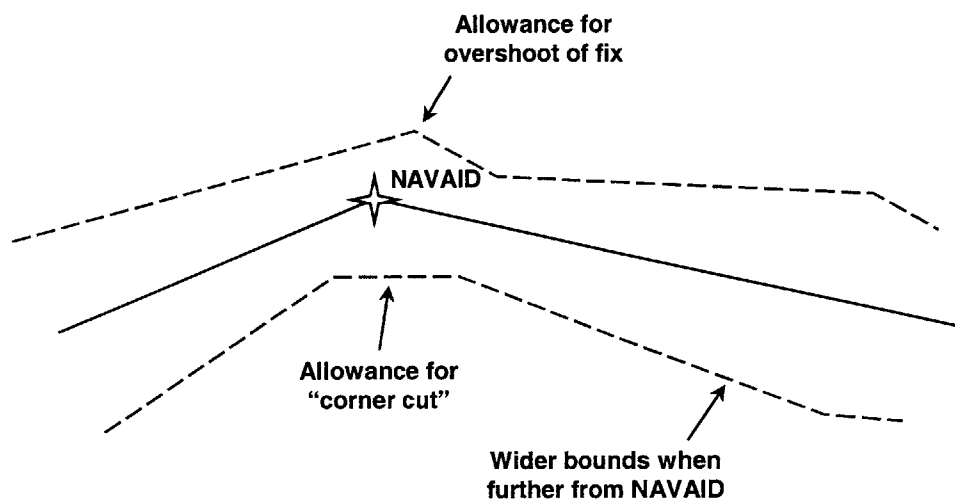


**Figure 2.6: AERA Lateral Conformance Bound Concept [Wetherby *et al.* (1993)]**

Similar bounds existed in the vertical and longitudinal domains also, such that their union defined a 4D conformance bound. The conformance monitoring function detected when an aircraft was outside of the appropriate conformance bound, whether because of pilotage, instrument failure, unexpected winds or a control action not yet entered into the automation. An appropriate alert was then made to the controller so that “reconformance” could be initiated to replan a new conflict-free trajectory for that aircraft. Conformance monitoring in URET refined this concept for the operational application by defining conformance bounds as functions of nominal or transitioning flight (as illustrated in Figure 2.7) and



navigational equipage (specifically whether the aircraft was equipped for area navigation (RNAV)<sup>†</sup> or not).

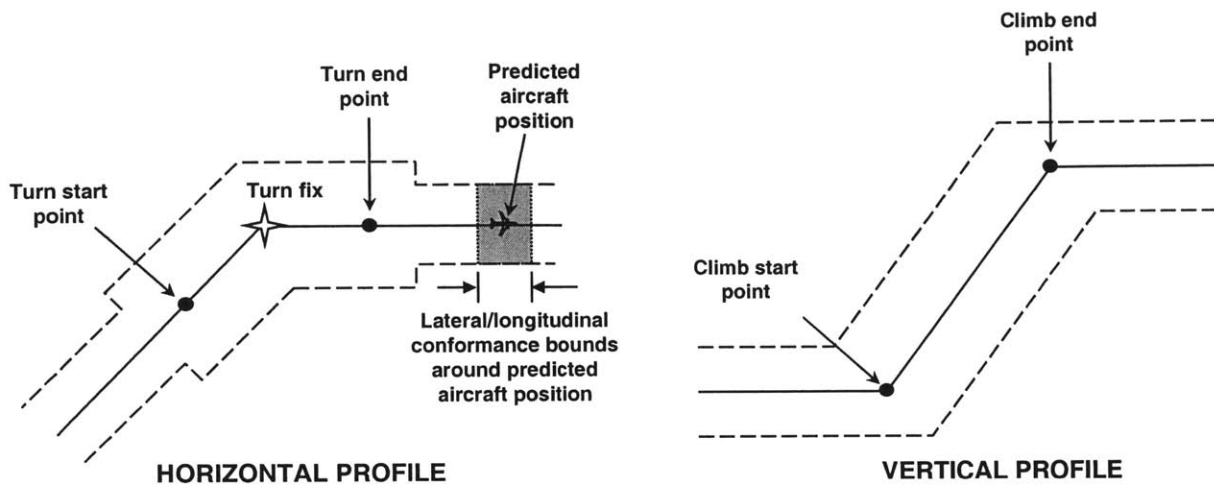


**Figure 2.7: URET Horizontal and Vertical Conformance Bounds [Celio *et al.* (2000)]**

Nominal conformance bound values for the various conditions are presented in Table 2.3. Note that the URET conformance bound values are generally much smaller than the HCS association checking thresholds despite the fact that URET utilizes HCS trajectory and surveillance inputs. This is especially noticeable relative to the lateral domains. Note also that vertical transition bounds do exist in URET, although the basis for the threshold values employed is unclear.

**Table 2.3: URET Nominal Conformance Bound Values [adapted from Celio *et al.* (2000)]**

Domain	RNAV-Equipped Aircraft		Non-RNAV-Equipped Aircraft	
	Non-Transition Region	Transition Region	Non-Transition Region	Transition Region
Lateral*	± 2.5 nm	± 3.5 nm	± 3.5 nm	± 4.5 nm
Longitudinal	± 1.5 nm	± 2.5 nm	± 2.5 nm	± 3.5 nm
Vertical	± 300 ft	± 1300 ft	± 300 ft	± 1300 ft

<sup>†</sup> An area navigation (RNAV) system is one capable of providing guidance along any desired flight path within the coverage of station-referenced navigation signals or within the limits of a self contained system capability [RTCA (2000)]. The aircraft is no longer restricted to flying along a track directly to or from a specific radio navigation aid, allowing more flexible routings. A Flight Management System (FMS) is one example of RNAV equipment.

\* By convention, positive lateral deviations correspond to those starboard of the route, while negative deviations correspond to those to port.

When the track and altitude of an aircraft are observed to be within the conformance bounds associated with the flight plan trajectory, URET determines that the aircraft is conforming, otherwise it is determined to be out of conformance. Again, this implies a signal-based fault detection approach utilizing position deviations from the flight plan route. The effectiveness with which URET can undertake its main task of CD&R relies in part on its ability to infer the actual trajectory of the aircraft once non-conformance to the HCS flight plan has been triggered. To achieve this, URET uses track position and velocity data plus heuristics of nominal ATC performance: a process referred to as “reconformance”. As a result, the URET system can also be considered to incorporate knowledge-based fault detection elements after non-conformance has been detected. The heuristics used in this process depend on the type of non-conformance detected and how the observed behavior could logically return to the nominal trajectory. Examples for lateral non-conformance scenarios are presented in Table 2.4. Note that the use of heuristics to account for some of the uncertainty present in the HCS flight plan data has also been utilized in the development of the trajectory synthesis elements of the Center-TRACON Automation System (CTAS) tools [Slattery & Zhao (1997)].

The two notable components of this discussion in the context of the present research are that the URET boundary definitions are one of the first to explicitly account for aircraft equipage (RNAV in this instance), while the “reconformance” element in URET highlights the need for inferred trajectory development after a non-conformance has been detected in order to undertake effective CD&R tasks. This latter element will be re-visited later in the context of extended applications of the research approach for “intent inferencing”.

**Table 2.4: URET Lateral Reconformance Scenarios [adapted from Celio et al. (2000)]**

Reconformance Scenario	Description	Schematic
Cut corner	If the track position history indicates the aircraft diverging from the route near a turn fix, then the aircraft is assumed to be cutting a corner. The new trajectory is modeled to rejoin the route either at an intersection point downstream or at a nearby fix.	
Direct to downstream point	If the track position indicates that the aircraft is diverging from the route and its extrapolated position is within a parameter distance from a downstream fix, then the new trajectory is modeled direct to that fix.	
Converging towards point	If the track position indicates that the aircraft is converging towards the route then the trajectory is modeled to converge to the route at an intersection point or, if the intersection point is near a fix, to that fix.	
Diverging from route, stable track history	If the track position indicates that the aircraft is diverging from the route but with a stable track history, an intermediate turn point is modeled from which the aircraft will be assumed to make a turn back to the flight plan route at a downstream location.	
Parallel offset	If the track history indicates a parallel offset, a return to route is modeled using the default "return to route at downstream position" processing discussed next.	
Returning to route at downstream position (default if none of the previous cases apply)	If none of the above cases apply, the default trajectory that is modeled is a return to the route at a downstream position. The initial route segment modeled is a direct turn to the flight plan route from the aircraft's current position.	

## 2.2.4 Canadian Automated Air Traffic System (CAATS)

The Canadian Automated Air Traffic System (CAATS) is a set of advanced ATM automation tools that have been deployed in Canada since the fall of 2002 [Raytheon (2000), Troutman & Pelletier (2002)]. One of these tools is an advanced flight data processor, which handles conformance monitoring functions. At its foundation is a detailed clearance that is maintained for each aircraft in the system. A detailed 4D trajectory is calculated based on the clearance and a region of “Airspace To Protect” (ATP) is defined around it. The size of the ATP is based on standards published by NavCanada for application by controllers and which have been adapted for the automated function. The ATP dimensions are functions of many factors such as the type of route segment being flown, distance from NAVAIDs, radar status, aircraft equipage, turn angles, etc. but the minimum size of the ATP is 4 nm from the trajectory laterally and 500 ft vertically. Although no specific information is available in this regard, it appears that the ATP dimensions have been set more by the desire to avoid separation minima violations than the desire to detect non-conformances in a timely fashion, since they are relatively conservative. This is consistent with the way conformance monitoring tools are used in other operational systems discussed in this Chapter. The conformance monitoring function checks the progress of the flight along the cleared trajectory and flags non-conformance whenever the observed position or altitude is outside of the applicable ATP at that point. Hence CAATS conformance monitoring is another approach that can be classified as a signal-based fault detection technique. Initial implementation highlights lateral non-conformance by the use of brackets around the aircraft icon on the controller’s display, while altitude deviations are indicated by a change of color of the altitude element in the datablock (see Figure 2.8). Longitudinal deviations are presented in an “announcements window” on the controller’s display [Pelletier (2002)].



**Figure 2.8: CAATS Display Symbology for Conforming (left) & Non-Conforming (right) Aircraft**  
[adapted from Pelletier (2002)]

The conformance monitoring in the CAATS system is notable for its use of a sophisticated trajectory description that is quite distinct from any other flight data processor. For the most part, this trajectory

exactly matches the official clearance negotiated between ATC and the flight crews of controlled aircraft. The clearance language in CAATS uses elements that correspond to standard ATC phraseology and CPDLC message elements and can express all aspects of route, altitude and speed along with all manner of complex restrictions with respect to altitude, speed, and time. It also includes many specific instructions including procedures for hold, offset, departure, arrival, approach, reporting, missed approach and special airspace usage [Pelletier (2002)]. Updates to the clearance can be entered quickly by the controller via a menu-driven interface, making it more likely that the clearance in the system accurately reflects the clearance communicated to the aircraft relative to more cumbersome data-entry techniques used in many other systems. The importance of this issue will be revisited later.

## **2.2.5 Other Operational Systems**

Many other modern automation systems have been deployed that incorporate conformance monitoring decision support functions, but for which exact details of their conformance monitoring techniques are not readily available. Some of the important systems are discussed briefly below.

### **2.2.5.1 The Australian Advanced Air Traffic System (TAAATS)**

Deployed in 2001, TAAATS now handles air traffic in approximately 11% of the Earth's airspace around Australia. This comprises diverse ATC operating environments, including oceanic, domestic en-route and terminal area airspace that are now integrated in TAAATS [Scott (2001)]. An automated flight data processing tool maintains a model of the assigned route for each aircraft, based on the flight plan, ADS intent messages (such as the current active waypoint) and pilot voice updates. Estimated time over waypoints are based on flight crew communication, ADS messages or calculations using flight plan true airspeed and aircraft performance data applied in a three-dimensional wind model. The system presents warning and alerts to the controller through the human-machine interface when required. Conformance monitoring alerts depend on the knowledge of the assigned aircraft trajectory and the available surveillance in the environment being considered, but include [Airservices (2002)]:

- “Lateral route conformance” warning when position deviations from the assigned route exceed some threshold value based on ADS or radar position inputs which are updated every 30 seconds.
- “Cleared level adherence” warning when the ADS or transponder altitude report deviate excessively from the assigned altitude.
- Unacceptable differences exist between pilot estimate and system estimate times (e.g. in proceduralized oceanic environments).

- A “Danger Area Infringement Warning” when restricted airspace has been intruded based on radar or ADS position reports.

All of these warning types are based on positional deviations exceeding threshold values, although exact details of the thresholds used for the various warning types under different operating conditions were not readily available.

### **2.2.5.2 The Gander Automated Air Traffic System (GAATS)**

GAATS was deployed in early 2002 for oceanic controllers in Gander who handle up to 1000 flights a day in the world’s busiest oceanic airspace over the North Atlantic [Koslow & Fekkes (2002)]. Since most oceanic airspace is beyond the range of land-based radar, traditional oceanic conformance monitoring is generally restricted to rudimentary checking for overdue position reports that are typically made every 10° of latitude or longitude depending on the direction of flight. Such position reports cannot be verified and may be updated only once or twice an hour. The GAATS system provides a radar-like display to the oceanic controller of aircraft identification, position, tracks and intent data based on more frequent ADS reports from equipped aircraft using the FANS 1/A technology [Bornemann & Kelley (2000), Galotti (1997)]. This enhanced knowledge of intent coupled with more accurate and timely position information for the aircraft allows much more sophisticated conformance monitoring to be conducted over the oceans than was previously possible. GAATS automatically compares the controller’s inputs and the position reports against the current flight profiles. Alerts are generated for the responsible sector controller when discrepancies exceed a threshold value or a position report is overdue by a given amount [NavCanada (2001)]. GAATS and CAATS are being integrated to allow for more efficient transition between domestic and oceanic ATC operations [Raytheon (2000)], while discussions are also underway to adapt the GAATS core functionality for the Shanwick Automated Air Traffic System (SAATS) to be used in the equivalent sector on the east side of the North Atlantic [Koslow & Fekkes (2002)].

### **2.2.5.3 Miscellaneous Other ATC Systems**

Many other ATC systems in use around the world contain functionality that could be defined as conformance monitoring but for which detailed information is either unavailable or their conformance monitoring elements are very similar to approaches described in the systems above. These include many other Flight Data Processing Systems (FDPS) such as the Icelandic FDPS for oceanic traffic and the European FDPSs used for en-route traffic in Europe, as well as many conflict probe tools such as the US Conflict Alert (CA) system, the European Short Term Conflict Alert (STCA) and the Medium Term

Conflict Detection (MTCD) tool. The flight data processing systems generally use conformance monitoring systems to associate flights to flight plans in a fashion similar to the US Host Computer System. The conflict probe systems generally use conformance monitoring to determine whether to use the flight plan (conforming) or a dead-reckoning (non-conforming) trajectory in the conflict detection process. This process will be observed in some of the developmental tools described in the next section.

### 2.3 Review of Developmental Tools

This section contains a review of three tools currently under development for use in ATC applications. These are the Flight Progress Monitor (FPM) being developed by Eurocontrol; NarSim being developed by NLR and the Tactical Separation Assisted Flight Environment (TSAFE) tool being developed at NASA Ames. These tools represent the current state-of-the-art in conformance monitoring support tools being developed for application in future ATC automation.

#### 2.3.1 Flight Progress Monitor (FPM)

The Flight Progress Monitor (FPM) is a research tool for ground-based conformance monitoring being developed as part of the Programme for Harmonised Air Traffic Management Research in Eurocontrol (PHARE) [Jansen *et al.* (1999)]. All of the PHARE tools are based on a 4D ATM philosophy, where an entire “tube” trajectory [Wilson (1996)] is verified to be conflict free during the planning phase, as illustrated in Figure 2.9. Once this trajectory has been accepted by an aircraft, it is assumed to agree to stay within its “contract tube” to ensure a conflict-free evolution of the flight.

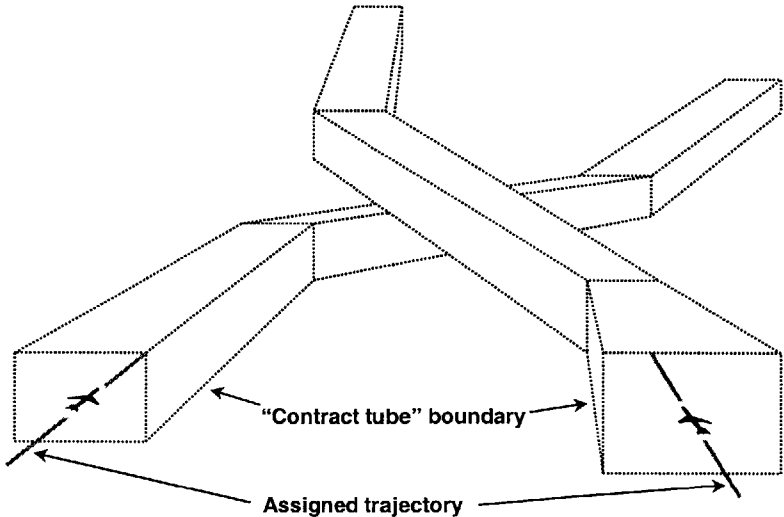
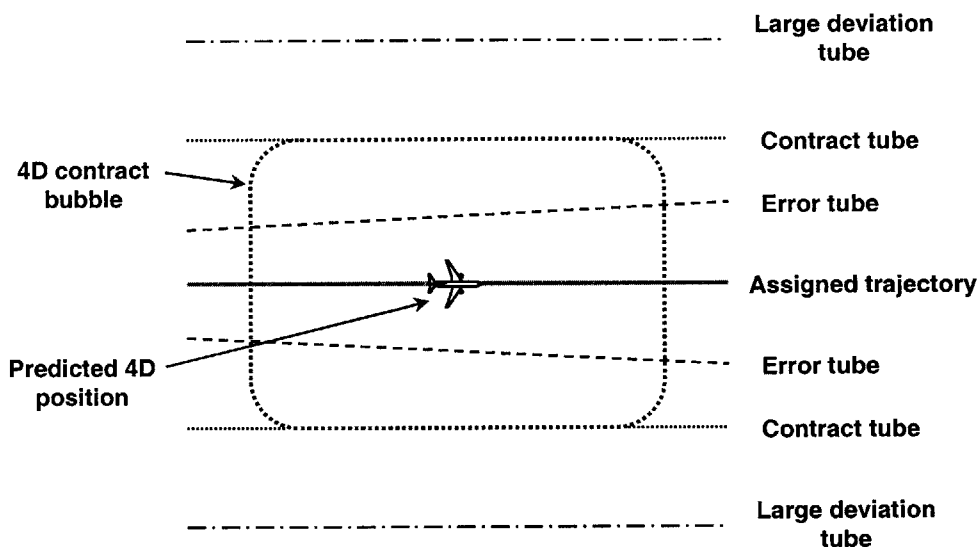


Figure 2.9: PHARE 4D Contract Concept [adapted from NRC (1998)]

Note that the “tube” shown in Figure 2.9 is the 3-dimensional component of the contract swept out over time. The actual airspace contracted with the aircraft is considered to be a 4D “bubble” defining lateral, vertical *and* temporal (longitudinal) contract components. This is illustrated in Figure 2.10 for the horizontal dimension, along with the additional tube types that are defined inside and outside the contract tube for use by the FPM tool. Each type are discussed in more detail in the next section.



**Figure 2.10: PHARE Tube Definitions [Wilson (1996)]**

Inside the contract tube resides an “error tube” which is used to account for the likely inaccuracies in the variables input into the forecasting process and the errors of the aircraft trying to follow the trajectory (i.e. the Flight Technical Error). Note that the errors may not be constant for a given trajectory (e.g. if the navigation system performance varies as a function of distance from a navigational aid). The contract tube is generated to be larger than or equal to the error tube in all dimensions so the aircraft should always have the navigational tracking capability to remain within it. The relative size of the tubes depend on the application: for example, at take-off and landing the contract tube and error tube may be coincident, while the contract tube is likely to be larger than the error tube in the en-route environment. Although the preliminary PHARE research studies used simple pre-determined contract tube dimensions of  $\pm 1$  nm laterally,  $\pm 200$  ft vertically and  $\pm 10$  seconds longitudinally [Wilson (1996)], it is suggested that in an operational system the contract tube sizing could be linked to the known navigational capabilities of the aircraft or the RNP specification of the airspace.



Outside of the contract tube resides a “large deviation tube” which defines the boundary of recoverable navigation errors for the aircraft, i.e. a deviation from the 4D trajectory which is small enough to allow the aircraft to recover within the contract tube by the current sector boundary and which causes no hazard to other aircraft. This tube is used by the FPM to issue a large deviation alert when the aircraft flies outside of its boundaries, and the trajectory must be renegotiated. Again, the size differential between the large deviation tube and the contract tube is a function of the operational environment. They may be coincident at the runway, while the large deviation tube is likely to increase in size relative to the contract tube in the en-route domain, or decrease in relative size as traffic density increases such that only small deviations can be tolerated if conflict-free trajectories are to be maintained.

The FPM tool compares the tracked 4D aircraft positions with the predicted 4D position from the contract bubble and calculates the deviation and deviation trends (i.e. increasing, steady or decreasing) in the lateral, vertical and longitudinal directions [Jansen *et al.* (1998)]. The sizes of the deviations are then classified into three types [Jansen *et al.* (1999)]:

- “Insignificant”, meaning that the aircraft has almost no deviation (i.e. inside the “error tube”).
- “Medium”, meaning that the aircraft is deviating (i.e. outside the “contract tube”) but is still able to return to its planned trajectory. Careful monitoring is required.
- “Large”, meaning the aircraft has deviated outside the “large deviation tube” and is no longer able to return to the contracted 4D trajectory. A new contract trajectory needs to be negotiated and separation from other traffic is a high priority.

This conformance monitoring process can be classified as three signal-based fault detection schemes operating simultaneously. The signal is the same in each case (the deviation of the observed 4D position relative to the predicted 4D position) but this is compared to three different thresholds. Graphical display of the relevant aircraft deviation status is given to the controller via a display for subsequent planning, although no information on the display element of the tool was available.

There are several interesting elements of the FPM architecture from a conformance monitoring perspective. Firstly, the use of sets of nested tubes defining various thresholds and the use of a contract scenario are unique to this tool. Again the tube dimensions are considered to vary as functions of the scenario of interest (such as aircraft equipage), although interestingly there is no explicit suggestion of different thresholds being required during transitioning flight regimes. However, the FPM documentation [Jansen *et al.* (1999)] indicates that the biggest research challenge is in the determination of the

dimensions of the various tube types under various environments, for example subject to differing traffic densities and meteorological conditions.

### 2.3.2 NarSim

NarSim is an ATC research simulator being developed by the National Aerospace Laboratory (NLR) in the Netherlands. Its main goal is to support ATM research through the development, building and evaluation of new operational procedures, decision support tools and human machines interfaces [NLR (2002)]. It has a component that supports the controller's conformance monitoring tasks by monitoring flight progress and detecting possible deviations from the planned route. A schematic of the scenarios considered in the development of the system are shown in Figure 2.11.

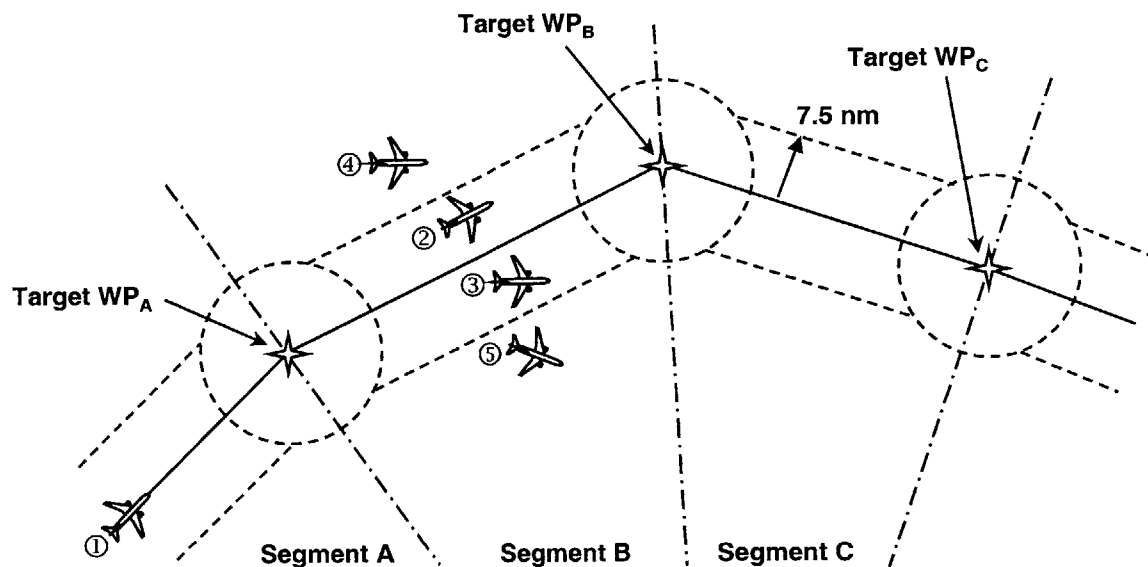


**Figure 2.11: NarSim Conformance Monitoring Scenarios [adapted from NLR (2002)]**

The nominal flight plan route is parsed into segments whose boundaries are defined by route bisectors at each waypoint, as shown in the figure. A waypoint is considered passed when it has crossed the associated segment boundary, and the active waypoint target becomes that existing at the next segment boundary.

Regions of allowable position deviations are defined around the nominal route comprising the union of a band of certain width (typically 7.5 nm) along the flight plan segment and circular regions around each waypoint. No information was available regarding why a circular shape was chosen at the transitions: it is simply implied that generic larger thresholds are required at these points. Various aircraft

behavior scenarios are illustrated in Figure 2.11. Aircraft ① is behaving in a conforming fashion, being both inside the allowable position conformance region and having a heading that is consistent with the heading towards the current target waypoint. Aircraft ② is also considered conforming so no alert would be generated, since it has a proper heading and has a position that remains inside the designated conformance region (although with a non-zero cross-track error). Aircraft ③, on the other hand, has the same cross-track error as aircraft ② but is headed away from the appropriate target waypoint—an alert is generated in this instance. Both aircraft ④ and ⑤ have position deviations outside of the allowable region and so alerts are generated in both instances, despite the fact that aircraft ④ is behaving in a manner consistent with a return to the proper route, while aircraft ⑤ continues to diverge. Although the heading state is not used in the conformance status determination, it is used to determine the appropriate flight plan update algorithm. In the instances where an alert is generated, the system checks to see whether the aircraft is headed towards the appropriate target waypoint. If the aircraft does appear to be headed towards the correct waypoint, then the nominal flight plan route remains unchanged. However, if the heading is not appropriate for the target waypoint, a flight plan update in the form of a direct-to command is suggested to the controller. It is then up to the controller to accept the suggested flight plan amendment or develop an alternative.

Hence the conformance monitoring concept in NarSim is novel in that it utilizes both cross-track position and heading to determine whether to alert for non-conformance and to assist in the determination of what future trajectory to use for a non-conforming aircraft. In terms of fault detection classification, elements of knowledge-based and/or model-based approaches are implied to determine expected heading states before determining conformance using a standard signal-based approach. However, no detail was found in the open literature regarding exactly how the heading expectations or signal-based threshold values are derived. In addition, the suggested allowable cross-track position deviations appear relatively large at 7.5 nm, implying that gross deviations could exist before a non-conformance alert would be generated. This may be a consequence of using a preliminary value that is acceptable for all aircraft types and operating environments before refining in the future.

### **2.3.3 Tactical Separation Assisted Flight Environment (TSAFE)**

The Tactical Separation Assisted Flight Environment (TSAFE) tool is part of the Automated Airspace concept currently being developed at NASA Ames [Erzberger & Paielli (2002)]. The primary ground-based component is the Automated Airspace Computer System (AACS) that will be designed to automatically generate efficient and conflict-free traffic trajectories over a 20-30 minute lookahead time. These trajectories are then communicated to equipped aircraft within the sector via datalink technologies

such as Mode S, ADS-B or VDL3. Several current CTAS tools, including the Direct-To/Trial Planner [Erzberger *et al.* (2001)], the En-route Descent Advisor (EDA) [Green *et al.* [1998]] and the Final Approach Spacing Tool (FAST) [Robinson & Isaacson (2000)] could be further developed and integrated for the AACS application. However, because of the high complexity of the tasks being automated in the AACS, a simpler “safety net” application (TSAFE) is also being developed with the sole objectives of identifying and resolving loss-of-separation events over a much shorter timeframe of approximately 3 minutes [Dennis (2003)]. A schematic representation of the TSAFE architecture is presented in Figure 2.12.

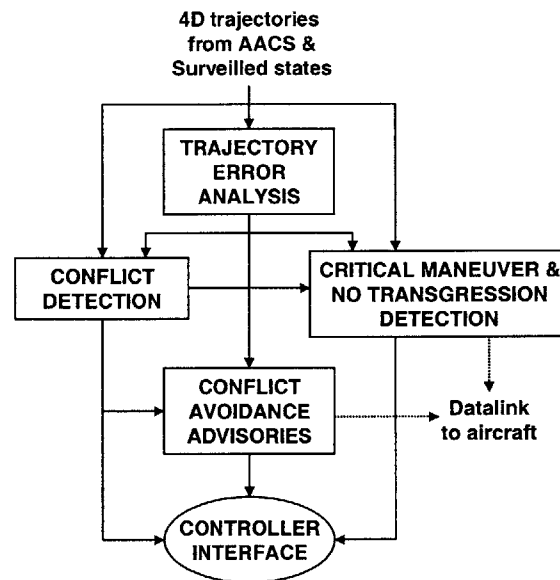


**Figure 2.12: TSAFE Architecture [adapted from Erzberger & Paielli (2002)]**

The 4D AACS trajectories and surveillance inputs are received by three modules: the trajectory error analysis module; the conflict detection module and the critical maneuver & no transgression zone detection module. These modules interface between themselves and also with the conflict avoidance module. The main TSAFE elements related to the conformance monitoring functionality are discussed in the next sections.

### 2.3.3.1 Trajectory Error Analysis

The role of the trajectory error analysis module is to compare the current position, heading, altitude and speed states of every aircraft to their assigned values in the planned 4D trajectory in order to determine whether they are within prescribed error tolerances. This can be considered a conformance monitoring function which can be described by a signal-based fault detection approach. Depending on

the outcome of the trajectory error analysis and the ATC scenario, the conflicts are probed along one of three trajectories: the AACS 4D trajectory; a dead-reckoning trajectory (i.e. at current heading & speed) or a “recovery trajectory” designed to return the aircraft to its proper path. These could involve processes described by both knowledge-based or model-based fault detection processes. If a conflict is detected along the appropriate trajectory, then conflict avoidance commands are calculated which can be datalinked to the aircraft if required. A simplification of these processes is illustrated in Figure 2.13.

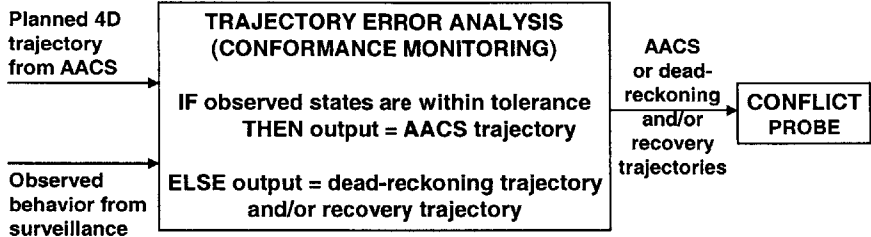


**Figure 2.13: Simplified TSAFE Functionality**

Early and accurate detection of errors in tracking the planned AACS trajectory through a trajectory tracking analysis/conformance monitoring function is essential to the effective operation of TSAFE and to the overall safety of the automated airspace operation. Various trajectory tracking scenarios have been examined [Erzberger (2001)] in an attempt to classify realistic error types for ATC operations so that effective conformance monitoring algorithms can be developed. For this purpose, trajectories were divided into two classes:

- Non-transitioning trajectories, characterized by flight at constant heading or altitude.
- Transitioning trajectories, characterized by changing heading or altitude.

Each class will be discussed in the following sections in the context of both horizontal and vertical environments.

**2.3.3.2 Non-Transitioning Trajectory Tracking Error Analysis**

Non-transitioning trajectory tracking errors and the associated conflict detection trajectories have been classified in the horizontal and vertical domains based on CTAS empirical analysis and observed traffic behaviors. The non-transitioning horizontal tracking error cases are presented in Figure 2.14. The specific type of deviation illustrated has been observed in operational data when pilots have attempted to avoid convective weather.

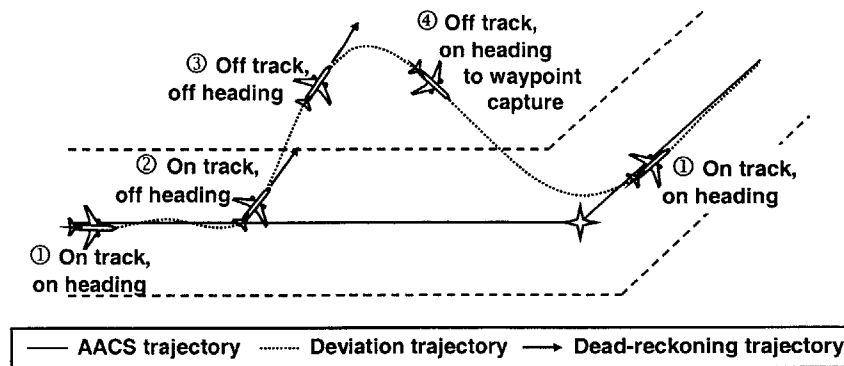


**Figure 2.14: TSAFE Non-Transitioning Horizontal Tracking Error Categories [adapted from Erzberger (2001)]**

The conflict detection strategy employed by TSAFE in the non-transitioning horizontal case depends on the tracking error category, as summarized in Table 2.5.

**Table 2.5: TSAFE Non-Transitioning Horizontal Conflict Detection Trajectories [Erzberger (2001)]**

Non-transitioning Horizontal Tracking Error Category	Conflict Detection Trajectory
① On track, on heading	AACS 4D
② On track, off heading	AACS 4D & Dead-reckoning
③ Off track, off heading	Dead-reckoning
④ Off track, on heading to capture waypoint	AACS 4D

When the aircraft is on track and on heading (case ①), it is behaving in a conforming manner to the AACS 4D trajectory and it is therefore appropriate to use in the conflict detection probe. However, when the aircraft gets off heading relative to the AACS trajectory, then the dead-reckoning trajectory is used in the probing strategy, either in addition to the nominal AACS trajectory (if on track in position, case ②) or instead of the AACS trajectory (if off track in position, case ③). If the aircraft is off track but heading back towards a waypoint on the AACS trajectory (case ④), then the conflict probing strategy reverts to probing along the AACS trajectory alone. The implicit assumption is that the aircraft is attempting to return to its assigned trajectory and will revert to flying along it once it has reached the waypoint it is flying towards. Lateral displacement thresholds of 4 nm are suggested to determine whether the aircraft is on or off track, while heading thresholds and how to handle trajectories that are consistent with a recovery to the trajectory but not coincident with a waypoint appear to be subject to future research since specific details are not given in the existing literature.

Vertical cases involving uncoordinated or unintended altitude excursions are presented in Figure 2.15. Although the represented vertical deviations occur less frequently than the example deviations used in the horizontal domain, they are easy for the controller to miss due to the lower observability of vertical behavior on the radar plan display relative to horizontal deviations. Whenever the aircraft altitude deviation exceeds the threshold (a value of 400 ft is suggested), vertical non-conformance is declared.

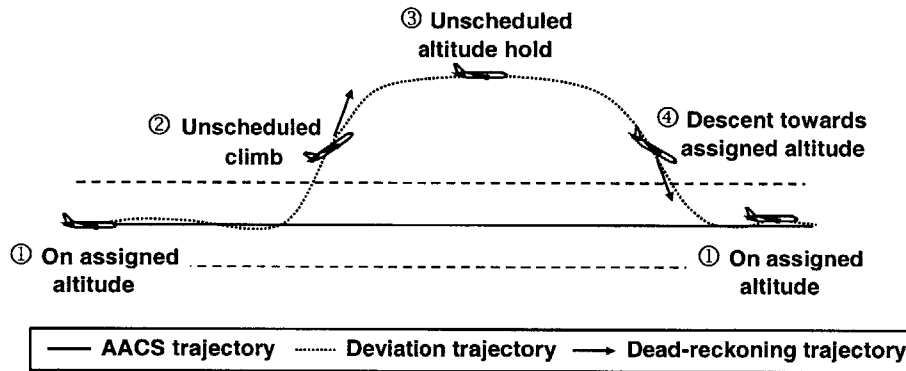


**Figure 2.15: TSAFE Non-Transitioning Vertical Tracking Error Categories** [adapted from Erzberger (2001)]

Again, the conflict detection strategy depends on the tracking error category in the vertical scenario as summarized in Table 2.6.

**Table 2.6: TSAFE Non-Transitioning Vertical Conflict Detection Trajectories** [Erzberger (2001)]

Non-transitioning Vertical Tracking Error Category	Conflict Detection Trajectory
① On assigned altitude	AACS 4D
② Unscheduled climb above/descent below assigned altitude	Dead-reckoning at observed altitude rate
③ Unscheduled altitude hold above/below assigned altitude	AACS at observed altitude level
④ Descent/climb towards assigned altitude after deviation	Dead-reckoning at observed altitude rate

When the aircraft is at its assigned altitude (case ①), then it is conforming and the AACS trajectory is the appropriate one to use in the conflict probe. When an unscheduled climb/descent away from (case ②) or back towards (case ④) the assigned altitude, then a dead-reckoning trajectory at the currently observed altitude rate is used in the conflict probe. The use of altitude rate in the dead-reckoning trajectory presents a significant challenge in that current Mode C altitude returns are discretized in 100 ft increments and updates can be up to 12 seconds apart. Significant uncertainty can exist in the altitude

rate as a result. If the non-conformance involves an unscheduled hold above or below the assigned altitude (case ③), then conflict probing is conducted along the AACS trajectory using the nominal lateral and longitudinal components but the observed (non-conforming) altitude component.

### 2.3.3.3 Transitioning Trajectory Tracking Error Analysis

Horizontal test cases and conflict detection trajectories for transitioning trajectories are presented in Figure 2.16 and Table 2.7.

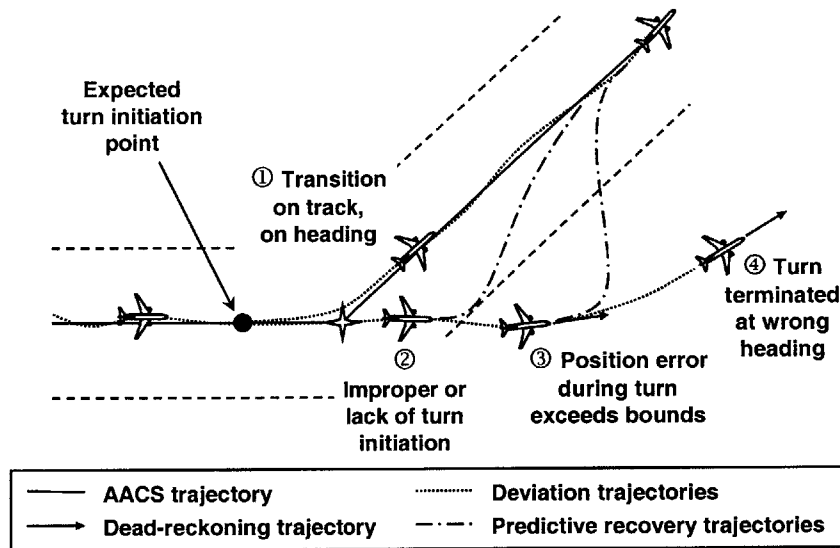


Figure 2.16: TSAFE Transitioning Horizontal Tracking Error Categories [adapted from Erzberger (2001)]

Table 2.7: TSAFE Transitioning Horizontal Conflict Detection Trajectories [Erzberger (2001)]

Transitioning Horizontal Track Error Category	Conflict Detection Trajectory
① Transition on track, on heading	AACS 4D
② Improper or lack of turn initiation	Recovery trajectory & Dead-reckoning
③ Position error during turn exceeds bounds	Recovery trajectory & Dead-reckoning
④ Turn terminated at wrong heading	Recovery trajectory & Dead-reckoning

TSAFE analysis determines whether the horizontal transition occurs within prescribed time limits and that state variables are behaving appropriately in terms of sign and rate towards expected target values. Erzberger indicates that allowable errors in transition are strongly dependent on the method used to execute the transition (e.g. whether it is flown manually or automatically via the FMS) and whether it originated from a standard flight plan transition or a controller vector. One of the most challenging



aspects when only position is surveilled is the determination of the start and end of the transition due to the relatively slow filters (such as the  $\alpha$ - $\beta$  trackers used for radar processing in the HCS [Brookner (1998)]) which are used to derive heading from the position data.

The proposed conflict detection trajectories used for deviant aircraft in horizontal transition scenarios (cases ②, ③ & ④ in Figure 2.16) involve probes along “predictive recovery trajectories”, in parallel with the dead-reckoning trajectory. In the current concept, these recovery trajectories are based on simple heuristics rather than the more detailed modeling required if specific aircraft dynamics were used. Experience with creating trajectory heuristics in the development of CTAS may assist in dealing with this issue in TSAFE.

Vertical test cases and conflict detection trajectories for transitioning trajectories are presented in Figure 2.17 and Table 2.8.

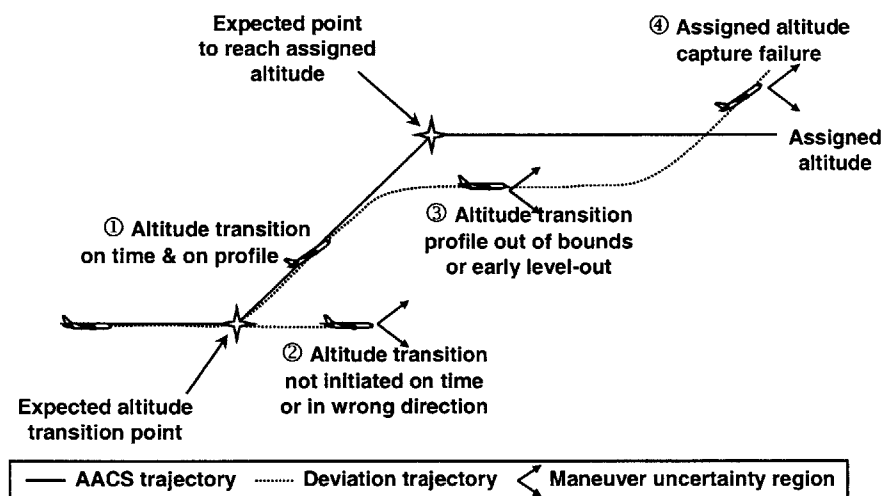


Figure 2.17: TSAFE Transitioning Vertical Tracking Error Categories [adapted from Erzberger (2001)]

Table 2.8: TSAFE Transitioning Vertical Tracking Error Conflict Detection Trajectories [Erzberger (2001)]

Transitioning Vertical Track Error Category	Conflict Detection Trajectory
① Altitude transition on time & on profile	AACS 4D & Dead-reckoning
② Altitude transition not initiated on time or in wrong direction	AACS & Maneuver uncertainty region
③ Altitude transition profile out of bounds or early level-out	AACS & Maneuver uncertainty region
④ Assigned altitude capture failure	AACS & Maneuver uncertainty region

Erzberger highlights the importance of vertical transition monitoring since loss of separation incidents often occur while aircraft are changing altitude or just after they have leveled out at a new altitude. However, as also seen in the discussion of other systems, vertical transition trajectories can be very hard to predict due to the substantial sources of error [McConkey & Bolz (2002)], and therefore much more leeway has to be allowed to aircraft in vertical transitions. The proposed approach to this in TSAFE is the use of vertical “maneuver uncertainty regions” as the basis for conflict search instead of the predictive recovery trajectories used in the lateral transition case. The maneuver uncertainty region is “pie-shaped” with its apex at the current location of the aircraft, its sides determined by the maximum and minimum flight path angles joined by a line defining a 3 minute flight time and aligned with the aircraft’s current heading. As such, this region theoretically contains all points that the aircraft could reach in the vertical plane over a 3 minute period if the current heading is maintained.

### 2.3.3.4 Critical Maneuver Detection

Another important feature of the TSAFE concept involves the detection of “critical maneuvers”. These are defined as planned transitions that must be performed accurately and on time in order to avoid a conflict with other aircraft, as illustrated in Figure 2.18.

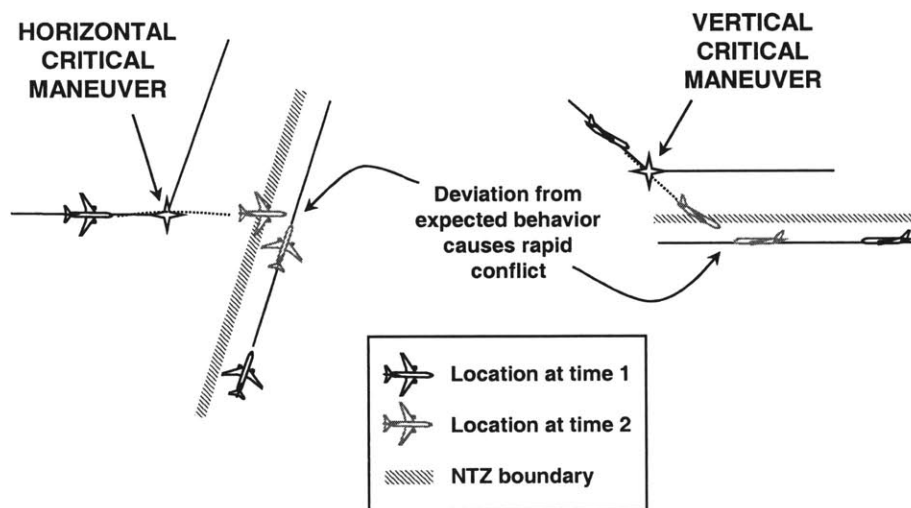


**Figure 2.18: Example Horizontal and Vertical Critical Maneuvers [adapted from Erzberger (2001)]**

Special monitoring attention must be given to critical maneuvers because of the adverse consequences associated with non-conformance under these conditions. This illustrates the critical relationship between conformance monitoring and allowable ATC operating procedures. In this case, if ATC procedures allow this situation to occur, then responsive and accurate conformance monitoring is

required to support it. However, if the conformance monitoring performance requirements could not be met or the implementation of a system was undesirable (e.g. for cost reasons), then ATC procedures could be used to prevent this potential aircraft encounter from ever occurring, even if there is non-conformance. The current concept envisions that a critical maneuver warning message would be displayed to the controller and datalinked to affected aircraft a few minutes before it is scheduled to occur. This would make both the pilot and controller aware of the criticality of the imminent maneuver. The message would then be cancelled as soon as surveillance data indicates that the critical maneuver has been conducted, or else pre-computed avoidance maneuvers would be immediately executed.

An extension of the No Transgression Zone concept (as used for close-spaced parallel approaches discussed previously) has also been proposed for more general application in this context. The NTZ would identify the airspace regions that another aircraft must avoid if a conflict is to be prevented, as illustrated in Figure 2.18. In principle, this could also be communicated to the flight crew of aircraft adjacent to this area in the form of “do-not-maneuver” messages. This is then complementary to the critical maneuver concept in that the critical maneuver message identifies what the aircraft *should* do, while the NTZ message would identify what it *should not* do. The concept of rapidly issuing conflict avoidance commands if a deviation is detected coupled with an NTZ illustrates the strong parallels between the operational close-spaced parallel approach concept and the current proposals for allowing improved conformance monitoring in a more general ATC environment in the TSAFE concept.

## 2.4 Summary

This Chapter has presented a discussion of a wide selection of ground-based ATC conformance monitoring tools that are operational or under development. In the operational systems, notable conformance monitoring issues have been highlighted through discussions of the HCS, AERA/URET and CAATS systems. The conformance monitoring in the HCS was one of the first to be implemented and identify the need for different thresholds at trajectory transitions than during steady flight and in the lateral and vertical domains. The early systems also have large threshold values that allow for surveillance uncertainty and the wide range of aircraft navigational tracking capabilities using the system. This has subsequently affected wider system operation such as acceptable separation minima. The AERA/URET system has more advanced conformance monitoring utilizing different threshold values depending on the equipage state of the aircraft being monitored and using more aggressive threshold placement so deviations can be detected more quickly. This system also highlights the importance of attempting to infer the intent of an aircraft once it has been determined to be non-conforming in order to

undertake its conflict detection and resolution task. The fundamental importance of detailed and accurate knowledge of the cleared trajectory and aircraft intent was highlighted in the implementation of CAATS. Developmental tools are involving more sophisticated conformance monitoring techniques. Eurocontrol’s FPM tool introduces a 4D contract concept and multiple nested thresholds that vary according to aircraft capability and operating conditions. NLR’s NarSim is one of the first with conformance monitoring techniques that explicitly involve the heading state in the determination of conformance. Finally, the detailed consideration of conformance monitoring in NASA’s new automated airspace concept has reinforced its fundamental importance to future ATC operations. Although still at an early stage of development, the designers of TSAFE are considering the benefits of utilizing multiple states (i.e. not just position), knowledge-based heuristics and simple aspects of model-based techniques to determine possible behaviors after non-conformance has been detected. The conformance monitoring approaches used by each of the tools can be classified according to the three fault detection categorizations of signal-based, knowledge-based and model-based techniques. These are summarized in Table 2.9, along with the primary states used

**Table 2.9: Fault Detection Categorizations & State Usage of Conformance Monitoring Tools**

Tool	Fault Detection Categorization			States Used in Conformance Monitoring Process
	Signal-Based	Knowledge-Based	Model-Based	
PRM	✓			Position deviation from approach path
HCS	✓			Position/altitude deviation from flight plan
URET	✓	✓ <sup>1</sup>		Position/altitude deviation from flight plan
CAATS	✓			Position/altitude deviation from flight plan
TAAATS	✓			Position/altitude deviation from flight plan
GAATS	✓			Position/altitude deviation from flight plan
FPM	✓			Position/altitude deviation from flight plan
NarSim	✓	✓ <sup>2</sup>	✓ <sup>2</sup>	Position/altitude & heading deviations from flight plan
TSAFE	✓	✓ <sup>3</sup>	✓ <sup>4</sup>	Position/altitude & heading deviations from flight plan

<sup>1</sup> URET reconformance process only

<sup>2</sup> NarSim heading expectations theoretically based on heuristics or an explicit model, but details not available

<sup>3</sup> TSAFE conflict probe trajectory determination only

<sup>4</sup> TSAFE conflict probe trajectory determination during vertical transition regimes only: bounds are defined by maximum climb/descent rates of different categories of aircraft.

. The dominant fault detection strategy is the signal-based approach where the observed states of an aircraft are compared to its expected states and non-conformance being declared when the deviation exceeds a threshold value. Early systems have been exclusively position-based, while the benefit of using

additional states (primarily heading) are now being studied as new technologies make them more accessible.

With the exception of the PRM system, in tools where threshold values have been implemented or suggested, there has found to be little in the way of quantitative analysis regarding how the suggested threshold values were developed or their impact on ATC operations. Many of the developmental tools are qualitative in nature and much more research is required to determine how the concepts could be implemented effectively in practice. General analysis approaches are therefore required to assist in the development of future conformance monitoring approaches and technology requirements to support future ATC system objectives. The research presented in the following chapter presents a framework identifying how novel conformance monitoring approaches can be developed and allowing a quantitative analysis of candidate approaches to be conducted. Its utility is demonstrated through several studies using both operational and simulated data in subsequent Chapters.

[This page intentionally left blank]

---

# CHAPTER 3: Development of the Conformance Monitoring Analysis Framework

---

## 3.1 Introduction

The previous Chapter demonstrated that existing ground-based conformance monitoring Decision Support Tools primarily use simple strategies that declare an aircraft to be non-conforming when the difference between the observed position deviation exceeds a pre-determined threshold. The rationale for the threshold values employed in these various systems is generally not well established. There is a need for general conformance monitoring analysis techniques that provide a framework for describing, developing and quantifying novel conformance monitoring approaches. A framework is described in this Chapter that allows a fundamentally new approach to conformance monitoring system development to meet these needs based on fault detection techniques.

## 3.2 Conformance Monitoring as Fault Detection

The previous Chapter discussed existing conformance monitoring automation systems and categorized them according to standard fault detection classifications. This was seen to be an effective way of *describing* the general conformance monitoring approaches employed by each tool. Fault detection techniques can also be used to help *develop* new conformance monitoring approaches. By formally defining an aircraft non-conformance as a fault that needs to be detected in the ATC system, a whole spectrum of fault detection analysis techniques developed in other domains can be employed to create new approaches for this application.

A general framework allowing the signal, knowledge and/or model-based fault detection techniques described in Chapter 1 to be employed is illustrated in Figure 3.1. After the analogy between fault detection and conformance monitoring has been made, this general framework can be tailored for the conformance monitoring application in ATC. The result is shown in Figure 3.2.

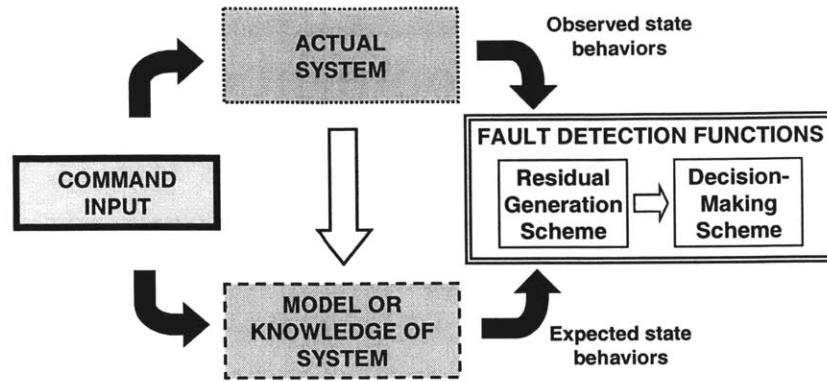


**Figure 3.1: General Fault Detection Framework**

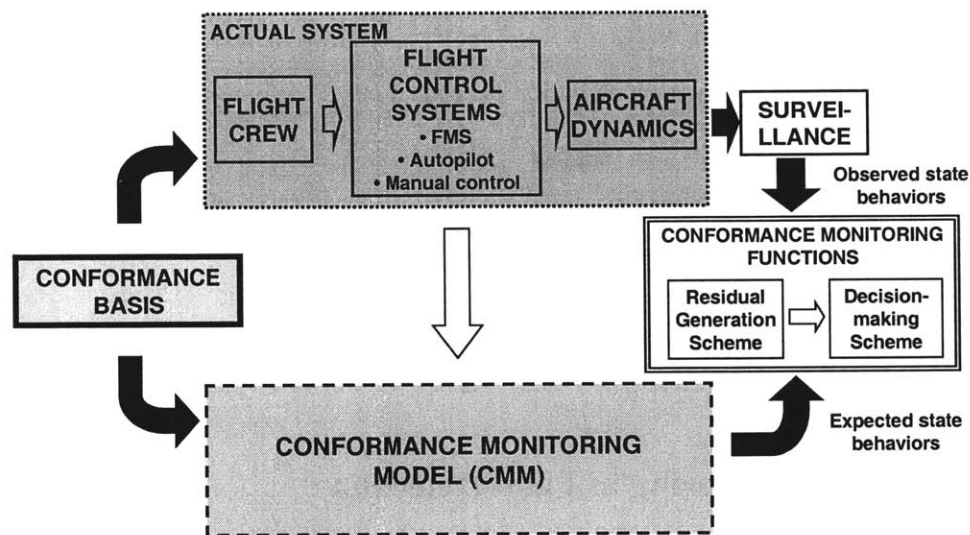


**Figure 3.2: Conformance Monitoring in General Fault Detection Framework**

In Figure 3.2, the command input is now considered the “Conformance Basis”, i.e. the basis against which the conformance of a subject aircraft is being compared, such as the assigned trajectory. The pilots nominally make inputs to the aircraft systems (flight automation or manual control) to manage the aircraft trajectory in a manner consistent with the active Conformance Basis. These “Actual System” processes are shown in the upper box of Figure 3.2 and some of the states are observable through the available surveillance systems. The expected state behaviors are based on a “Conformance Monitoring Model” (CMM) shown in the lower box. This model requires sufficient form and fidelity to determine expectations on the observable states that are to be used in the residual generation task. The block at the right receives the observed states from the surveillance systems and determines at any given time whether they are consistent with the expected behaviors from the CMM by using the fault detection-inspired



techniques of residual generation and decision-making. Note that the generic fault detection functions of Figure 3.1 have been tailored to the task of detecting aircraft non-conformance in Figure 3.2 through the definition of a Conformance Residual generation scheme.

### 3.3 The Conformance Monitoring Analysis Framework (CMAF)

The general conformance monitoring representation of Figure 3.2 is the basis for the more evolved form shown in Figure 3.3. This form is referred to as the Conformance Monitoring Analysis Framework (CMAF) in the rest of this document and is the foundation of the research approach.

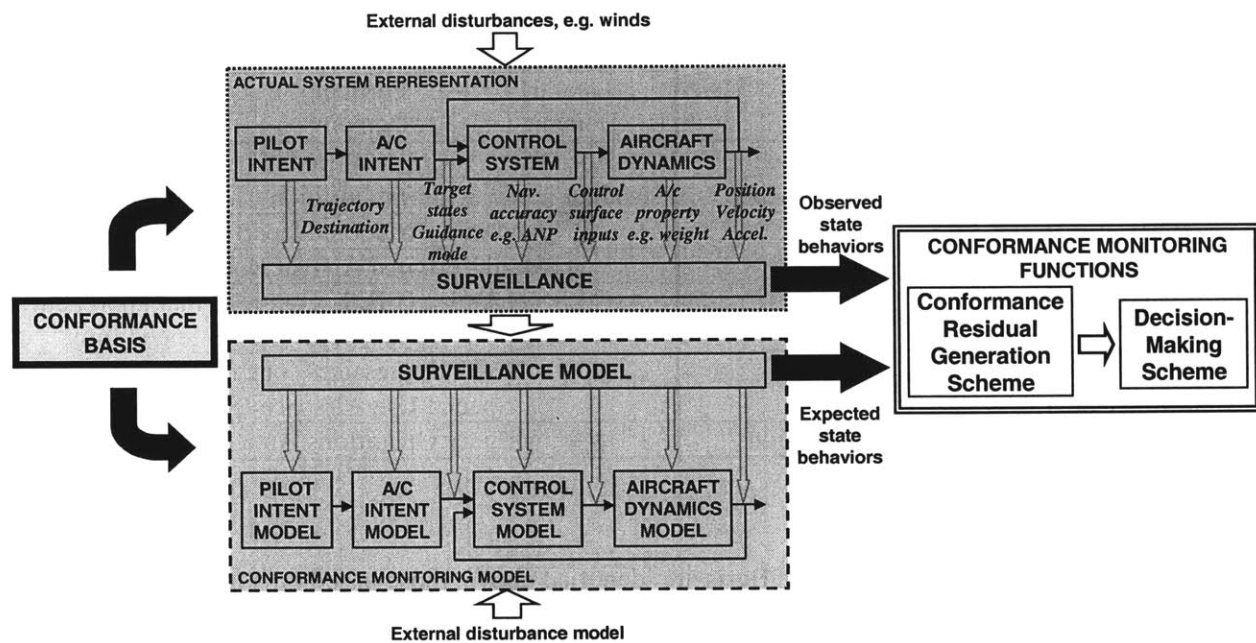


Figure 3.3: The Conformance Monitoring Analysis Framework (CMAF)

The main components of the framework are defined as:

- Conformance Basis
- Actual System Representation
- Conformance Monitoring Model
- Conformance Residual Generation Scheme
- Decision-Making Scheme

Each component is discussed in detail in the following subsections.

### 3.3.1 Conformance Basis

The concept of a Conformance Basis was developed in this research in order to define the basis against which the observed behavior of an aircraft may be monitored. More explicitly, it is a representation of the currently-active clearances or procedures that can be monitored against in the lateral, vertical and longitudinal ATC domains. Example forms of a Conformance Basis, or sub-elements that make up a Conformance Basis in the various domains, are presented in Table 3.1.

**Table 3.1: Example Forms of Conformance Basis**

	Example Conformance Basis	Example Conformance Basis Sub-Elements		
		Lateral Domain	Vertical Domain	Longitudinal Domain
Trajectory-Based Conformance Bases	Active Flight Plan	Assigned route	Cruise altitude	Cruise speed
	Tactical Amendments	Heading vector	Interim altitude	Interim speed
	Standard Procedures	Standard Instrument Departure (SID)		
		Standard Terminal Arrival Route (STAR)		
		ILS localizer	ILS glide slope	Final approach speed limit
Region-Based Conformance Bases	No-Fly Zones	No-Transgression Zone (NTZ)		
		Special Use Airspace (SUA)		
	Containment Regions	Military Operations Area (MOA)		

Two general forms of Conformance Basis are identified above: those based on a trajectory and those based on a region. Trajectory-based Conformance Bases are the most common type and identify a specific trajectory in state space against which observed behavior can be monitored. A Conformance Basis based on a region can be considered an inverse of the trajectory-based form: rather than monitoring for what an aircraft should be doing, the requirement is to monitor an aircraft against what it *should not* be doing, such as traveling inside a no-fly zone (e.g. NTZ) or outside a containment region (e.g. MOA). The analyses presented in this document will focus primarily on the trajectory-based Conformance Bases.

The complete Conformance Basis for an aircraft can be a complex collection of sub-elements in the various domains. Conformance monitoring could be conducted on the union of the Conformance Basis in each domain, or on one of the elements individually, depending on the task at hand and the information available. For example, in today's en-route ATC environment, it is common for controllers to primarily conduct conformance monitoring in the lateral and vertical domains and less in the longitudinal domain.

Currently, specific longitudinal conformance monitoring is mainly conducted by the HCS to prevent flight plan time-outs rather than for tactical operational needs of the controller. This priority placed upon lateral and vertical monitoring in the en-route domain is partly as a result of the greater reliance of the procedures on these axes (e.g. lateral and vertical separation minima) and partly as a result of the lack of adequate information to undertake longitudinal conformance monitoring. This is both in terms of lack of an accurate longitudinal Conformance Basis (e.g. limited to estimated arrival time at a single discrete point printed on the flight strip—see Figure 2.4) and a lack of surveillance of en-route progress in the longitudinal dimension. However, as the use of ATC procedures that call for longitudinal conformance monitoring increase (such as the wider use of minutes-in-trail restrictions), it will become important to support improved monitoring in this domain. Regardless of the dimension in which monitoring is being conducted, consistent knowledge of the currently active Conformance Basis among the various agents in the ATC system (e.g. controller, pilot, aircraft and ground automation systems) is of paramount importance since the Conformance Basis defines the baseline from which the expected state behaviors are generated and against which the observed behaviors are compared.

### 3.3.2 Actual System Representation

The observed state behaviors in the CMAF are sourced from surveillance of the Actual System processes. In order to illustrate them as more than a “black box”, these processes are represented in the CMAF of Figure 3.3 by the key elements that are involved in the execution of the Conformance Basis, thus becoming an Actual System Representation. A simplified form of the Actual System Representation is shown in Figure 3.4: it includes a classical feedback representation of the aircraft control system and dynamics, supplemented with upstream pilot and aircraft “intent” components. Pilot intent represents the intended actions on the part of the flight crew to execute their understanding of the Conformance Basis, while the aircraft intent represents the future behavior of the aircraft assuming no further control inputs.

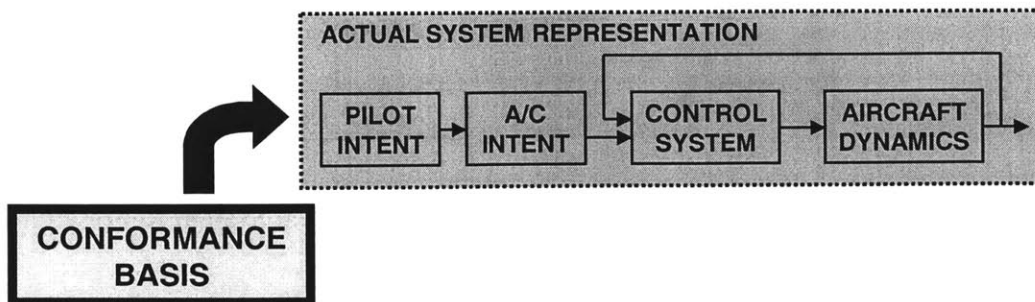
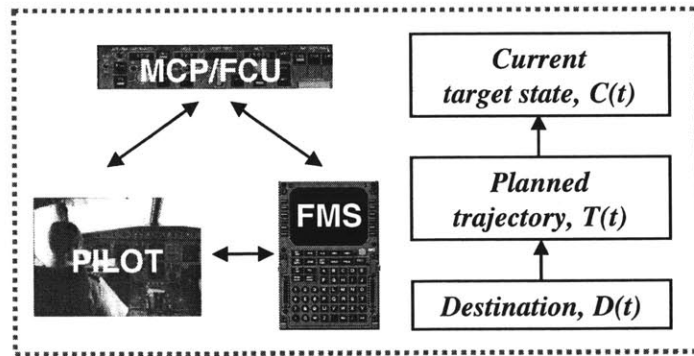


Figure 3.4: Simplified Actual System Representation

The notion of intent needed to be developed as part of this research in order to formalize the future behavior of an aircraft that is often contained within a Conformance Basis. For example, a cleared trajectory defines the future route that an aircraft should follow, while an ATC vector defines the heading to which the aircraft should turn. The ‘‘Surveillance State Vector’’  $X(t)$  [Reynolds & Hansman (2001)] was created to describe the different forms of intent used in the ATC system and to formalize the relationship with the traditional dynamic states of position, velocity and acceleration, as shown in Equation 3.1.

$$\text{Surveillance State Vector, } \underline{X}(t) = \left[ \begin{array}{l} \textit{Position states, } P(t) \\ \textit{Velocity states, } V(t) \\ \textit{Acceleration states, } A(t) \\ \textit{Current target states, } C(t) \\ \textit{Planned trajectory states, } T(t) \\ \textit{Destination states, } D(t) \end{array} \right] \begin{array}{l} \textit{Traditional dynamic} \\ \textit{states} \\ \\ \textit{Defined intent} \\ \textit{states} \end{array} \quad \text{Equation 3.1}$$

Under this representation, the future behavior of the aircraft is defined by intent at current target state, planned trajectory state and destination state levels. These definitions were chosen since they accurately mimic the way intent is communicated and executed in the operational ATC system as illustrated in Figure 3.5, as well as being consistent with the way it is defined in the ADS-B specifications [RTCA (2002), Barhydt & Warren (2002)].



**Figure 3.5: Intent & Dynamic State Relationships in the Actual System Representation**

For example, intent is communicated in the ATC system at the various defined levels: controllers give current target state commands (heading vectors, altitude assignments) and planned trajectory commands (re-routes, standard procedures) to manage the path of the aircraft. These intent clearances

can be executed through a number of autoflight systems. For example, a Flight Management System (FMS) can be programmed to take the flight to its destination ( $D(t)$ ) via a programmed trajectory ( $T(t)$ ). This in turn implies current target states ( $C(t)$ ) such as heading, altitude and speed targets are output from the FMS or directly programmed by the pilot via a Mode Control Panel (MCP) or Flight Control Unit (FCU). These target states manage the aircraft along the planned trajectory by providing the reference inputs to the traditional feedback control loops governing the acceleration ( $A(t)$ ), velocity ( $V(t)$ ) and position ( $P(t)$ ) dynamic state components. In this way, each element can be considered as existing at an incrementally higher level and producing inputs for the next state in the Surveillance State Vector formalism, just as each element in the Actual System Representation generates appropriate control system target states for the downstream elements. The example discussed above could also be repeated for the case of a pilot performing the function of the FMS/autopilot elements when manually controlling the aircraft, where analogous mental intent at the various levels can be considered to exist.

One of the advantages of representing the processes occurring in the actual system in this manner is that it allows different surveillance environments to be visualized, as demonstrated in Figure 3.6 for radar and ADS-B surveillance environments. The downward arrows illustrate where potentially-surveillable states could be extracted from various points in the Actual System Representation. Traditional surveillance systems such as radar generally extract states from the point represented by the arrow at the far right. However, enhanced surveillance systems such as Automatic Dependent Surveillance-Broadcast (ADS-B) may enable more dynamic states, as well as intent and supporting states to be surveilled. These additional states could lead to a better understanding of the actual system behavior for the user provided with the surveillance information and possibly significantly enhance conformance monitoring capability.

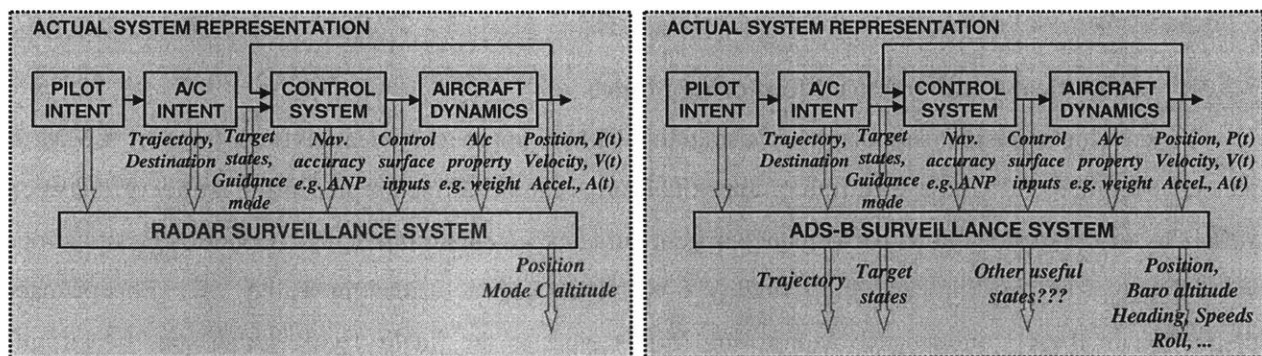


**Figure 3.6: Visualization of Surveillance Environments using the Actual System Representation**

### **3.3.3 Conformance Monitoring Model (CMM)**

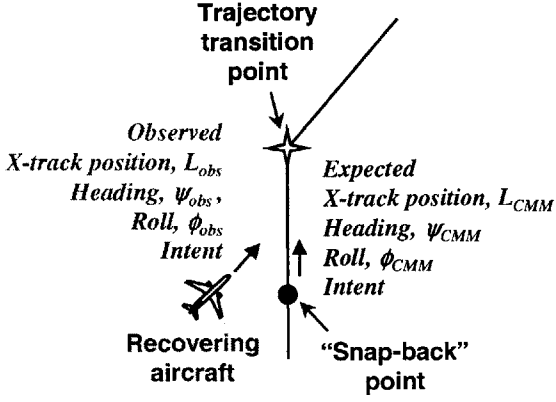
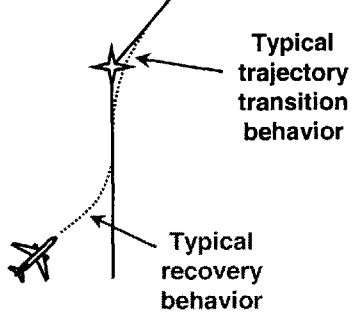
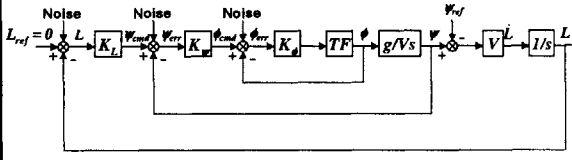
The Conformance Monitoring Model is used to generate the expected values of states for comparison with those surveilled from the actual system. In the Conformance Monitoring Analysis Framework of Figure 3.3, the Conformance Monitoring Model is shown as containing elements that mirror those in the Actual System Representation. Hence, another benefit of using the chosen form of the Actual System Representation is that it provides insight regarding the key elements that may need to be modeled to generate appropriate state expectations. Note that the states surveilled from the various points in the Actual System Representation can be used to help populate or provide inputs to appropriate Conformance Monitoring Model elements. This is illustrated by the downward arrow from the Actual System Representation to the Conformance Monitoring Model in the framework of Figure 3.3.

There are many potential forms that the Conformance Monitoring Model could take, both explicit analytical models implemented in a decision support tool or “mental models” employed by controllers. Within each category, model types could exist at many different levels of fidelity or abstraction depending on the conformance monitoring performance requirements, along with other factors. One of the greatest challenges in exercising the CMAF approach is the development of the Conformance Monitoring Model at an appropriate level of abstraction and fidelity. It requires sufficient fidelity to undertake effective conformance monitoring (e.g. to meet non-conformance time-to-detection targets), but not be so detailed that modeling uncertainty and sampling issues introduce too much noise into the residual (thereby increasing false alarm rates). A tradeoff is therefore required to determine what level of fidelity is required in the conformance monitoring model in the ATC environment being monitored. Model fidelity issues are discussed in the following sections in the context of the two general categories of CMM-type: analytical and mental model forms.

#### **3.3.3.1 Analytical Conformance Monitoring Models**

To develop decision support tools using the CMAF approach, an analytical form of CMM is generally required. A whole spectrum of analytical forms can be defined representing a tradeoff between simplicity of the model and its performance in generating expected aircraft states. Generic classifications according to low, medium and high fidelity CMM types are described in Table 3.2. The primary distinction in these Conformance Monitoring Model types is the fidelity with which specific aircraft dynamics are modeled in order to generate the expected state behaviors, particularly during nominal transitioning flight regimes and also during recovery from a deviation.

**Table 3.2: Example Conformance Monitoring Model Fidelities**

CMM Fidelity	Description	Schematic
<p>Low Fidelity CMM</p>	<p>No explicit modeling of aircraft dynamics either at nominal transitions or during recovery from a deviation. Assumes discrete heading changes at transitions (no smoothing) and no credit is given for being off-track but attempting to return to the proper trajectory.</p> <p>Expected state behaviors governed by Conformance Basis at a closest “snap-back” point closest to the Conformance Basis.</p>	 <p>The schematic illustrates a vertical trajectory with a sharp upward transition point. An aircraft is shown below the transition point, labeled 'Recovering aircraft'. A dashed line indicates the 'Observed' path, and a solid line indicates the 'Expected' path. Key parameters are listed: Observed X-track position, <math>L_{obs}</math>, Heading, <math>\psi_{obs}</math>, Roll, <math>\phi_{obs}</math>, Intent; and Expected X-track position, <math>L_{CMM}</math>, Heading, <math>\psi_{CMM}</math>, Roll, <math>\phi_{CMM}</math>, Intent. A 'Snap-back' point is marked on the expected path below the transition point.</p>
<p>Medium Fidelity CMM</p>	<p>Transitioning and/or recovery aircraft behaviors based on curve fit or heuristics of nominal conforming behavior.</p>	 <p>The schematic shows a smooth curve for the trajectory transition and a curved path for the aircraft's recovery behavior, both labeled as 'Typical'.</p>
<p>High Fidelity CMM</p>	<p>Transitioning and/or recovery aircraft behavior based on an explicit model of the aircraft being monitored under the expected environmental conditions.</p>	 <p>The block diagram represents a control system. It starts with a reference input <math>L_{ref} = 0</math> and a disturbance <math>L</math>. The signal passes through a gain block <math>K_L</math>, then a summing junction with 'Noise'. This is followed by a gain block <math>K</math>, another summing junction with 'Noise', and a gain block <math>K_d</math>. The signal then goes through a transfer function block <math>TF</math>, a gain block <math>g/V_s</math>, a summing junction with 'Noise', a gain block <math>V</math>, and finally an integrator <math>1/s</math> to produce the output <math>L</math>.</p>

The low fidelity CMM employs no specific model of transition or recovery dynamics. Instead, the expected states output from this CMM are based upon what they would be if the aircraft were flying exactly to the Conformance Basis, either at the position defined by the longitudinal element of that basis or the closest point to the route given the observed position (the “snap-back point”). Note that a trajectory defined by waypoints is often approximated with straight-line segments, implying a discrete heading change at the waypoint as illustrated at the top of Table 3.2. This simple type of CMM is employed by the majority of the existing ground-based tools discussed in Chapter 2, where the expected position,

altitude, speed and heading (if used) are based on the aircraft flying the exact flight plan route. The primary advantage of this type of approach is the simplicity with which expected states can be derived with knowledge of the current Conformance Basis. However, since it incorporates no transition dynamics, it does a poor job of generating realistic expected aircraft behaviors during transitioning flight regimes. In addition, if an aircraft deviates slightly off the planned track and attempts to recover back, this type of model does not distinguish or give credit for recovery behavior over behavior that indicates further divergence.

Improvements can be made by employing higher fidelity CMM types which do account for the aircraft dynamics, either generically using curve fit or heuristically-derived transition and recovery dynamics (as in the medium fidelity CMM description) or a more explicit attempt to model realistic aircraft behaviors (in the high fidelity CMM description). Although, these medium and high fidelity models are more challenging to develop and implement efficiently, they generally produce more accurate state expectations in a given situation than the more simple approach that models no transition or recovery dynamics.

Conformance Monitoring Model fidelity issues will be examined in detail in the following chapters where various fidelities of CMM are compared under different flight regimes and operating environments.

### **3.3.3.2 Mental Conformance Monitoring Models**

An example of a simple “mental model” of expected behavior in a controller’s mind [Reynolds *et al.* (2002)] is illustrated in Figure 3.7. The surveillance systems (e.g. radars) provide input for each aircraft being monitored through the controller’s perception and attention channels (note that the controller is responsible for monitoring multiple aircraft: separate conformance monitoring tasks are required for each). This provides both the observed state behavior to the controller’s internal conformance monitoring function and also aids in the construction of the working mental model, which transforms the intended Conformance Basis into an expectation for each aircraft’s behavior. The working mental model is represented at a higher level of abstraction than the actual system processes consistent with controller abstractions and heuristics identified through interviews and field observations. In this example representation, the working mental model contains sub-models of the pilot, aircraft, surveillance and disturbance (not shown in Figure 3.7 for clarity) components, which are populated through appropriate abstractions. It is assumed that there is a default abstraction for each of the key components in the mental model. These default abstractions can be supplemented by more situation-specific models from a reserve of standard abstractions or can be synthesized in real time for non-standard cases. The default



abstractions and model reserves are thought to be developed through training and operational experience [Davison & Hansman (2003a)].

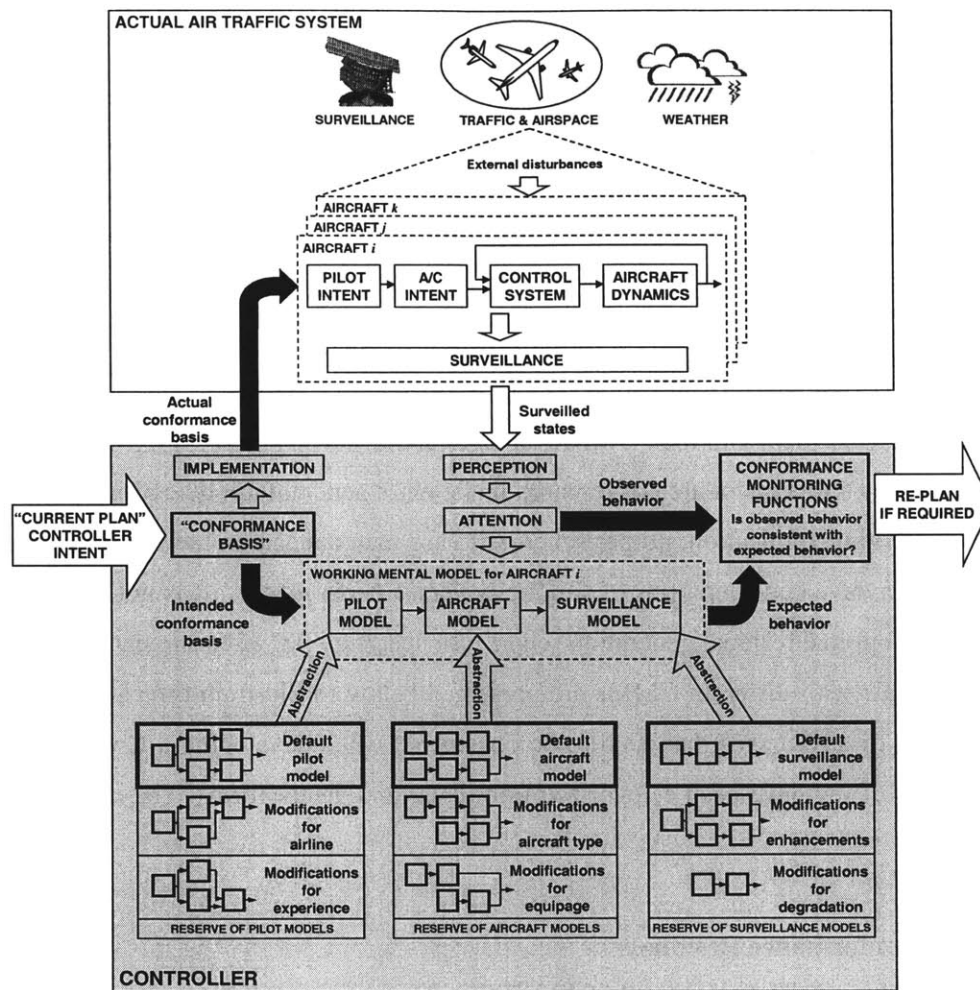


**Figure 3.7: Conformance Monitoring Model as a Mental Model in the Controller**

This mental model interpretation of the CMM will not be explicitly considered further in this document. It is included here to demonstrate that the same framework structure can be employed for the case where the controller is responsible for conformance monitoring. The residual generation and decision-making processes discussed next can be considered to be occurring internal to the controller at some level, but detailed discussion of these processes in the human is beyond the scope of this thesis. However, this view of the controller’s monitoring task may be beneficial in human factors research.

### 3.3.4 Conformance Residual Generation Scheme

In the context of the Conformance Monitoring Analysis Framework, the residual is called the Conformance Residual,  $CR$ . This represents a quantification of the difference between the observed aircraft states available through surveillance of the actual system and the expected aircraft behaviors generated from the Conformance Monitoring Model. The generation of the residual is reducing the problem back to a signal-based approach, but enables a more sophisticated signal (i.e. Conformance Residual) to be used as appropriate.

The challenge in Conformance Residual generation is to create a residual that effectively describes whether an aircraft is behaving in a conforming fashion or not under the environment of interest. There are a large number of residual generation functions that could be employed to generate effective Conformance Residuals, each with their own advantages and disadvantages. Indeed, residual generation scheme formulation is still a major area of research in the more general fault detection community. In the conformance monitoring application, proper schemes to use may depend on the ATC environment under consideration and involve considerations of simplicity versus performance. It is not the intention of this thesis to determine optimal residual generation scheme for specific ATC environments. However, several examples of residuals with different CMMs are presented below to illustrate typical forms and some of the advantages and disadvantages that need to be considered when developing a Conformance Residual generation scheme. They have been categorized into scalar and vector forms. The next sections discuss each of these types.

#### 3.3.4.1 Scalar Conformance Residuals

The simplest type of Conformance Residual is a scalar where the difference between the observed and expected state behaviors are combined into a single value. The general form of a scalar residual is given by:

$$CR_{scalar} = \sum WF_x \cdot f(x_{obs}, x_{CMM}) \quad \text{Equation 3.2}$$

where  $x$  is a useful observed state,  $x_{obs}$  is the observed value for each of those states from the actual system,  $x_{CMM}$  is the expected value of the state from the Conformance Monitoring Model,  $f(x_{obs}, x_{CMM})$  is some function applied to the observed and expected state values and  $WF_x$  is a weighting factor applied to this function on each state  $x$ . Any number of different functions could be employed to achieve different residual characteristics, such as linear, quadratic, differential and integral forms. Similarly, many

different weighting factor philosophies could also be employed, such as normalizing states according to some standard or to weight states according to some perceived or calculated importance. Example Conformance Residual generation schemes are discussed next to illustrate the scalar form, as well as some of the different function and weighting factor issues. These example forms are subsequently demonstrated in a simple aircraft deviation and recovery scenario in the next Chapter.

**Example 1: Absolute Linear Function Residual Generation With Normalization Weighting Factors**

This example residual generation scheme employs the magnitude of the difference between the observed and CMM states, multiplied by a weighting factor and averaged over the number of states. Thus,  $CR_I$  is defined by:

$$CR_I = \frac{\sum WF_x |x_{obs} - x_{CMM}|}{n} \quad \text{Equation 3.3}$$

where  $n$  is the total number of states used to define this Conformance Residual. The individual state components thus add to  $CR_I$  in proportion to the weighted magnitude of the difference between the observed and expected values of the state  $x$ . This form of residual generation is arguably the simplest.

Many types of weighting factor strategies could be employed. One approach is to design the weighting factors to reflect each state’s relative importance. For example, if the timely initiation of a turn is critical to maintaining safe system operation, a higher weighting factor could be assigned to those states that are indicative of the start of turn initiation (e.g. roll angle). At other times, the extra noise existing in these higher order states may require that a smaller weighting factor be employed.

An alternative weighting factor strategy could be designed to normalize each state to acceptable conforming behavior limits so that each contributes equal weight in the final Conformance Residual. This concept already has a precedent in ATC with the Required Navigation Performance (RNP) concept introduced in Chapter 1. This defines 95% probability containment limits based on twice the standard deviation in the cross-track position state deviations during nominal operation. As such, an aircraft’s RNP-qualification level (or surveilled Actual Navigation Performance (ANP) plus Flight Technical Error (FTE)) is a reasonable basis for normalizing an aircraft’s cross-track position error. Under this assumption, a cross-track position error weighting function in the Conformance Residual formalism would be the reciprocal of the RNP value, which can be alternatively represented by twice the standard

deviation limit on the cross-track position for the required 95% containment. This philosophy of using 95% confidence and/or two standard deviation containment limits as the basis for developing weighting functions can be extended for other states that might be available. Observation of conforming behavior could be used to determine appropriate weighting factors in these cases. A weighting factor that is the reciprocal of an observed two standard deviation range may then be appropriate, as shown in Equation 3.4 below.

$$CR_1 = \frac{\sum WF_x |x_{obs} - x_{CMM}|}{n} = \frac{\sum \frac{|x_{obs} - x_{CMM}|}{2\sigma_x}}{n} \quad \text{Equation 3.4}$$

Overall normalization of a residual is desirable so that a comparison can be made between surveillance environments where differing amounts of state information may be available, for example from different levels of the surveillance state vector. In the example used here, this can be achieved by simply dividing the sum of the various weighted components by the number of components used in the summation. As an example,  $CR_1$  in an environment containing surveilled position (from which cross-track position error,  $L$ , can be determined if the planned trajectory intent state  $T(t)$  is also known), heading angle ( $\psi$ ), roll angle ( $\phi$ ) and heading target state intent ( $\psi_T$ ) information would be:

$$CR_1 = \frac{\left[ \frac{|L_{obs} - L_{CMM}|}{RNP\ spec} + \frac{|\psi_{obs} - \psi_{CMM}|}{2\sigma_\psi} + \frac{|\phi_{obs} - \phi_{CMM}|}{2\sigma_\phi} + \frac{|\psi_{T_{obs}} - \psi_{T_{CMM}}|}{2\sigma_{\psi_T}} \right]}{4} \quad \text{Equation 3.5}$$

### Example 2: Quadratic Function Residual Generation

It is common practice in classical control system design to use quadratic functions. A typical form of a quadratic Conformance Residual would be defined by:

$$CR_2 = \frac{\sum WF_x [x_{obs} - x_{CMM}]^2}{n} \quad \text{Equation 3.6}$$

With this form of residual, small deviations about the expected value are reduced relative to an absolute linear function and can be neglected more readily, while deviations beyond a certain point cause a more rapid increase in the deviation parameter and an associated more rapid response from the

Conformance Residual relative to an absolute linear function. These differing properties are illustrated in Figure 3.8. Amplification of these properties can be obtained by using higher powers such as quartics.

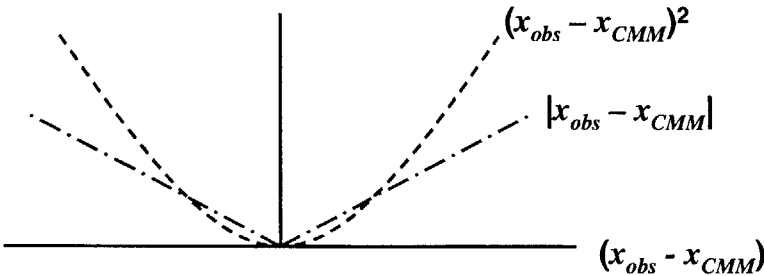


**Figure 3.8: Comparison of Absolute Linear & Quadratic Functions in Residual Generation**

Although this type of behavior may be desirable for some conformance monitoring applications, the non-linear nature makes it harder to map the residual value to the deviations in each state in a multi-state Conformance Residual. In addition, it can be harder to define appropriate weighting factors for states in order to normalize them in a common fashion.

**Example 3: Differential and Integral Function Residual Generation**

Differential and integral functions can also be employed in Conformance Residual generation schemes. A differential element to a residual can be useful to account for the rate of change of a residual element, for example to distinguish between a scenario indicative of a continually deviating aircraft (i.e. with a positive  $d(CR)/dt$ ) versus a scenario indicative of a recovering aircraft (i.e. with a negative  $d(CR)/dt$ ).

An integral element to a residual can be used to account for behavior over a certain time period. For example, a residual based on the integral of an aircraft’s cross-track deviation over time could allow the notion of equivalency between a small deviation over an extended period of time and a large deviation over a small period of time to be captured.

**Example 4: Combined and Parallel Function Residual Generation**

A logical extension of the individual functions discussed above is to combine their various properties to create a hybrid form or to run multiple forms in parallel to benefit for their various properties. For example, a quadratic function could be employed to damp out the effects of small state deviations, while a linear function could be employed for larger deviations so the output would be proportional to the

deviation. A residual with proportional, integral and derivative (PID) control characteristics could also be implemented through combined functional forms. Alternatively, different Conformance Residual generation schemes could be run in parallel, for example one to detect non-conformance and another to indicate whether an aircraft is performing in a recovering fashion or not based on the sign of the residual derivative. Examples of these combined and parallel scalar forms will be presented in the next Chapter in a realistic flight deviation scenario.

### 3.3.4.2 Vector Conformance Residuals

Despite their simplicity, scalar residuals have an inherent limitation in that they limit the ability to distinguish between behaviors in multivariable residuals which represent totally different actual behaviors and which therefore might require different conformance monitoring approaches. For example, consider the two cases illustrated in Figure 3.9. Assume also that a CMM with no recovery dynamics is used to determine the expected aircraft behaviors and that a scalar Conformance Residual is generated using the position, heading and roll angle states. Case ① represents an aircraft which has deviated significantly in position but has heading and roll angle state that are expected given the assumed Conformance Basis and form of CMM. Case ② represents an aircraft that is deviating only slightly in position, heading and roll angle (e.g. due to some atmospheric disturbance), but because of their additive nature they develop a scalar conformance residual of a similar value to the totally different behavior of case ①. These different behaviors could have totally different consequences to the ATC operation but would not be immediately distinguishable from the characteristics of the Conformance Residual alone given the form of the CMM and residual generation scheme.

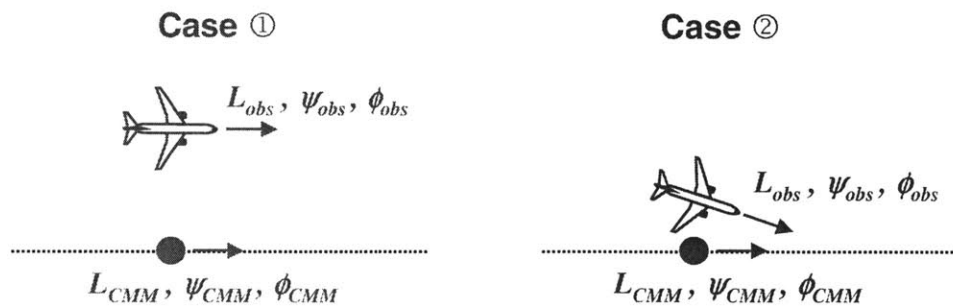


**Figure 3.9: Example Non-Conformance Scenarios**

One way around this problem is to use a vector Conformance Residual where each component of the vector represents the difference between the expected and observed behaviors for each state in the residual generation scheme:

$$\underline{CR}_{vector} = \begin{Bmatrix} WF_{x_1} \cdot f(x_{1_{obs}}, x_{1_{CMM}}) \\ WF_{x_2} \cdot f(x_{2_{obs}}, x_{2_{CMM}}) \\ \vdots \\ WF_{x_n} \cdot f(x_{n_{obs}}, x_{n_{CMM}}) \end{Bmatrix} \quad \text{Equation 3.7}$$

The same two cases discussed above now produce very different residuals in vector space compared to the scalar space, as illustrated in Figure 3.10 for the case where a simple difference is taken between the observed and expected states to generate position, heading and roll error states. Applying generalized functions or weighting factors on the various states can be employed in the vector case in the same way as in the scalar case, only now they are defined in state space rather than on a scalar.

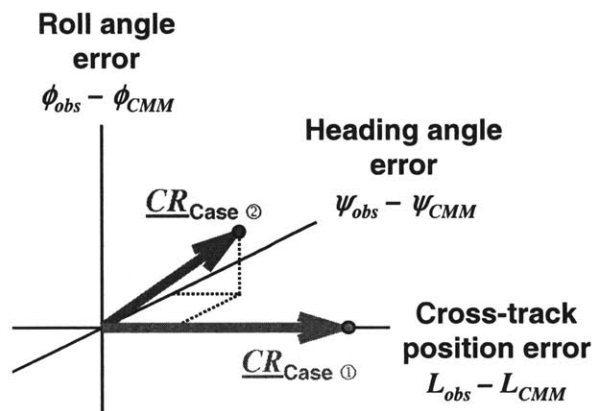


**Figure 3.10: Example Vector Conformance Residuals**

Examples of each of these types of Conformance Residual generation scheme are presented in the next Chapter. Note that, just as there is a trade-off in the form and fidelity of the Conformance Monitoring Model employed to generate expected state values, so there is a tradeoff in the form (scalar vs. vector) and function (e.g. linear, quadratic, derivative, integral) in the Conformance Residual generation scheme in order to achieve certain conformance monitoring objectives.

### 3.3.5 Decision-Making Scheme

Once a residual has been generated, the decision making process involves a determination of whether the residual behavior is characteristic of a conforming aircraft or not. The simplest technique is to use a threshold-based approach on the Conformance residual, such that:

$CR(t) < Threshold(t)$  implies a conforming aircraft at time  $t$   
 $CR(t) > Threshold(t)$  implies a non-conforming/deviating aircraft at time  $t$   
 $CR(t) = Threshold(t)$  implies an aircraft at its conformance limit at time  $t$

Notice that regardless of the techniques used in the Conformance Monitoring Model or the development of the Conformance Residual, a threshold-based technique such as this ultimately distills the process back to a simple signal-based approach, albeit on a (presumably) more effective Conformance Residual.

It is often a challenge to determine the appropriate threshold to use with different Conformance Residual generation schemes, under different ATC environments and at different times in that environment. For example, the review of existing conformance monitoring automation systems suggest that larger thresholds are required at trajectory transitions than away from transitions, and that different thresholds should be used for aircraft of different equipages. It is not apparent how the threshold values used in these various existing systems were established, but they have all been pre-determined in the form of “look-up” tables, many of which are presented in Chapter 2. However, in principle “smart thresholds” could be employed where real-time observations of individual or group aircraft behaviors were observed over a certain period of time and these observed behavior used to establish appropriate threshold placements.

Setting thresholds on a scalar signal has already been illustrated in the discussion on signal-based fault detection. Establishing thresholds for vector residuals can again be achieved in an analogous fashion to the scalar case, only in state space. Indeed, the use of observed behavior under a presumption of conforming behavior to define thresholds of conforming/non-conforming behavior in vector space have been employed in a closely-spaced parallel approach analysis conducted at MIT [Winder & Kuchar (2001)]. Cross-track and heading errors states relative to the final approach path were recorded and used to establish thresholds in vector space based on three standard deviation statistics from the observed data. This is illustrated in Figure 3.11 alongside the generic scalar decision threshold concept for comparison.



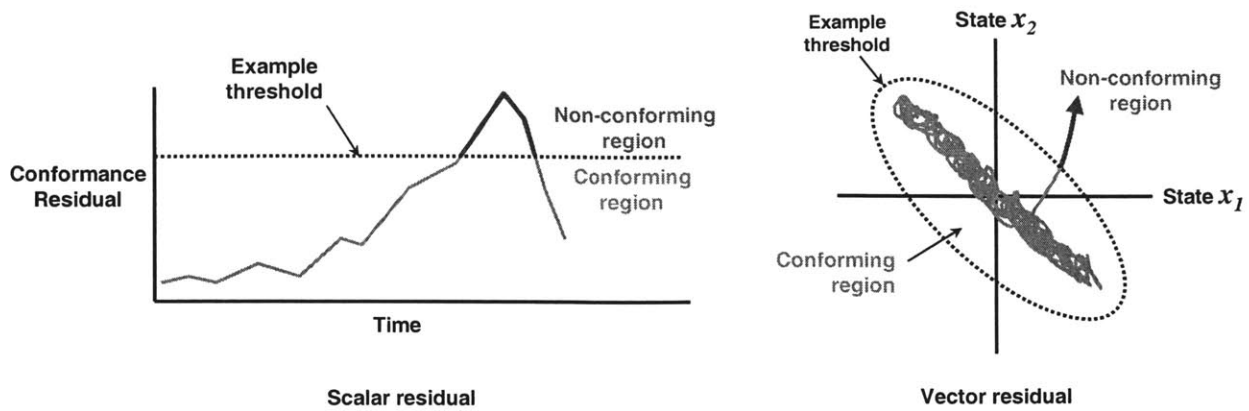


**Figure 3.11: Scalar & Vector Decision Thresholds** [vector case adapted from Winder & Kuchar (2001)]

Note that the threshold strategy can also be employed in a system with multiple alert stages, such as one with a caution stage that is to be issued prior to a full non-conformance alert. This can be achieved by using nested thresholds in both scalar and vector residuals, as illustrated in Figure 3.12.

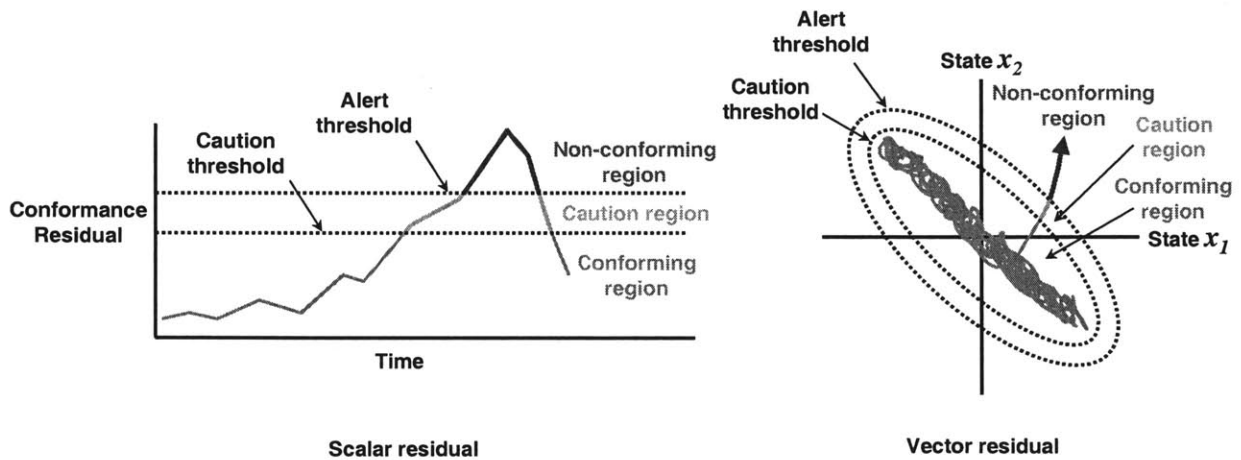


**Figure 3.12: Multiple Alert Stages Enabled by Nested Thresholds**

### 3.4 Designing CMAF Elements to Meet Conformance Monitoring Requirements in ATC

The properties required of a conformance monitoring system vary from one ATC environment to another. For example, rapid detection of a deviant aircraft may be critical to maintaining proper system operation under some conditions, even if it is at the expense of a few false alarms involving an alert of a

deviation when one is not actually occurring. Examples of where this may be the case include during closely-spaced independent parallel approaches or at “critical maneuver” points where the proper conformance to a clearance is critical to maintaining safe separation from other aircraft or high-security regions. However, at other times, rapid detection may be less important than low numbers of false alarms, such as in the en-route domain where aircraft separations are larger (so there is more time to react to a non-conformance) but the high number of aircraft involved means that too many false alarms might reduce the user’s trust in the system.

The various properties required from the conformance monitoring system under different applications can be defined by “figures of merit”. These could include the time-to-detection and false alarms measures discussed above, as well as other quantitative measures like missed detections and maximum deviation values. Figure of merit could also include more abstract measures such as simplicity or cost.

The Conformance Monitoring Analysis Framework allows conformance monitoring approaches to be created and their performance analyzed in terms of a number of these figures of merit. For example, for a given surveillance system, Conformance Monitoring Model and Conformance Residual generation technique, the placement of the decision threshold will affect time-to-detection, false alarm, missed detection and maximum Conformance Residuals figures of merit, while the fidelity of the CMM and the type of Conformance Residual generation technique will affect the overall simplicity of the resulting conformance monitoring system design. The figures of merit can be then used to determine whether the resulting system is appropriate for use in a given ATC application, for example by comparing the specific value of the chosen figure of merit to a target value established for the operation from empirical analysis or operational data. This procedure is illustrated schematically in Figure 3.13. If the achieved figure of merit for the chosen framework implementation meets a specified target, then the design of the resulting conformance monitoring system can be considered acceptable. However, if this figure of merit target is not met, then a re-design of one or more of the elements will be required. For example, the figure of merit used during the development of the PRM system was collision risk after a 30° blunder had occurred, and the calculated risk with chosen system variables was compared to the target collision risk established from accident data.

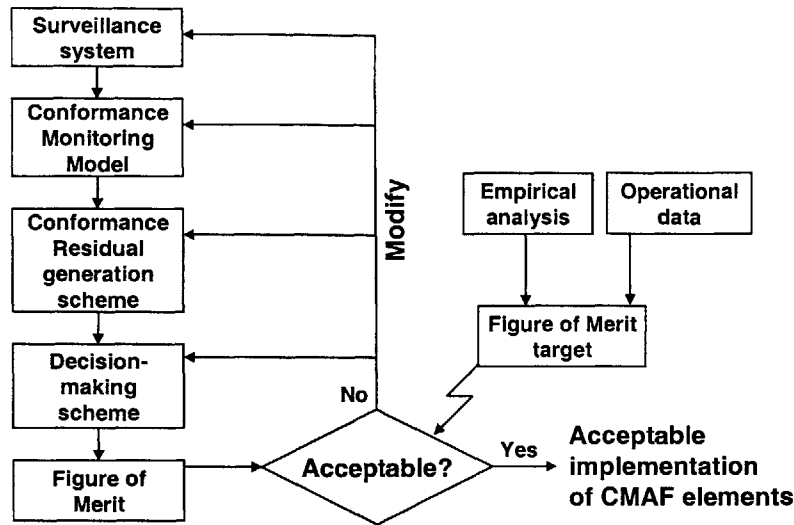


**Figure 3.13: Example Use of Figures of Merit to Determine Appropriate CMAF Implementations**

Under certain circumstances when a figure of merit target is known for a given environment, it can be used to “back-out” appropriate threshold placements and even residual generation schemes that will meet the required level of performance [Yang *et al.* (2003)].

Clearly many figures of merit could be defined for different conformance monitoring applications. Those that will be considered in this document include time-to-detection of a true deviation, false alarms that alert of a deviation when one is not occurring, and a maximum conformance residual metric. Each will be described conceptually in the next sections and then examples of their use will be presented in the following chapters.

### 3.4.1 False Alarm & Time-To-Detection Figures of Merit

Two important figures of merit in the conformance monitoring task are False Alarms (FAs) of alerting non-conformance when the aircraft is actually conforming, and Time-To-Detection (TTD) of an alert of a true non-conformance. These two figures of merit often compete against each other. For example, a small threshold implies rapid detection of a deviation but is susceptible to false alarms created by nominal variations in state behavior of a conforming aircraft due to navigational tracking or ground surveillance system limitations. On the other hand, a large threshold would reduce the false alarm rate but at the expense of much longer time-to-detection of a true deviation. In addition, since the surveillance system and CMM cannot provide a perfectly accurate and complete representation of the processes occurring in the actual system, challenges exist to distinguish effects observed in the residual due to uncertainty introduced from the surveillance system and limited fidelity model, from those due to real

non-conforming behavior. Signal detection theory [e.g. Barkat (1991)] can be used to set thresholds based on False Alarm and Time-To-Detection performance goals. Figure 3.14 illustrates in schematically the general tradeoff that exists when determining appropriate placement for decision thresholds in order to meet certain FA/TTD targets. This representation is analogous to an inverse System Operating Characteristic (SOC) curve that has found widespread application in alerting system design. The SOC curve illustrates the tradeoff of false alarm and correct detection probabilities [Kuchar (1996)] as shown in Figure 3.15.

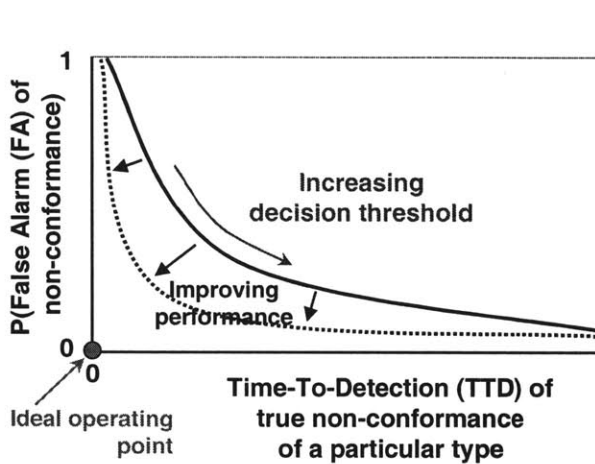


**Figure 3.14: False Alarm/Time-To-Detection Trade-Off Schematic**

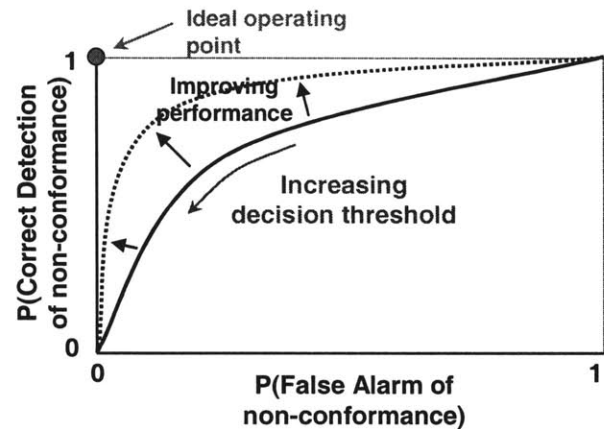


**Figure 3.15: System Operating Characteristic (SOC) Curve Schematic**

On any given curve in these figures, varying the placement of the decision threshold causes the operating point of the decision system to move along the curve as shown. Just as there is an ideal operating point at the top left of the SOC curve, the ideal operating point in the FA/TTD space is in the bottom left hand corner, representing 0% false alarms and immediate detection of a deviant aircraft. The CMAF elements can be designed for improved performance by producing a curve that has a point close to this ideal operating point (e.g. through a combination of the use of proper state information, generation of effective Conformance Residuals together with a reduction in the amount of noise in that residual) and then determining the threshold placement that puts the system operation at that point.

### 3.4.2 Maximum Conformance Residual Figure of Merit

Although the Time-To-Detection and False Alarm metrics are intuitive ones to use to identify conformance monitoring system performance, sometimes it can be problematic to define the start of a deviation and therefore the “zero-time” point required to generate the TTD metric. This is particularly

true when the aircraft performs a slowly evolving deviation rather than a more abrupt blunder type of deviation. For this type of slow deviation, an alternative metric is proposed based on the theoretical maximum Conformance Residual that would exist if the aircraft initiated a “perfect recovery response maneuver” at any given time as illustrated schematically in Figure 3.16.

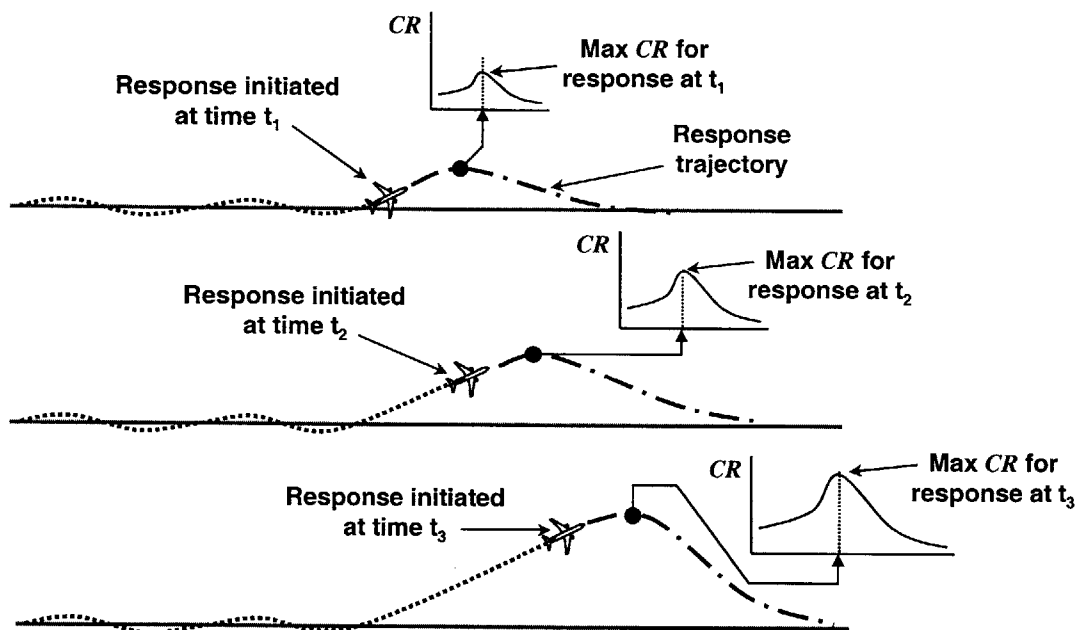


**Figure 3.16: Maximum Conformance Residual Figure of Merit Definition**

The recovery behavior could be based on a knowledge-based heuristic or an explicit dynamic model of the aircraft. This type of metric has the distinct advantage of being definable at all times based on a standard recovery response behavior. Target values could then be set on the maximum allowable Conformance Residual in a given environment. The decision of non-conformance could be made whenever the aircraft could no longer possess a Conformance Residual below that threshold value even if a perfect response was initiated immediately. This is similar to the philosophies contained within the designs of the PRM and FPM tools described earlier. For example, a PRM alert of likely penetration of the NTZ is issued when the aircraft can no longer stay out of that region, while the FPM large deviation tube defines the boundary of recoverable navigation error for an aircraft. Note that a related figure of merit could also be defined based on the *time* to recovery if a perfect recovery response maneuver were conducted at each instant in time and defining a limit of acceptable time to recovery to determine when to issue an alert.

### 3.5 Summary

The Conformance Monitoring Analysis Framework has been presented that applies fault-detection techniques to the conformance monitoring task in ATC. It provides a framework for investigating conformance monitoring issues and developing conformance monitoring methods in the ATC domain. The various elements of the framework have been identified as a Conformance Basis, Actual System Representation, Conformance Monitoring Model, Conformance Residual generation and decision-making schemes. The relationships of each of the elements has been discussed in detail. The various forms of Conformance Basis in ATC have been elucidated. The Actual System Representation was discussed in terms of a classic feedback control representation supplemented by upstream pilot and aircraft intent components representing the future behavior of the aircraft. This representation utilizes the surveillance state vector concept that formalizes the notion of intent and which maintains consistency with real-world ATC operations. Various forms of Conformance Monitoring Model, both analytical and mental in form, have been presented. Finally the conformance monitoring functions have been discussed in terms of several processes as inspired by the fault detection analogy. The various forms of Conformance Residual generation have been discussed in terms of scalar and vector forms, and some examples types of each have been presented. The related issue of setting decision-thresholds to determine when these residuals indicate conforming or non-conforming aircraft behavior has been discussed. The impact that the chosen threshold has on specific figures of merit trade-offs that can be used to design a conformance monitoring system to a level appropriate for conformance monitoring priorities in a given ATC application were also discussed.

---

# CHAPTER 4: Investigating Implementation Issues of the Conformance Monitoring Analysis Framework Elements

---

## 4.1 Introduction

The Conformance Monitoring Analysis Framework presented in the previous Chapter provides a conceptual means by which conformance monitoring research can be conducted. This chapter utilizes specific implementations of the CMAF elements to illustrate several forms of Conformance Monitoring Model, Conformance Residual generation schemes, decision-making techniques and the use of various figures of merit applied to a simple non-conformance event flown during a flight test.

## 4.2 Flight Test Non-Conformance Scenario

### 4.2.1 Flight Test Data Collection

Flight test data was obtained from a flight test of a specially-equipped Boeing 737-400 commercial aircraft illustrated in Figure 4.1. *It should be noted that the test aircraft was in an experimental configuration, so its performance should not be considered representative of the production model.*



**Figure 4.1: Experimental Boeing 737-400 Flight Test Aircraft [photograph courtesy of Boeing]**

The test aircraft was equipped with an ARINC 429<sup>†</sup> databus from which the flight parameters listed in Table 4.1 were recorded at a rate of 10 Hz. The latitude and longitude states available on the ARINC 429 databus were based on the outputs of an IRU system which are susceptible to drift at a rate of approximately 1 nm/hour. Higher accuracy positional states were archived at 1 Hz from a separate GPS system on board the aircraft and which also provided additional states as outlined in Table 4.2. A roll angle state was also calculated from the GPS course over ground state.

**Table 4.1: ARINC 429 Databus Parameters Archived During Flight Test**

Time	GMT (hhmmss)
	Seconds after midnight
Position	Latitude from Left IRU (degs)
	Longitude from Left IRU (degs)
Altitude	Barometric (ft)
	Radar (close to ground only) (ft)
Velocity	Groundspeed (knots)
	Calibrated airspeed (knots)
	Vertical speed (ft/min)
Heading angle	Magnetic (degs)
	True (degs)
Roll angle	(degs)
Pitch angle	(degs)
FMS states	Desired track angle (degs)
	Distance to active FMS waypoint (nm)
	Bearing to active FMS waypoint (degs)
	Destination ETA (hrs, mins)
Deviation states	Cross-track error (nm)
	Vertical deviation (ft)
	ILS localizer deviation (DDM) <sup>*</sup>
	ILS glide slope deviation (DDM) <sup>*</sup>
Environmental states	Wind speed & direction (knots & degs)
	Air temperature (static and total) (°C)
	Pressure (static) (inches Hg)

<sup>†</sup> The ARINC 429 is one of the industry-standard commercial aircraft databus protocols [ARINC (2001)]. Specifically, it defines the local area network protocol for the transfer of digital data over the databus (comprising a pair of twisted/shielded wires) to up to 20 receiving elements that require the information.

<sup>\*</sup> DDM stands for “Difference in Degree of Modulation” and is a measure used for deviations during Instrument Landing System (ILS) approaches. A full description is provided in the discussion of the ILS approach data in Chapter 5.



**Table 4.2: GPS Parameters Archived During Flight Test**

Time (hhmmss)
Latitude (degs)
Longitude (degs)
Altitude (m)
Course over ground (degs)
Speed over ground (knots)

#### 4.2.2 Non-Conformance Scenario

The analyses in this Chapter will focus on a simple lateral non-conformance scenario flown during a test flight that involved a deviation from a straight path. The ground track derived from the aircraft GPS latitude/longitude states was categorized into three segments, as presented in Figure 4.2.

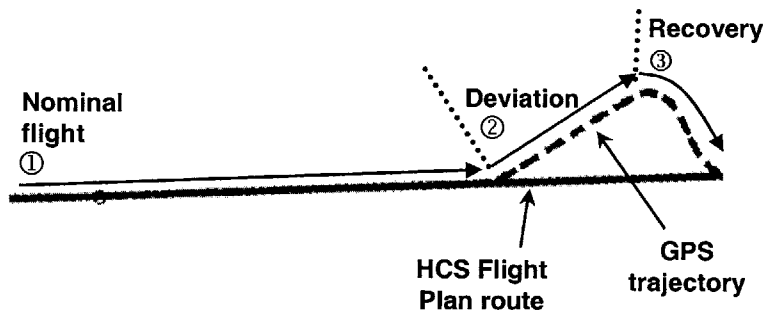


**Figure 4.2: Flight Test Lateral Non-Conformance Scenario**

The non-conformance scenario comprised approximately 10 minutes (600 seconds) of “nominal flight” (segment ①) where the aircraft flew the assigned flight plan trajectory. The pilot then initiated an intentional “deviation” phase (segment ②) where the aircraft was turned left off the HCS flight plan course by 10° until a positional deviation of approximately 3 nm from the flight plan route had been achieved. At this time a “recovery” phase (segment ③) of flight returned the aircraft to the HCS flight plan trajectory.

The dynamic states recorded from the aircraft databus and GPS during each of the segments in the scenario are presented in Figure 4.3. The offset in the position data from the aircraft databus is due to the drift in the IRU system from which the position data is sourced. The autoflight system utilizes both the IRU and the GPS data to track its position and so the IRU data would be ignored in this case. Hence, the GPS position information was combined with the databus heading and roll states to represent a

surveillance system providing the best information available on-board the aircraft at a rate of 1 Hz to a conformance monitoring system.

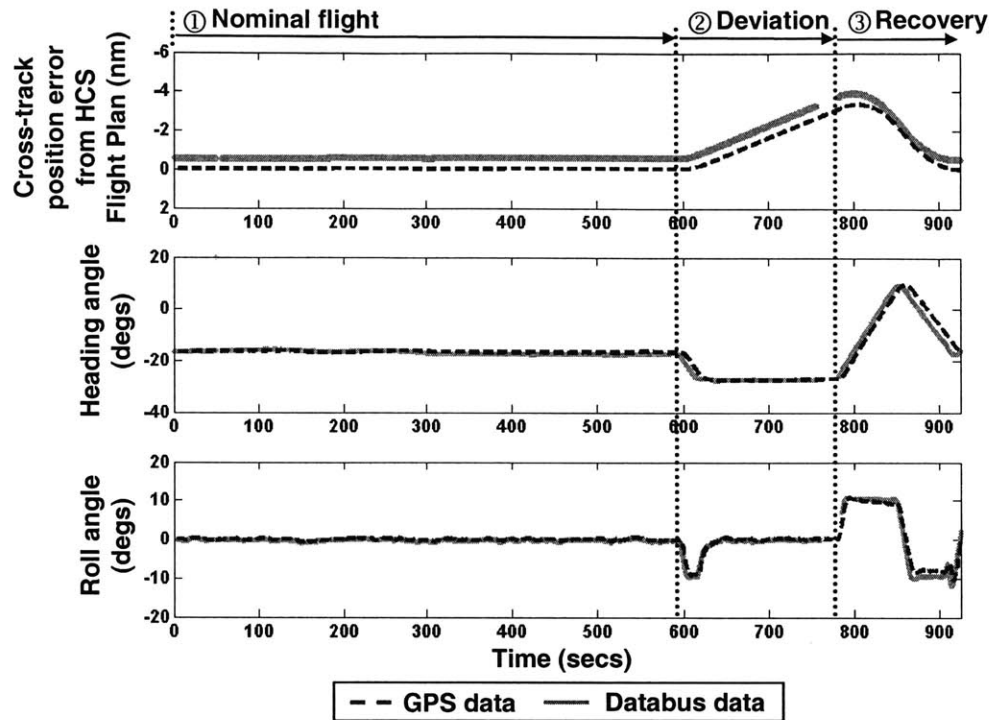


**Figure 4.3: Lateral Non-Conformance Scenario Dynamic States**

Example forms of each Conformance Monitoring Analysis Framework elements discussed in Chapter 3 are used to illustrate its application and the insights that can be gained, specifically in terms of various:

- Conformance Monitoring Models involving low, medium and high fidelity approaches
- Conformance Residual generation techniques, in terms of various forms of scalar functions and a comparison of scalar and vector forms of residual
- Threshold decision-making techniques
- Figures of merit

The demonstrations of the specific element forms presented here are not designed to show that they are necessarily optimal, but to provide a basis for discussion of the wider issues.

### 4.3 Investigating Conformance Monitoring Model Fidelity Issues

In the introduction to Conformance Monitoring Models presented in Chapter 3, various model fidelities were discussed, ranging from simple, low fidelity models where no transition or recovery dynamics were modeled, medium fidelity models where dynamics were based on curve fits to data or heuristics, to high fidelity models of the specific aircraft dynamics under the currently-existing conditions. In this section, a comparison of the performance of various CMM fidelities during the non-conformance scenario will be compared. Since this scenario does not contain a nominal flight plan transition, the comparison will focus on differences during the recovery flight phase of the scenario (segment ③). Transition modeling issues will be discussed in detail in Chapters 5 and 6.

The simple, low fidelity type of CMM incorporates no transition or recovery dynamics into its calculation of the expected state components for the residual generation. Instead, the expectations are based on assumption of what the aircraft states should be at any given time or location if the aircraft was in perfect conformance to the assumed Conformance Basis. For the scenario presented here, the expected states for a perfectly conforming aircraft coming from a low fidelity CMM would be:

- CMM cross track position,  $L_{CMM} = 0$  (i.e. no cross-track position error from flight plan route).
- CMM heading angle,  $\psi_{CMM} = \text{flight plan track angle corrected for wind}$ .
- CMM roll angle,  $\phi_{CMM} = 0$  (i.e. no bank angle so there is no tendency to turn off the flight plan route).

This is the approach implicitly used in many existing automation tools discussed in Chapter 2, where the observed aircraft states are compared to the extrapolated three or four-dimensional position along the flight plan route and the course angle of the current flight plan segment (corrected for wind). However, as discussed briefly in the context of CMM fidelities in the previous chapter, this may not be the best philosophy to adopt during a nominal aircraft transition or after an aircraft deviation from the expected Conformance Basis has occurred since it does not account for any recovery behaviors on the part of the aircraft.

Incorporating expected recovery behaviors into a CMM for an aircraft during a deviation is a complex task, however. A typical lateral trajectory-following autopilot can be represented as a three-loop control system about the cross-track, heading and roll angle errors as illustrated in Figure 4.4. This can be considered a high fidelity CMM since the aircraft dynamics and control loops are explicitly modeled.

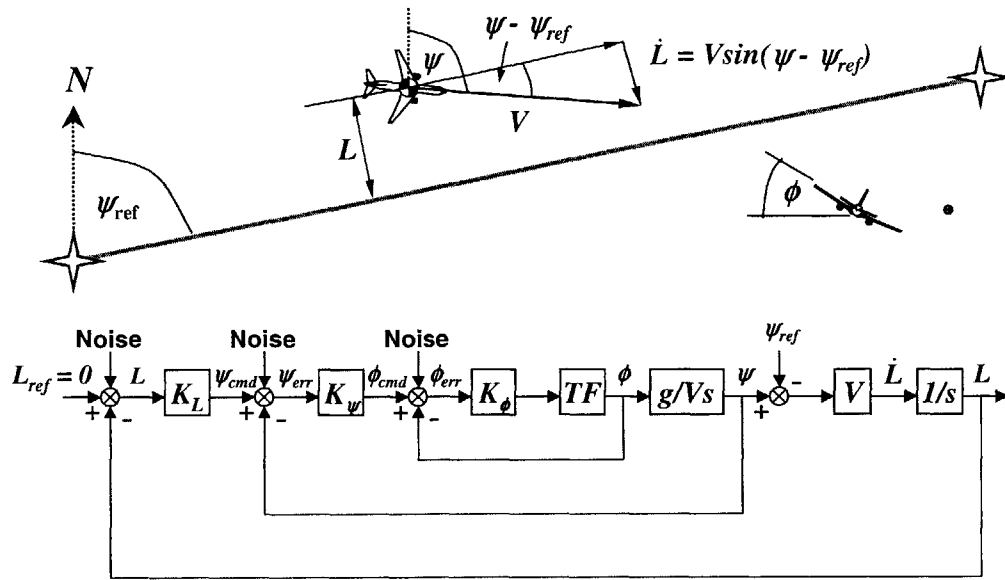


**Figure 4.4: High Fidelity CMM Representation of Trajectory-Following Autopilot**

This representation requires many model parameters to be identified and defined, such as the control loop gains ( $K_L$ ,  $K_\psi$ ,  $K_\phi$ ) and the roll to aileron transfer function ( $TF$ ). Realistic values for many of these parameters are documented for generic aircraft types in a few flight regimes [e.g. Roskam (1995)], but the parameters can vary significantly as functions of aircraft type (e.g. geometry and mass distribution), operating conditions (e.g. speed), aerodynamic configuration (e.g. flap settings) and atmospheric properties (e.g. density, temperature). Therefore, it is challenging to develop realistic simulations of aircraft recovery behaviors. This high level of fidelity is probably unnecessary for most conformance monitoring applications and medium fidelity approaches defining sensible recovery behaviors in the heading and roll states may be sufficient in order to realize some advantage over the low fidelity model that takes no account of aircraft dynamics.

The medium fidelity approach to be demonstrated here involves defining the heading CMM states as a function of observed cross-track error and roll CMM states as a function of the difference between the resulting CMM and observed heading states, as shown in Figure 4.5.

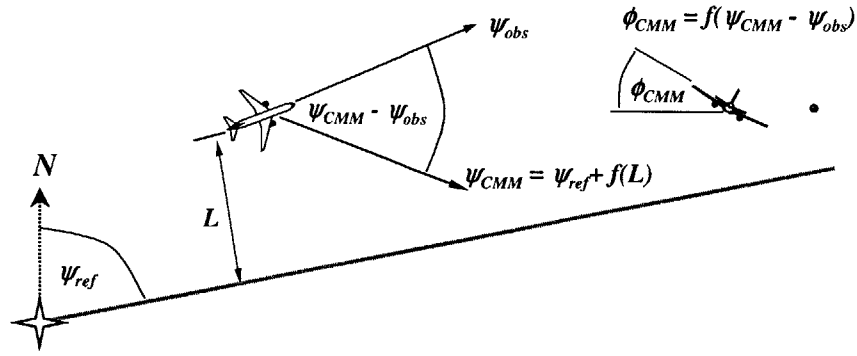


**Figure 4.5: Medium Fidelity CMM Heading and Roll State Behaviors**

In this example, typical heading correction behavior as a function of cross-track error during the recovery response is inferred by curve fitting to the flight test data during the recovery response portion of the flight test scenario, as shown in Figure 4.6. It is seen that a quadratic curve fit is an excellent match to the observed recovery data for  $L \leq -0.05$  nm. Although an explicit model of the aircraft dynamics is not being employed, this is analogous to backing out typical aircraft dynamics, as could be achieved through a machine-learning algorithm that was observing nominal system operation.

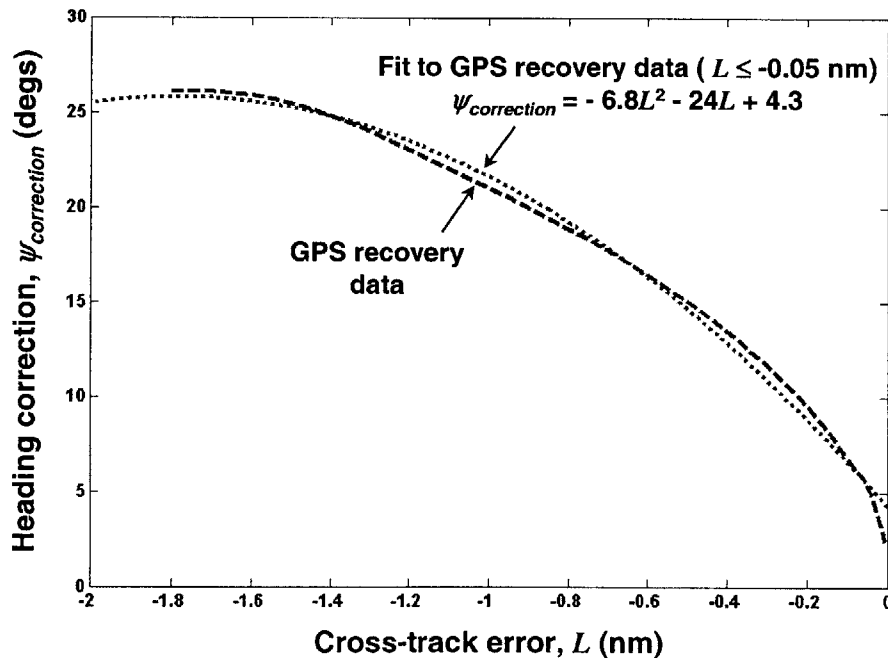


**Figure 4.6: Observed Relationship Between Heading Correction and Cross-Track Error During Recovery Flight Segment**

The medium fidelity CMM heading state during recovery can then be calculated according to:

$$\begin{aligned}
 \psi_{CMM} &= \psi_{ref} + \psi_{correction} \\
 &= \psi_{ref} - 6.8L^2 - 24L + 4.3 \quad \text{for } -2nm < L \leq -0.05nm \\
 &= \psi_{ref} + 25.1 \quad \text{for } L \leq -2nm
 \end{aligned}
 \tag{Equation 4.1}$$

where  $\psi_{ref}$  is the flight plan track angle corrected for wind shown in Figure 4.5. Note that  $\psi_{CMM} = \psi_{ref}$  when no recovery dynamics are included in the CMM, while the extra  $\psi_{correction}$  term is added when recovery dynamics are included.

The expected roll angle,  $\phi_{CMM}$  in the recovery segment was calculated from the difference between the resulting CMM and observed heading states according to [Johnson (1995)]:

$$\phi_{CMM} = \frac{V_{TAS}}{g} \dot{\psi}_{desired} \approx \frac{V_{TAS}}{g} [\psi_{CMM}(t+1) - \psi_{obs}(t)]
 \tag{Equation 4.2}$$

where  $V_{TAS}$  is the true airspeed,  $g$  is acceleration due to gravity and  $\dot{\psi}_{desired}$  is the desired heading change rate. The roll angle is limited to any bank angle limit imposed on the aircraft:  $\pm 10^\circ$  in the case of the flight test aircraft. Note that  $\phi_{CMM} = 0$  when no recovery dynamics are included in the CMM, while the term defined above is used when recovery dynamics are included.

A comparison of the magnitude of the differences between the observed and expected heading and roll states for the low and medium fidelity CMM types (i.e. with and without a recovery dynamics) are presented in Figure 4.7. Several effects are visible. Firstly, the inclusion of the recovery dynamics in the medium fidelity CMM accentuates the difference between the observed and expected states during the deviant behavior region (segment ②) relative to the low fidelity CMM. Secondly, during the recovery portion (segment ③), the state errors (especially roll) values are considerably lower with the medium fidelity CMM relative to the low fidelity CMM. Conformance Residuals based on the differences between observed and expected states would therefore generally produce desirable results of larger residuals in the truly deviant portion of the flight and smaller residuals during the recovery portion with the medium fidelity CMM relative to the low fidelity CMM.

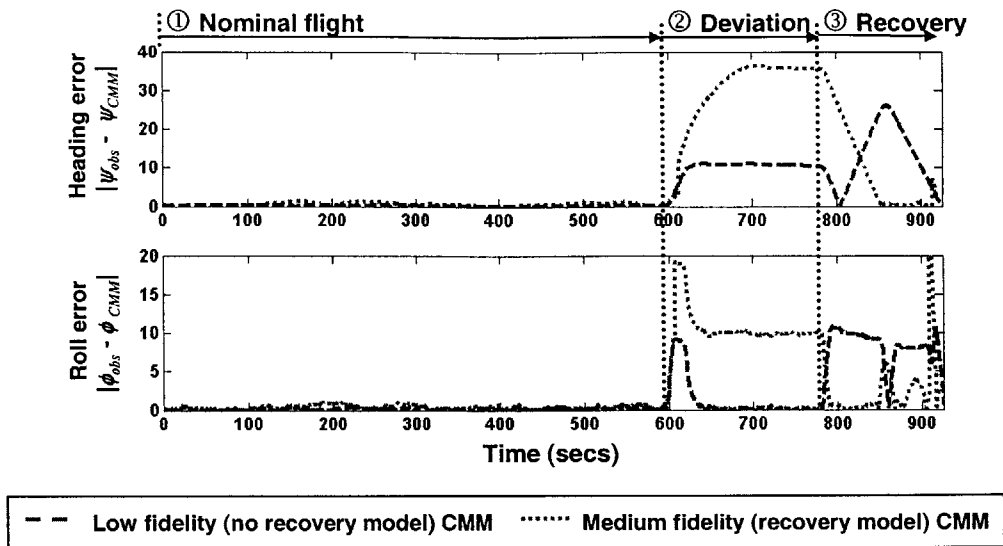


**Figure 4.7: Heading and Roll State Errors for Low & Medium Fidelity CMMs**

The problems with using models that attempt to capture recovery behaviors are that they are often very case-specific and so may not be as effective as the more simple non-recovery CMM in some circumstances. The curve fit model used in this example may not produce comparably small state errors under different circumstances. Even this model based on a curve fit of the actual behavior was not effective at capturing all the recovery behaviors: right after the recovery was initiated (i.e. the transition from segment ② to ③), the difference between the observed and expected heading states are actually larger for the medium fidelity CMM case than the much simpler low fidelity CMM case for about 60 seconds after recovery had started. Similarly, the spikes visible in the roll state error during the recovery segment are likely caused by poor modeling of the “roll-in” and “roll-out” behavior as the desired heading is captured by the autoflight dynamics. These types of problems indicate why it is often desirable to stay with the simpler low fidelity CMM in many conformance monitoring applications, especially since both low and medium fidelity CMMs produce comparable results for nominal conforming behavior, while the low fidelity CMM is, of course, much simpler to develop and use.

This discussion has concentrated on the issues of modeling recovery behavior after a deviation has occurred. Equally, if not more, important is the more common issue of properly modeling nominal transitions in the flight path, such as lateral turns at waypoints, vertical transitions during altitude changes and longitudinal transitions during speed changes. These issues will be examined in detail in the context of the operational and simulated data analysis presented in the next two Chapters.

## 4.4 Investigating Conformance Residual Generation Issues

### 4.4.1 Absolute Linear vs. Quadratic Scalar Functions Example

The main properties of the absolute linear and quadratic scalar residuals were outlined in Chapter 3. Absolute linear functions benefit from the linear mapping between aircraft and residual behaviors, while the quadratic functions are more widely employed in control applications for damping out small deviations while accentuating more major ones. These properties are demonstrated here in the context of the non-conformance test scenario with the general Conformance Residual forms of:

$$\begin{aligned}
 CR_{absolute\ linear} &= \frac{\sum WF_x |x_{obs} - x_{CMM}|}{n} \\
 CR_{quadratic} &= \frac{\sum WF_x [x_{obs} - x_{CMM}]^2}{n}
 \end{aligned}
 \tag{Equations 4.3}$$

In order to generate Conformance Residuals using these functions, the weighting factors  $WF_x$  need to be determined to account for nominal variations in the various dynamic states. As described in Section 3.3.4, one way to determine appropriate weighting factors is to establish bounds on the state values under nominal conforming behavior. This can be achieved through the use of the standard deviation ( $\sigma$ ) in the nominal state variations: Figure 4.8 illustrates the nominal flight segment variations for this scenario. If the state variations are normally-distributed, then weighting factors equal to  $1/2\sigma$  would be consistent with the 95% confidence interval philosophy contained within the Required Navigational Performance (RNP) described in earlier chapters. This method was used here, with resulting weighting factors shown in Table 4.3. These were then used in the generation of the sample Conformance Residuals components using the absolute linear and quadratic functions in Figure 4.9 for segment ① and for the entire deviation scenario in Figure 4.10.

**Table 4.3: Non-Conformance Scenario Weighting Factors**

Weighting Factor	Nominal Flight Segment $1/2\sigma$
$WF_L$	1 / 0.05 nm
$WF_v$	1 / 1.12°
$WF_d$	1 / 0.52°



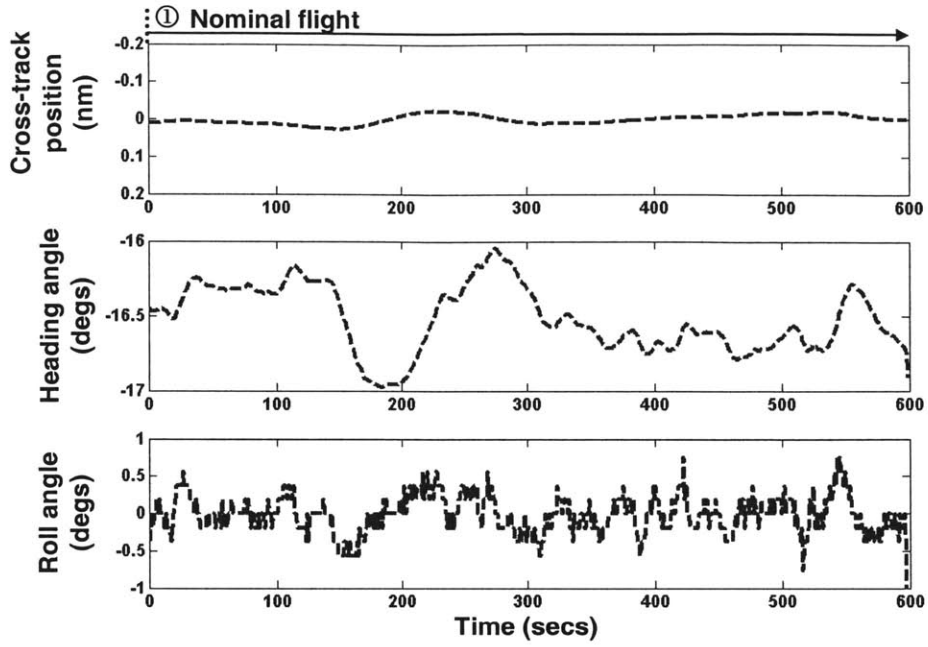


Figure 4.8: Dynamic State Variations During Nominal Flight Segment

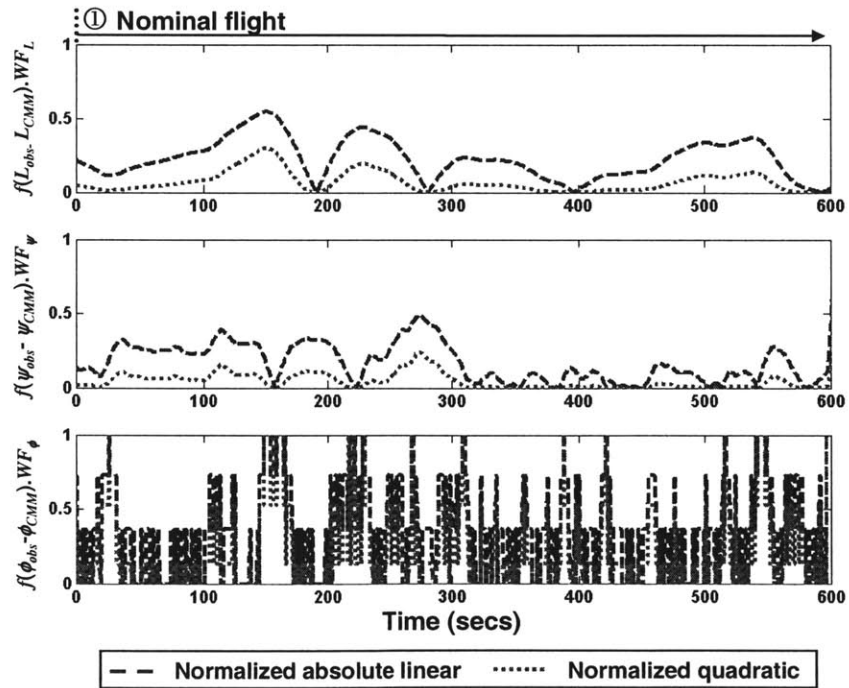
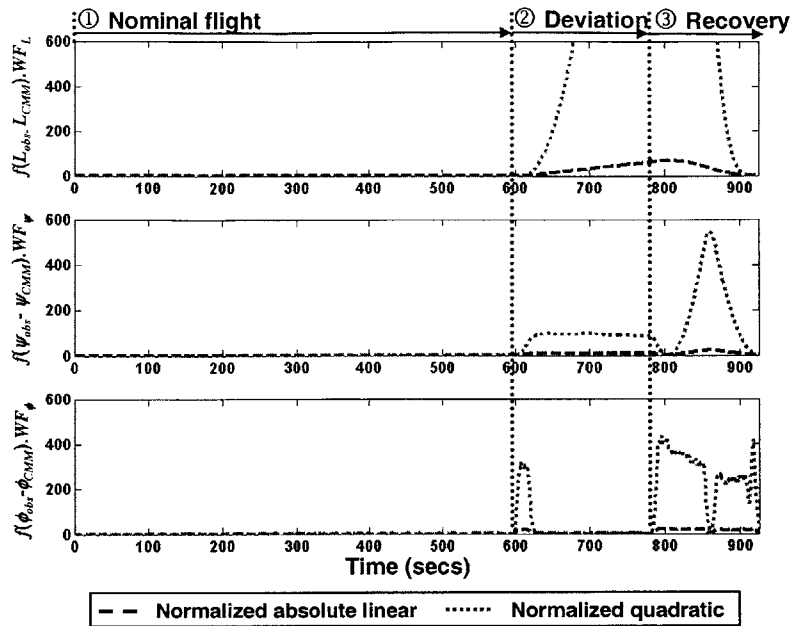


Figure 4.9: Absolute Linear vs. Quadratic Scalar Function During Nominal Flight Segment



**Figure 4.10: Absolute Linear vs. Quadratic Scalar Function for Entire Non-Conformance Scenario**

These results vividly demonstrate the relative properties of the two approaches. The normalized absolute linear function approach displays a value in each state that is directly proportional to the difference between the expected and the observed value of that state normalized to the nominal variation. So, for example, a value of  $|L| = 0.5$  indicates a cross-track deviation that is half of the nominal variation that could be expected in that state during conforming behavior. A value of  $|L| = 0.25$  indicates a cross-track deviation that is half of the previous case. This property may be desirable in the interpretation of relative Conformance Residual values and to aid in the setting of appropriate weighting factors. The normalized quadratic function lacks this property, but does have the property of greatly accentuating the difference between behavior within the nominal state variation range and behavior outside of that range. As discussed in Chapter 3, a Conformance Residual could easily be defined that combines the quadratic function for small deviations and a linear function for larger deviations. In that way, small state deviations would be damped out, while the residual would be proportional to the deviations in the larger deviation regime.

#### 4.4.2 Scalar vs. Vector Forms Example

The scalar residual provides a simple numerical representation of the amount of deviation that is evident in the observed states used to generate the residual. An example scalar residual defined by an absolute linear function utilizing normalization on the cross-track and heading error states is used here:

$$CR = \frac{\left[ \frac{|L_{obs} - L_{CMM}|}{0.05} + \frac{|\psi_{obs} - \psi_{CMM}|}{1.12} \right]}{2} \quad \text{Equation 4.4}$$

This Conformance Residual for the non-conformance scenario is presented in Figure 4.11 for a simple form of CMM that does not include recovery dynamics.

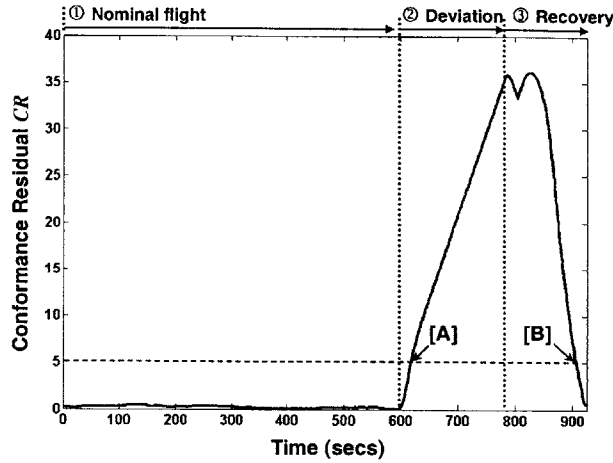


Figure 4.11: Example Scalar Conformance Residual

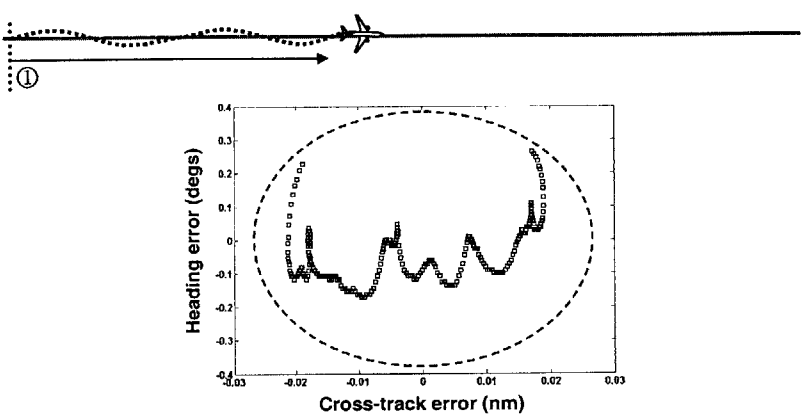
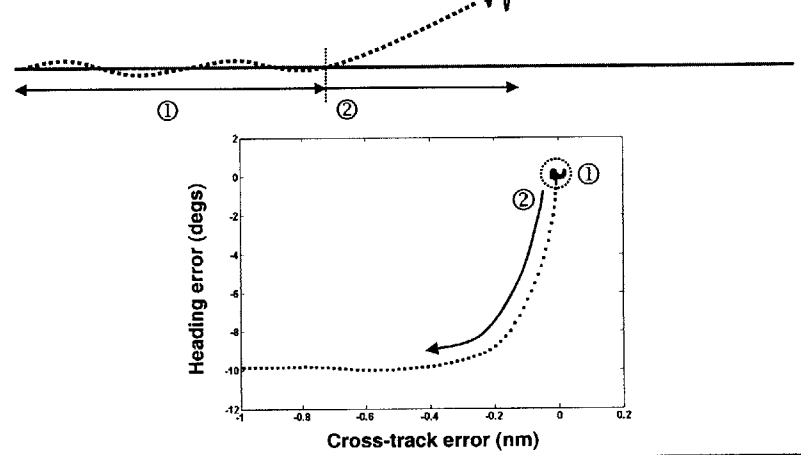
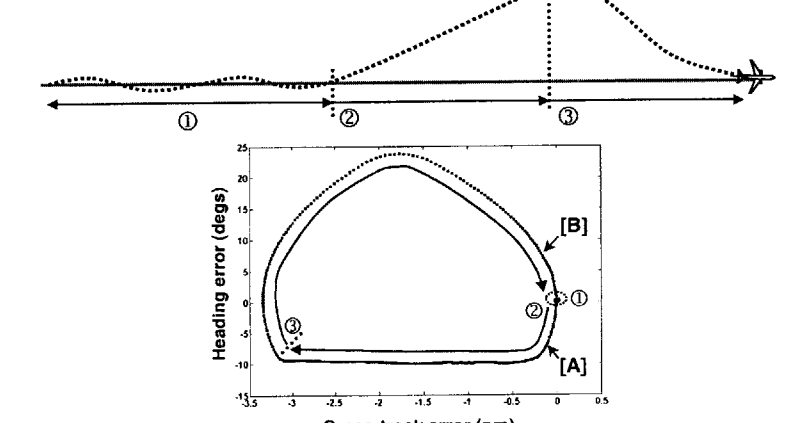
The simplicity of the scalar residual does come at the expense of losing specific information about the observed situation at any given point in time. For example, the two points marked [A] and [B] in Figure 4.11 represent very different conformance behaviors for the aircraft (point [A] being in the deviation phase and point [B] being in the recovery phase), but each has exactly the same scalar Conformance Residual value in this case.

In order to distinguish the specific different behaviors at these two points, a vector representation is most effective. A vector can be defined whose components are the differences between the observed and expected behaviors in each state. Table 4.4 illustrates the evolution of a two-dimensional vector composed of cross-track and heading error components for the non-conformance scenario, i.e.:

$$\underline{CR}_{vector} = \begin{Bmatrix} L_{obs} - L_{CMM} \\ \psi_{obs} - \psi_{CMM} \end{Bmatrix} \quad \text{Equation 4.5}$$

Figure 4.12 shows the effect of adding the roll angle error to form a 3D vector for the complete scenario. The different aircraft behaviors throughout the various segments, and at the points marked [A] and [B] are now clearly distinguishable.

**Table 4.4: Evolution of Vector Residuals During Lateral Non-Conformance Scenario**

Segment	Vector Residual
<p style="text-align: center;">Segment 1: Nominal Flight</p>	
<p style="text-align: center;">Segment 2: Deviation</p>	
<p style="text-align: center;">Segment 3: Recovery</p>	

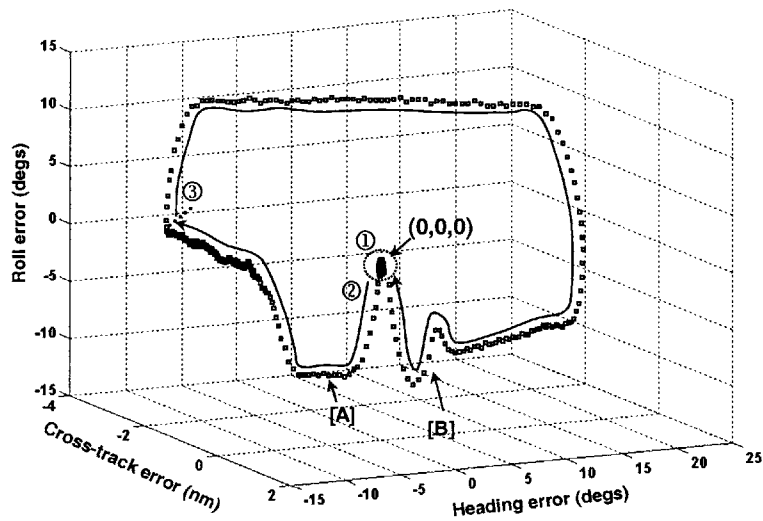


**Figure 4.12: Example 3D Vector Conformance Residual**

The vector components in the preceding figures are the straight differences between the observed and expected behaviors in each state. However, these can be normalized just as the scalar components were, by defining nominal behavior thresholds. One such threshold around nominal behaviors in vector space is shown in the top figure of Table 4.4. Such a threshold would preserve the shape of the vectors displayed in the figures but would re-scale the axes according to the weighting factor values.

It is apparent that the vector approach provides the capability to distinguish the specific behaviors at various times and a limited ability to infer future behavior a short time in advance due to the lead provided from the higher order dynamic states. This may be a highly desirable attribute under certain conformance monitoring circumstances, such as diagnosing the type of non-conformance behavior (if any exists). However, in more general monitoring applications, the simplicity and intuitiveness associated with a scalar residual may be more desirable. In addition, the ambiguity associated with various state combinations resulting in a similar scalar Conformance Residual value is only really an instantaneous problem. The instantaneous observation of the residual relative to previous and future evolutions of the residual (e.g. to determine whether the residual is increasing or decreasing at the time of the observation) would provide sufficient context to ameliorate many of the problems. For example, other combined or parallel Conformance Residual schemes could easily be developed that utilize the derivative and/or integral of the state behaviors. Examples are illustrated in Figure 4.13 for the cross-track error state,  $L$ .

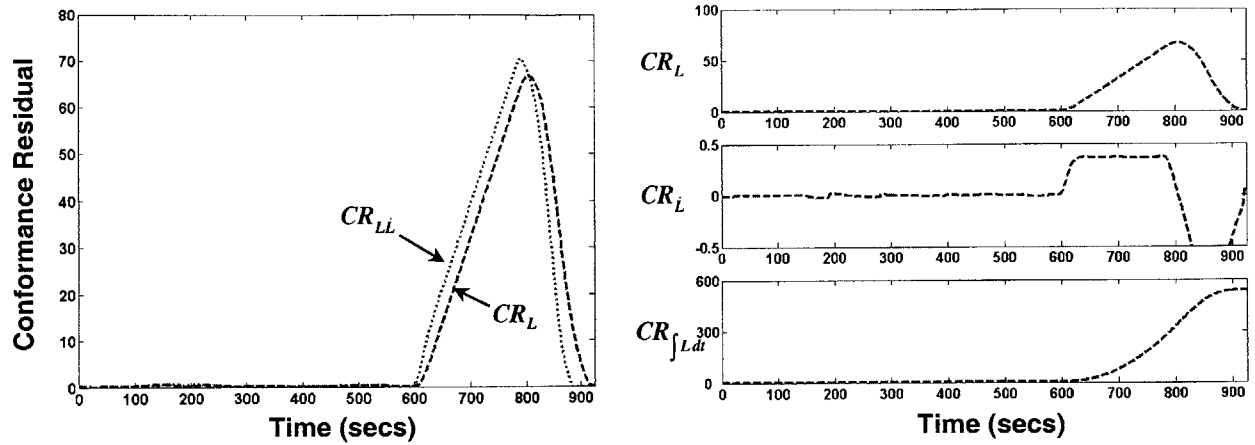


**Figure 4.13: Combined & Parallel Conformance Residuals Using Derivative and Integral Functions**

A combined Conformance Residual utilizing both cross-track position and its derivative (annotated as  $CR_{LL}$ ) is shown on the left side of Figure 4.13. This combined residual was calculated according to:

$$CR_{LL} = \frac{|L_{obs} - L_{CMM}|}{0.05} + \frac{dL/dt}{0.0025} \quad \text{Equation 4.6}$$

The effect of the derivative is to increase the Conformance Residual value relative to the no derivative case when the aircraft is in the deviant phase and to reduce it in the recovery phase. Note that the weighting factor on the derivative could be varied to accentuate or reduce the effect of the derivative element of the residual. Of course the addition of the derivative element is comparable to the use of a heading state with a suitable weighting factor since the rate of change of the cross-track error is proportional to the aircraft heading state. The effects of the derivative, and also the integral of a suitable Conformance Residual could also be examined in parallel, as shown on the right of Figure 4.13. The top Conformance Residual could be used as an instantaneous measure of the conformance status of the aircraft, the derivative could be used as an indication of whether the aircraft is deviating further or recovering, while the integral measure could be used as an indication of the total deviation accrued over a certain period of time. The different proportional, integral and derivative (PID) aspects of these residuals could be considered separately or combined as desired.

## 4.5 Investigating Decision-Making & Figure of Merit Issues

In order to make a determination of whether an aircraft is conforming or not, a decision must be made based on the characteristics of the Conformance Residual. The most common form of decision-making strategy involves the use of a threshold, with the outcome of the decision changing as the threshold is crossed. Chapter 3 described in detail how different threshold settings can change the performance of the conformance monitoring function relative to certain figures of merit. This section will use the lateral non-conformance scenario with example implementations of the other elements of the Conformance Monitoring Analysis Framework to illustrate the threshold-based decision-making approach and two types of figures of merit: a False Alarm/Time-To-Detection tradeoff and a maximum Conformance Residual measure.

### 4.5.1 False Alarm/Time-To-Detection Figure of Merit Example

The lateral non-conformance scenario is investigated here with the following CMAF elements:

- Conformance Basis: the HCS flight plan route.
- Conformance Monitoring Model: simplest form of CMM where the expected states were determined from an assessment of what they would be for a perfectly conforming aircraft with no disturbances, i.e.  $L_{CMM} = 0$  nm,  $\psi_{CMM} =$  route track angle corrected for wind and  $\phi_{CMM} = 0^\circ$ .
- Conformance Residual generation scheme: example absolute linear function scalar of form

$$CR = \frac{\sum WF_x |x_{obs} - x_{CMM}|}{n} \quad \text{Equation 4.7}$$

In order to investigate the influence of using different state combinations, Conformance Residuals were generated using lateral cross-track position ( $L$ ) only (i.e. representative of the simple position-based criteria used today); position and heading ( $\psi$ ); and position, heading and roll ( $\phi$ ) according to the equations:

$$\begin{aligned} CR_L &= WF_L |L_{obs} - L_{CMM}| \\ CR_{L\psi} &= \frac{WF_L |L_{obs} - L_{CMM}| + WF_\psi |\psi_{obs} - \psi_{CMM}|}{2} \\ CR_{L\psi\phi} &= \frac{WF_L |L_{obs} - L_{CMM}| + WF_\psi |\psi_{obs} - \psi_{CMM}| + WF_\phi |\phi_{obs} - \phi_{CMM}|}{3} \end{aligned} \quad \text{Equations 4.8}$$

The subscripts on  $CR$  are used to identify the states being used in that Conformance Residual. This convention is used throughout the rest of this document. Residuals with these forms were generated using data archived from the aircraft during the non-conformance scenario. The weighting factors for each state were inferred from twice the standard deviation ( $2\sigma$ ) of each state error observed in the aircraft data during the nominal flight phase as before. The resulting Conformance Residuals based on these assumptions are presented in Figure 4.14. The residuals are plotted relative to the time of the start of the deviation established from evaluation of the aircraft roll state.

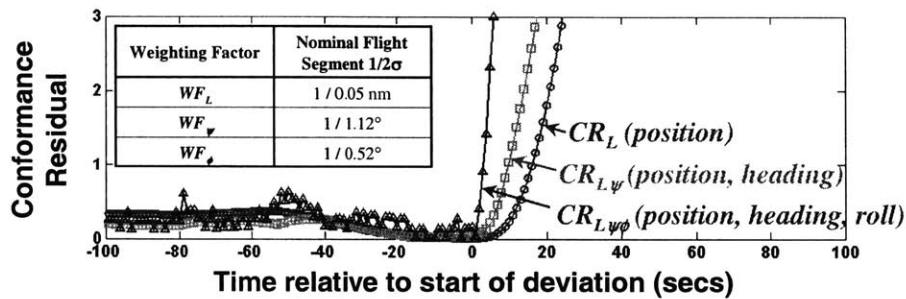


Figure 4.14: Lateral Non-Conformance Scenario Conformance Residuals

The Conformance Residuals resulting from this scenario with the assumptions for the other elements of the CMAF outlined above form a basis for making a decision of the conformance status of an aircraft. The generic threshold-based decision-making strategy is outlined in Figure 4.15.

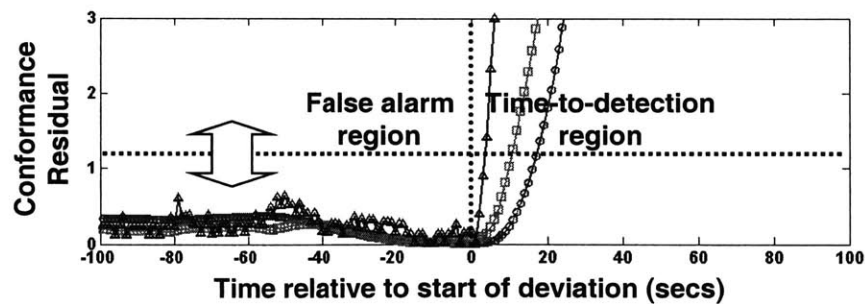
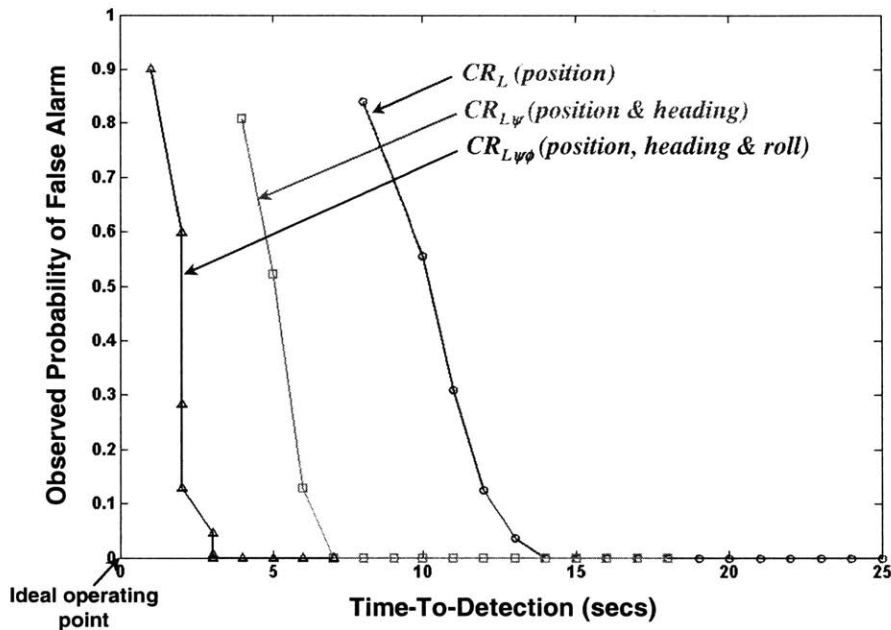


Figure 4.15: Generic Threshold-Based Decision-Making Strategy

Assuming that non-conformance is declared when the Conformance Residual exceeds the threshold value, as the threshold is moved up and down the Conformance Residual axis the performance of the decision-making will change. In this example, the performance is measured relative to the chosen figures



of merit of the probability of false alarm (i.e. declaring non-conformance when the aircraft is conforming) and time-to-detection of a true non-conformance. These metrics were calculated from the Conformance Residuals above. For a given threshold value, the observed proportion of Conformance Residual values above the threshold in the nominal region (negative times relative to the start of the deviation) is a measure of observed probability of false alarm. The time-to-detection was considered to be the first update time after the Conformance Residual exceeded the threshold value in the deviation (positive time) region of flight. Different False Alarm/Time-To-Detection (FA/TTD) metrics will therefore exist for each threshold location, and FA/TTD curves can be traced out as the threshold location is increased from low to high values. Curves for the non-conformance scenario with the three Conformance Residuals using different state combinations outlined above are shown in Figure 4.16.



**Figure 4.16: Lateral Non-Conformance False Alarm/Time-To-Detection Metrics**

Recalling that the ideal operating point is in the lower left hand corner of the above metric space (representing zero false alarms when the aircraft is conforming and immediate non-conformance detection), the relative placement of the curves with respect to this point gives an indication of the performance the overall CMAF implementation. The curves using higher order dynamic states have points closer to the ideal operating point, suggesting superior performance of these residuals relative to those using position alone. The implications of these results in this, and many other ATC scenarios, are discussed in detail in the next Chapters, so further discussion will not be included here.

#### 4.5.2 Maximum Conformance Residual Figure of Merit Example

As discussed in Chapter 3, a potential problem with the previous figures of merit is that under some conditions it can be difficult to define the start time of a deviation from which a time-to-detection measure can be calculated. This is especially true for non-conformance scenarios that do not involve a sudden deviation action, but rather a more slowly-evolving situation that gradually turns into a non-conformance event. An alternate figure of merit that does not suffer from this problem was proposed based on a *perfect recovery response maneuver being initiated at a given time* and then setting a threshold on the maximum Conformance Residual that is allowable in a given environment. Exceedance of this threshold would imply that the aircraft was no longer capable of behaving acceptably, even if an ideal recovery were initiated immediately. A method is demonstrated here for calculating such a metric for the lateral non-conformance scenario.

In order to calculate the maximum Conformance Residual figure of merit, the following procedure was developed for each point in time:

1. Read current aircraft states (e.g. cross-track position and heading states).
2. Extrapolate aircraft states along standard recovery trajectory into the future (see Figure 4.17).
3. Calculate Conformance Residual along recovery trajectory using chosen residual generation scheme.
4. Find maximum Conformance Residual along recovery trajectory from current time,  $t$  ( $CR_{max}(t)$ ).
5. Compare with target  $CR_{max}(t)$  given ATC operation.

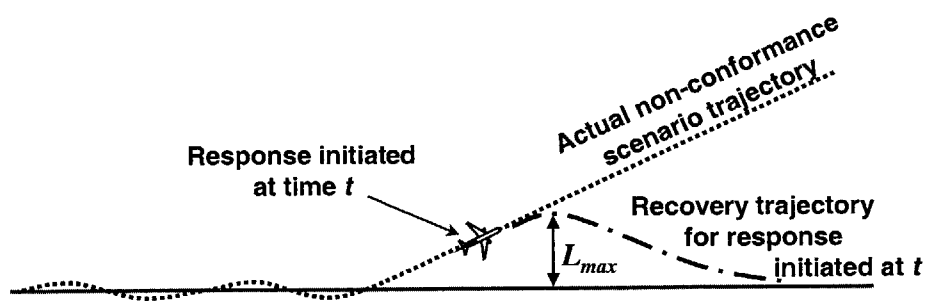


Figure 4.17: Recovery Trajectory in Maximum Conformance Residual Figure of Merit

The major challenge with implementing this approach is to establish the protocol for the recovery response maneuver. Just as there are various model fidelities that can be employed in the Conformance Monitoring Model, so too various recovery response model fidelities can be employed here. These can

range from full dynamic models of the aircraft and autoflight dynamics during the recovery, to more simple point-mass models. The recovery response dynamics used to analyze the non-conformance scenario were based on standard turn dynamics. Given that the flight test aircraft was using a  $\pm 10^\circ$  bank angle limit, the heading change rate was limited to  $\pm 0.54^\circ/\text{second}$  (from Equation 4.2). For simplicity, the chosen Conformance Residual generation scheme consisted of a simple position-based absolute linear scalar, appropriately weighted as before:

$$CR_L = WF_L |L_{obs} - L_{CMM}| \quad \text{Equation 4.9}$$

Therefore, the maximum Conformance Residual for the response trajectory occurred at the extrapolation time coinciding with the maximum cross-track position of the recovery trajectory (shown as  $L_{max}$  in Figure 4.17). State extrapolation out from time,  $t$  along the recovery response trajectory therefore consisted of:

$$\begin{aligned} \psi(t+1) &= \psi(t) + 0.54 \\ L(t+1) &= L(t) + V_{TAS} \sin(\psi(t) - \psi_{ref}) \\ \text{repeat until } L(t+1) &< L(t) \text{ indicating } L(t) = L_{max} \end{aligned} \quad \text{Equation 4.10}$$

For simplicity, the roll angle state was not considered in the analysis undertaken here, but it could be included if desired. The resulting maximum Conformance Residual figure of merit ( $CR_{max}$ ) for the non-conformance scenario is presented in Figure 4.18. The standard  $CR_L$  values for the actual non-conformance trajectory flown are also included for comparison. In the nominal flight segment, there is no recovery behavior to be modeled, so the two curves are very similar. However, during the deviation flight segment, there is an offset between the two curves. This represents the extra Conformance Residual increase from the current  $CR_L$  due to the response maneuver if it were initiated at that time. An example is shown in Figure 4.18: at time = 650 seconds, the maximum Conformance Residual would be approximately 17 on this scale if the response maneuver were initiated at that time, compared to an actual Conformance Residual of approximately 13 that currently existed. In the recovery flight segment, the aircraft is already following a recovery trajectory, so the maximum Conformance Residual in this segment overlays the  $CR_L$  plot, i.e. the current Conformance Residual at all times is higher than anything along the extrapolated trajectory.

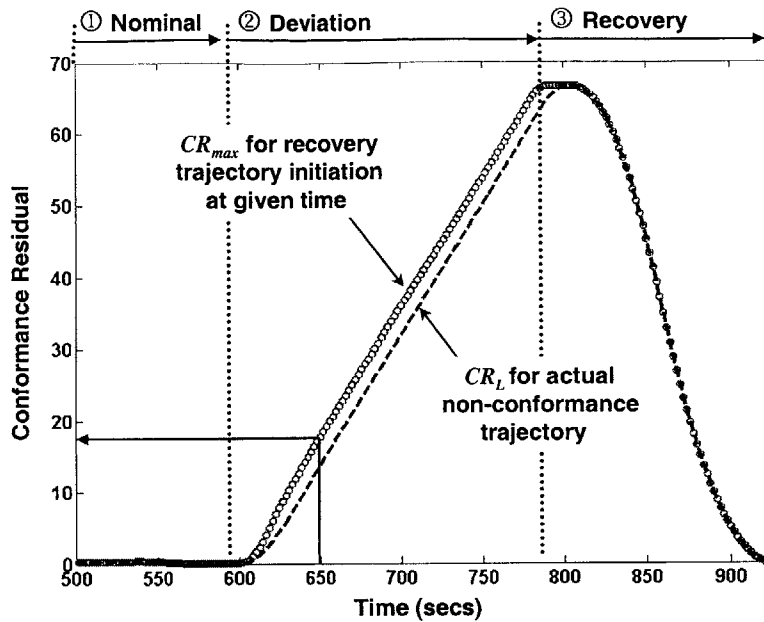


**Figure 4.18: Lateral Non-Conformance Maximum Conformance Residual Figure of Merit**

This procedure can act as a basis for determining decision-making threshold for a given ATC application. When the aircraft can no longer possess a Conformance Residual lower than that acceptable for a given application, then a decision of unacceptable non-conformance can be made. For example, in the close-spaced parallel approach scenario, when the aircraft is no longer capable of staying outside of a No Transgression Zone (even if it is not currently inside it), then it would be appropriate to declare non-conformance.

## 4.6 Summary

Several forms of each element of the Conformance Monitoring Analysis Framework have been demonstrated in this Chapter in order to compare and contrast different implementations under a simple non-conformance scenario flown by a commercial aircraft during a flight test.

Firstly, Conformance Monitoring Model fidelity issues were explored by comparing a simple low fidelity CMM (where state expectations were based exclusively on the Conformance Basis trajectory) and a more sophisticated medium fidelity CMM that included a model of recovery behavior based on curve-fit parameters. The latter model was found to be effective at accentuating the differences between observed and expected state behaviors during the deviation flight segment and reducing the errors during the

recovery portion. However, these advantages would be reduced (or potentially even negated) if the same model were applied to a different non-conformance scenario since the model would have to be re-tuned. The results illustrate the potential power of using higher fidelity Conformance Monitoring Models, but these potential advantages come at the expense of significantly more complicated CMM development.

Secondly, different Conformance Residual generation schemes have been examined. Differences between absolute linear and quadratic scalar functions have been illustrated, especially the former's simplicity and the latter's characteristics of damping out small differences from an operating point while amplifying those far away. An examination of the non-conformance scenario flight segments using a two and three-dimensional vector Conformance Residual was also conducted to illustrate how characteristics masked in a scalar residual can be made visible in a vector form. Combined or parallel use of other functions, particularly derivative and integral information was also demonstrated. In all cases, the use of weighting factors based on observed nominal performance was found to be an effective technique for combining different states together while expanding on the confidence interval philosophy contained in the Required Navigation Performance concept.

Finally, different decision-making and figure of merit issues were examined using threshold-based decision-making, False Alarm/Time-To-Detection and maximum Conformance Residual metrics. The FA/TTD figure of merit was found to be effective at examining the relative performance of different CMAF implementations under scenarios where a non-conformance event start time could be defined and allowed for comparison with FA/TTD targets if they existed for given ATC applications. The maximum Conformance Residual figure of merit was demonstrated as a possible alternative approach which can be defined at all times and compared to target values in given ATC applications and which does not depend on knowledge of the specific start time of a non-conformance event.

[This page intentionally left blank]

---

# CHAPTER 5: Investigating Conformance Monitoring Issues Using the Analysis Framework & Operational ATC Data

---

## 5.1 Introduction

A variety of different implementations of the Conformance Monitoring Analysis Framework elements for a single lateral non-conformance scenario were presented in the previous Chapter. In this Chapter, simple implementations of the different elements of the framework are used to investigate conformance monitoring issues under a variety of different scenarios that occurred in the actual ATC system during the course of two test flights with a commercial jet aircraft. Data from the aircraft databus and GPS systems, as well as ground-based radar surveillance systems were analyzed in the MATLAB<sup>†</sup> computing environment for this purpose, as illustrated in Figure 5.1. This provided an opportunity to compare conformance monitoring approaches in today's radar surveillance environment with an environment where aircraft-derived data may also be available (such as through ADS-B) in a range of flight regimes. It also enabled fundamental insights to be gained with regard to conformance monitoring issues in the operational ATC system.

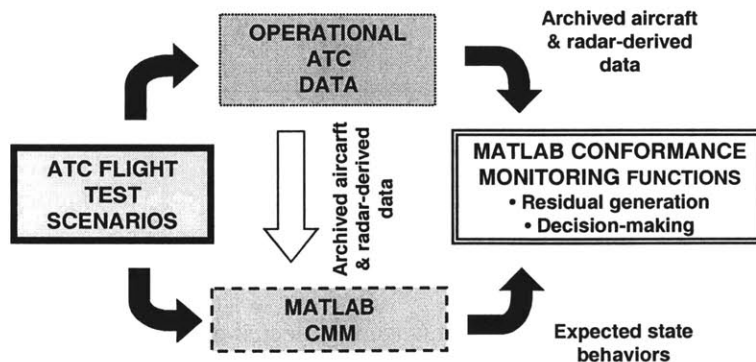


Figure 5.1: Implementation of Analysis Framework Using Operational Data

---

<sup>†</sup> MATLAB is a registered trademark of The MathWorks, Inc.

## 5.2 Operational ATC Data Collection

The test aircraft was the same specially-equipped Boeing 737-400 used in the non-conformance scenario discussed in Chapter 4. However, in this Chapter, operational data is analyzed from two complete test flights conducted by the Boeing ATM group during January and February 2003. It is reiterated that *the test aircraft was in an experimental configuration, so any performance characteristics observed during these test flights should not be considered representative of the production aircraft model*. Each of the two flights originated from and returned to Boeing Field/King County International Airport (BFI) near Seattle, WA and lasted several hours. During the flights, the aircraft flew various flight profiles over the north-western portion of the United States as illustrated in Figure 5.2. The flight tests also included a number of lateral and vertical deviations (conducted with the agreement of ATC) that provide an opportunity to test non-conformance detection algorithms.

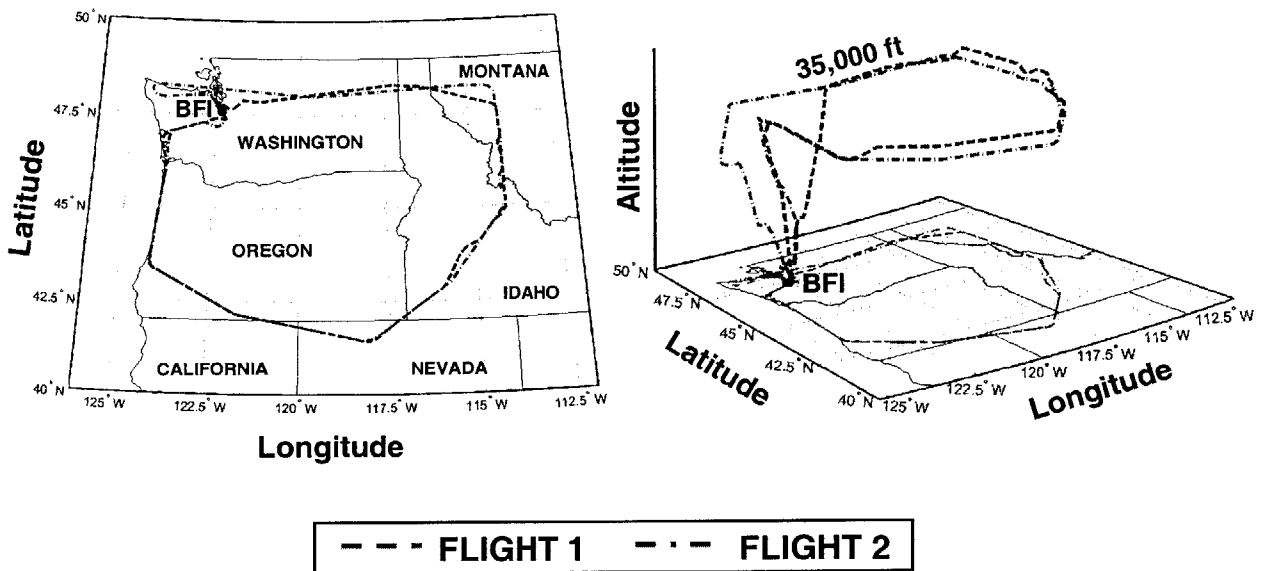


Figure 5.2: Flight Test Profiles

The same aircraft ARINC 429 and GPS states were collected as summarized in the previous Chapter (Table 4.1 and Table 4.2 respectively).

Although not considered in the earlier analyses conducted in Chapter 4, ground-based surveillance data was also collected from the FAA Host Computer System (HCS). This information was sourced from



the System Analysis Recording (SAR) tapes that are used to archive HCS outputs. Usable data was extracted from the SAR tapes using additional FAA analysis programs, namely the Data Analysis and Reduction Tool (DART) and National Track Analysis Program (NTAP). The outputs of these programs included mosaiced radar data<sup>†</sup> from long-range en-route ATC radars (generally ARSR-3 and ARSR-4 radar), HCS-derived additional states (such as heading and speed inferred from  $\alpha$ - $\beta$  trackers), and assigned Flight Plan/altitude amendments as entered into the HCS by the controller. The complete list of extracted states applicable to this study are outlined in Table 5.1. These states were updated on a 6 second update cycle to ensure effective data capture from the unsynchronized radar sites used in the mosaicing process, each updating on independent 12 second intervals. The textual flight plan was converted into latitude/longitude coordinates using NAVAID databases and NOAA aeronautical charts.

**Table 5.1: HCS Parameters Archived During Test Flights**

Parameter	Source Tool
Time (hhmmss)	DART & NTAP
Latitude (degs)	NTAP
Longitude (degs)	NTAP
Stereographic x,y coordinates*	DART
Reported Mode C altitude (ft)	DART
Derived heading (degs)	DART
Derived speed (knots)	DART
Assigned altitude (ft)	DART
Flight Plan (textual)	DART

This HCS data was recorded from the feed to the Seattle Air Route Traffic Control Center (ZSE). Data was only available for times that the aircraft was inside Seattle Center airspace or its “buffer region” (i.e. the airspace just outside the ZSE boundary where arriving or departing aircraft are tracked for ZSE controllers). These regions are shown in Figure 5.3. Certain portions of the test flights were outside of these regions and consequently no ground-based surveillance data was available during these times.

---

<sup>†</sup> The HCS Radar Data Processor (RDP) takes data from overlapping radar sites and uses an internal mosaic of “radar sort boxes” to determine which radar site should be used to provide surveillance data at any given location. Each radar sort box is a 16 nm square within which up to 4 radars are chosen to provide surveillance, in priority order. For example, if the quality of data from the first choice radar degrades below a certain level, the second choice is used, etc. [Lincoln (1998)].

\* Radar-centric polar coordinates (i.e. range,  $\rho$  & angle,  $\theta$ ) are converted to a stereographic x,y coordinate frame by the HCS Radar Data Processor for mosaicing, tracking and display purposes (details can be found in [Lincoln (1998)]). These Cartesian coordinates were subsequently converted to latitude/longitude coordinates in the NTAP tool for use in this analysis.

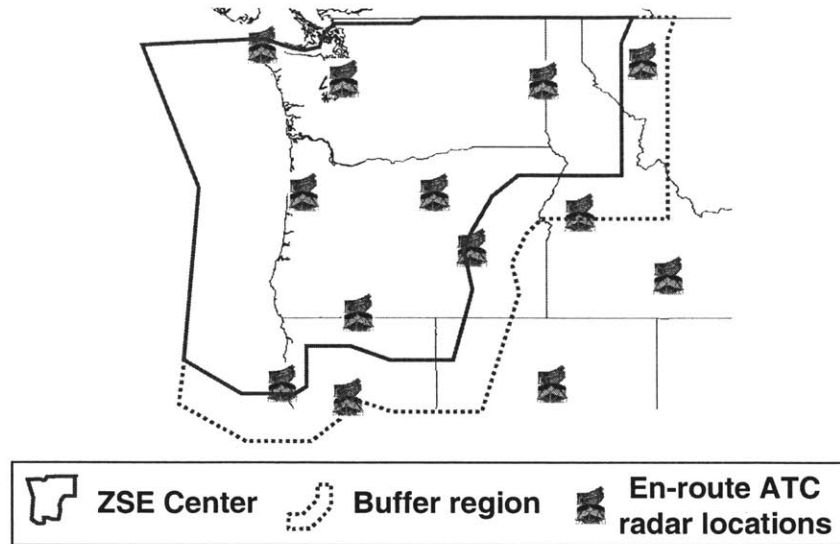


Figure 5.3: Seattle Center (ZSE) Airspace & En-Route Radar Locations

### 5.3 Operational Conformance Monitoring Issues in Key Flight Regimes

This flight test data provided an opportunity to exercise the Conformance Monitoring Analysis Framework under different operational environments of the flight test flight regimes and also under different surveillance environments representative of current and possible future technologies. It is apparent from the discussion of the existing ground-based conformance monitoring tools that fundamental differences exist in the approaches to conformance monitoring in the lateral, vertical and longitudinal conformance monitoring environments and also in the non-transitioning and transitioning environments within each of these domains. In order to investigate fundamental conformance monitoring issues in each of these domains, the Conformance Monitoring Analysis Framework was applied to each. The subsections that follow describe findings from:

- Lateral conformance monitoring during straight (non-transitioning) flight.
- Lateral conformance monitoring during transitioning flight.
- Vertical conformance monitoring during level (non-transitioning) flight.
- Vertical conformance monitoring during transitioning flight.
- Longitudinal conformance monitoring during constant speed flight.
- Longitudinal conformance monitoring during accelerating/decelerating flight.

A specific comparison of the results with radar and aircraft-based data are discussed in each domain.

The general form of each CMAF element used during this operational data analysis were as follows:

- Conformance Basis: defined in each scenario discussed.
- Conformance Monitoring Model: low, medium and high fidelity forms as appropriate.
- Conformance Residual generation scheme: absolute linear function scalar with weighting factors on each state based on twice the nominal flight phase standard deviations ( $\sigma$ ):

$$CR = \frac{\sum WF_x |x_{obs} - x_{CMM}|}{n} = \frac{\sum \frac{|x_{obs} - x_{CMM}|}{2\sigma_x}}{n} \quad \text{Equation 5.1}$$

This generation scheme is an extension of the approaches used by many of the existing tools described in Chapter 2, most of which compare an absolute difference of position deviation relative to a static threshold. This allows for easier comparison of results generated here with those from existing tools.

- Decision-making: threshold-based.
- Figures of merit: False Alarm/Time-To-Detection (FA/TTD) metrics.

These forms were chosen primarily for simplicity, not to imply that they are necessarily the best approaches, but to illustrate application of the CMAF approach to the major flight regimes and to gain further insight into its utility.

### 5.3.1 Lateral Conformance Monitoring: Straight Flight

Lateral conformance monitoring during straight flight is one of the most basic forms of conformance monitoring conducted in the ATC environment since aircraft spend most of their flight time in straight, level and constant speed flight regimes. In order to illustrate conformance monitoring issues for this case, the same lateral non-conformance scenario as was discussed in Chapter 4 is analyzed further using the Conformance Monitoring Analysis Framework. Here, the results from both the aircraft-based and ground-based data are compared. The scenario is illustrated in Figure 5.4 showing ground tracks recorded by the available sensor systems.

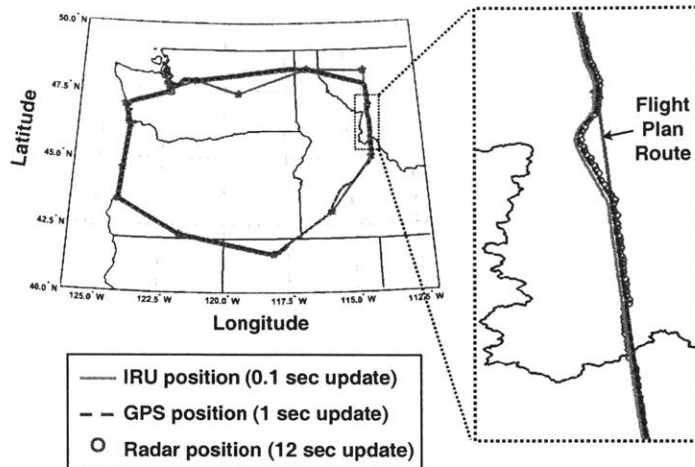


**Figure 5.4: Lateral Non-Conformance Scenario**

Recall that the scenario comprised approximately 10 minutes (600 seconds) of “nominal flight” where the aircraft flew the assigned flight plan trajectory, followed by a “deviation” phase where the aircraft was turned left off the HCS flight plan course by  $10^\circ$  until a positional deviation of approximately 3 nm from the flight plan had been achieved. At this time a “recovery” phase of flight returned the aircraft to the HCS flight plan trajectory. The dynamic states recorded from the aircraft and ground-based systems during the scenario are presented in Figure 5.5. Note the extra noise and delayed observability of the deviation and recovery behaviors in the radar data.

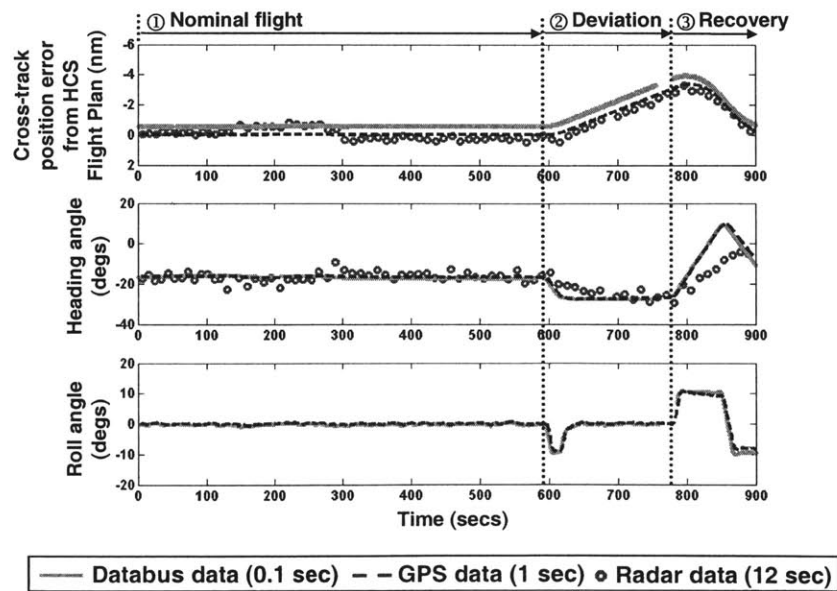


**Figure 5.5: Lateral Non-Conformance Scenario Dynamic States**

The Conformance Basis for this lateral deviation scenario was the HCS flight plan route identified in Figure 5.4. A simple low fidelity CMM was used: the expected states were determined from an assessment of what they would be for a perfectly conforming aircraft with no disturbances. Conformance Residuals were generated according to the example absolute linear function scalar form proposed earlier, but this time were compared for the aircraft and radar-based data cases:

$$\begin{aligned}
 CR_L &= WF_L |L_{obs} - L_{CMM}| \\
 CR_{L\psi} &= \frac{WF_L |L_{obs} - L_{CMM}| + WF_\psi |\psi_{obs} - \psi_{CMM}|}{2} \\
 CR_{L\psi\phi} &= \frac{WF_L |L_{obs} - L_{CMM}| + WF_\psi |\psi_{obs} - \psi_{CMM}| + WF_\phi |\phi_{obs} - \phi_{CMM}|}{3}
 \end{aligned}
 \tag{Equations 5.2}$$

$L_{CMM} = 0$  nm,  $\psi_{CMM} =$  route track angle corrected for wind and  $\phi_{CMM} = 0^\circ$  in this case. Residuals with these forms were generated using data from the aircraft and radar systems separately to demonstrate the difference between the aircraft and ground-based information for detection of the lateral deviation. The weighting factors for each state were inferred from twice the standard deviation ( $2\sigma$ ) of each state error (i.e.  $x_{obs} - x_{CMM}$ ) observed in the aircraft and radar data during the nominal flight phase as shown in Figure 5.6 and summarized in Table 5.2. The resulting Conformance Residuals based on these assumptions are presented in Figure 5.7. The residuals are plotted relative to the time of the start of the deviation established from evaluation of the aircraft roll state.

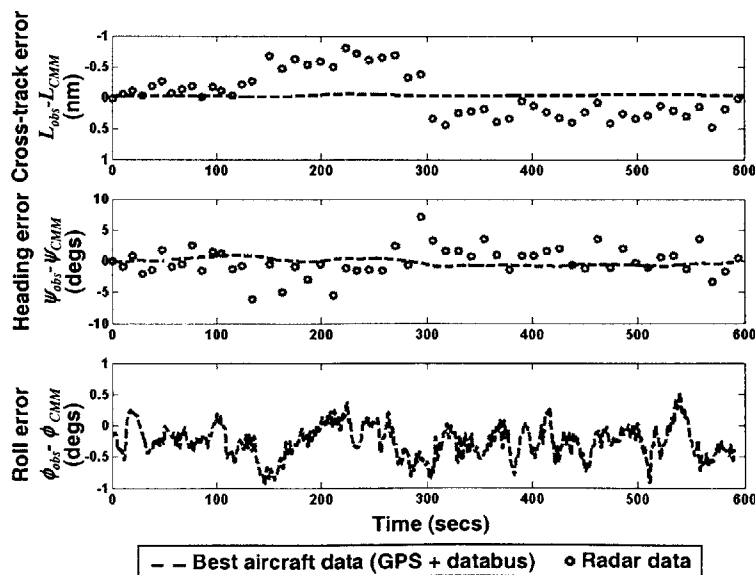
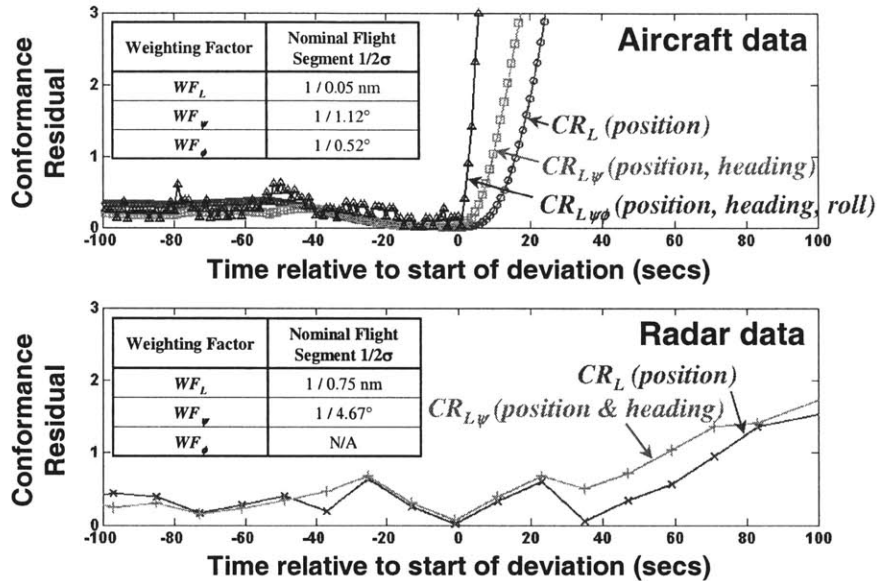


Figure 5.6: Lateral Non-Conformance Scenario Weighting Factor Determination

**Table 5.2: Lateral Non-Conformance Scenario Weighting Factors**

Weighting Factor	Nominal Flight Segment $1/2\sigma$	
	Aircraft Data	Radar Data
$WF_L$	1 / 0.05 nm	1 / 0.75 nm
$WF_\psi$	1 / 1.12°	1 / 4.67°
$WF_\phi$	1 / 0.52°	N/A



**Figure 5.7: Lateral Non-Conformance Scenario Conformance Residuals with Aircraft & Radar Data**

The False Alarm and Time-To-Detection metrics were calculated using the same approach described in Section 4.5.1 for the two sets of surveillance data, with the resulting curves for various threshold values presented in Figure 5.8. These results vividly demonstrate the trade-off of false alarm and time-to-detection and illustrate the significantly better performance associated with access to higher quality/higher update rate aircraft data. Realistic detection times are found from the point at which the various curves first increase from the zero false point, although the slope of the curves at higher false alarm probabilities give an indication of the signal to noise ratio in each case. Note how the aircraft based curves have significantly steeper curves indicating much higher signal to noise ratio with this data relative to the radar system data case.

For the 1 Hz update aircraft data, detection times were 80-90% lower than were possible with the ground data updated at 12 second intervals for a given Conformance Residual and false alarm rate. For example, realistic (low false alarm) detection times of 5-15 seconds were observed with aircraft data compared to 60-85 seconds with ground data.

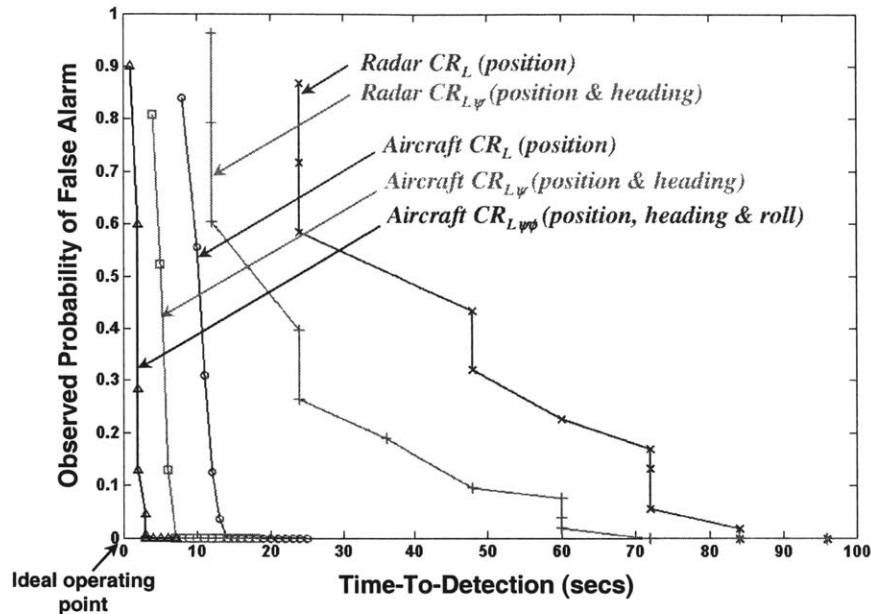


**Figure 5.8: Lateral Non-Conformance Scenario False Alarm/Time-To-Detection Metrics**

Access to higher order dynamic states (heading and roll) was observed to shorten the detection times in this analysis due to the lead provided by these states. However, care must be exercised in the extension of these results to more general ATC situations, since only a simple deviation scenario from a very clear Conformance Basis (i.e. a straight flight segment) under nominal autopilot control was analyzed. For this case, the higher order states were not expected to be changing (see the example CMM definition above) so the deviation was readily detected when these states *did* start to change. However, in more dynamic scenarios where the higher order states are expected to change (e.g. in nominal lateral and vertical transition maneuvers), it is harder to accurately define the expected values. These issues are demonstrated in the sections that follow. Other deviation non-conformance angles and guidance modes would also produce different results than those presented above. For example, the effect of deviation angle at different threshold settings is presented in Figure 5.9. Although the absolute time-to-detection values are generic for this example, the relative values for different non-conformance angles are informative. Note how the time-to-detection values can get large at very small deviation angles. The effect of guidance mode will be discussed in more detail in the simulation studies of the next Chapter.

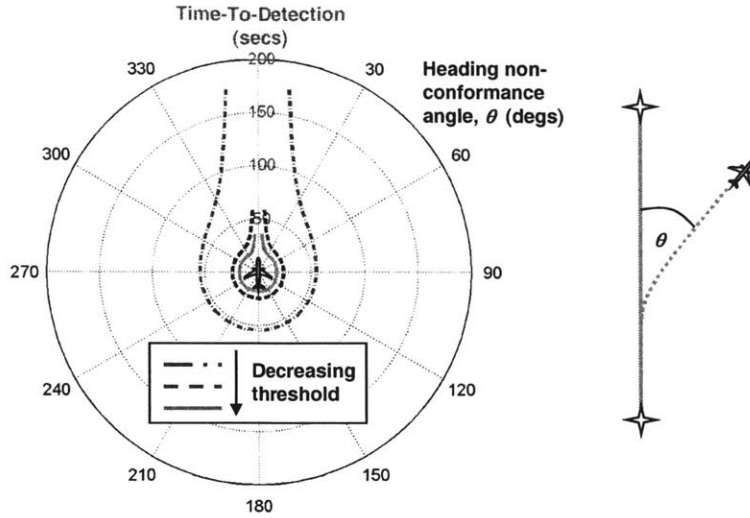


**Figure 5.9: Effect of Non-Conformance Angles on Position-Based Time to Detection**

It is also instructive to compare the false alarm/time-to-detection rates presented in Figure 5.8 to those achievable by existing systems under the same  $10^\circ$  heading non-conformance scenario. A simple comparative analysis of the time-to-detection for various heading non-conformance angles and speeds from a straight path with the different systems and their lateral non-transition thresholds is presented in Figure 5.10. Here the aircraft heading deviation was modeled by a standard  $1.5^\circ/\text{sec}$  turn off the expected route until the desired heading non-conformance angle was reached. Time-to-detection was determined from the elapsed time between the start of the turn and when the cross-track deviation of the aircraft first exceeded the threshold value appropriate for each tool.

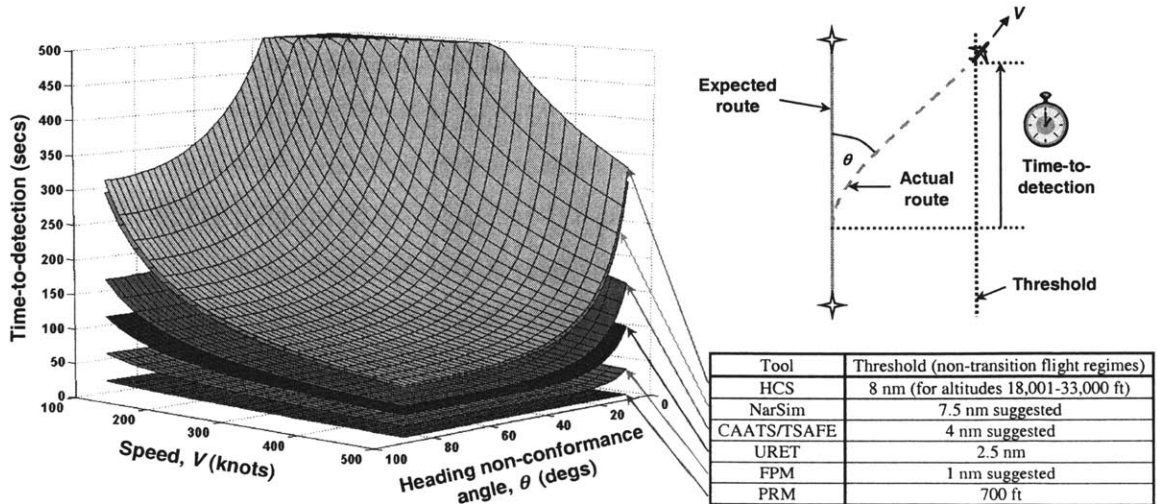


**Figure 5.10: Analysis of Heading Non-Conformance Detection in Existing Systems**



By taking a slice through this surface plot at the 10° heading non-conformance angle, the appropriate Times-To-Detection measure for each tool are presented in Figure 5.11. Given typical operating speeds of 140 knots at approach for PRM and 425 knots during cruise for all of the other tools, the appropriate time-to-detection for each tool in its operational environment are summarized in Table 5.3.

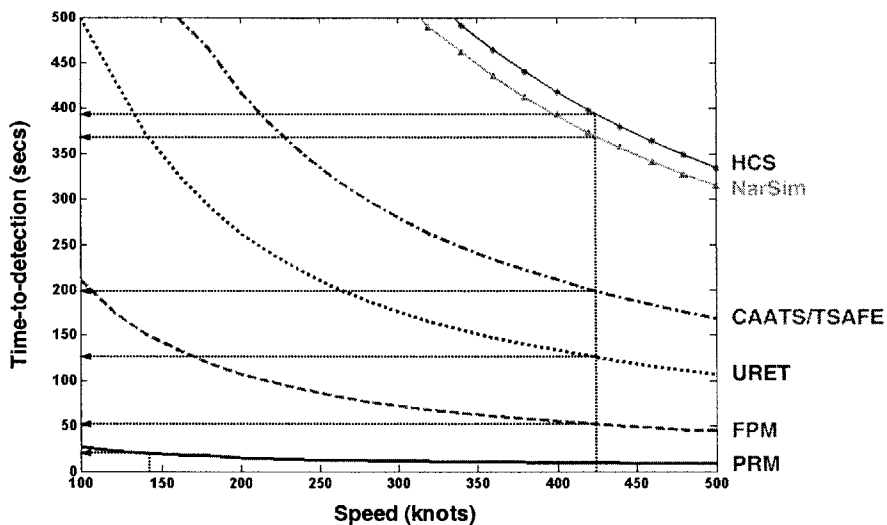


**Figure 5.11: Time-To-Detection of 10° Heading Non-Conformance in Existing Systems**

**Table 5.3: Time-To-Detection of 10° Non-Conformance with Existing System Thresholds under Nominal Operating Conditions**

Tool	Time-to-detection
PRM	25 secs
FPM	50 secs
URET	125 secs
CAATS	200 secs
TSAFE	200 secs
NarSim	360 secs
HCS	390 secs

A comparison of these time-to-detection values for the existing tools with the FA/TTD results of Figure 5.8 suggests that even this simple implementation of the CMAF produces superior time-to-detection at zero false alarm rates than all of the existing en-route operational tools and comparable times to many developmental tools. The analysis enabled by the new framework allows a comparison of different conformance monitoring approaches in terms of different Conformance Monitoring Models,

Conformance Residual generation and decision-making schemes producing different figures of merit that assist in the design of the system for a given application. This was not achievable before, where only time-to-detection values under various conditions (such as those presented above) could be calculated with little indication of whether they were appropriate for a given application.

### 5.3.2 Lateral Conformance Monitoring: Transitioning Flight

Two cases will be considered in this Section. The first case demonstrates the challenges associated with lateral transition conformance monitoring due to the errors that exist in a typical Conformance Residual even for a conforming aircraft. The second case discusses how these challenges affect the detection of non-conformance at a lateral transition.

#### 5.3.2.1 Conforming Transition Behavior

It is common for a flight plan to be simplified into straight-line segments joining waypoints that define the assigned trajectory. This simplification is appropriate for conformance monitoring along the segments themselves (as in the previous analysis), but implies that a low fidelity CMM would have discrete heading changes and an impulse roll state at the transition points. However, aircraft dynamics dictate that more gradually changing heading and roll states are to be expected and need to be described in higher fidelity CMMs for use at transitions.

A lateral transition scenario involving a properly conforming transition at a waypoint (SDO) is used as an example. The scenario is shown in Figure 5.12.

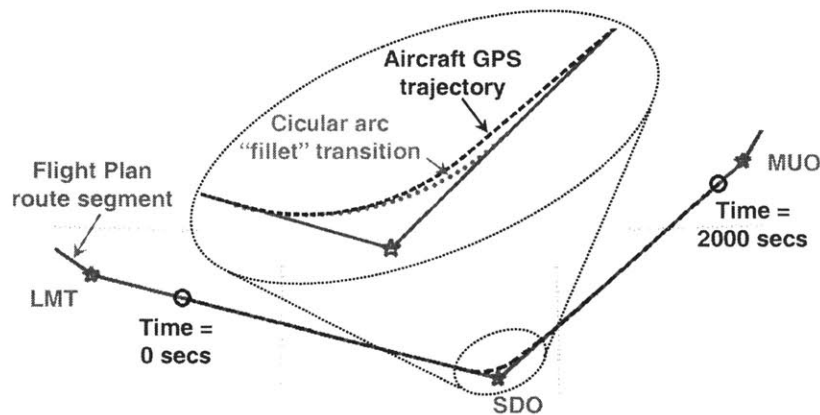


Figure 5.12: Lateral Transition Scenario

This shows the flight plan route based on straight-line segments, the GPS track from one of the flight tests and a simplified circular arc “fillet” that can be considered a medium fidelity CMM used to approximate the transition trajectory. This fillet is inspired by the boundary of the transition containment region defined in the RNP Minimum Aviation System Performance Standards (MASPS) [RTCA (2000)] and is also supported through a turn radius parameter in the ADS-B MASPS [RTCA (2002)]. It defines the radius of curvature and initiation point of a transition containment region, as presented in Figure 5.13.

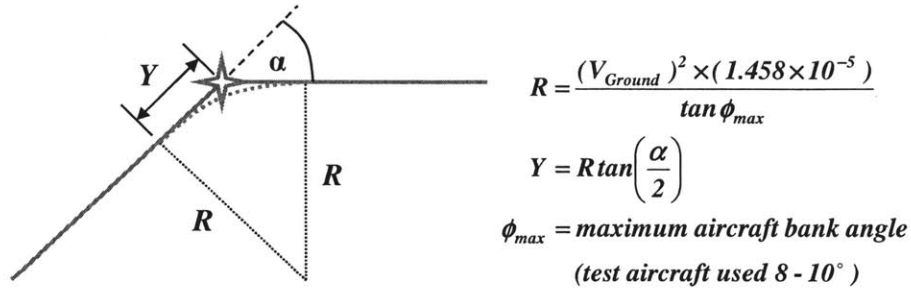


Figure 5.13: Circular Arc Fillet Definition [adapted from RTCA (2000)]

The conformance monitoring issues during the transition maneuver are highlighted in the figures below. These concentrate solely on aircraft-based data for clarity. Figure 5.14 presents the dynamic states during the transition and the expected states associated with a discrete transition and the simple fillet transition based on the circular arc. Figure 5.15 presents the state error components (i.e.  $x_{obs} - x_{CMM}$ ) that would be used to generate Conformance Residuals similar to those used in the previous section.

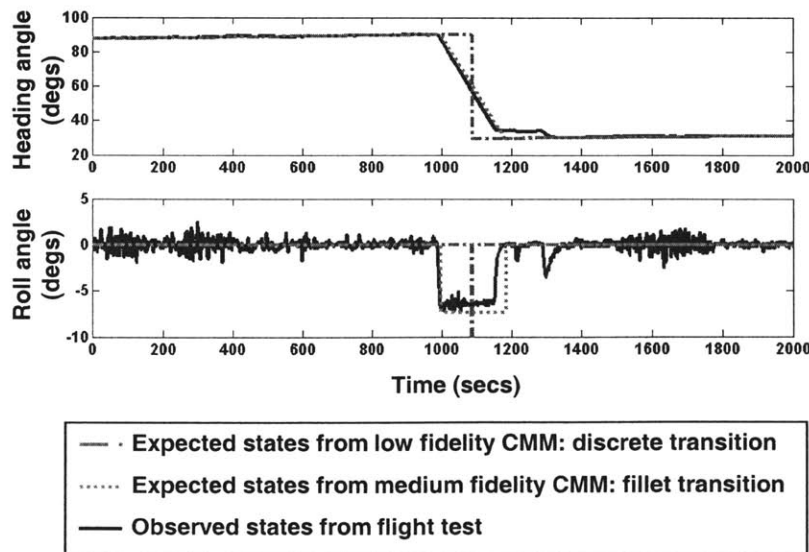
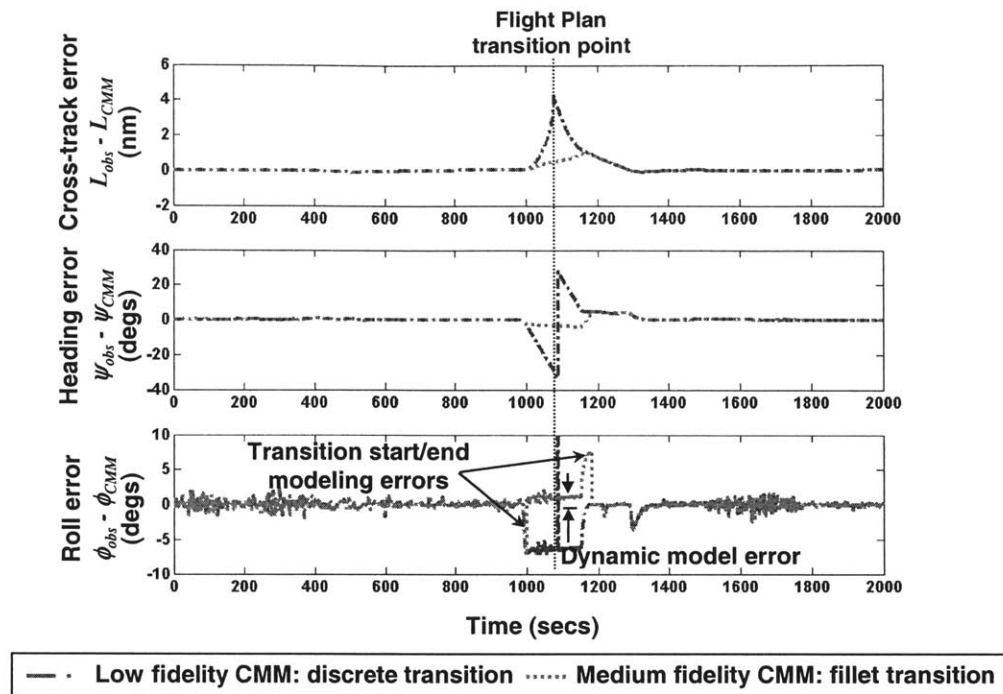


Figure 5.14: Lateral Transition Scenario Dynamic States



**Figure 5.15: Lateral Transition Scenario Error States**

It is clear that the observed errors using the low fidelity CMM are significant during the transition, *despite the fact the aircraft is nominally conforming*. These errors can be substantially reduced using the medium fidelity CMM with the simple circular fillet since it allows approximations of the aircraft dynamics during the transition to be captured. However, even when the medium fidelity model is used, some errors still exist due to the mismatches between the simple fillet and the actual trajectory flown. These mismatches are caused by dynamic modeling errors and autoflight timing differences, as identified in Figure 5.15. The timing differences manifest themselves as the spikes in the roll angle state due to the small differences between the expected start and end times of the lateral transition predicted using the fillet, and the actual start and end of the transition governed by the logic used in the autoflight system. Note that these spikes could be filtered out using a low pass filter on the Conformance Residual if required, but this could reduce the response time of the detection of a non-conformance.

Conformance Residuals generated using the same generation scheme and state weighting factors as outlined in the previous section are presented in Figure 5.16. These reinforce the main points: that significant errors occur in the Conformance Residuals at transition points for even a conforming aircraft

when a low fidelity CMM is used. These errors can be reduced, but not eliminated, by medium fidelity modeling of the transition trajectory.

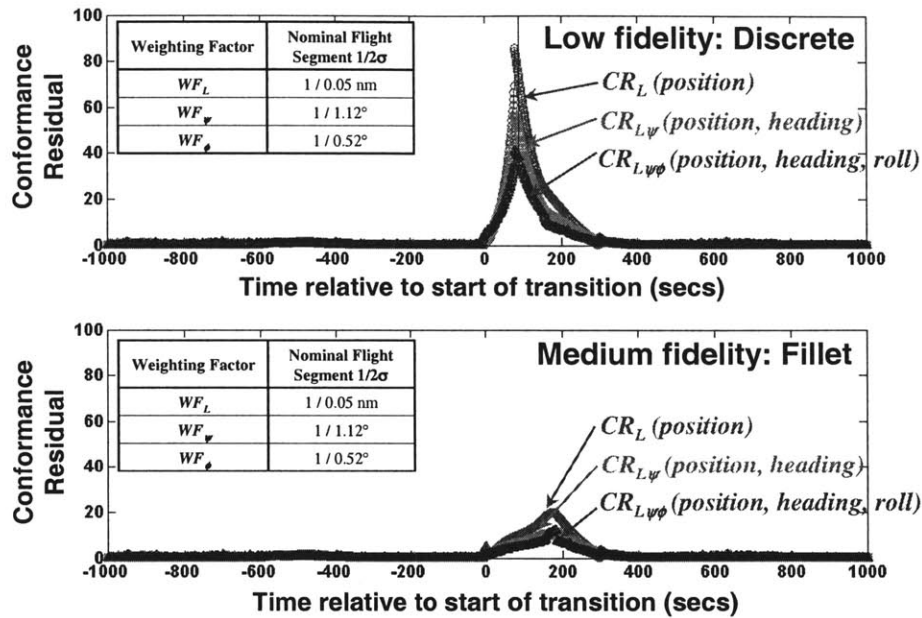


**Figure 5.16: Lateral Transition Scenario Conformance Residuals**

Some of these errors could theoretically be reduced further using a high fidelity CMM, as described in Chapters 3 and 4. However, since the actual transition flight path of an aircraft is a function of a number of variables (such as airspeed, maximum bank angle, autoflight logic, winds, etc.) it is neither repeatable nor predictable with an *a priori* model. Rather, the errors can be reduced by “tuning” the more sophisticated model parameters (such as the gains and transfer function of Figure 4.4) to minimize the errors with an observed trajectory. However, this tuned model may not be effective at minimizing the transition errors at a different transition for the same aircraft or at the same transition for different aircraft than that used in the tuning process. Figure 5.17 illustrates the issue. The flight paths for the test aircraft at the transition shown are very different across the two test flights. Hence, even if a model were developed that accurately predicted the transition trajectory for the first test flight, the same model would not have been as effective at reducing errors for the second. Since these issues are more prominent in the higher order states, the benefits associated with using higher order dynamic states discussed in the context of the straight flight scenario are harder to realize in the transitioning environment.



**Figure 5.17: Comparison Between Lateral Transition Trajectories for Flight Tests 1 & 2**

As a result, the fine-tuned high fidelity CMM is generally impractical for normal ATC operations, although they may find application for some specialized conformance monitoring tasks where detailed transition conformance monitoring is essential. The errors inherent in the more widely-applicable low and medium fidelity CMMs require that much larger thresholds are required relative to the non-transitioning domains in order to achieve an equivalent false alarm rate. This is illustrated in Figure 5.18 for the transition scenario considered here. With a low fidelity CMM, a transition region threshold value of approximately ten times the non-transition region value is required. With a medium fidelity CMM, the transition region threshold value is approximately three times the non-transition region value. Note that different relative values may be required for different transition angles. The findings above are compared to the relative sizes of the thresholds for the HCS and URET conformance monitoring tools in Table 5.4. Note that the relative sizes of the transition/non-transition thresholds in these tools is somewhat smaller than those suggested from the analysis with the CMAF. However, this may be explainable by the much lower threshold suggested in the CMAF analysis resulting from the RNP specification being used as a normalization basis, compared to the much larger thresholds employed in the HCS and URET tools which account for a wider spectrum of aircraft tracking capabilities and transition angles.

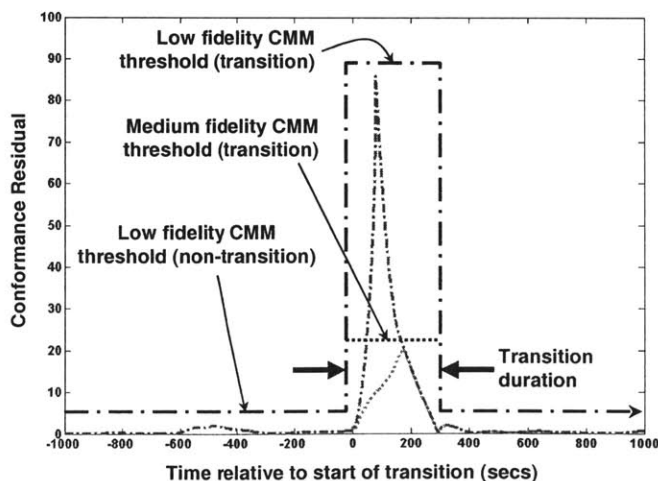


**Figure 5.18: Relative Non-Transition/Transition Threshold Values for Example Scenario**

**Table 5.4: Relative Non-Transition/Transition Threshold Values for Existing Tools**

Tool	Example Lateral Non-Transition Threshold Value	Example Lateral Transition Threshold Value	Relative Threshold Size (Transition/Non-Transition)
HCS	8 nm	12 nm	1.5
URET	2.5 nm	3.5 nm	1.4

Note also that the size of the “transition region” is an indication of the expected duration of the transition, i.e. the expected time between the initiation and termination of the transition maneuver. Since there can be significant variability in how the transition is executed (this is demonstrated in the simulation studies presented in the next Chapter), there can also be significant uncertainty in the transition duration. Hence, the size of the transition region may have to be based on a “worst case” prediction if no additional information is available. Alternatively, this could be proceduralized through “standard transition procedures”, or even surveilled in advanced surveillance systems. For example, the ADS-B MASPS support surveillance of the transition behavior through provision in the message-set of the turn radius parameter [RTCA (2002)] from which the transition initiation and termination points can be calculated, as shown in Figure 5.13.

### **5.3.2.2 Non-Conforming Transition Behavior**

Because of the larger thresholds required at transitions, there are significantly greater challenges to detecting non-conformance at transitions relative to the straight flight environment. This is illustrated through a transition non-conformance scenario shown in Figure 5.19. It uses an alternate assumed scenario where the aircraft was expected to fly to BOI after SDO but actually flew towards MUO, resulting in a path with a 10° heading difference from that expected. This simulates a scenario where a 10° heading non-conformance occurs at a transition point in the Conformance Basis, allowing this situation to be directly comparable with the 10° heading non-conformance from the straight flight segment described in Section 5.3.1.

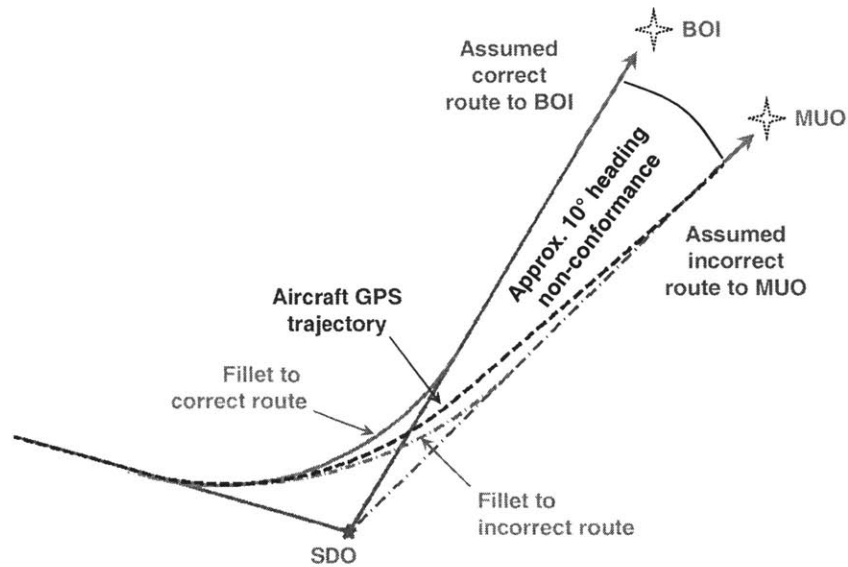


**Figure 5.19: Transition Non-Conformance Scenario**

Figure 5.20 presents the False Alarm/Time-To-Detection results for this scenario when the same Conformance Monitoring Models and Conformance Residuals as the previous MUO section are used. These results demonstrate the difference between the low and medium fidelity models, but this time in the FA/TTD space. The low fidelity CMM is associated with curves much farther from the optimal operating point, while the medium fidelity CMM shows improved performance but it is still much worse than the case in the straight flight environment due to the modeling errors that exist.

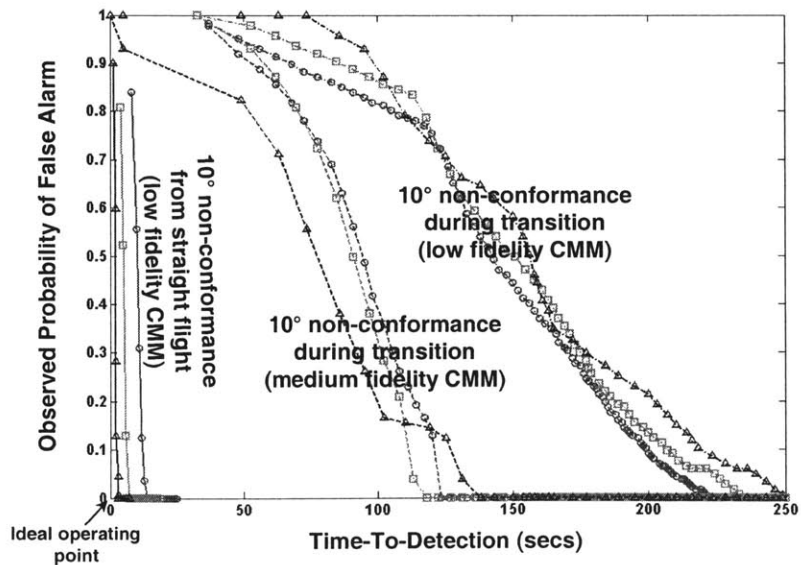


**Figure 5.20: Transition Non-Conformance False Alarm/Time-To-Detection Metrics**



These results also illustrate that the benefits associated with using higher order states observed in the straight flight case of the previous section are reduced or even negated in the transitioning case. This is illustrated in Figure 5.21. Note that the larger errors associated with noise and modeling inaccuracies in the higher order states can produce residuals that give worse performance than those that do not use the higher order state at all. This reiterates why it can be worse to use an inaccurate high fidelity model than a more generally-applicable medium fidelity model where the ranges of error are known more accurately.

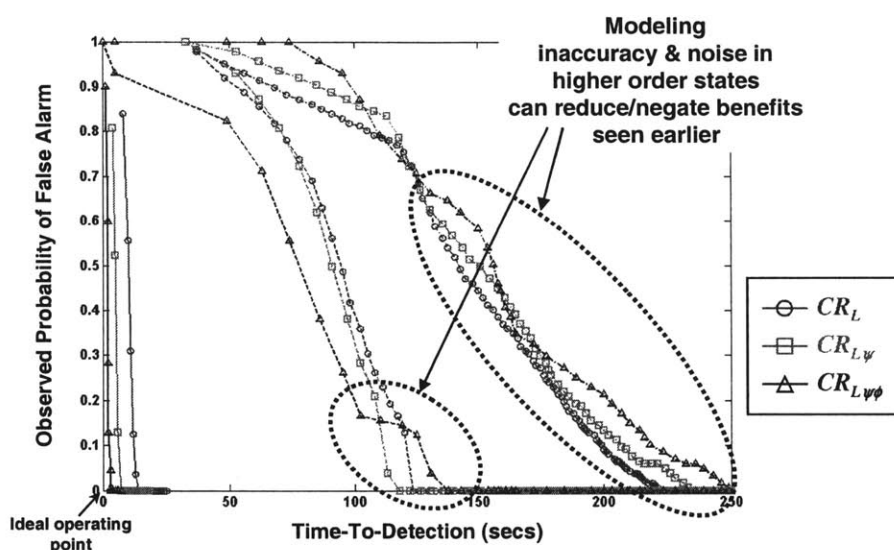


**Figure 5.21: Reduced Benefit of Higher Order States During Transitions**

Due to these challenges at transitions, it is clearly much harder to detect non-conformance in this domain using traditional dynamic states. However, as described earlier, advanced surveillance systems such as ADS-B hold the promise of enabling intent states to be made available for conformance monitoring purposes. This could have particular benefit in the transitioning domains, as shown in Figure 5.22. For example, access to the trajectory or target state level intent states could allow rapid detection of any non-conformance through a direct comparison of the trajectory or target state observed relative to that expected for the conforming case. Incorrect programming of the FMS to fly to MUO after SDO rather than the assumed correct route to BOI could be detected immediately that the trajectory level intent state was surveilled. Access to the target state level intent (e.g. the expected ground track angle target value to BOI versus the observed ground track angle target to MUO) would reveal the non-conformance as soon as the transition was initiated and the new ground track angle target became active.

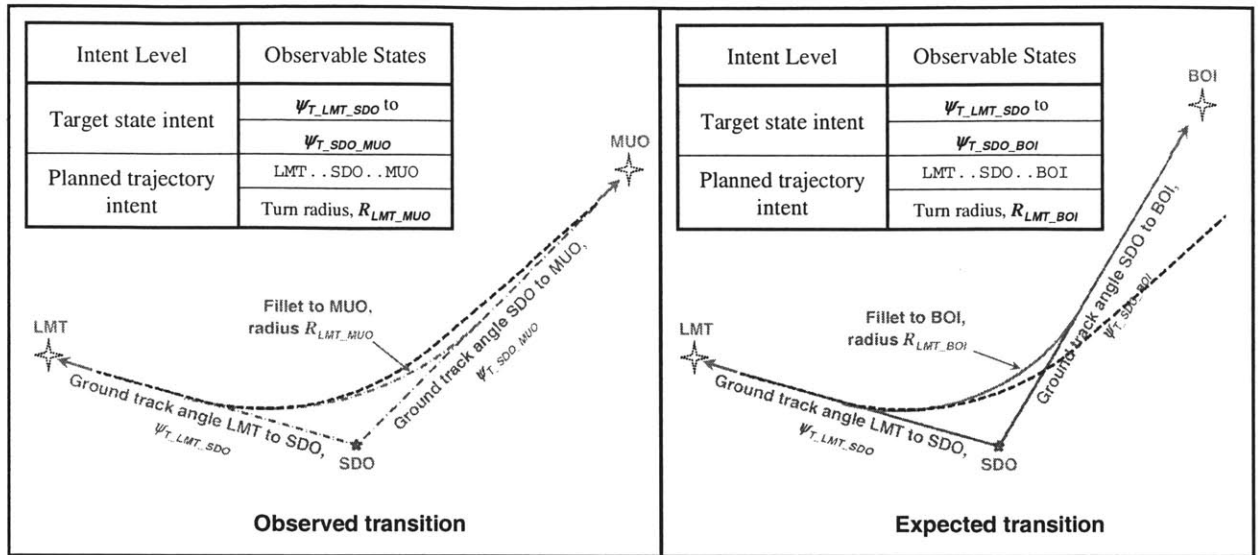


**Figure 5.22: Intent State Usage During Transition Non-Conformance Scenario**

This highlights the significant potential associated with surveillance of intent information in future ATC environments. Access to the trajectory level intent would allow potential non-conformances to be detected before the aircraft is anywhere near the transition at which the non-conformance would occur. Access to the target state level intent would allow detection as soon as the target became active and sooner than would be possible with the dynamic states alone which are controlled to that target. These benefits would appear to be limited only to the degree that there can be uncertainty as to whether the aircraft is in a flight guidance mode to follow the programmed intent, that there is noise in the target level states if directly surveilled from a Mode Control Panel/Flight Control Unit and that there is sufficient bandwidth in the surveillance system to make the required states available.

### 5.3.3 Vertical Conformance Monitoring: Level Flight

When a stable altitude target is presented for an extended period of time such that the aircraft has time to reach and stabilize to it, the variation of the barometric altitude profile relative to the assignment is incredibly small, as illustrated in Figure 5.23 for one of the test flights.

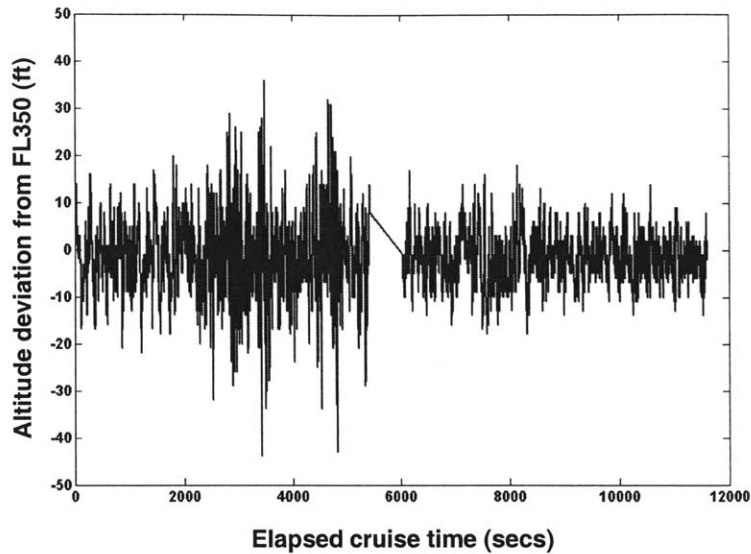


**Figure 5.23: Barometric Altitude Deviations Recorded During Cruise Phase**

After removing the intentional altitude deviation performed as part of the test flight procedures (causing the gap in the data around 6000 seconds), the difference between the barometric altitude recorded on the databus and the assigned altitude of FL350 had a mean of  $-1.6$  ft and a standard deviation of  $6.9$  ft during over 3 hours of cruise flight. Instantaneous altitude measurements were all within  $50$  ft of the assigned flight level. These observations validate prior discussions regarding the challenges associated with conformance monitoring in vertical transitions and the relative ease with which it can be conducted during non-transitioning vertical phases due to the excellent vertical tracking performance that can be expected from advanced autoflight-equipped aircraft.

Another interesting issue visible in the data from these test flights is the significant differences that can exist between the altitudes provided by the barometric and GPS systems. Differences of up to  $350$  ft were observed in this case, as illustrated in Figure 5.24. One explanation for this difference is the local pressure field. An aircraft autoflight system tracks *pressure altitude* which is referenced to a standard sea-level atmospheric pressure of  $29.92$  inches Hg. However, if the actual local sea-level pressure differs from the standard pressure and varies from one location to another, then the aircraft's *true altitude* above the ground (as measured by the GPS) will vary as a function of the local pressure contours. A variation of  $100$  ft altitude is observed for every  $0.1$  inches Hg difference from standard. So if the local sea-level pressure is higher than  $29.92$  inches of Hg, the actual aircraft altitude measured by the GPS will be higher than the barometric altitude, as is the case observed in the figure. An additional contributing factor to this altitude discrepancy between the two systems could be the reduced accuracy of GPS systems from

Vertical Dilution of Precision (VDOP) caused by unfavorable geometry of GPS satellites for vertical measurements [Spilker (1996)].

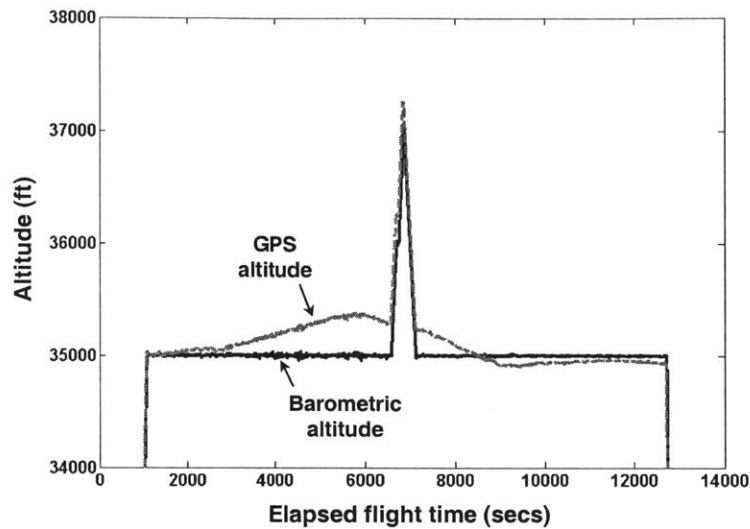


**Figure 5.24: Barometric & GPS Altitude Comparison During Cruise**

In order to illustrate the application of the analysis framework for vertical conformance monitoring during level flight, a vertical deviation scenario was examined. Unfortunately, no Mode C altitude information was available for any of the intentional vertical deviations conducted during the test flights. Instead, a vertical deviation scenario was synthesized from the nominal descent behaviors by simply assuming that a scheduled descent during the test flight had not been cleared, as illustrated in Figure 5.25. The primary altitude data sources from the flight tests were barometric altitude onboard the aircraft (updated at 10 Hz) and the Mode C transponder altitude (updated on a 6 second cycle) available through the ground Host Computer System. No other vertical information was available from the ground surveillance systems. However, the flight path angle,  $\gamma$  could be calculated from the vertical speed ( $V_{VS}$ ) and ground speed ( $V_{GS}$ ) states available on the databus, according to:

$$\gamma = \text{atan}\left(\frac{V_{VS}}{V_{GS}}\right) \quad \text{Equation 5.3}$$

The resulting dynamic states available during the vertical deviation are presented in Figure 5.25.

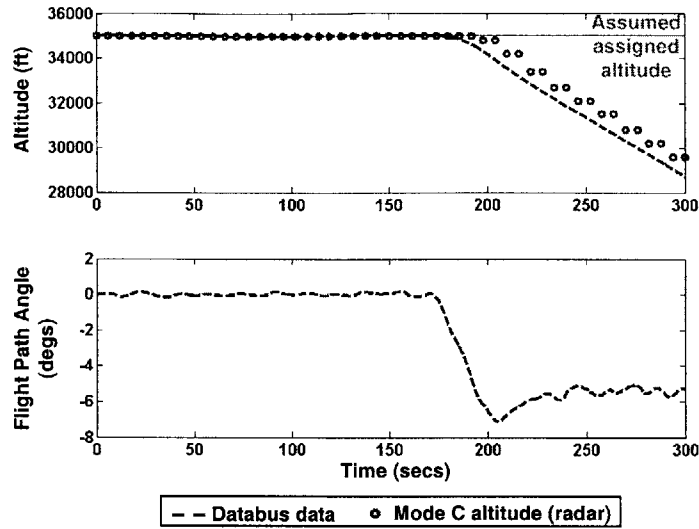


Figure 5.25: Vertical Deviation Dynamic States

Conformance Residuals using combinations of altitude ( $A$ ) and flight path angle ( $\gamma$ ) states were generated of the same form used in the lateral case according to the equations:

$$\begin{aligned}
 CR_A &= WF_A |A_{obs} - A_{CMM}| \\
 CR_{A\gamma} &= \frac{WF_A |A_{obs} - A_{CMM}| + WF_\gamma |\gamma_{obs} - \gamma_{CMM}|}{2}
 \end{aligned}
 \tag{Equations 5.4}$$

A low fidelity vertical Conformance Monitoring Model was used again where the expected states were defined by a perfectly conforming aircraft, i.e.  $A_{CMM} = 35,000$  ft and  $\gamma_{CMM} = 0^\circ$ . Similar to the lateral analysis, weighting factors for the states were based on twice the observed standard deviations in data with aircraft and ground systems during the nominal (conforming) part of the flight. This indicated that barometric altitude variations during cruise were generally contained within a  $\pm 50$  ft envelope from the assigned altitude. Given that Mode C altitudes are discretized in 100 ft increments<sup>†</sup>, a  $\pm 100$  ft envelope was used as the inverse of the radar altitude weighting factor. The resulting Conformance Residuals based on these assumptions are presented in Figure 5.26. The time scale has again been shifted to be relative to the start of the vertical deviation. False Alarm/Time-To-Detection (FA/TTD) metrics can also be generated from these Conformance Residuals as presented in Figure 5.27.

<sup>†</sup> Newer Mode S transponder altitudes are discretized in 25 ft increments

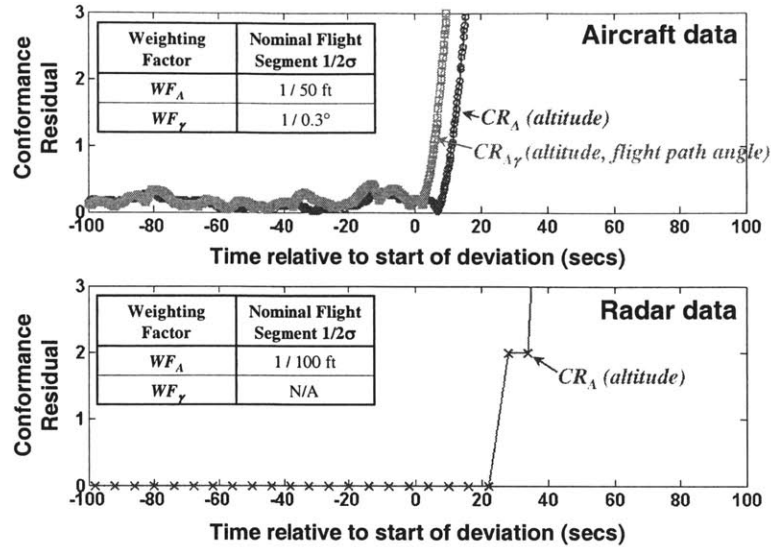


Figure 5.26: Vertical Deviation Conformance Residuals with Aircraft & Radar Data

Results similar to the lateral deviation scenario exist for the vertical case. The higher quality/higher update rate aircraft-based data is associated with more rapid detection of the vertical deviation relative to the ground case, and that the higher order dynamic state (flight path angle) provides added lead time. Note how the discretized Mode C transponder data allows only a binary decision about the conformance status of an aircraft, with either 100% or 0% false alarms and nothing in-between. The TTDs are lower than equivalent results in the lateral case, indicating easier detection of aircraft deviations in the level vertical domain relative to the straight lateral case.

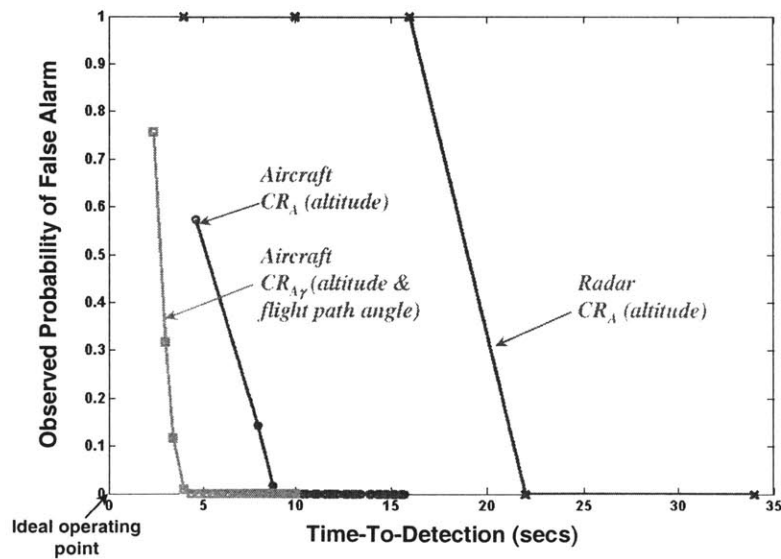


Figure 5.27: Vertical Deviation False Alarm/Time-To-Detection Metrics

Realistic detection times of 8 seconds with the aircraft altitude data compare to 22 seconds with the Mode C radar data. It is interesting to note in Figure 5.28 that by the time the deviation could be detected by current ground system information, the aircraft had already descended 700 ft from the assigned altitude. This is a significant proportion of the current 1000 or 2000 ft vertical separation minima.

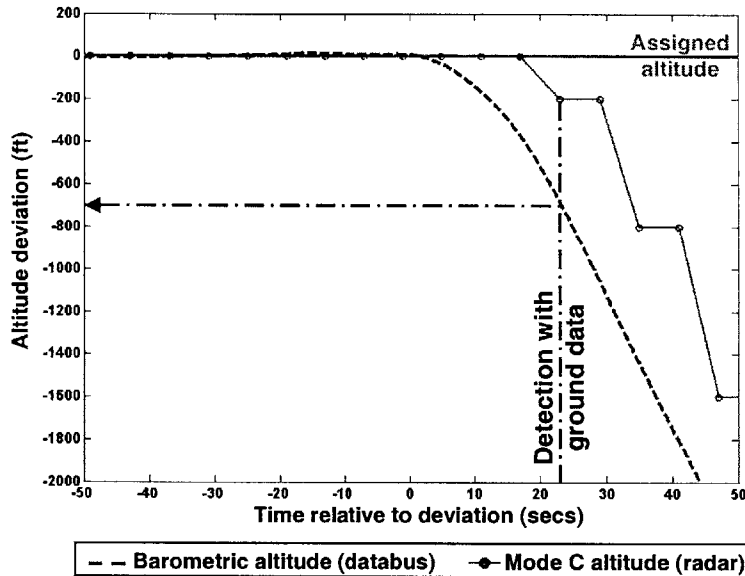


Figure 5.28: Vertical Deviations at Detection

### 5.3.4 Vertical Conformance Monitoring: Transitioning Flight

Conformance monitoring in the vertical transitioning environment is extremely challenging for a number of reasons:

- There is poor knowledge of the Conformance Basis during vertical transitions.
- There is poor predictability of the aircraft dynamics and logic during vertical transitions: this is analogous to the problem discussed in the context of the lateral transition path and the various transition logics that can be employed in this domain. However, the path to be followed during vertical transitions is even more difficult for ground-based automation tools to predict since it depends on many more factors than the lateral path [McConkey & Bolz (2002)], including:
  - Larger numbers of vertical automation modes than lateral automation modes: modern autoflight-equipped aircraft can have up to 14 vertical modes [Vakil (2000)], each of which may be associated with different trajectory logic.

- Dependence on aircraft configuration and properties such as weight, aerodynamic configuration, thrust setting, etc. which affect the actual profile flown.
- Sensitivity to atmospheric property forecasts such as wind and temperature profiles used in FMS calculations to calculate optimal profiles.
- Sensitivity to atmospheric properties actually experienced in flight which affect engine thrust, speed transition points, etc.
- There is poor surveillance in the vertical channel: discretization and lag effects.

Detailed discussions of the Conformance Basis issues are contained in the next section (Section 5.4). Aircraft dynamics/automation issues cannot be readily demonstrated using the operational data: rather they are demonstrated using simulation techniques in the next Chapter. Finally, the limited surveillance issue is visible in the altitude profiles presented in Figure 5.28 which represents the Top Of Descent (TOD) point for one of the flight tests. Altitudes reported from Mode C transponders are discretized in 100 ft intervals, while the 6 second update cycle of the HCS and the altitude tracking filter dynamics lead to approximately 30 second lags in the observed altitude on the ground relative to the true altitude.

### **5.3.5 Longitudinal Conformance Monitoring: Constant Speed Flight**

Advanced flight management systems are capable of “four-dimensional navigation” which provide the capability of computing an Estimated Time of Arrival (ETA) at a specified point along its route and which it is generally capable of meeting within a few seconds [Moir & Seabridge (2003)]. This new capability is being used in ATC through Required Time of Arrival (RTA) instructions to aircraft in order to optimize traffic flows. In addition, Miles-In-Trail (MIT) and Minutes-In-Trail (MINIT) restrictions are becoming increasingly common in ATC operations to manage delays and maximize throughput. Research is underway to discover how automated systems can be employed to support the controllers in the longitudinal domain, especially with the process of projecting aircraft positions into the future [Davison & Hansman (2003b)] to ensure that RTA, MIT and MINIT restrictions are met. For these projections of aircraft positions in the future to be valid, conformance monitoring in the longitudinal domain is essential.

The primary aircraft dynamic state that is used for longitudinal conformance monitoring is airspeed, although this is generally converted to a position at some point in the future for both existing conformance monitoring tools with longitudinal elements (e.g. HCS, URET, FPM) and projection tasks in ATC. Figure 5.29 contains a plot of the calibrated airspeed (CAS) during a cruise portion of one of the



flight tests. With an inferred speed target of 250 knots, the CAS varies only by about  $\pm 5$  knots during the 60+ minutes of flight time shown.

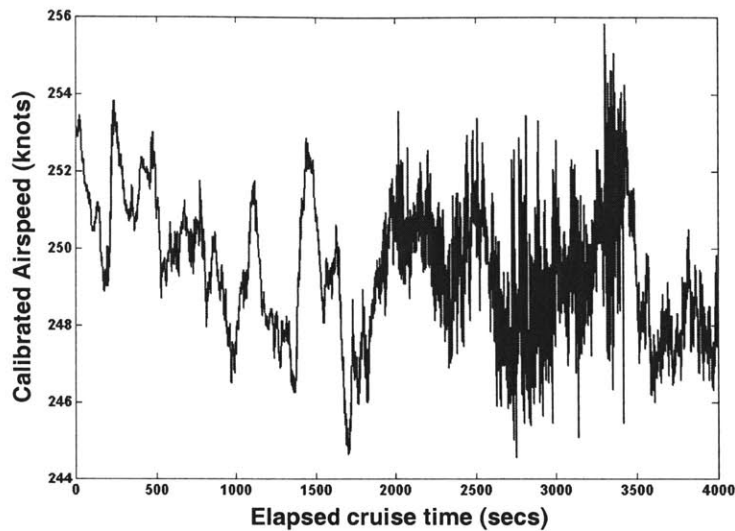


**Figure 5.29: Calibrated Airspeed During Cruise Flight**

Although no known intentional speed deviations were conducted during the test flights, for the sake of discussion one can again be synthesized from the nominal behaviors during the course of the flights by assuming that an observed speed change had not been authorized. The example speed transition to be considered for this purpose is displayed in Figure 5.30.

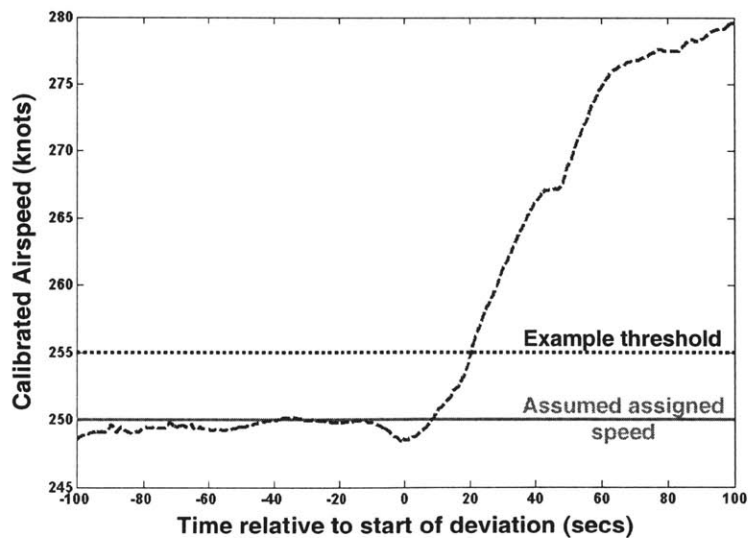


**Figure 5.30: Calibrated Airspeed Deviation Scenario**

With only one state being used to check longitudinal conformance monitoring, the simple threshold-based strategy employed in the existing systems described in Chapter 2 can be used effectively here. Assuming a nominal variation about an assigned speed of  $\pm 5$  knots, threshold placements of  $250 \pm 5$  knots CAS can be employed. With this setup, the synthesized speed deviation could have been detected after approximately 20 seconds.

### 5.3.6 Longitudinal Conformance Monitoring: Transitioning Flight

Just as the vertical transition conformance monitoring is difficult, so too the speed conformance monitoring during accelerating or decelerating flight regimes is difficult for similar reasons, namely:

- Poor knowledge of the Conformance Basis during speed transitions since commands are *indicated airspeed* while the radar outputs *ground speed*.
- Poor predictability of the aircraft dynamics during speed transitions:
  - Dependence on aircraft configuration and properties such as weight, aerodynamic configuration, thrust setting, etc. which affect thrust/drag and thus the speed profile
  - Sensitivity to atmospheric disturbances, especially wind gusts
  - Sensitivity to atmospheric properties affecting engine thrust level
- Poor surveillance in the speed channel: discretization and lag effects in the filters from which ground speed is derived.

Due to the lack of information on the longitudinal Conformance Basis during the test flights, demonstration of this issue was not possible. This, in itself, may be an indication of the lack of observability of the speed Conformance Basis in the current ATC system.

Aircraft dynamics issues could also not be demonstrated using the operational data, but are considered in more detail in the simulation studies described in Chapter 6.

Finally, the speed surveillance issues are demonstrated in Figure 5.31. This presents the calibrated airspeed recorded from the aircraft databus and the ground speed derived from the  $\alpha$ - $\beta$  trackers in the HCS for a small portion of one of the test flight during an acceleration maneuver. The vertical offset between the two profiles simply represents the difference in the definition of these two types of speed, primarily due to winds. However, the horizontal offset in the two profiles is not for this reason. It represents the lag introduced into the HCS-derived ground speed due to the dynamics of the  $\alpha$ - $\beta$  tracker.

In this example, the HCS speed lags the airspeed being recorded on the databus by approximately 60 seconds, or about double the lag in the vertical transitioning case. This is the primary reason why speed deviations are so difficult to detect in a timely fashion. This function is not supported by the performance of the surveillance systems, and as a result longitudinal conformance monitoring is challenging during speed transitions.

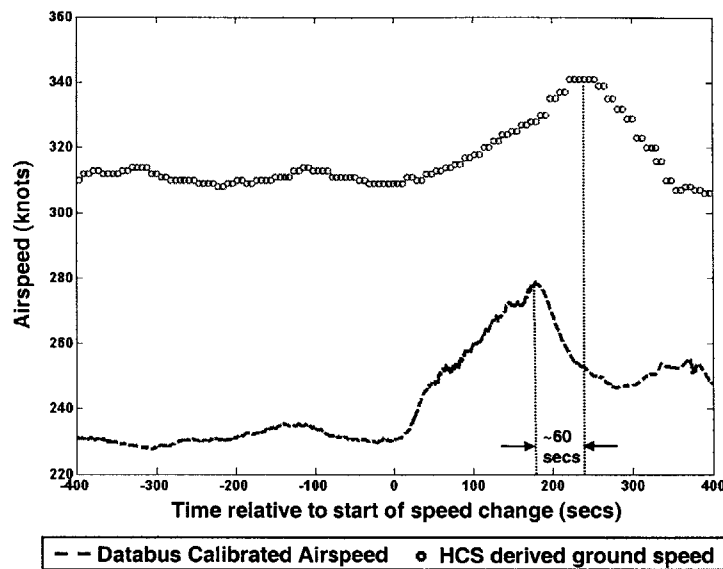


**Figure 5.31: Speed Surveillance Limitations**

### 5.3.7 Implications of Conformance Monitoring Issues for Future ATC System Design

The analyses presented in this section have fundamental implications for future ATC operations and procedural design. With even the simple forms of the CMAF elements employed (such as the low fidelity CMM), more effective conformance monitoring can be conducted in the non-transitioning environments with the aircraft-derived data, with higher order dynamic states and/or with more sophisticated algorithms compared to what is possible with today’s tools. This suggests that the introduction of advanced surveillance systems such as ADS-B that can provide higher accuracy, update rate and content states to a monitoring tool hold significant potential for allowing improved conformance monitoring in future ATC environments in these non-transitioning domains.

The improvements with higher order dynamic states suggested in the non-transitioning environments are harder to realize in the transitioning case. Medium or high fidelity CMMs are required to reduce the effects of modeling errors during transitioning domains. However, high fidelity models are not practical for most ATC operations and the more general medium fidelity models are often most appropriate. The

modeling errors that then have to be accepted require larger thresholds be utilized in the decision-making scheme. These larger thresholds increase the time to detect a non-conformance for a given false alarm level. These findings imply that ATC procedures should generally not require rapid detection of non-conformances at transition points when only dynamic states are available. If rapid detection is essential to a particular ATC operation, more accurate modeling of the aircraft transition dynamics are needed, either through the development of sophisticated high fidelity modeling techniques or through strict proceduralization. It was also shown that the use of intent states can significantly improve conformance monitoring capability in the transitioning domain. Hence the introduction of advanced surveillance systems that allow intent information to be surveilled also hold significant potential for allowing improved conformance monitoring in future ATC environments in the transitioning domains.

Many of these issues will be examined in more detail in the simulation studies presented in the next Chapter.

#### 5.4 Conformance Basis Observability Issues in Key Flight Phases

The previous discussions of the Conformance Monitoring Analysis Framework have stressed the fundamental importance of accurate knowledge of the Conformance Basis. Consistent knowledge of the Conformance Basis among the various agents in the ATC system (controller, pilot, aircraft and ground automation systems) is of importance since when inconsistencies exist between the agents, the potential for false alarm or missed detection of non-conformance increases. This is shown schematically in Figure 5.32.

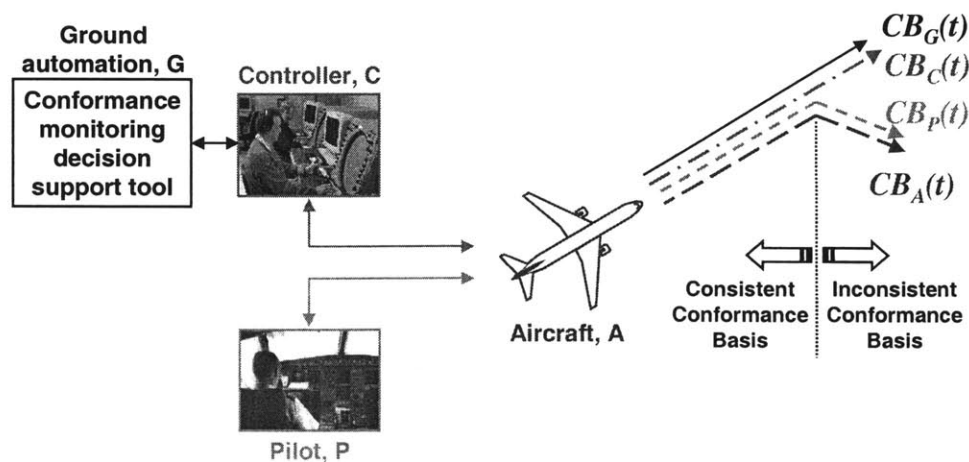
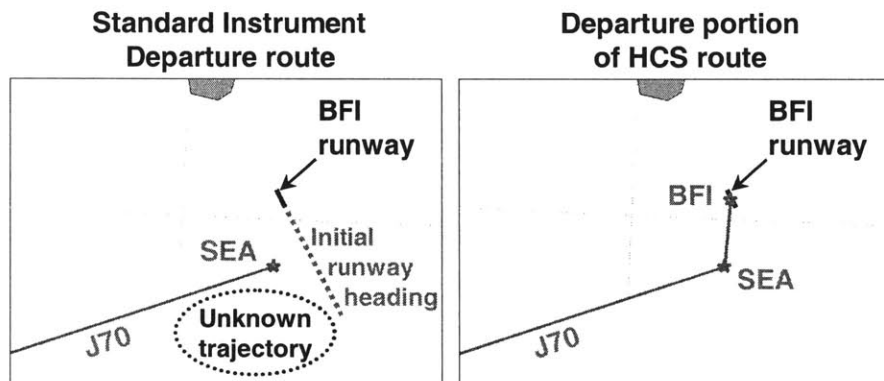


Figure 5.32: Importance of Consistency of Conformance Basis Among ATC Agents



Although SIDs provide an effective means to communicate general standard procedures, they contain insufficient data to determine a consistent departure route, and therefore Conformance Basis, that any given aircraft will follow since they allow flexibility for the departure controller to issue tactical radar vectors. These are often necessary to allow the controller to achieve efficient sequencing, spacing, and separation between aircraft given the current traffic conditions and are therefore determined in real-time given the current operating environment. The Kent Four Departure description contains the text “Climb runway heading, expect radar vectors to assigned route/fix...”, illustrating the proceduralized use of vector control by the departure controllers for BFI. The resulting variability present during the SID departure is illustrated on the left of Figure 5.34, with a trajectory discontinuity existing between the initial runway heading and the first flight plan route segment. Although the controller is capable of internal conformance monitoring from memory of the vectors issued to any given aircraft, this information is not entered into any ground automation, thereby reducing the benefit of any decision support tool employed in this environment at present.



**Figure 5.34: Trajectory Uncertainty During Departure**

After the end of the SID, the next Conformance Basis information source is the HCS flight plan route. The departure portion of the HCS route was :

BFI . . SEA . J70 . HQM

indicating a departure out of BFI towards SEA VOR before joining jet route J70 towards the HQM VOR. This portion of the flight plan route is illustrated on the right of Figure 5.34. The actual tracks of the two flight tests relative to the flight plan route are presented in Figure 5.35, where it is apparent that both

tracks deviate significantly from the HCS flight plan route immediately after departure before converging to it.

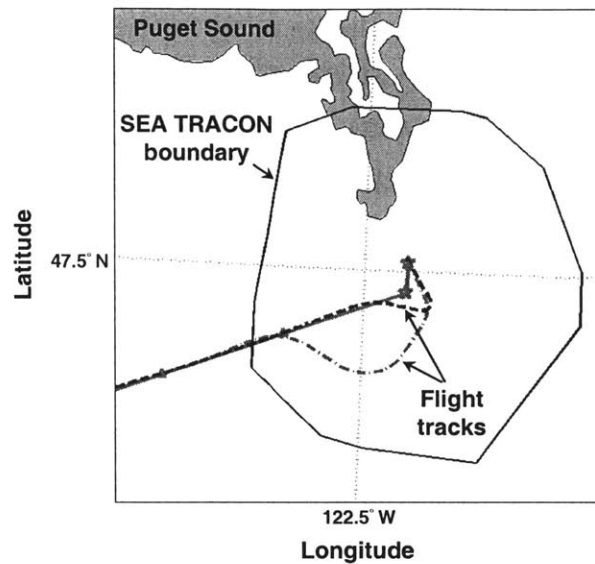


**Figure 5.35: Flight Test Departure Tracks Relative to HCS Flight Plan Route**

It is apparent that neither the SID nor the HCS route are adequate for describing the departure trajectory with enough accuracy to undertake automated conformance monitoring on the ground. Given the real-time nature of the tactical vectoring being used, no consistent route was flown by the two flights even though they were nominally on the same flight plan. If conformance monitoring is conducted using the departure portion of the HCS flight plan as the Conformance Basis, lateral deviations of up to 12 nm were observed during the second test flight. But these deviations are due to the lack of knowledge in the ground automation of the proper Conformance Basis rather than non-conformance to the verbal clearance on the part of the aircraft. This discussion demonstrates the high level of uncertainty in the Conformance Basis from the perspective of the ground automation under vectoring conditions and a concomitant difficulty in creating conformance monitoring decision-support tools during departure operations. The implication is that either a large conformance region is required around a departure Conformance Basis, high levels of false alarms have to be accepted or more accurate communication of the Conformance Basis to the support tool is required.

The flight tracks observed in Figure 5.35 imply that all of the tactical vectoring is contained within the TRACON boundary so that by the time the aircraft enters en-route (ZSE) airspace, the aircraft are established on their flight plan route. This would imply that by the time the aircraft enter the en-route

airspace, the HCS flight plan is an accurate Conformance Basis to use for conformance monitoring. However, the SEA TRACON airspace only extends up to 11,000 ft and a three-dimensional analysis of the flight data reveals that the flights were in fact *not* established on their HCS flight plan routes prior to leaving SEA TRACON airspace, as shown in Figure 5.36. Field studies at other TRACONs and ARTCCs around the US suggest that Standard Operating Procedures (SOPs) or Letters Of Agreement (LOAs) often exist between facilities allowing certain common operating practices to be formalized. Although this could not be verified, it is likely that in this case an LOA exists between SEA TRACON and ZSE allowing aircraft to be on a tactical vector to intercept the HCS route when they enter ZSE's airspace, rather than already being established on the route. The implication of this practice for conformance monitoring is that the en-route controller needs to infer what vector the aircraft entering their airspace are initially on (something that may be defined in the LOA), and ensure that they properly intercept the active flight plan route when they eventually reach it. Conformance to the expected intercept maneuver becomes a critical task for the ZSE controller handling the first en-route sector after the TRACON since all subsequent traffic plans for the center rely on the aircraft being established on the HCS route.

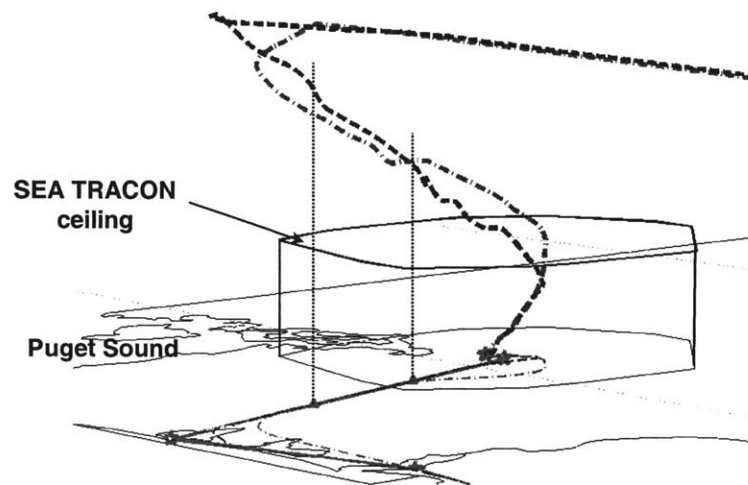


**Figure 5.36: Three-Dimensional Departure Flight Tracks**

#### **5.4.1.2 Vertical Departure Environment**

The primary indication of the controller's vertical Conformance Basis is given by the assigned altitude that appears on the datablock for each flight on the radar screen and which is also logged in the HCS. A comparison of this assigned altitude and the actual aircraft altitude recorded from the databus during one of the test flights is illustrated in Figure 5.37. Several issues are illustrated in this figure.



Firstly, no assigned altitude existed immediately after take-off. This corresponds to the time when the departure vectoring discussed above was being conducted by the departure controller. The first assigned altitude appearing in the HCS system was the filed cruising altitude at point ① (35,000 ft in this case), and this was the only assignment while the aircraft was inside TRACON airspace. This indicates that intermediate altitude assignments are not entered into the automation system inside the TRACON. Given the high workload level of controllers in this airspace, the extensive use of dynamic vectors and the close proximity of controllers in charge of adjacent sectors, standard operating practices preclude the requirement to update any automation system with the clearances issued inside the TRACON. When the aircraft transitioned into ZSE Center airspace at point ②, a series of intermediate step altitudes assignments (of 23,000 and 27,000 ft in this case) were made before the cruising altitude was reassigned as the aircraft climbed through these flight levels. This general pattern was also observed in the other flight test profile.

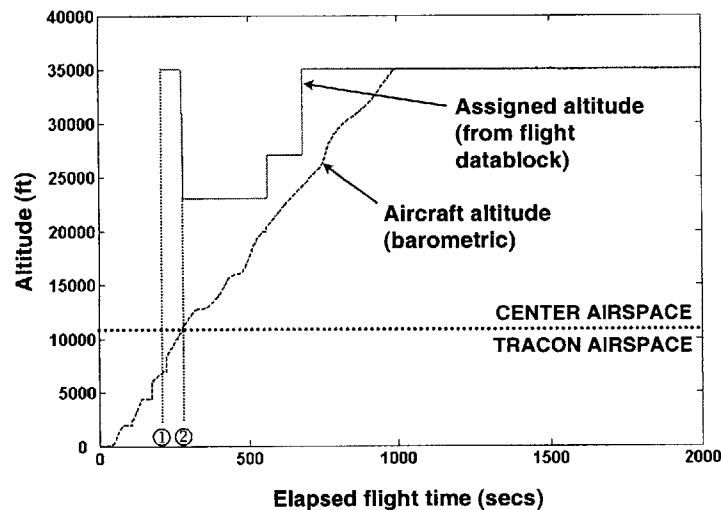


**Figure 5.37: Vertical Profile Relative to Assigned Altitude During Flight Test Departure**

It is apparent from Figure 5.37 that, similar to the case in the horizontal domain, vertical conformance monitoring is extremely difficult to undertake with automation in the current ATC environment during the departure phase of flight due to a lack of vertical Conformance Basis. Either no assigned altitude exists in the automation or it is not a valid or meaningful target (such as the filed cruising altitude used in the TRACON). In addition, while the actual altitude of the aircraft is increasing during climb in center airspace, the interim assigned altitudes are stepped up as the aircraft gets within a few thousand feet of the current target. As such, the vertical conformance monitoring is not possible without additional information during the aircraft's climb to its cruising altitude.

## 5.4.2 Conformance Basis Observability Issues: En-Route Phase

### 5.4.2.1 Lateral En-Route Environment

Once aircraft leave the TRACON airspace, they are transferred to Seattle Center for en-route control. In the en-route domain, it is expected that the lateral dimensions of the HCS route accurately represent the current clearance for the flight (apart from initial uncertainty due to vectoring initiated prior to entering en-route airspace, as discussed previously). It is common for a flight plan to evolve as the flight proceeds due to changing controller constraints and pilot preferences. The evolution of the lateral HCS flight plan route for one of the test flights relative to the actual path flown is presented in Figure 5.38.

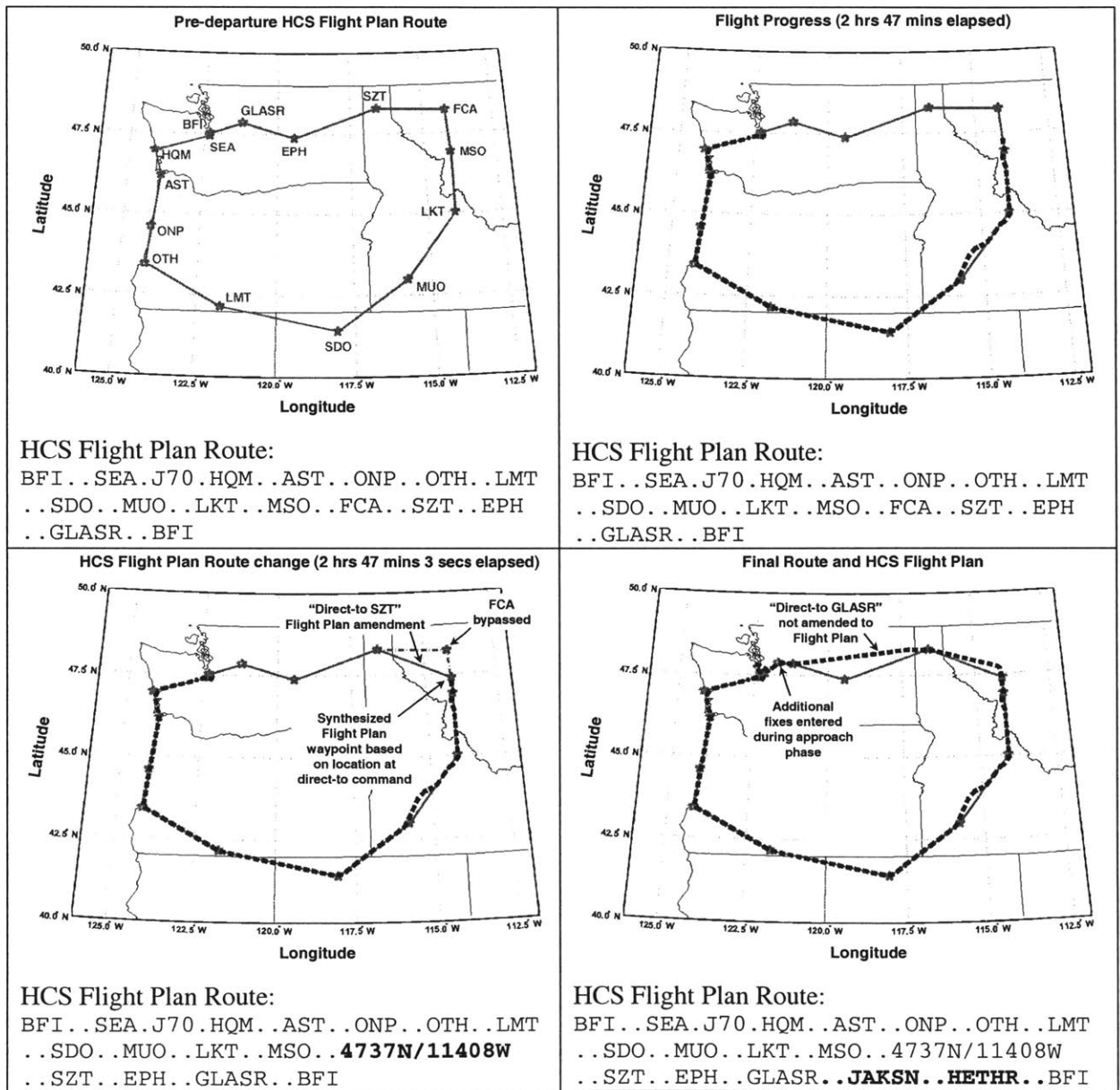
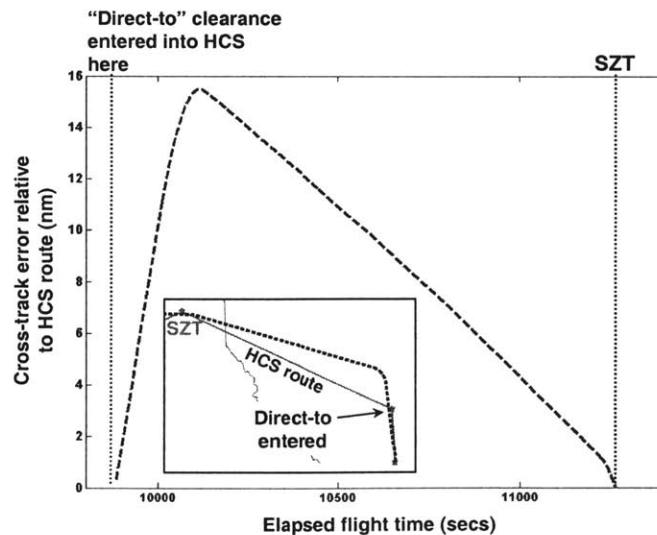


Figure 5.38: Evolution of Lateral HCS Flight Plan and Actual Flight Path Flown

The first 2 hours and 47 minutes of this test flight followed the pre-departure flight plan route, as illustrated in the top half of Figure 5.38 (the deviations observable near MUO, LKT & MSO were intentional parts of the flight test procedure and would not be observed in nominal ATC operations). Apart from the departure vectoring issues discussed in the previous section, the HCS flight plan during this time appears to be an effective Conformance Basis away from transition points.

With the flight still 50 nm from the FCA waypoint, the HCS flight plan route archive indicates that a “direct-to SZT” clearance was issued, as shown by the flight plan message in the bottom left of Figure 5.38. The aircraft location at the time the command was issued (approximately N47.37°, W114.08°) became a new “virtual waypoint” in the HCS flight plan route, followed immediately by the identifier of the fix to which the direct-to command was issued (SZT in this case). Notice that the flight plan trajectory formed by the straight line connecting these points was not indicative of the path that the actual aircraft flew, since the pilot still had to initiate and complete the turn after the new clearance had been given. As can be seen in the bottom right of Figure 5.38, there is a significant difference between the path flown and the direct line segments joining the command issuance point and the SZT waypoint. Hence, if the direct line segments are used as the Conformance Basis in the CMAF implementation, large lateral deviations result as illustrated in Figure 5.39. However, it is clear that the aircraft stabilizes on a path demonstrating intent to fly towards SZT, suggesting that a more effective Conformance Basis might be based primarily on the direct-to heading towards the next waypoint. Alternatively, the time delay and aircraft maneuver dynamics need to be accounted for in the determination of the Conformance Basis.



**Figure 5.39: Lateral Deviations from HCS Route After Direct-To SZT Amendment**

The flight track suggests that another direct-to was also issued (to airspace fix GLASR) immediately after the SZT waypoint was reached since the EPH waypoint was also bypassed. However, the HCS route does *not* have an amendment reflecting the change in this case, suggesting that this clearance was issued without being entered into the automation. As a result, the actual flight deviates from the HCS flight plan route by as much as 40 nm north of EPH. Examination of the high altitude air traffic control sectors in this region (depicted in Figure 5.40) reveals that much of the flight towards the new direct-to fix was within a single sector (ZSE07), suggesting that the controller may have preferred to simply remember the amendment that primarily only affected his/her own sector rather than explicitly update the HCS with the amended route. The impact on the downstream sector (ZSE31) could have been covered by a formal ZSE procedure, or explicitly communicated to the ZSE31 controller through verbal channels (the two controllers for these neighbouring sectors may even be sat next to each other to facilitate this) rather than through the HCS. This type of informal verbal communication is a standard operating practice that has been observed often on site visits to ATC facilities. It is a major reason why HCS flight plan routes may not always accurately reflect the clearances issued to the aircraft.

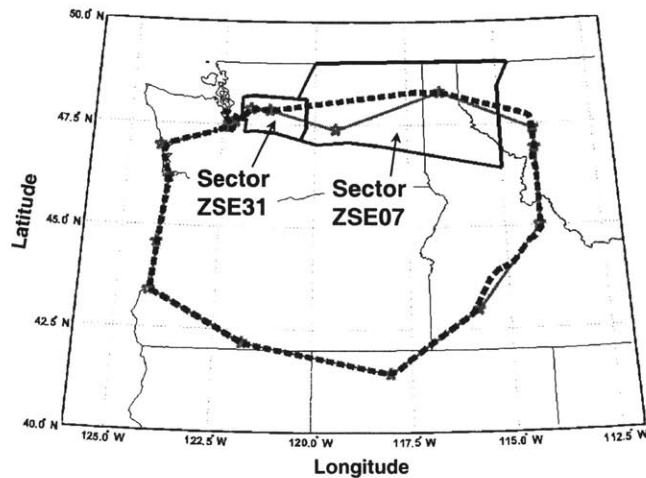


**Figure 5.40: High Altitude Sectors Involved in the Direct-To GLASR Route Amendment**

It is apparent from this discussion that the lateral flight plan route evolves as a flight progresses through the application of various amendments such as re-routes and direct-to clearances. Some of these amendments are entered into the automation systems, while others appear to be communicated between the controllers involved through other channels such as voice. Those amendments that are not entered into the automation clearly have implications for any conformance monitoring functions, such as the association checking routines of the HCS described in Chapter 2.

The reliance of conformance monitoring algorithms on an accurate internal representation of the trajectory to be flown relative to that communicated to the aircraft is of paramount importance if effective ground-based conformance monitoring is to be conducted. Without accurate knowledge of this conformance basis, the function will not be able to perform effectively since the observed positions will not be compared to the proper expected positions. Studies based on observations in several ATC centers in 1997 and 1999 [Lindsay (2000a), Lindsay (2000b)] indicated that as many as 70-80% of controller route clearances issued to flight crew by voice did not have matching HCS update entries and that position deviation from the internal HCS route often exceeded 4 nm even though the aircraft were correctly following the route assigned to them by the controllers. Although most route clearances that are not updated in the HCS are likely to have been self-contained within a controller's own sector (and therefore the controller should have a mental model of the "correct" Conformance Basis [Reynolds *et al.* (2002)]), the automation functions are using the original trajectories so an aircraft could appear non-conforming to the automation. The need to be robust to such issues is one reason why many existing ground-based conformance monitoring tools use large threshold parameters. If more effective conformance monitoring is required, operating practices that bypass the updating of the Conformance Basis in the automation may need to be eliminated.

#### **5.4.2.2 Vertical En-Route Environment**

The evolution of the assigned altitude and the actual aircraft profile during the en-route phase of the first test flight are shown in Figure 5.41. It was seen in the previous section that the assigned altitude in the HCS was not an effective vertical Conformance Basis in the departure phase of flight, and this statement can be extended for vertical transitions in the en-route domain as well. The assignments evolve in discrete steps, while the altitude profile itself is governed by the aircraft flight mode, dynamics and atmospheric properties. Often the assignment is changed well before the aircraft actually reaches the interim assigned altitude.

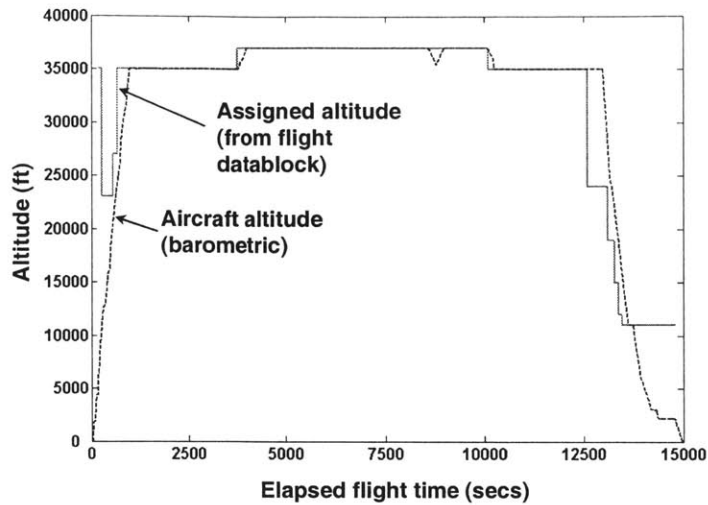


**Figure 5.41: Evolution of Assigned Altitudes and Actual Altitude Profile**

However, when a stable altitude target is presented for an extended period of time such that the aircraft has time to reach and stabilize to it, the variation of the barometric altitude profile relative to the assignment is incredibly small, as discussed in the previous section on vertical conformance monitoring (Section 5.3.3). As such, an assigned cruising altitude level that has been reached provides a solid Conformance Basis from which effective conformance monitoring can be conducted.

### 5.4.3 Conformance Basis Observability Issues: Descent Phase

A more detailed view of the vertical behavior during the descent phase of the test flight is provided in Figure 5.42.

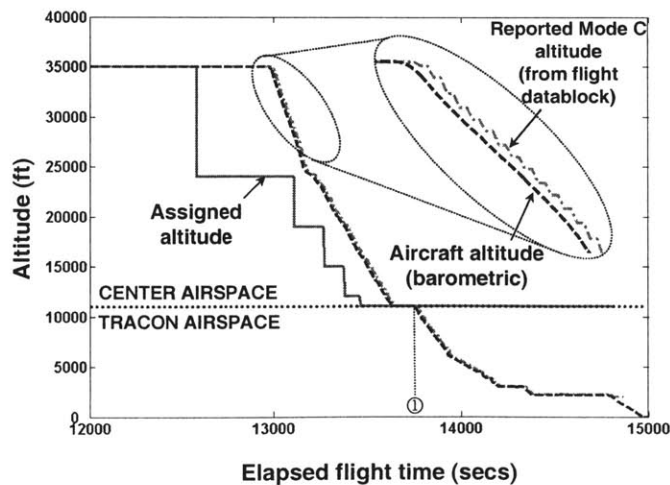


**Figure 5.42: Vertical Conformance Basis and Surveillance Issues on Descent**

Some interesting insights into ATC operations can be observed in the data presented in this figure. Firstly, it was seen in previous sections that the assigned altitude was not an effective vertical Conformance Basis during the vertical transitions in the departure and en-route environments. This statement can be extended for all vertical transition environments since the same issues discussed previously are also evident on descent. The main difference is that the actual aircraft altitude is now consistently *above* the assigned altitude, while during climb portions they are consistently *below* the assigned altitude. In the descent data, it can also be seen that the reduced altitude assignment on the initial descent in the HCS occurred about five minutes before the actual descent was initiated. For this whole time, the assigned altitude from the perspective of the HCS was 11,000 ft below the actual altitude. The likely explanation for this discrepancy between when the descent altitude was assigned and when it was initiated is that the assignment may have been to descend at the pilot's discretion or a command to cross a particular waypoint at a particular altitude. Faced with commands such as these, pilots often choose to descend as late as possible or at the top of descent (TOD) point predicted by an FMS to achieve a more fuel-efficient descent profile than if the descent was initiated as soon as the clearance had been given. Although this type of flexibility is highly desirable from an operational perspective, it contributes to the significant challenges associated with defining the Conformance Basis in the vertical transitioning environment.

Secondly, the assigned altitudes only extend down to the ceiling of the TRACON airspace (11,000 ft). The aircraft briefly levels out at this altitude, and this was probably the crossing-restriction altitude given during the descent from cruising altitude to get the aircraft at an LOA-approved altitude ready for hand-off to the TRACON. However, once the aircraft enters TRACON airspace (after point ④ in the figure), no additional updates to the HCS assigned altitude take place. This is consistent with the observation made in the context of the departure aircraft that TRACON controllers do not update the assigned altitude in the HCS. Again, there is no viable vertical Conformance Basis existing in the HCS in the descent domain against which automated conformance monitoring can be conducted.

Finally, the lag and discretization of the ground-based surveillance is clearly evident.

#### **5.4.4 Conformance Basis Observability Issues: Approach Phase**

In the lateral flight plan evolution presented in Figure 5.38, it is seen that additional airspace fixes (JAKSN and HETHR) were entered prior to returning into SEA TRACON airspace for landing at BFL. Just as standard instrument departures exist at aircraft takeoff, so standard procedures called Standard

Terminal Arrival Routes (STARs) exist for approaches to the destination airport. These provide a set of pre-defined arrival instructions under a standard name. An inspection of the STARs for BFI that include the added fixes suggest that at least part of the GLASR FIVE ARRIVAL was utilized in this flight. This STAR is presented in Figure 5.43. Knowledge of the STAR being used during an arrival would improve the knowledge of the Conformance Basis during this operation.

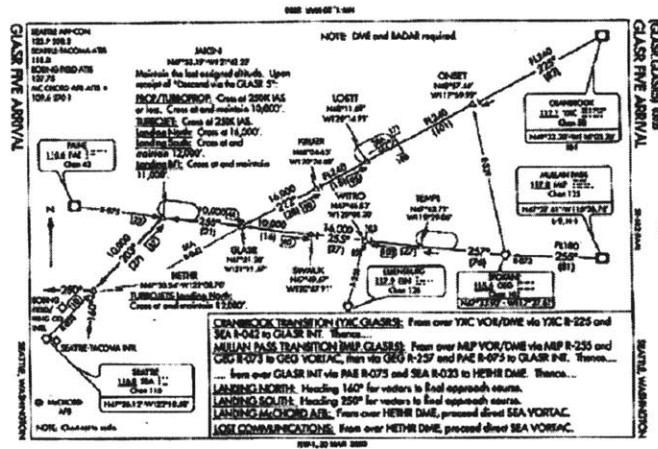


Figure 5.43: Standard Terminal Arrival Route (STAR) to BFI

A comparison of the arrival flight track for this flight and the amended flight plan route containing JAKSN and HETHR is presented in Figure 5.44. Note that the STAR calls for vectors to the final approach course at HETHR. As discussed in the context of the departure, tactical vectors can reduce the predictability of the actual trajectory to be flown (and hence increase the uncertainty in the Conformance Basis for an automated system), but increase flexibility to account for various traffic conditions for ATC. The issuance of the vector in this case is apparent when the aircraft turns off the course in Figure 5.44.

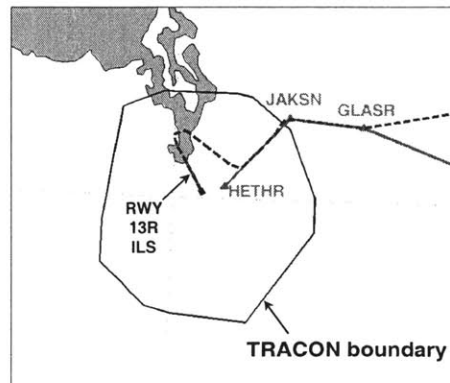
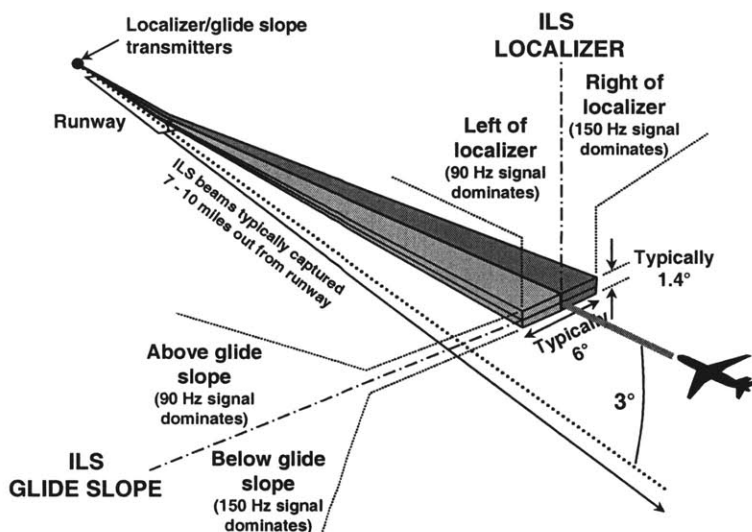


Figure 5.44: Flight Test Arrival Tracks Relative to HCS Flight Plan Route



However, a definitive Conformance Basis in both the lateral and vertical axes is re-established when the tactical vectors intercept the final approach course. Due to the limited number of runways at airports, most aircraft fly an almost identical final approach path. To facilitate this operation, many runways at larger airports utilize the Instrument Landing System (ILS) which provides guidance to flight crew during instrument conditions along a well-defined path made up of lateral and vertical elements called the localizer and glide slope respectively. Each is made up of two signals of different frequency whose relative degree of modulation change as a function of the aircraft location within the beams [Kayton & Fried (1997)], as illustrated in Figure 5.45. When the aircraft is exactly on the ILS path, the two signals have equal strength, while one of the signals dominates if the aircraft deviates to one side or the other. The signals are used by systems on-board the aircraft to provide guidance cues along the ILS path to the pilot or an autoland system.



**Figure 5.45: Instrument Landing System (ILS) Schematic**

Those airports with ILS technology installed have standard approach procedures defined to assist pilots in capturing and flying the proper path defined by the signals, as illustrated in Figure 5.46 for runway 13R at BFI which was used in the test flights. This procedure defines the proper heading and altitude targets to be flown (130° and 2200 ft respectively) in order to intercept the ILS beams at the final approach fix (6.4 nm from the runway threshold in this instance). A comparison of the ILS path extended out 10 nm from the runway and the final approach flight paths for the two test flights considered here are

shown in Figure 5.47. The approach at 2200 ft to intercept the glide slope before following the ILS path to the runway at BFI is clearly evident.

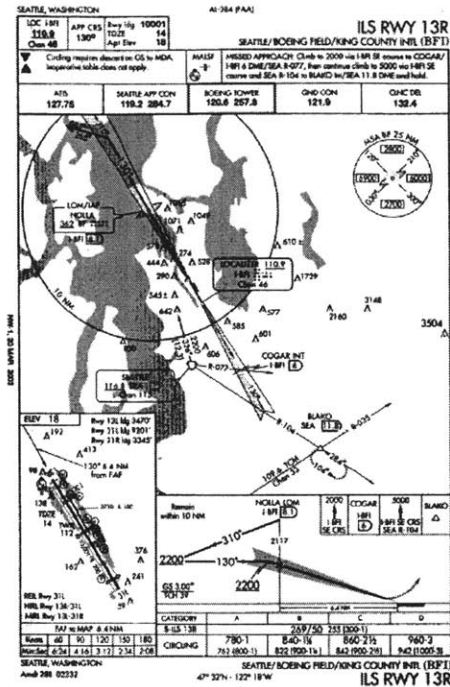


Figure 5.46: ILS Approach Procedure into BFI Used During Test Flights

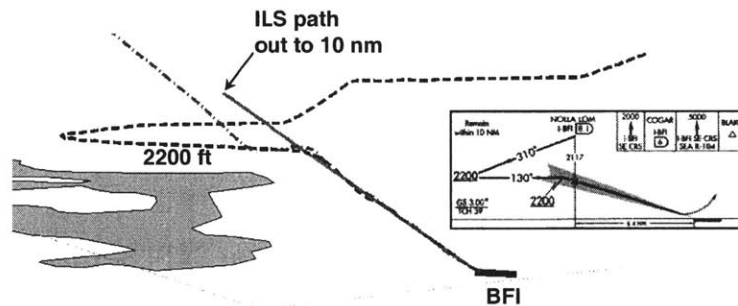


Figure 5.47: Flight Test Arrival Tracks Relative to ILS Path

The systems providing ILS path guidance on the aircraft measures the Difference in Depth of Modulation (DDM) of the 90 Hz and 150 Hz signals making up the localizer and glide slope paths. The DDM metric is a measure of the angular deviation within the localizer and glide slope fan beams, calibrated to a value of  $\pm 0.155$  for a full scale  $3^\circ$  deviation on the localizer, and a value of  $\pm 0.175$  for a full scale  $0.7^\circ$  deviation on the glide slope [Kayton & Fried (1997), ICAO (1985)]. Hence, using the

localizer and glide slope DDM values recorded on the databus during the flight tests enables positional deviations relative to the ILS path to be derived according to:

$$\text{Localizer deviation} = \left( \frac{DDM_{LOC}}{0.155} \right) \times \left( \frac{3^\circ \times \pi}{180^\circ} \right) \times \text{Distance to localizer antenna}$$

**Equations 5.5**

$$\text{Glide slope deviation} = \left( \frac{DDM_{GS}}{0.175} \right) \times \left( \frac{0.7^\circ \times \pi}{180^\circ} \right) \times \text{Distance to glide slope antenna}$$

Since the locations of the localizer and glide slope antennas were not known, the distance to the touchdown point on the runway was used as a surrogate in these calculations. The resulting localizer and glide slope deviations for the two test flights are presented in Figure 5.48. The use of the runway location in the calculations may affect the accuracy of the absolute values displayed here (especially as the distance to the runway decreases), but comparison of relative values at different distances is still valid. Note also that no information was available regarding whether these approaches were flown manually or through an autoland system and the experimental nature of the test aircraft is reiterated such that the behaviors illustrated in Figure 5.48 are not representative of any production commercial aircraft performance level.

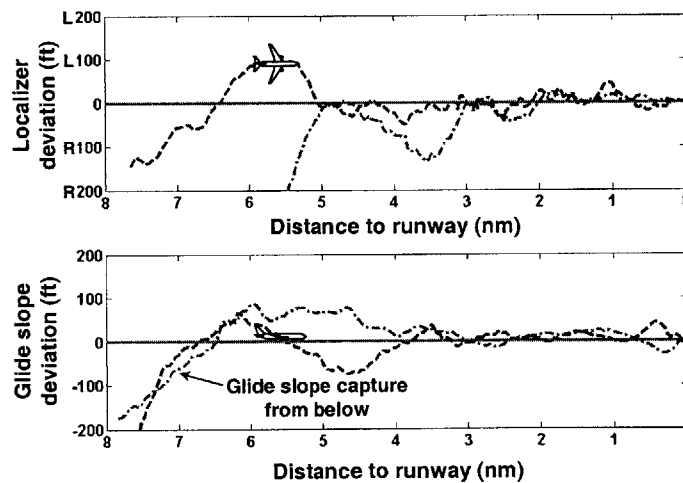


**Figure 5.48: Flight Test ILS Localizer and Glide Slope Deviations**

From a conformance monitoring perspective, the ILS path provides a highly reliable and well-defined lateral and vertical Conformance Basis. Certification requirements exist for ILS landing systems that enable bounds on nominal deviations about the ILS path to be defined for various system operational

procedures such as CAT I/II/III instrument approaches [Braff *et al.* (1996)]. The combination of the well-defined Conformance Basis coupled to the knowledge of likely deviations allows for effective conformance monitoring to be conducted in the final approach environment. Advantage has been taken of these properties in the independent closely-spaced parallel approach used in the Precision Runway Monitor system discussed in earlier chapters.

### 5.4.5 Implications of Conformance Basis Observability for Future ATC System Design

A block diagram representation of the Conformance Basis update procedure in the current US ATC system is illustrated in Figure 5.49. Flight plans reside in the HCS, from which flight progress strips (Figure 2.4) are printed for use by the controllers. This same flight plan information is used by the conformance monitoring Decision Support Tools (such as URET) to determine an internal model of the Conformance Bases for each aircraft being monitored. A simultaneous Conformance Basis model can be considered to reside internal to the controller consistent with the clearances communicated to the aircraft within the ATC airspace. Nominally, whenever the controller issues a clearance that amends the current flight plan clearance, a corresponding update is made to the HCS through a keyboard interface. In practice, such updating of the HCS is not always performed, as observed in the operational data described in the preceding subsections. As a result, the Conformance Basis model internal to the DST can be different from that internal to the controller and active in the ATC airspace. Under these conditions, the observed behaviors available from the surveillance systems would be compared to invalid Conformance Bases in the DST, leading to the potential for missed detections of actual instances of non-conformance or false alarms of alerting non-conformance when none has actually occurred.

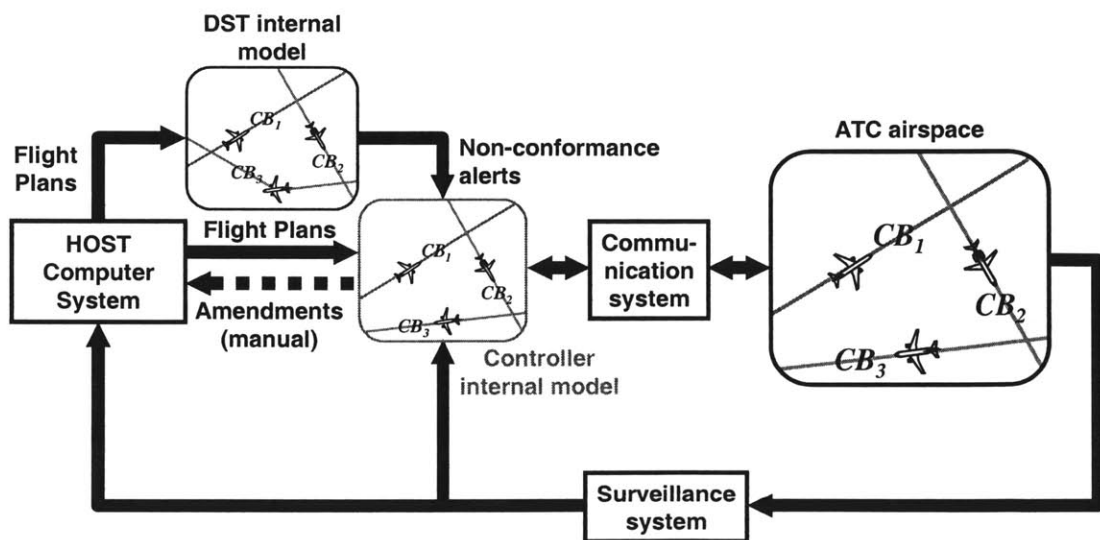
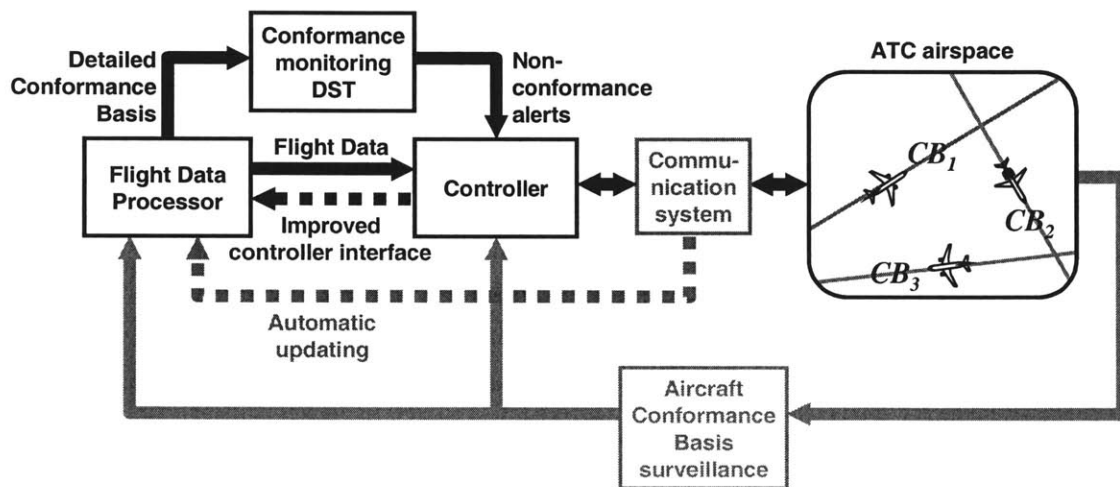


Figure 5.49: Conformance Basis Updating in Current ATC System

Missed detections and false alarms severely limit the utility of a conformance monitoring decision support tool, whether through poor overall performance figures or degraded trust on the part of the operator [Lee & Moray (1992)]. Therefore, the wider application of DSTs for the conformance monitoring task requires higher accuracy of the Conformance Basis being used by the automation. Several enhancements to the current system that could be used to achieve higher Conformance Basis accuracy in future ATC systems are illustrated in Figure 5.50. These include:

- Improved human-machine interfaces to make updating of the automation easier, more accurate and requiring lower workload.
- Advanced communication systems that allow automatic routing to the automation of clearances issued to the aircraft, e.g. through voice-recognition systems or automatic routing of datalink clearance messages to the DST.
- Advanced surveillance systems that allow direct verification of the Conformance Basis being utilized on board the aircraft being monitored.



**Figure 5.50: Potential Conformance Basis Updating Enhancements in Future ATC System**

## 5.5 Summary

This Chapter has contained an in-depth analysis of conformance monitoring issues as a function of flight regime in the ATC system using operational aircraft and ground-based data archived during two test flights and example implementations of the Conformance Monitoring Analysis Framework.

In the analysis of lateral conformance monitoring during straight flight, a detailed comparison of the use of various state combinations to generate Conformance Residuals and FA/TTD curves from air and radar surveillance sources was conducted. Results suggest that significantly better conformance monitoring performance is associated with the higher quality/higher update rate aircraft-based information relative to the ground-based data, and with the use of higher order dynamic states in this flight regime. A comparison of the results with those for existing systems under the same non-conformance scenario suggests that even this simple implementation of the CMAF produces far superior time-to-detection at zero false alarm rates than all of the existing en-route operational tools and comparable times to many developmental tools. Similar results were observed in the vertical domain during level flight with access to higher order dynamic states such as flight path angle.

The greater challenges in the lateral transitioning environment have been discussed by demonstrating the errors that exist in the Conformance Residual using a low and medium fidelity CMMs (through discrete and circular fillet transitions respectively) for a properly conforming aircraft. These errors could theoretically be reduced with a tuned high fidelity model but this is generally not practical for wide ATC application, suggesting that generic medium fidelity models may hold most promise. Hence, larger thresholds are required during transitioning flight regimes than non-transitioning flight regimes. In all cases, errors were seen to be larger in the higher order dynamic states, implying that the benefits of these states suggested from the straight flight case may not be realizable in the transitioning regimes. However, the potential availability of intent states in advanced surveillance systems holds significant promise to enable improved transition conformance monitoring in future. Overall, these results suggest that the introduction of advanced surveillance systems, such as ADS-B, that could provide various aircraft-derived dynamic and intent states to a monitoring system hold significant potential for allowing improved conformance monitoring in future ATC environments.

Significant challenges were also identified in the vertical transitioning domain. The reasons for these challenges include the greater dependence on automation mode, aerodynamic configuration and atmospheric properties than other domains. A demonstration of these issues is presented in the simulation studies of the next Chapter. Longitudinal conformance monitoring issues during constant speed flight were briefly demonstrated by analyzing how quickly a speed deviation could be detected using a simple threshold-based strategy. Longitudinal monitoring challenges during changing speed flight were described in terms of poor knowledge of the Conformance Basis, unknown aircraft dynamics and

limited/delayed surveillance of the speed state. These issues will also be demonstrated in the simulation studies presented in the next Chapter.

Finally, a detailed survey of the observability of the lateral and vertical Conformance Bases in the various phases of the test flights was conducted. Poor knowledge of the Conformance Basis inside the HCS in both axes was observed during the departure phase as the controllers require significant flexibility to maneuver aircraft for separation purposes inside the TRACON. In the en-route phase, the flight plan resident in the Host Computer System provides a lateral Conformance Basis. The flight plan was seen to evolve throughout the course of the flight test, and although it provided an accurate basis for conformance monitoring for much of the time, it did not provide an accurate representation of the clearance issued to the aircraft after several direct-to amendments or at the trajectory transition points. The assigned altitude during the en-route phase was generally found to be an effective Conformance Basis during level flight, although it was totally ineffective during altitude transitions, especially after the Top of Descent point due to the uncertainty in the descent initiation time and profile to be flown. In the approach phase, the Standard Terminal Arrival Route to the airport provided some knowledge of the lateral and vertical Conformance Basis, before vectoring was commenced for sequencing to the final approach course. Once established on the final approach course, the ILS localizer and glide slope paths provide an unambiguous Conformance Basis which allows for detailed conformance monitoring during the final approach flight phase.

The issue of Conformance Basis observability is of critical importance to the conformance monitoring application. In the environments described above where the Conformance Basis did not exist or was inaccurate in the ground automation, effective conformance monitoring could not be conducted. Without accurate knowledge of the Conformance Basis, no amount of aircraft behavior surveillance will improve the conformance monitoring capability in that environment. Future ATC environments will therefore need to ensure the observability and accuracy of the Conformance Basis whenever conformance monitoring is required, for example through improved human-machine interface design, or the application of advanced communications and surveillance technologies.

[This page intentionally left blank]



---

# CHAPTER 6: Investigating Conformance Monitoring Issues Using the Analysis Framework & Simulated ATC Data

---

## 6.1 Introduction

The operational studies described in the previous Chapter were effective at illustrating actual conformance monitoring issues encountered in today's ATC system and highlighting many fundamental issues. However, the analysis was limited to those scenarios that were actually encountered in the two flight tests. In order to expand the investigation of conformance monitoring issues into other potentially interesting areas that were not seen in the test flights, the analysis framework was also exercised through simulation studies, as illustrated in Figure 6.1. A study using Microsoft® Flight Simulator 2002 (FS2002) is described in this chapter where conformance monitoring issues and approaches are investigated under a number of ATC scenarios representative of actual system operation in the lateral, vertical and longitudinal domains.

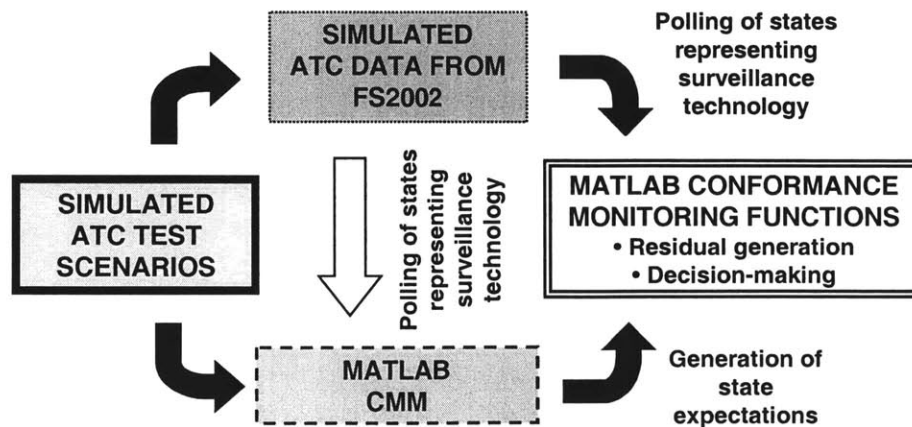


Figure 6.1: Implementation of the Analysis Framework Using Simulated ATC Data

## 6.2 Simulated ATC Data Collection

Microsoft® Flight Simulator 2002 (FS2002) was chosen as the Actual System Representation element of the analysis framework in the simulation studies. This is a commercial flight simulation program that has the advantages of being readily available, inexpensive and contains an excellent user interface representing several modern glass-cockpit commercial aircraft. The program contains simulations of the primary autopilot interfaces (Flight Management System<sup>†</sup> and Mode Control Panel) available in the real aircraft. The display, automation and control interfaces are illustrated in Figure 6.2. Limited control over environmental parameters such as wind speed and direction, gust level and turbulence is also provided. However, it was found that there were some limitations in the atmospheric and aircraft dynamic models, the effects of which will be discussed in the context of the individual domain investigations.

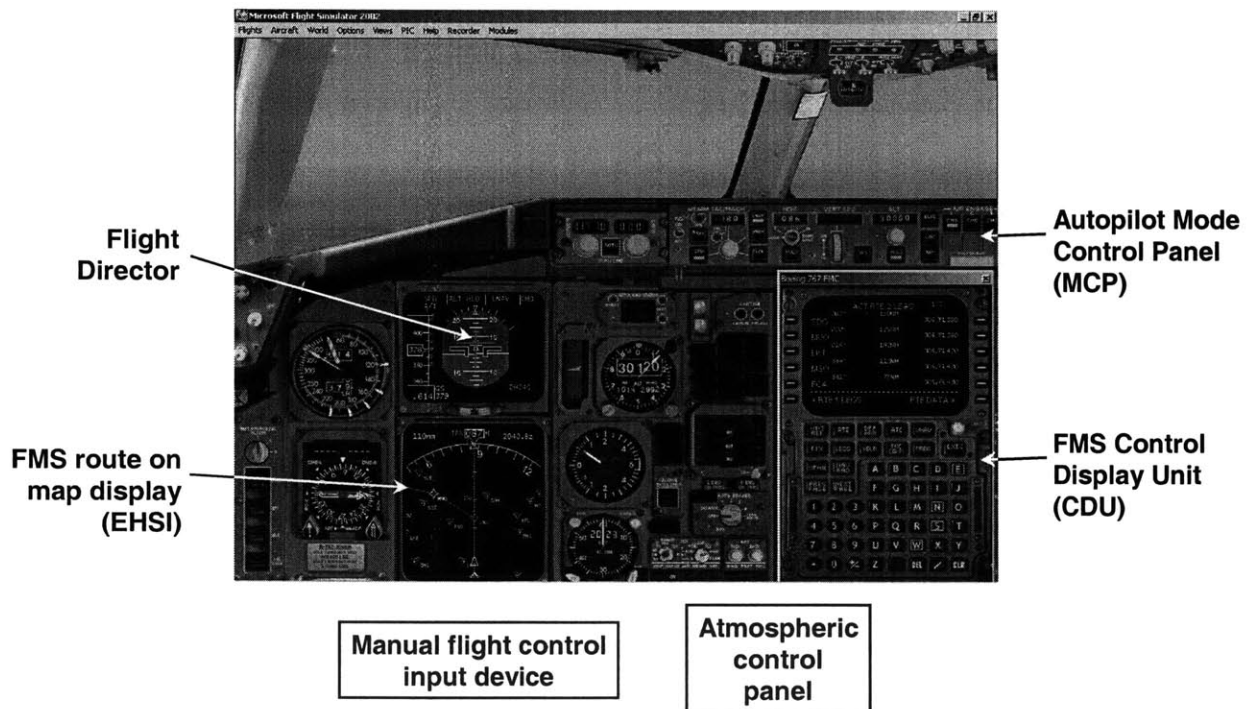
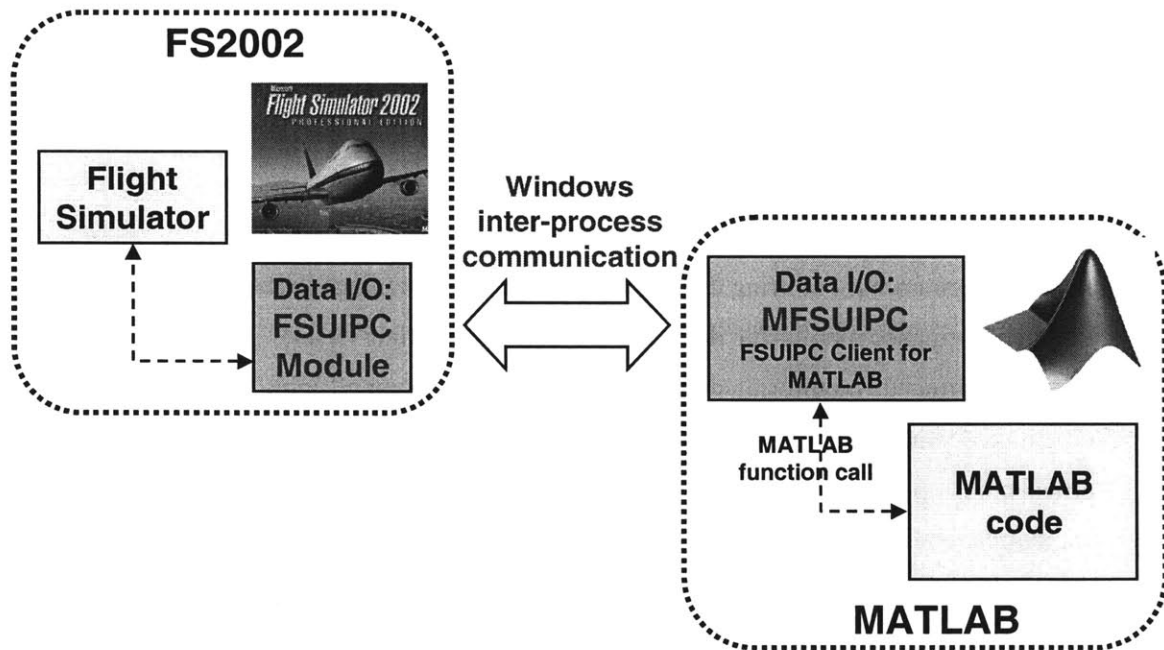


Figure 6.2: Flight Simulator Cockpit Screenshot

In order to implement the Conformance Monitoring Analysis Framework with the FS2002 simulation, a software utility was developed (called MFSUIPC [Pollock (2003)]) which resided in the

<sup>†</sup> The FMS simulation capability required an additional third party software called 767 Pilot In Command, developed by Wilco Publishing for FS2002.

MATLAB environment. This acted as a complement to existing third-party software (called FSUIPC\*) that is a module residing within FS2002 and provides access to and control over numerous variables used within the flight simulator. Together, these utilities provided a real-time, duplex link between the FS2002 and MATLAB computing environments, as illustrated in Figure 6.3. This enabled the same MATLAB models and code developed for the operational data analysis to also be used for the simulation studies. By placing models of various surveillance technologies in this communication path, analysis of different surveillance environments and candidate CMM and Conformance Residual/decision-making schemes could be performed in real-time with FS2002 simulated data.



**Figure 6.3: Flight Simulator/MATLAB Integration Capability**

In order to allow for comparison with the operational data analysis, a similar set of implementations of the other framework elements were employed in the simulation studies. The states to be observed,  $x_{obs}$ , were “surveilled” from the aircraft simulation by polling them at 1 second intervals. This simulated an advanced surveillance technology with sufficient bandwidth to make the polled states available at a 1 Hz update rate and were thus directly comparable with the flight test GPS data. By changing the content and frequency of the polled states, the impact of different surveillance technologies on conformance monitoring could be analyzed.

---

\* FSUIPC was written by Pete Dowson and is readily available on the internet.

Expectations for each of these states,  $x_{CMM}$ , were developed from a simple low fidelity CMM with no recovery dynamics. Position, heading angle, roll angle and heading target state expectations were therefore based on what they would be as they evolved along the defined lateral Conformance Basis of each simulated scenario if no disturbances or system noise were present. Conformance Residuals were then generated according to an absolute function scalar residual of the same form used in the previous Chapters using different combinations of the observed states and various weighting factor parameters based on two standard deviation variability depending on the scenario. A threshold-based decision-making strategy was employed with variable threshold placement to develop False Alarm/Time-To-Detection figures of merit as before.

The following sections contain discussions of the findings from implementing the analysis framework under a variety of simulated ATC scenarios involving the key lateral, vertical and longitudinal domains in non-transitioning/transitioning flight regimes, namely:

- Lateral conformance monitoring during straight (non-transitioning) flight.
- Lateral conformance monitoring during flight plan transitioning flight.
- Lateral conformance monitoring during ATC vector transitioning flight.
- Vertical conformance monitoring during level (non-transitioning) flight.
- Vertical conformance monitoring during transitioning flight.
- Longitudinal conformance monitoring during constant speed (non-transitioning) flight.
- Longitudinal conformance monitoring during transitioning speed flight.

## **6.3 Simulated Conformance Monitoring Issues in Key Flight Regimes**

### **6.3.1 Lateral Conformance Monitoring: Straight Flight**

The findings from the analysis of conformance monitoring during straight flight in the operational data were discussed in the context that the aircraft was flying under autopilot guidance and that the environmental conditions were unknown. A caveat was therefore included indicating that the findings could be affected by environmental disturbance effects and different guidance modes. The simulation study provided an opportunity to investigate the influence of these issues.

The FS2002 aircraft was flown on a straight flight plan leg for 5 minutes and then a 10° heading deviation to the left of the leg was initiated. This scenario is identical to the lateral deviation scenario flown during the operational flight tests discussed in the previous chapters, allowing comparisons to be

drawn with the previous findings. Several runs were made under a range of environmental conditions and flight guidance modes, namely:

- Calm and turbulent environmental conditions under autopilot control.
- Autopilot and manual flight control modes under zero environmental disturbance conditions.

### 6.3.1.1 Effects of Environmental Disturbances

Figure 6.4 presents the FS2002 cross-track position error, heading and roll angle states during the runs with no turbulence/no gust and severe turbulence/15 knot gust environmental conditions under autopilot control. The severe turbulence/15 knot gusts run is associated with much higher noise in the higher order dynamic states. The limited environmental modeling fidelity in the simulation is evident in these plots since under these conditions, higher noise would normally be expected in the roll angle than the heading angle, which does not appear to be the case in this plot. This limitation is consistent with previous investigations into modeling fidelity of FS2002 [Billarant (2003)] that uncovered similar issues with the higher order dynamic states during high frequency disturbances. As a result, the roll angle was not considered a viable state to employ in Conformance Residuals during this particular study.

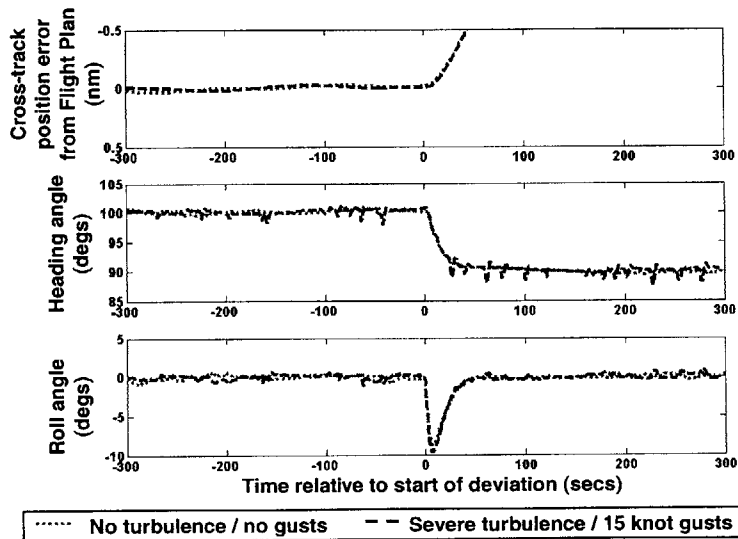


**Figure 6.4: Simulated Lateral Non-Conformance Dynamic States with Environmental Disturbances (Autopilot Guidance)**

Figure 6.5 shows the effect of the two environmental conditions on the False Alarm/Time-To-Detection metrics. The weighting factors used on the Conformance Residual generation schemes were calculated from an analysis of deviations in the cross-track position and heading angle states during the

non-deviation portion of the flight profile under the no disturbance condition. Rapid detection times were possible under these conditions, with somewhat faster detection possible with the position and heading states compared to the position state alone. These findings, and the False Alarm/Time-To-Detection values observed, are comparable to those obtained during the same scenario flown in the operational flight tests.

The same weighting factors on the position and heading states were then also used with the data from the severe turbulence/gust case to illustrate the impact of turbulence on the detection of a deviation when calm conditions are used to set the weighting factors. It is seen that the disturbances cause a general shift in the curves to the right in the FA/TTD space, indicating deterioration in the performance (i.e. slower TTD for a given FA or higher FA for a given TTD) of the residuals under these disturbed conditions relative to the no disturbance case. However, the shift is relatively small, being equivalent to approximately 2-4 seconds extra detection time for this type of deviation. These results indicate that although the effects of high frequency environmental disturbances such as turbulence and gusts can influence the FA/TTD metrics, it appears their effect is relatively minor. Weighting factors calculated under different environmental conditions than those being experienced will not induce large errors. Note that the effect of more sustained winds and environmental disturbances can generally be very important and this issue will be discussed in the context of environmental parameter estimation in Chapter 7.

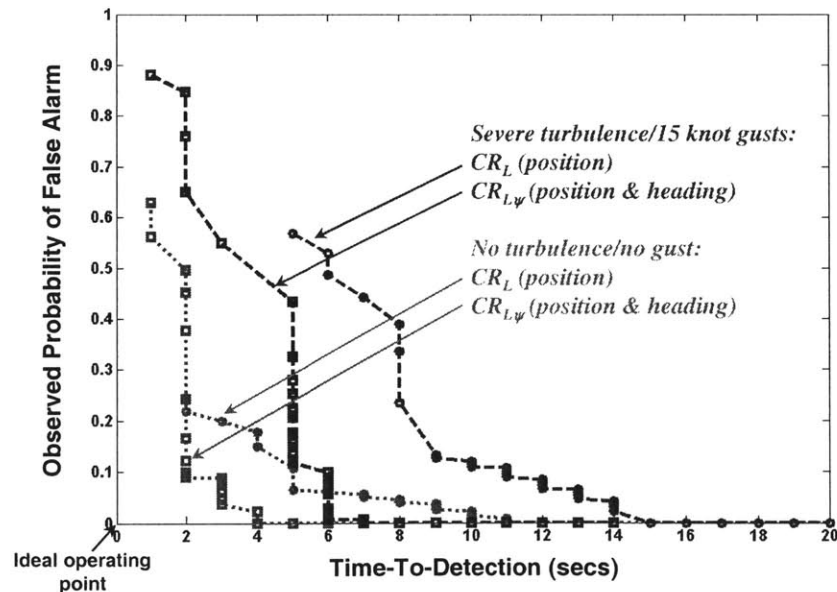


**Figure 6.5: Effect of Environmental Disturbances on FA/TTD Metrics During Lateral Non-Conformance (Autopilot Guidance)**

### 6.3.1.2 Effects of Guidance Mode

A potentially larger influence on the weighting factors used in the Conformance Residual is that of guidance mode. Boeing data has already been presented in Chapter 1 (Figure 1.8) indicating that the Flight Technical Error during manually-controlled flight can be as much as a factor of ten times higher than during full autopilot-controlled flight. The FS2002 simulator was used to investigate this issue during the same lateral deviation maneuver considered in the previous section during zero turbulence conditions. Guidance conditions considered were autopilot (LNAV) guidance and manual guidance where the subject pilot made inputs to the simulator through a flight yoke with flight director and map display guidance cues (see Figure 6.2). This simulated the same conditions used in the published Boeing data. The dynamic states during these scenarios are presented in Figure 6.6. It can be seen that there is slightly more variability in the states for the manual control modes with flight director compared to the autopilot control states as the pilot attempts to follow the flight director cues to track the FMS route. The variability increases with the manual control and EHSI display since it provides poorer feedback of the aircraft's position relative to the FMS route, even at the lowest range setting of the display. A slight offset in the path flown relative to the FMS route is visible in the figure, even though it was not discernable on the display, and larger discrete corrections are also evident.

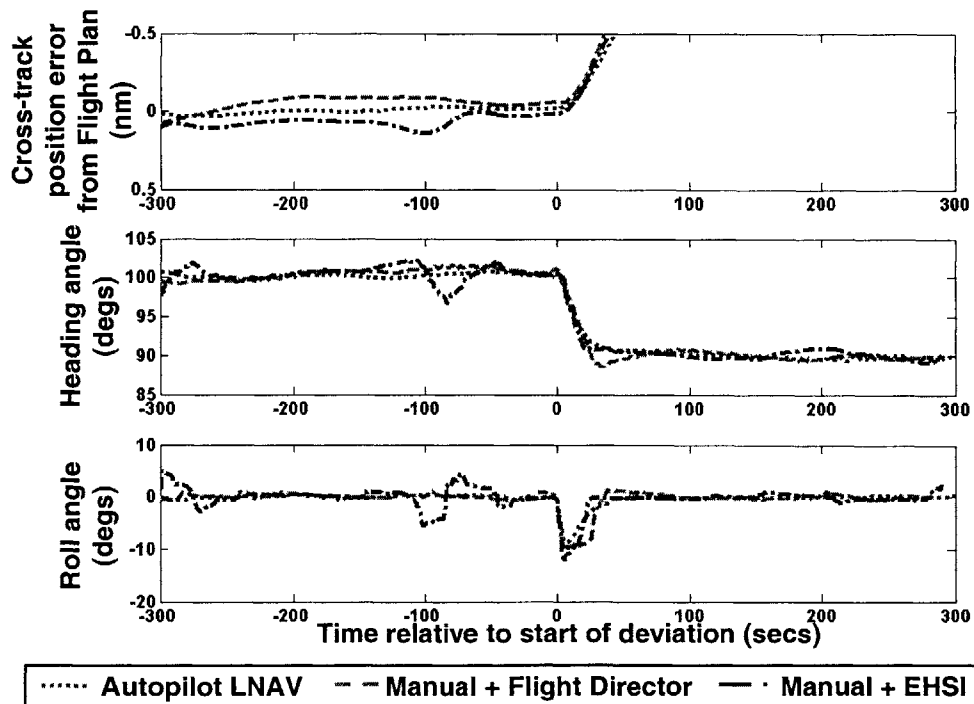
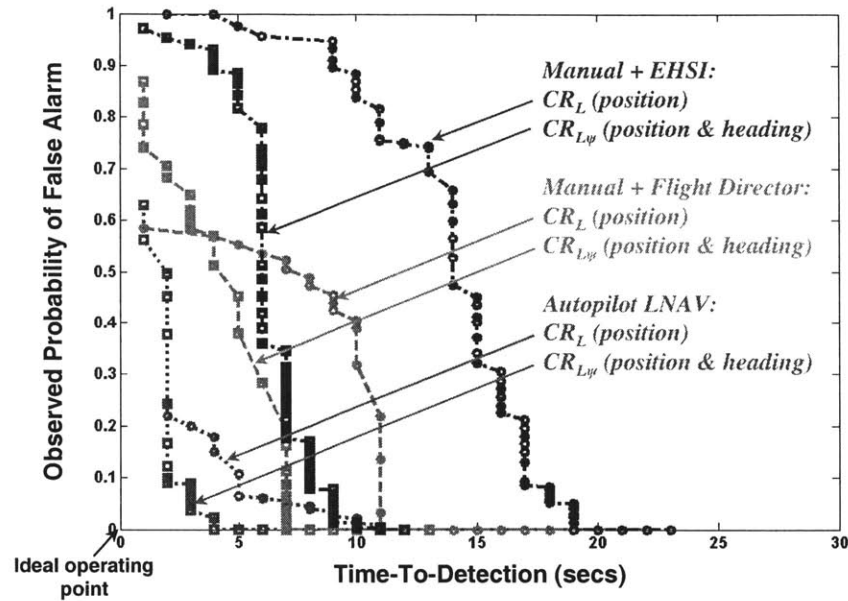


Figure 6.6: Simulated Lateral Non-Conformance Dynamic States with Different Guidance Modes (Zero Turbulence)

The impact of using weighting factors derived from the autopilot case when the aircraft is actually being flown under manual guidance is presented in Figure 6.7. This is representative of the situation where the aircraft is expected to be capable of very low FTE and the conformance monitoring scheme is set up appropriately, but a less capable guidance mode is actually being used.



**Figure 6.7: Effect of Guidance Mode on FA/TTD Metrics During Lateral Non-Conformance (Zero Turbulence)**

It is apparent that the manual guidance modes cause a general shift of the curves to the right indicating a deterioration in performance away from the ideal operating point, just as in the environmental disturbance case. But here the shifts are more significant, ranging from a high of 15-20 seconds increased TTD at a given FA for the manual guidance with the EHSI display, to 5-10 seconds increased TTD at a given FA for manual guidance with the flight director display in the cases where position alone is used in the Conformance Residual. The curve shifts are less for the cases where position and heading are used in the Conformance Residuals for both manual control modes, indicating that the benefit of using the higher order heading state observed in the previous analyses is preserved in this case too. However, these results indicate that it is necessary to account for the guidance mode of the aircraft in the design of the conformance monitoring system, especially during applications which require small time-to-detections of non-conformance.



### 6.3.2 Lateral Conformance Monitoring: Flight Plan Transitions

The operational data analysis highlighted the importance of accounting for the aircraft dynamic behavior at flight plan transition points. The simulation study provided an opportunity to demonstrate a range of typical transition maneuvers, and also investigate a selection of non-conformance scenarios.

#### 6.3.2.1 Ranges of Conforming Flight Plan Transition Maneuvers

For these studies, the simulator FMS was programmed to fly the same flight plan as in the operational flight tests. The same SDO waypoint transition that was examined in the operational data was simulated under a variety of typical conditions that could be encountered in an ATC environment:

- A fly-by transition with a 10° bank angle limit set on the MCP.
- A fly-by transition with a 25° bank angle limit set on the MCP.
- A fly-over transition.

The simulator flight tracks for each of these conditions are presented in Figure 6.8.

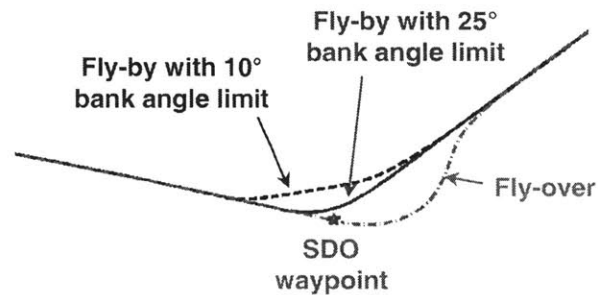


**Figure 6.8: Simulated Flight Tracks Under Various Flight Plan Transition Modes**

These tracks illustrate the diversity of flight behaviors that can be involved in even a simple flight plan transition point, all of which could be associated with behavior of a conforming aircraft. For example, the flight test aircraft employed a small bank angle limit of approximately 10° resulting in a shallow and extended turn at the waypoint, similar to that in the figure above. However, more typical ATC operations use higher bank angles of up to 25° resulting in much shorter transition periods. In addition, if the transition were interpreted as a “fly-over” type, the automation would not initiate a transition until after the waypoint had been passed, resulting in the extended trajectory presented above. At its furthest point from the straight-line trajectory, this fly-over trajectory is more than 3 nm in a cross-track direction from the fly-by trajectories.

A full presentation of the Conformance Residuals and FA/TTD metrics for these cases under various assumed conditions will not be conducted since the main points are consistent with those made in the operational data analysis. This can be summarized as: unless the behaviors of different aircraft and in different environments can be made more predictable and repeatable at flight plan transition points, accurate conformance monitoring in this domain is extremely challenging. While multiple aircraft manufacturers employ different autoflight logics and while ATC operations allow multiple transition behaviors, a level of uncertainty in the trajectory flown at transitions will continue to exist. Therefore, the best conformance monitoring will likely consist of checking that aircraft remain within an envelope defined by the extremes of possible conforming aircraft behaviors. This conclusion supports the approach to define RNP at transitions [RTCA (2000)] and the generic approaches employed by some of the existing systems described in Chapter 2.

### 6.3.2.2 Non-Conforming Transition Maneuvers

Due to the inherent challenges of conducting conformance monitoring at transitions previously discussed, aircraft deviations at transitions are much harder to detect compared to the non-transitioning environment. One case of transition non-conformance where the aircraft turns in the correct direction but stops at the wrong heading was discussed in the context of lateral transition conformance monitoring with the operational data in Section 5.3.2. This situation was found to be particularly challenging since the evidence of non-conformance in the dynamic states is delayed until it emerges from the increased noise that exists during the transition maneuver. Another interesting case that can be simulated involves a transition in the opposite direction to that expected. An example of this type of non-conformance at the SDO waypoint transition was flown in the simulator as presented in Figure 6.9, as well as a turn in the correct direction but stopping at the wrong heading.

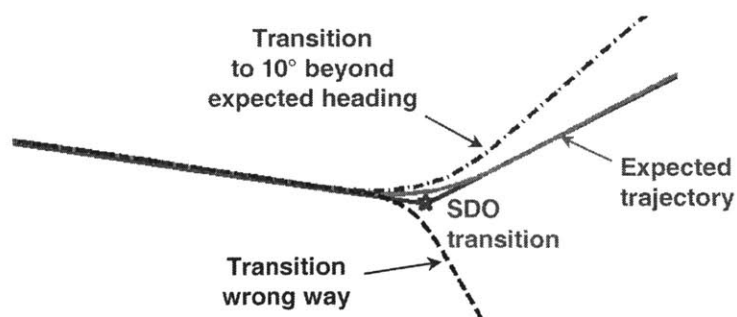


**Figure 6.9: Simulated Lateral Transition Non-Conformance Scenarios**

The dynamic states for the scenarios are presented in Figure 6.10. For the maneuver in the wrong direction, there is rapid divergence of the heading and roll states for the conforming and non-conforming cases. This makes this type of transition non-conformance much easier to detect with the higher order states compared to the case where the turn is in the correct direction but to the wrong heading.

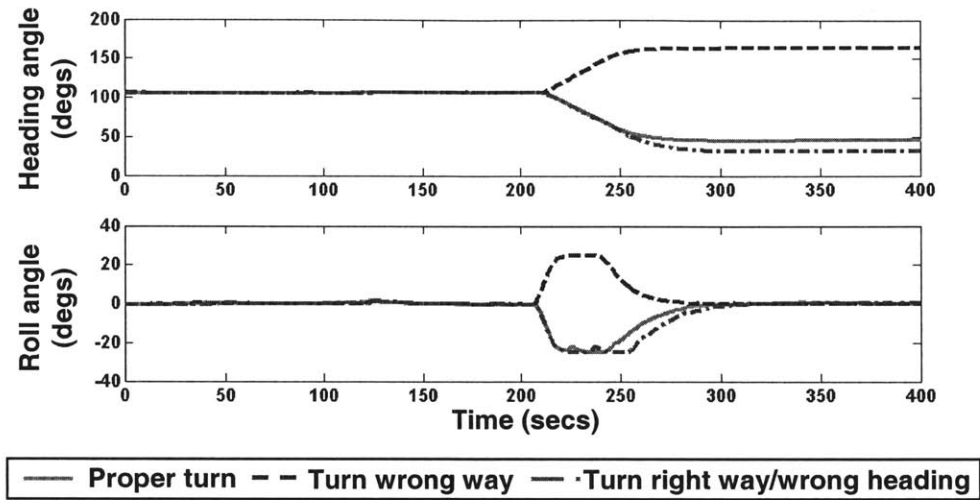


**Figure 6.10: Simulated Lateral Transition Non-Conformance Scenario Dynamic States**

### 6.3.3 Lateral Conformance Monitoring: ATC Heading Vector Transitions

An ATC heading vector transition is quite different from a conformance monitoring perspective than a flight plan route transition. The latter has a definitive position element defined by the trajectory to the next waypoint, while an ATC heading vector is typically used to achieve a change in aircraft direction for some tactical ATC objective, such as separation assurance or path stretching for sequencing purposes. As a result, there is no useful positional element to the Conformance Basis in the vector case, but a definite heading basis defined by the vector instruction.

In the ATC heading vector scenario simulated, a command requesting a left turn to 030° was assumed to have been issued by ATC to an aircraft as it approached the BOS waypoint, as illustrated in Figure 6.11 below.

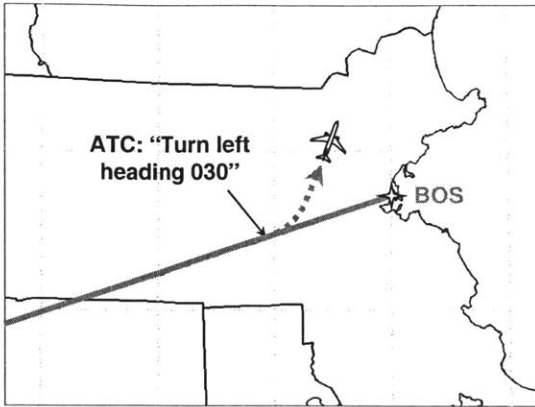


**Figure 6.11: Heading Vector Transition Scenario**

Flight crew typically implement heading vectors by engaging heading select mode on the Mode Control Panel with the appropriate heading target state. Variability in aircraft response time to the ATC vector Conformance Basis can be expected since the flight crew are involved in the control loop dialing the heading target into the MCP. Figure 6.12 below shows the aircraft state behaviors over three separate runs of this scenario with a human pilot inputting appropriate commands to the MCP in the FS2002 simulation. Note that a current target intent state is included here: the heading target state,  $\psi_T$ . The human-induced variability in the states is clearly evident. A standard response time of 10 seconds and turn rate of  $1.5^\circ/\text{sec}$  were assumed for the expected state values.

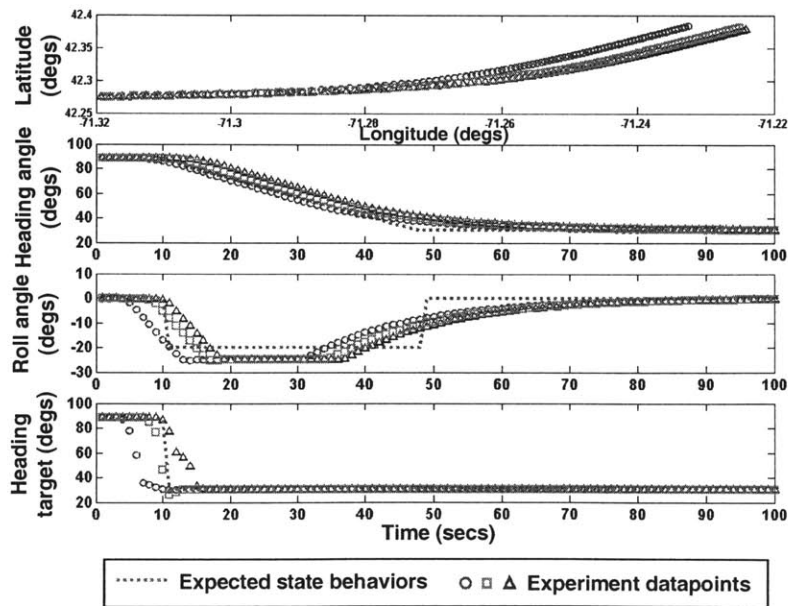


**Figure 6.12: Heading Vector Scenario State Behaviors**

The reliance on detailed modeling of the aircraft dynamics in order to accurately generate expectations in the heading and roll states is again clearly evident. Since the model used for the CMM in this example is simple, another way to use the higher order states while reducing the effect of modeling uncertainty is to reduce the weighting factors. The Conformance Residuals presented in Figure 6.13 were calculated using reduced weighting factors identified in Table 6.1.

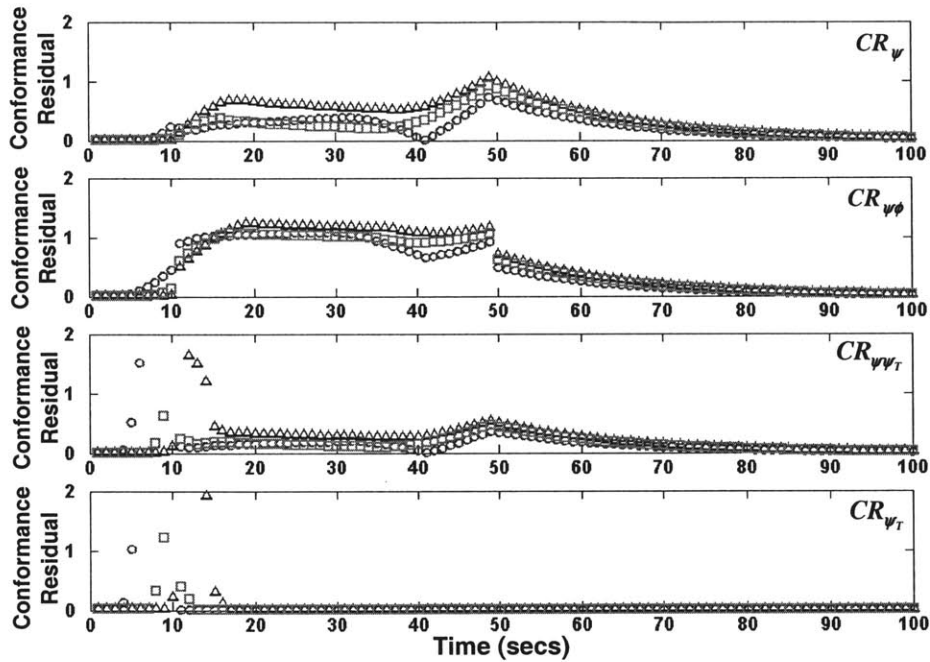


Figure 6.13: Heading Vector Scenario Conformance Residuals

Table 6.1: Weighting Factors in Heading Vector Scenario

Weighting Factor	Assumed value
$WF_{\psi}$	1/10 degs
$WF_{\phi}$	1/25 degs
$WF_{\psi T}$	1/10 degs

Since there is no positional component to the Conformance Basis, there is no cross-track error component to the Conformance Residuals. Even with the reduced weighting factors, the Conformance Residuals that use higher order dynamic states contain significant errors throughout the maneuver due to the limited modeling fidelity. The best indication of conformance under this scenario comes from the

heading target intent state: it is a state that is directly comparable to the active Conformance Basis. However, notice that even this state would not allow immediate deviation detection due to the pilot-induced variability visible in the heading target state plots as they dial the value into the MCP. The resulting time shifts can be identified by calculating the cross-correlation function between the observed heading target state for the three runs and the expected heading target state. The cross-correlation function of two sequences  $x[n]$  and  $y[n]$  is a third sequence  $r_{xy}[k]$  defined as:

$$r_{xy}[k] = \sum x[n] y[n-k] \quad \text{Equation 6.1}$$

where the second sequence  $y[n]$  is delayed by  $k$  units relative to  $x[n]$ , and the sum of the products is then evaluated for all applicable values of  $k$  [Denbigh (1998)]. Hence, if  $x[n]$  and  $y[n]$  are similar sequences that are simply shifted by a certain value,  $r_{xy}$  will be large for the value of  $k$  that corresponds to this shift value and small for all other values of  $k$ . In the context of the ATC vector scenario, the cross-correlation function between the observed and expected states can be used to identify time shifts in actual behavior. Figure 6.14 presents the results for the heading target state. Note that vectors flown manually may not have access to the heading target state: cross-correlation calculations with states could be used in a similar fashion.

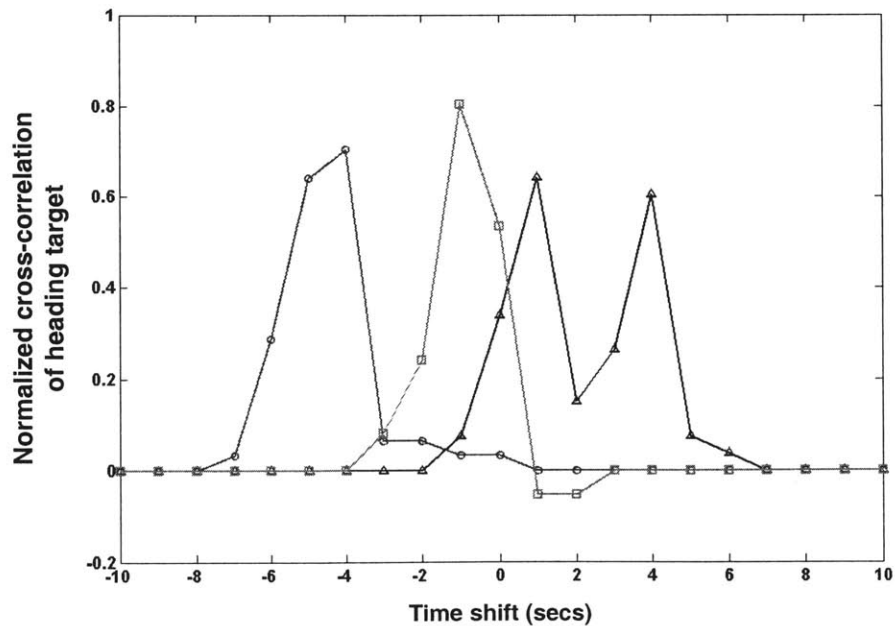


**Figure 6.14: Using Cross-Correlation Functions to Detect Timing Issues in Heading Vector Scenario**

The peaks in the curves above identify the time shifts in the observed behaviors: one vector transition was initiated 4 seconds earlier than expected, another occurred 1 second earlier and the third occurred a few seconds late. This last curve has two distinct peaks since the pilot paused part-way through dialing the target value into the MCP, resulting in ambiguity in the time of initiation that was picked up in the cross-correlation function.

Note that the cross-correlation function presented here has been normalized so that identical signals would have a value of 1.0 at their shift value. The fact that these curves peak below 1.0 indicates that some dissimilarity exists between the expected and observed state behavior curves. This is the same issue discussed previously regarding the fidelity of the CMM used to generate state expectations, only this time it is observable through the cross-correlation function rather than via a Conformance Residual. Indeed, the use of cross-correlation functions has a number of applications in conformance monitoring. They can be used to identify any behaviors that are correct in space but uncertain in time. The technique can also identify generic non-conformance: for example if the ATC vector was not initiated at all, the cross-correlation function would be zero for all time shifts. However, the technique is limited in that it contains no information about what the aircraft has done instead and is primarily useful for identifying delays *a posteriori*, i.e. after they have occurred, rather than being able to identify them in real-time.

#### **6.3.4 Vertical Conformance Monitoring: Level Flight**

In order to illustrate the impact of environmental disturbances and flight guidance mode in the vertical domain, the simulator was used to investigate the detection of vertical flight deviations under the same conditions tested in the lateral domain, namely:

- Calm and turbulent environmental conditions under autopilot control.
- Autopilot and manual flight control modes under zero environmental disturbance conditions.

The simulator was flown under calm and severe turbulence/15 knot gusts environmental disturbance conditions while under vertical navigation (VNAV) mode with the autopilot commanded to hold an altitude of 30,000 ft. These conditions were held for a period of 5 minutes, at which time a descent to 20,000 ft was initiated to simulate a vertical non-conformance maneuver. In the vertical scenarios considered in the operational data, the dynamic states considered were the altitude and flight path angle. These will be the states considered here also. In order to assess the impact of vertical guidance mode, the autopilot-controlled flight from the previous section was compared to the scenarios where manual vertical

guidance using flight director and altimeter/vertical speed indicator (VSI) displays were used under zero environmental disturbance conditions. Again, these conditions were held for a period of 5 minutes after which a descent to 20,000 ft was initiated to simulate a vertical non-conformance maneuver.

The altitude and flight path angle states recorded during these simulator flights are presented in Figure 6.15. Note the significantly larger variation in the states for manual control relative to the cases under autopilot control for both environmental conditions. Slightly more variation is visible in the states for the severe environmental disturbance conditions relative to the no disturbance conditions as expected, although caution must be exercised in analyzing the effects too much due to the uncertain environmental modeling fidelity in the simulator. Overall, the vertical deviations about the stationary altitude target are much smaller than lateral deviations about a stationary lateral target by about an order of magnitude. This implies that the vertical conformance region during cruise segments can be much smaller than the equivalent conformance region in the lateral domain, as observed in practice.

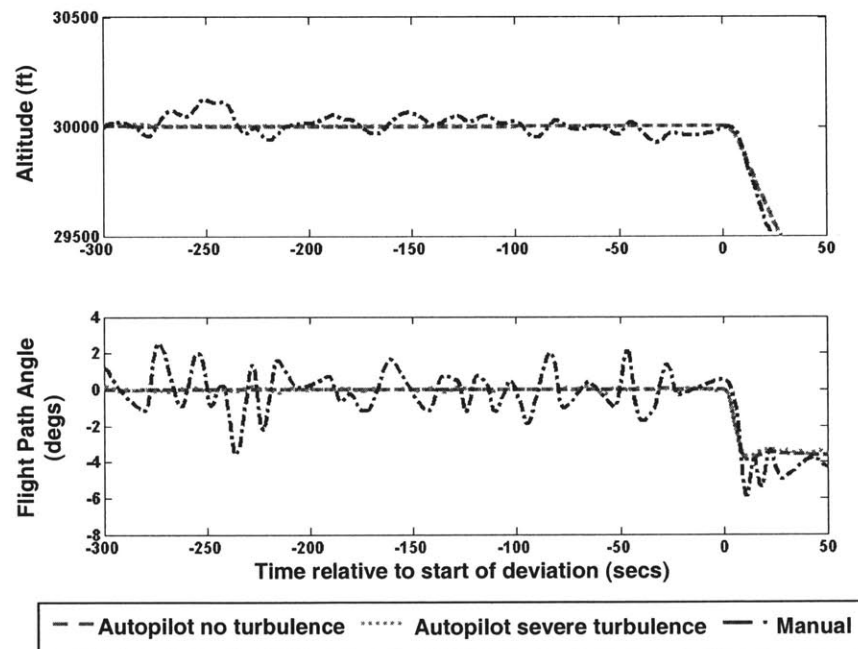


**Figure 6.15: Simulated Vertical Non-Conformance Dynamic States with Environmental Disturbance and with Different Guidance Modes**

As in the lateral cases, Conformance Residuals were generated using the simple absolute scalar function with weighting factors determined from two standard deviations in the pre-deviation flight phase. Residuals were generated for all the simulated conditions using weighting factors derived from the



autopilot/no turbulence conditions, and the resulting FA/TTD metric curves for these cases are presented in Figure 6.16 below.

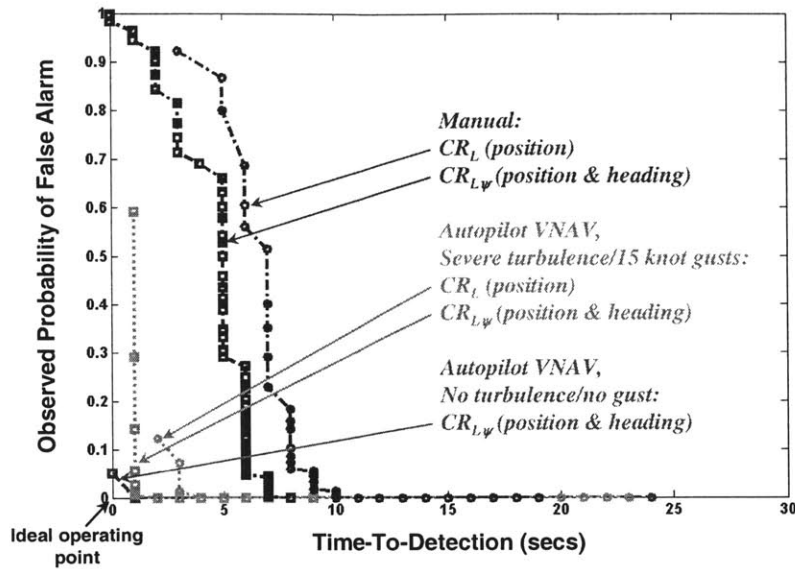


**Figure 6.16: Effect of Environmental Disturbance and Guidance Mode on FA/TTD Metrics During Vertical Non-Conformance**

A number of interesting issues are observable in these results. Firstly, when an aircraft is under autopilot control under calm conditions, vertical deviations can theoretically be detected very rapidly, as evidenced by the location of the curves for these conditions close to the ideal operating point in the lower left of the metric space. Curves move progressively further away from this ideal operating point as the effects of turbulence and manual guidance are factored in. However, even the relatively large deviations introduced by a novice pilot tracking the altitude target by hand only introduces a 5-10 second time-to-detection penalty with the residual scheme and weighting factors considered here. Overall, this illustrates that vertical deviations from a level altitude Conformance Basis are relatively easy to detect in a timely fashion under most conditions when access to high accuracy and update rate information is available.

### 6.3.5 Vertical Conformance Monitoring: Transitioning Flight

In order to demonstrate the problem with defining a Conformance Basis during vertical transitions introduced in Section 5.3.4, a vertical transition scenario was flown comprising straight and level flight at 30,000 ft for one minute followed by a descent to 25,000 ft. To illustrate the wide variety of vertical transition profiles that can occur, this scenario was flown under the following conditions:

- Autopilot guidance under vertical speed mode with descent commanded at  $-1500$  ft/minute.
- Autopilot guidance under flight level change (FLCH) mode with the descent profile calculated by FMS.
- Manual guidance attempting to descend at  $-1500$  ft/minute using altimeter and VSI cues.
- Autopilot guidance under FLCH mode with speedbrakes deployed to illustrate impact of aerodynamic configuration.
- Autopilot guidance under FLCH mode with “heavy” aircraft (12,000 extra gallons of fuel added to center fuel tank).

The resulting vertical states archived for one simulation run for each condition are shown in Figure 6.17.

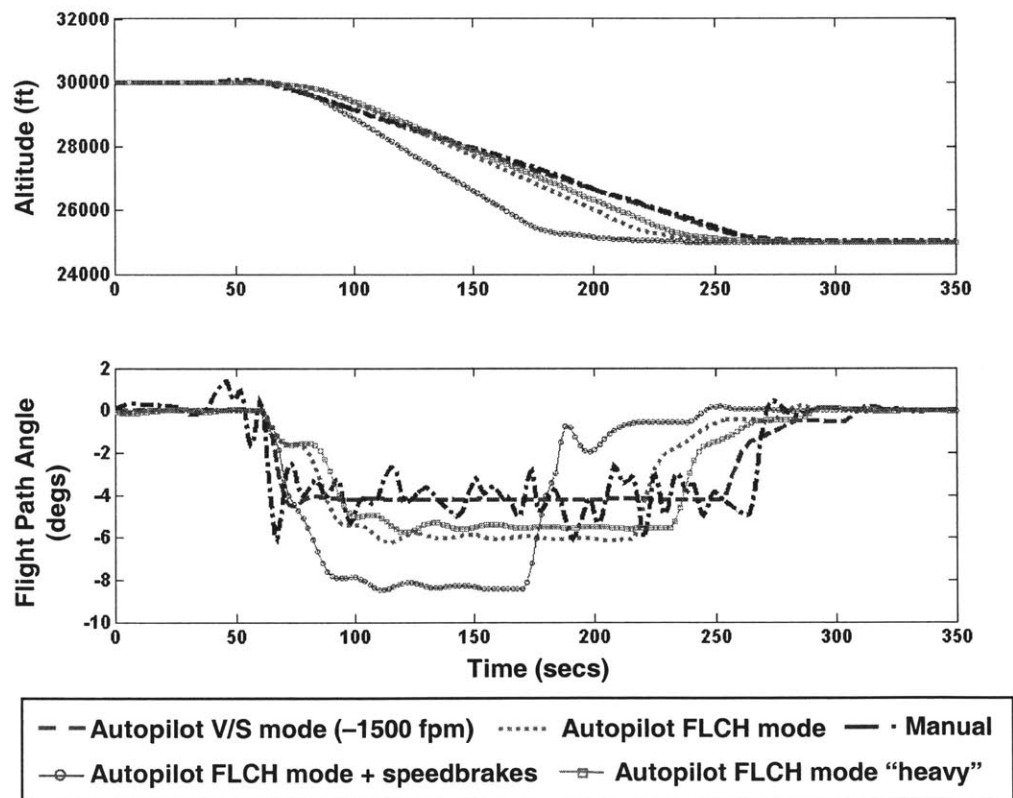


**Figure 6.17: Simulated Vertical Transition Dynamic States**

The fundamental issue evident in this data is the lack of predictability of the transition path across the various scenarios. Note how the autopilot FLCH mode transition has an initial  $-2^\circ$  flight path angle segment for a period of approximately 10 seconds, followed by a steeper descent at  $-6^\circ$  until the target

altitude is captured. By contrast, the V/S descent is associated with a much more constant  $-4^\circ$  flight path angle throughout the majority of the descent. The effect of the application of speedbrakes is to cause a steeper descent profile, consistent with the higher drag in this scenario.

This uncertainty in the vertical transition profile to be flown, coupled with the uncertainty in the initiation of the top of descent point described in the operational data (Section 5.4.3) is the reason why conservative “altitude blocking” is commonly employed in current ATC. This effectively assumes that the aircraft could be at any point in a column of airspace with a height defined by the current and cleared altitudes, and diameter defined by some conservative estimate of the descent profile. Larger thresholds are required as a result. This analogous to the larger thresholds required in the lateral domain, but the relative increase from the non-transitioning to transitioning scenarios is much larger in the vertical domain, as shown schematically in Figure 6.18.

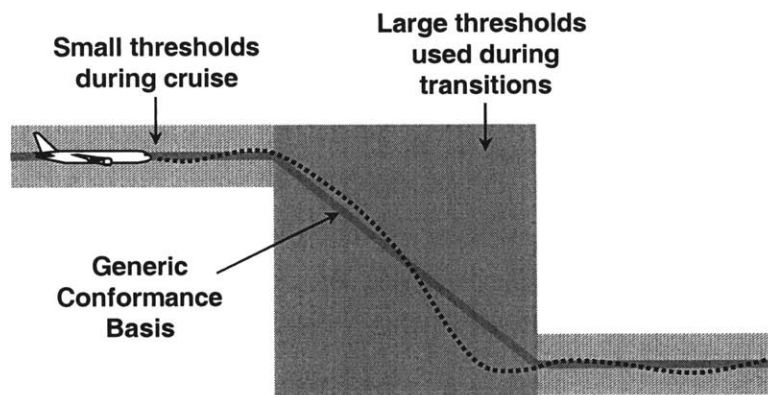


**Figure 6.18: Vertical Transition Thresholds Schematic**

In this situation, uncertainty in the Conformance Basis is being accounted for by assuming some generic Basis and simply assigning a large acceptable conformance region around it. This leads to very inefficient use of airspace in the current system. Research efforts are investigating whether VNAV paths computed by an aircraft’s FMS could be downlinked to the ground to assist in vertical transition path prediction [Palmer *et al.* (1999)] and hence reducing the uncertainty in the Conformance Basis. Although these are likely to be much more accurate than anything possible today (since many of the aircraft, aerodynamic and automation variables discussed above will be known or controllable by the FMS), some vertical profile uncertainty is still likely to exist due to errors in factors such as wind predictions used in the VNAV algorithms. Until accurate vertical profile forecasts are available to define the vertical

positional Conformance Basis, conformance monitoring during vertical transitions will continue to be a challenge.

### 6.3.6 Longitudinal Conformance Monitoring: Constant Speed Flight

In order to illustrate the impact of environmental disturbances in the longitudinal domain, the simulator was used to investigate the detection of speed deviations under light and severe turbulence environmental conditions while the speed axis was under autopilot control

The simulator was flown under 5 (“light”) and 15 (“severe”) knot gust environmental disturbance conditions while under IAS guidance mode selected on the autopilot with a commanded speed of 220 knots. These conditions were held for a period of 5 minutes, at which time a deceleration to 200 knots IAS was initiated to simulate a speed non-conformance maneuver. The speed states recorded during these simulator flights are presented in Figure 6.19.

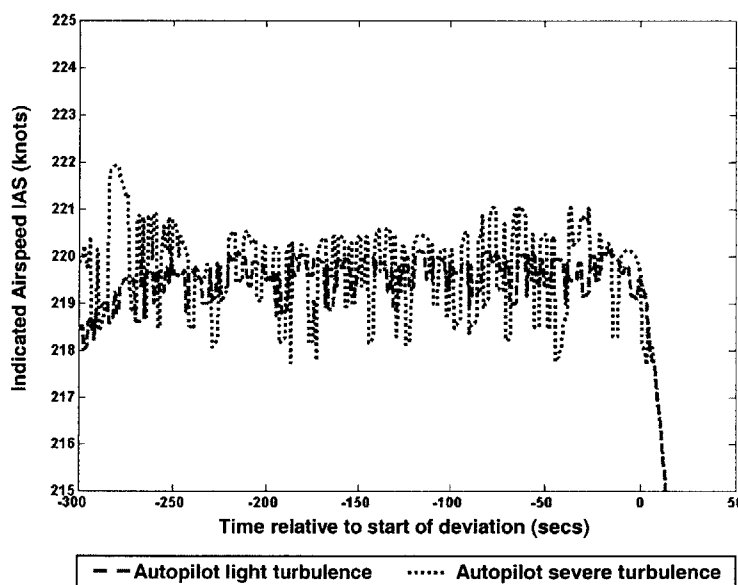


**Figure 6.19: Simulated Speed Non-Conformance with Environmental Disturbances**

Note the significantly larger variation in the speed for the severe environmental disturbance conditions relative to the light disturbance conditions, although again caution must be exercised in analyzing the effects due to the uncertain environmental modeling fidelity in the simulator. Although these larger variations imply the need for larger thresholds under severe disturbance conditions, it actually has little affect on the time of detection of the speed non-conformance if access to aircraft-derived states

is provided due to the short time it takes for the aircraft speed to change significantly. Under both conditions, thresholds set just outside the nominal state variation range would lead to detection of the non-conformance after 5-10 seconds. However, if ground-based speed data were being used to monitor for speed conformance, much longer times would be required due to the discretization and lag in the speed surveillance algorithm presented earlier. But again, the effect of the environmental disturbances on this process would be negligible.

### 6.3.7 Longitudinal Conformance Monitoring: Transitioning Flight

In order to demonstrate the problem with defining a Conformance Basis during longitudinal (speed) transitions introduced in Section 5.3.6, a speed transition scenario was flown comprising constant speed flight at 220 knots IAS for one minute followed by a deceleration to 200 knots IAS. To illustrate the variety of speed transition profiles, this scenario was flown under the following conditions:

- Autopilot guidance under IAS mode.
- Autopilot guidance under IAS mode with speedbrakes deployed to illustrate impact of aerodynamic configuration.
- Autopilot guidance under IAS mode with “heavy” aircraft (12,000 extra gallons of fuel added to center fuel tank).

Resulting speed states archived for one simulation run for each condition are shown in Figure 6.20.

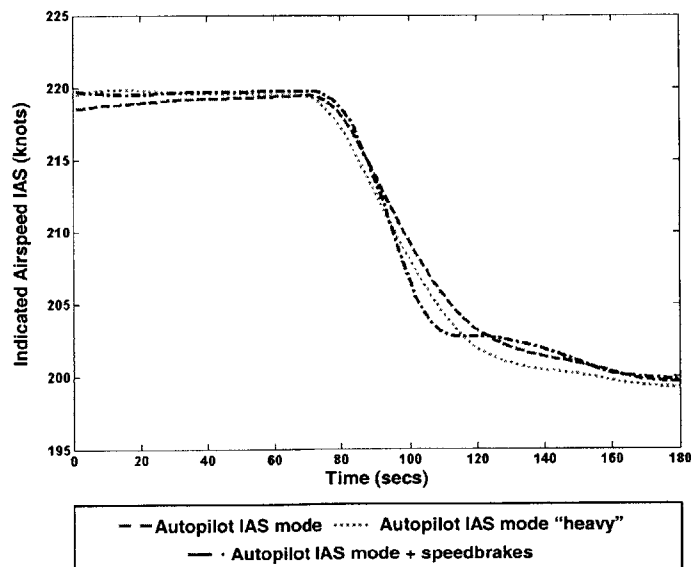


Figure 6.20: Simulated Speed Transition States

It is seen that there is much less variability in the speed profile across these various configurations than were observed in the vertical transition profile. This may simply be a result of the limited fidelity dynamic model employed in the flight simulation program. Even if this is not the case, the lack of definition of a longitudinal Conformance Basis (except for Required Time of Arrival restrictions at a limited number of waypoints, if at all), together with the poor surveillance in the speed channel (due to discretization and lag effects) severely limits the ability to undertake longitudinal conformance monitoring in the current ATC system. If more accurate monitoring in this domain is required in the future, then both of these issues need to be addressed.

## 6.4 Summary

This chapter has presented example implementations of the CMAF approach using a commercial flight simulation program to generate behavior outputs under a variety of realistic ATC environments to expand upon those studied with the operational flight data. Additional capability was developed to allow for 1 Hz polling and analysis of data from the flight simulator in the MATLAB computing environment. This simulated an ATC environment with an advanced surveillance system which allowed direct comparison with the aircraft-based data studies presented in the previous Chapter. Lateral, vertical and longitudinal flight regimes under non-transitioning and transitioning flight regimes have been studied.

The simulation analysis of lateral conformance monitoring during straight flight examined the effects of environmental disturbances and guidance mode on the baseline findings from the operational analysis. The effect of environmental disturbances was found to be relatively minor, with a time-to-detection burden of only a 2-4 seconds for a given probability of false alarm compared to the calm environmental condition case. The effects of guidance mode were demonstrated to be far more significant, with manual guidance modes having 15-20 seconds extra time-to-detections at a given false alarm rate compared to the autopilot guidance case. This implies that if rapid time-to-detection is required from a conformance monitoring system, then the monitor must be aware of the current guidance mode of the aircraft.

Simulation studies also demonstrated the wide variety of different behaviors that are possible at a flight plan transition point, due to different autoflight settings (such as bank angle limits) and waypoint designation (such as fly-by versus fly-over). As a result, lateral transition conformance monitoring is currently restricted to checking that the aircraft remain within an envelope defined by the extremes of conforming transition behaviors.

The ATC vector scenario was used to demonstrate the lags and variability issues added by the human element in the control loop. Cross-correlation techniques were found to be an effective way to analyze the amount of lag in the aircraft behaviors, but these are limited to post-processing operations. The fact that different states become better or worse indicators of conformance depending on the scenario were also discussed: in the flight plan scenario, the cross-track error is a prime indicator of conformance, while it has no meaning once a tactical vector has been issued. Under the latter scenario, the heading or heading target intent state becomes the primary conformance indicators since they are directly comparable to the form of the Conformance Basis.

The effects of atmospheric disturbances and guidance mode on the vertical conformance monitoring during level flight conditions was examined. Consistent with the operational data results, it was found that very rapid detection of deviations was possible in the vertical domain even under environmental disturbance conditions. The effect of manual control was to delay deviation detectability by only 5-10 seconds relative to the autopilot case.

The simulation capability was used to demonstrate the wide variety of vertical transition profiles flown by aircraft under different autopilot modes, aircraft weights and aerodynamic configurations. This uncertainty in the vertical transition profile, coupled with the uncertainty in the point of initiation of the vertical transition prevalent in today's ATC system, makes vertical transition conformance monitoring the most challenging of conformance monitoring applications.

Finally, the effect of atmospheric disturbances and aerodynamic configuration on the longitudinal conformance monitoring task was briefly assessed. It was found that the effect of atmospheric disturbances, speedbrakes and aircraft weight was negligible due to the rapid dynamic response of the aircraft in the scenario as long as aircraft-based data was available. The challenges in the longitudinal domain are currently caused by the poor surveillance in the speed axis, with slow and discretized speed surveillance. This severely limits the longitudinal conformance monitoring capability, but improved surveillance should allow significant improvements in this regard.

[This page intentionally left blank]



---

# CHAPTER 7: Extended Applications of the Conformance Monitoring Analysis Framework

---

## 7.1 Introduction

The previous Chapters have included a detailed description of the development of the Conformance Monitoring Analysis Framework and its application to ATC conformance monitoring research using operational and simulated data. Much of the emphasis in these Chapters has been on the task of detecting aircraft deviations using parallels with fault *detection*. However, the approach provides a framework for applications beyond this task, two of which are discussed in this Chapter. The first extended application is that of “intent inferencing”, in which parallels with fault *isolation* techniques are drawn in an attempt to infer an aircraft’s intent after non-conformance has been detected. The second extended application demonstrates how the framework can be used as a basis for inferring environmental parameters within the observed system to aid in the development or calibration of the various elements used in the analysis framework.

## 7.2 Intent Inferencing

Once a fault has been detected in a system, it is often necessary to also perform fault isolation in an attempt to identify the location of the fault so that the system can be reconfigured to account for the failure. In the conformance monitoring context, once an aircraft deviation has been detected, it is necessary to try to determine what new path the aircraft is following so that ATC tasks such as conflict detection and resolution can be conducted.

Fault isolation theory typically employs a “bank” of models of the actual system to perform fault isolation tasks [Frank (1996)], as illustrated in Figure 7.1. Numerous models of the system being considered are run in parallel, each representing a model of the system with a different type of fault. In essence this is a hypothesis testing function, where each alternative system model represents the hypothesis “a fault of type (1, 2, ... ,  $n$ ) has occurred in the system” [Frank (1992)]. Multiple

expectations for system states under various degraded system states are predicted and multiple associated residuals are generated. A decision-making process uses these residuals to identify which (if any) faults exist in the system as represented by the model with the lowest residual. Of course, if none of the degraded models represent the failure that exists in the actual system, then this approach may not be effective in identifying the fault. However, it does allow failures represented by those models that are tested to be eliminated.

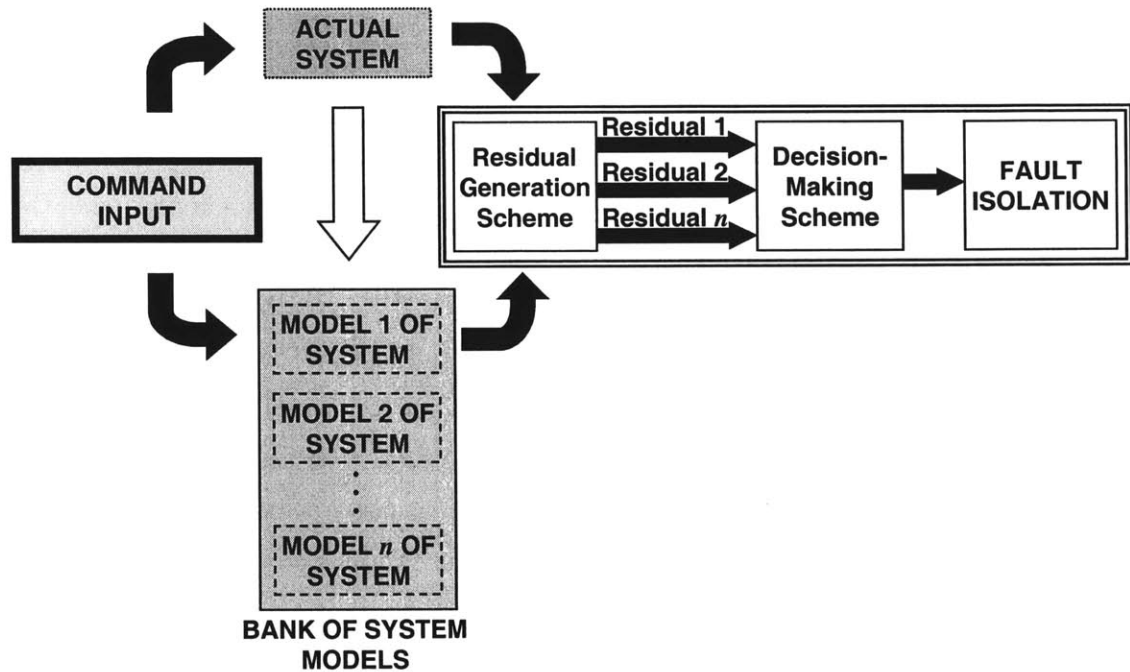


**Figure 7.1: Fault Isolation Using a Bank of System Models**

This approach can be used in the conformance monitoring application to run multiple CMMs, for example to represent different aircraft operating modes under conditions where it may be important to know which is currently being used. However, after an aircraft deviation has been detected, it is more important to infer what the aircraft's Conformance Basis is (i.e. inferring the aircraft's intent) rather than the operating mode so that essential functions such as conflict detection and resolution can be conducted on the most likely alternate trajectories. This can be achieved using a similar approach to that discussed above, but rather than using a bank of system models, a bank of command inputs (Conformance Bases) is used instead, as illustrated in Figure 7.2.

Each Conformance Basis inside the bank represents a hypothesized alternate to the true expected Conformance Basis. Residuals are generated for each of these alternates and then a decision-making

function is used to establish which, if any, is most likely. Again, it is possible that none of the hypothesized alternate Conformance Bases are consistent with the actual deviation, but it allows certain Conformance Bases (such as those reflecting trajectories towards high security targets or other aircraft) to be checked against and eliminated if the Conformance Residuals for those trajectories are too large.

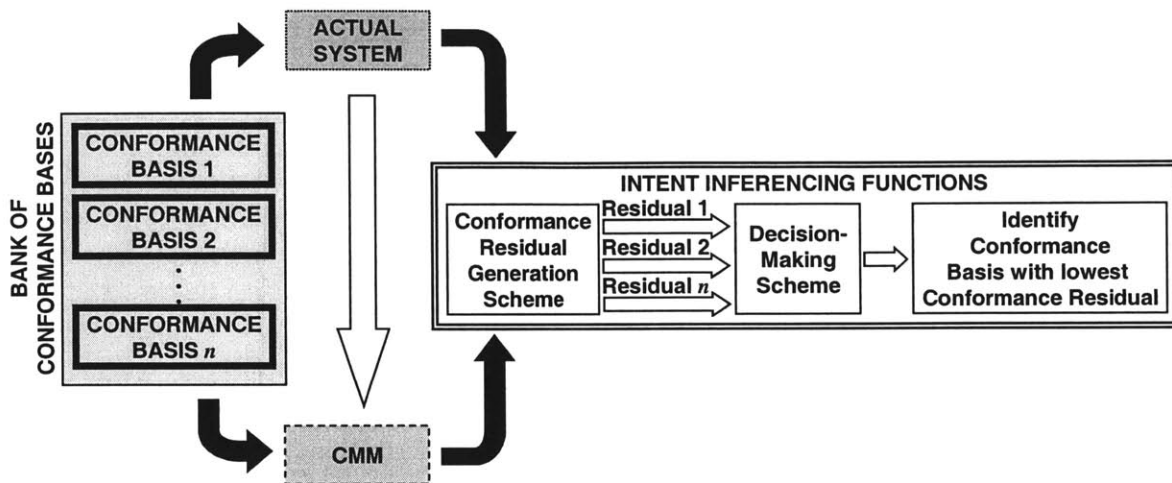


**Figure 7.2: Intent Inferencing Using a Bank of Conformance Bases**

In general, the set of hypotheses used to form the bank of Conformance Bases can be as extensive as required to determine or eliminate certain behaviors to a level of confidence appropriate for the application domain. The proposed alternates can be based on prior knowledge of system operation, heuristics or sensible assumptions of likely aircraft behavior in various contexts. Some examples include:

- A no change trajectory (i.e. dead-reckoning).
- Trajectories based on historical data of operational events, such as errors seen in incident/accident data for the nominal Conformance Basis trajectory, e.g. having waypoints with similar names in close proximity.
- Trajectories precipitating critical events, such as errors that could have immediate hazardous consequences, e.g. unauthorized flights into very busy or high security areas (such as Special Use Airspace (SUAs) or Temporary Flight Restrictions (TFRs)) or those which are known to cause a rapid loss of separation with another aircraft.
- A direct-to trajectory (i.e. by-passing the next fix).
- An alternate procedure trajectory with a transition point common to the expected procedure.

To illustrate this approach to intent inferencing, a number of alternative Conformance Bases are postulated and tested for the case of an aircraft turning late at a planned transition in a simple flight plan route from JFK to BOS via BDL, as illustrated in Figure 7.3. The route was flown using the FS2002 flight simulation capability described in Chapter 6 at a constant speed and altitude.

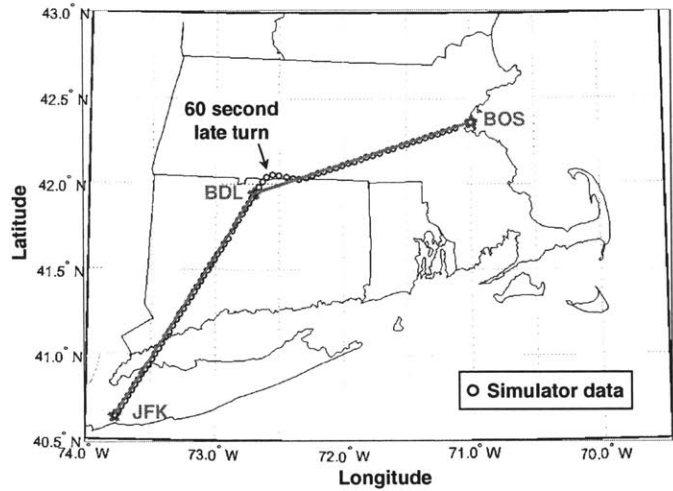


**Figure 7.3: Intent Inferencing Late Turn Scenario**

Such a situation could arise if a pilot accidentally engaged a heading hold autoflight mode before the BDL transition, then re-engaging autopilot LNAV mode after the mistake was realized. This was how the simulation was run to generate the data used in this example. The proposed alternate Conformance Basis trajectories hypothesized for this example scenario are shown in Figure 7.4.

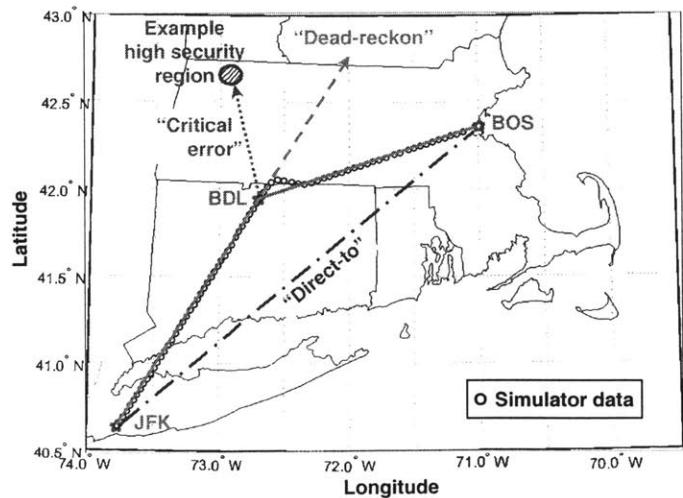


**Figure 7.4: Hypothesized Alternate Trajectories for Intent Inferencing Scenario**

Three alternate trajectories were tested in parallel with the default flight plan trajectory. These represented a “direct-to” trajectory which bypassed the BDL fix; a “dead-reckon” trajectory where the turn at BDL was not made at all, and an example “critical error” trajectory representing behavior consistent with flight towards a high-security area. Each of these trajectories were tested in parallel with the nominal flight plan trajectory by running a separate CMAF implementation for each. Example Conformance Residuals for each are presented in Figure 7.5. A simple CMM with no recovery dynamics and a Conformance Residual utilizing position and heading states in an absolute function scalar Conformance Residual generation scheme with weighting factors determined from nominal behavior were used.

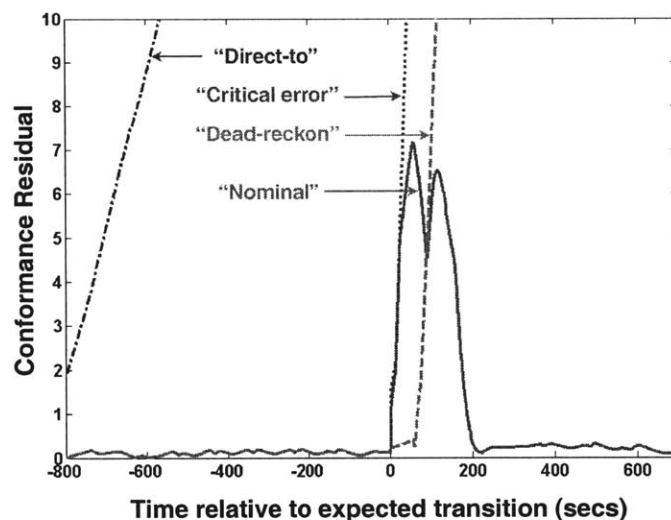


**Figure 7.5: Conformance Residuals for Alternate Trajectories**

In general, trajectories closest to the actual one being flown are those associated with the smaller Conformance Residuals. And just as a threshold was used to determine when a Conformance Residual was indicative of conforming behavior or not, a sensible decision-making scheme for intent inferencing uses a similar criteria to discard hypothesized trajectories that are clearly not supported by the observed evidence. In this example, a hypothesis discard threshold of  $CR = 10$  was used such that all trajectories with Conformance Residuals above this threshold were discarded. Note that a more detailed assessment of proper threshold placement could be conducted in a similar fashion to the deviation detection threshold analyses described earlier if required. Relative likelihoods of the remaining trajectories were inferred from the relative values of the Conformance Residuals, such that the most likely trajectory had the lowest residual. Using these criteria, the relative likelihood of the various trajectories and whether they are kept or discarded is illustrated in Figure 7.6.

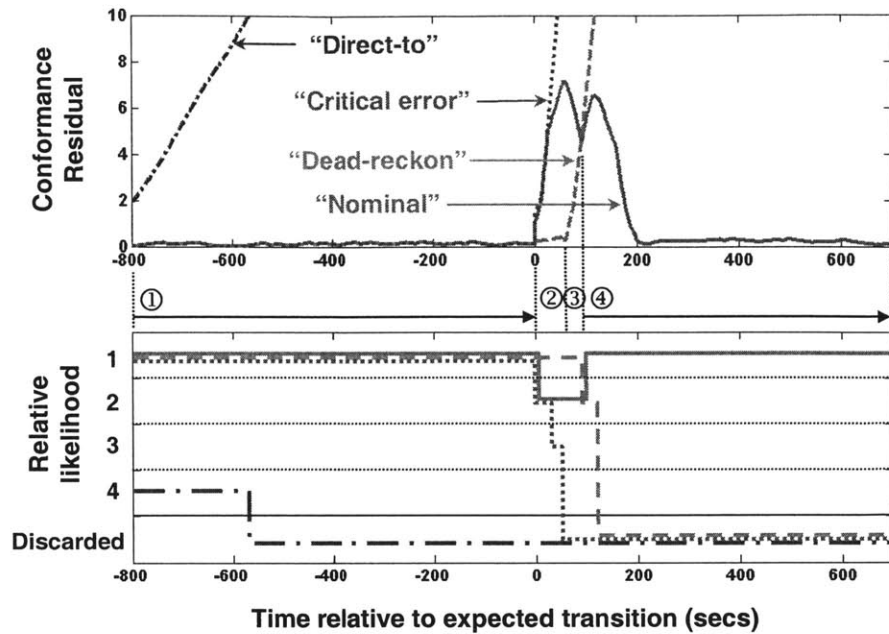


**Figure 7.6: Relative Likelihood of Alternate Trajectories**

The “direct-to” hypothesis (that directly connecting the initial aircraft position to BOS, bypassing BDL altogether) immediately has the lowest relative likelihood of being followed and is quickly discarded as its Conformance Residual climbs above the discard threshold. The Conformance Residuals for the other three alternate trajectories are initially very low and thus they represent viable hypothesized trajectories. Since the initial portion (segment ①) of the remaining trajectories are identical, each alternate has equal likelihood of being closest to the actual trajectory at this time. When the aircraft does not make the turn at the expected position (either way), the “nominal” and “critical error” trajectory Conformance Residuals increase relative to the “dead-reckoning” (segment ②). At this point, the highest likelihood is associated with the aircraft following close to the “dead-reckon” trajectory. This is consistent with the fact that, at this point, the aircraft is in a heading hold mode that in fact produces a dead-reckoning trajectory. However, when the turn towards BOS is finally initiated, the “nominal” trajectory Conformance Residual decreases while the “dead-reckon” and “critical error” trajectory Conformance Residuals increase, indicating a relative shift in the likelihood that the trajectory being followed is back towards the “nominal” (segment ③). Finally, all trajectories other than those close to the “nominal” become highly unlikely (segment ④). If none of the proposed trajectories result in a small enough Conformance Residual, additional feasible trajectories may be required or other means of inferring intent initiated.

### 7.3 Environmental Parameter Estimation

Rather than using the Conformance Monitoring Analysis Framework to determine whether an aircraft is conforming given *assumed environmental parameters*, it can be used in the opposite sense to determine what environmental parameters must be existing if it is *assumed that all the aircraft are conforming*, without direct surveillance of those parameters. Up to now it has been assumed that the effects of the environment have been known, either through forecast, observation or assumption. For example, the heading state expectations were explicitly pre-corrected for wind effects. This effect, as well as others such as pressure effects on the altitude state and density effects on the engine thrust states can have significant impacts in the conformance monitoring problem, especially with respect to the generation of expected aircraft state behaviors in the Conformance Monitoring Model. Non-conformance observed across numerous aircraft may be suggestive of improper modeling of the aircraft or environment in the CMM rather than being a true indication of widespread aircraft non-conformance. This fact can be used to refine the CMM, such as the environment parameters used. This is illustrated conceptually in Figure 7.7.

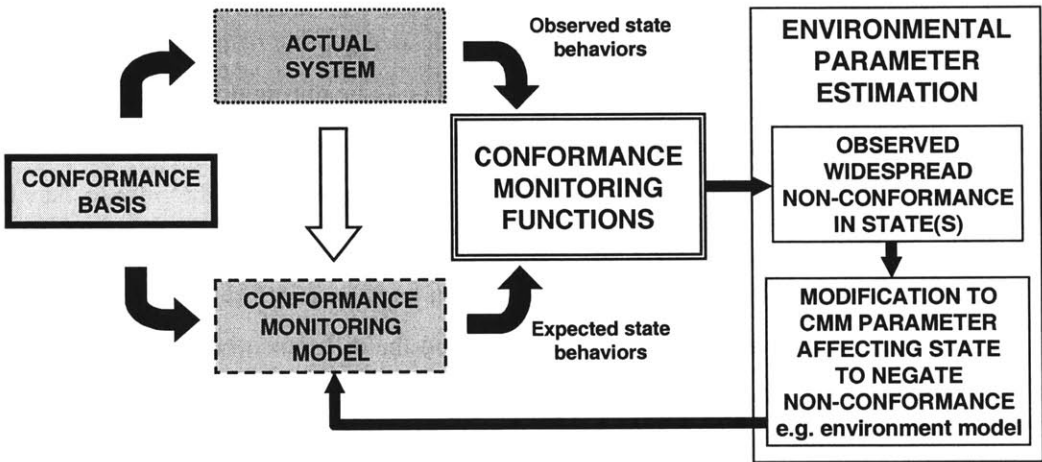


**Figure 7.7: Environmental Parameter Estimation Using the Conformance Monitoring Analysis Framework**

The example scenario of inferring the wind field in a lateral ATC domain is used to illustrate the approach described above. The effect of wind on an aircraft is illustrated in Figure 7.8. In the no wind condition, the aircraft heading,  $\psi$  is directly comparable with the ground track angle of the Conformance Basis,  $\psi_{CB}$  and the true airspeed of the aircraft,  $V_{TAS}$  is the same as the speed of the aircraft across the ground,  $V_{GS}$ . However, when a wind field of speed  $V_{wind}$  and direction  $\theta_{wind}$  is introduced, a conforming aircraft has a different heading from its ground track angle by an amount defined by the wind correction

angle,  $\omega$ , and a different ground speed from the airspeed. In the example scenario shown in Figure 7.8, a conforming aircraft's heading is less than the ground track angle, while the ground speed is higher than the airspeed due to a slight tailwind component of the wind field.

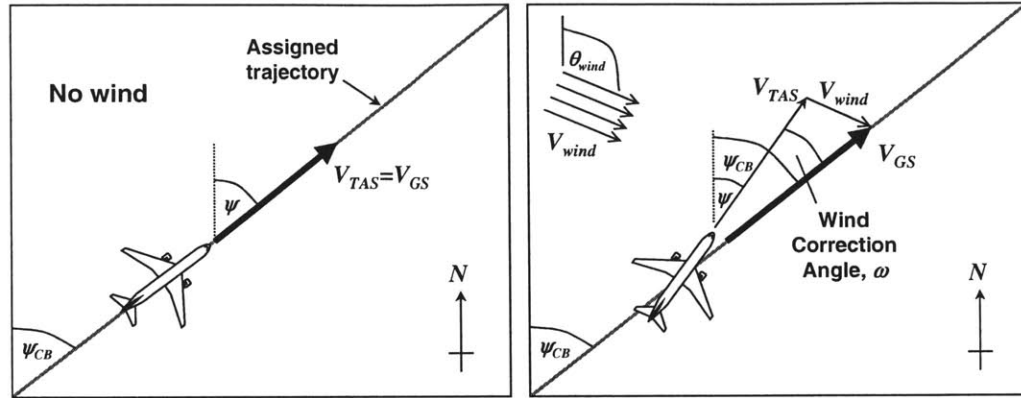


**Figure 7.8: Wind Effects in a Lateral ATC Scenario**

The effects of wind are typically an issue during tactical vectoring operations where the controller assigns a *heading angle* to an aircraft in order to achieve a desired *ground track angle*, so explicitly has to determine an appropriate wind correction angle. It is less of an issue during nominal flight plan-following operations since there is limited feedback of the actual heading of an aircraft in the current system (currently heading is only available with an explicit communication request to the pilot to “say heading”). However, aircraft heading may be directly surveilled in future. ATC site visits suggest that controllers infer the wind field from knowledge of the wind correction angle required during tactical vectoring that achieves a conforming ground track for a given aircraft and the difference between its assigned air and observed ground speeds. When a steady wind field exists in an ATC sector, details of this are often included in the standard hand-over communications given by an outgoing sector controller to an incoming sector controller to assist the latter’s calibration of the wind environment [Davison (2003)]. Information on the wind speed and direction can also be determined analytically in a DST from knowledge of the airspeed, ground speed, wind correction angle and track angle for a particular aircraft using vector analysis with the sine and cosine rules:

$$V_{wind} = \sqrt{V_{TAS}^2 + V_{GS}^2 - 2V_{TAS}V_{GS} \cos(\omega)}$$

**Equations 7.1**

$$\theta_{wind} = \psi_{CB} - \text{asin} \left[ \frac{V_{TAS} \sin(\omega)}{V_{wind}} \right]$$



These wind field parameters can then be used to determine proper wind correction angles for other aircraft according to the equation:

$$\text{Wind correction angle for aircraft } i, \omega_i = \text{asin} \left[ \frac{V_{wind} \sin(\psi_{CB_i} - \theta_{wind})}{V_{TAS_i}} \right] \quad \text{Equation 7.2}$$

In the current ATC environment, it is challenging to apply these equations since the ground speeds calculated in the HCS are discretized to the nearest 10 kts [Nolan (1999)], and the controllers assign *indicated* airspeeds which have to be converted to *true* airspeeds either using forecast pressure and temperature data, or heuristics. These issues result in significant uncertainty in the aircraft speed parameters. In addition, during vectoring operations the controller is limited to applying wind correction factors that are whole degree amounts. These issues limit the accuracy with which the wind field can be determined. In order to illustrate the proposed approach and the effects that some of these uncertainties introduce, assume a scenario illustrated in Figure 7.9 in which the following parameters exist:

- A constant wind field (unknown on the ground), defined by  $V_{wind} = 30$  kts,  $\theta_{wind} = 100^\circ$ .
- Required Conformance Basis ground track angle,  $\psi_{CB} = 40^\circ$ .
- Controller assigns airspeed to achieve  $V_{TAS} = 350$  kts (i.e. assume assigned indicated airspeed achieves this true airspeed and that perfect conformance to assignment exists).
- Controller assigns aircraft heading  $\psi = 035^\circ$  (assume conformance within  $\pm 2^\circ$ , i.e. wind correction angle,  $\omega = -5 \pm 2^\circ$ ).
- HCS-reported ground speed,  $V_{GS} = 360$  kts (assumed error  $\pm 5$  kts).

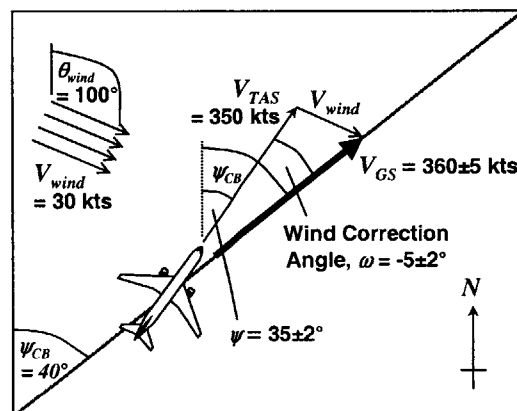


Figure 7.9: Wind Field Estimation Example (1 Aircraft)

Due to the uncertainties in the heading and ground speed parameters, the wind field parameters cannot be fully determined. Using Equations 7.1, a range of possible parameters result:

$$19 \text{ kts} \leq V_{wind} \leq 46 \text{ kts}$$

$$63^\circ \leq \theta_{wind} \leq 114^\circ$$

**Equations 7.3**

implying an uncertainty of over 25 knots in the wind speed and over  $50^\circ$  in its direction. This uncertainty can be reduced by considering other aircraft within the same airspace: assume two other aircraft are involved in the same airspace such that they can be considered to be in the same wind field, as shown in Figure 7.10. Calculating the wind parameters for all three of these aircraft results in the wind field parameters shown in Table 7.1.

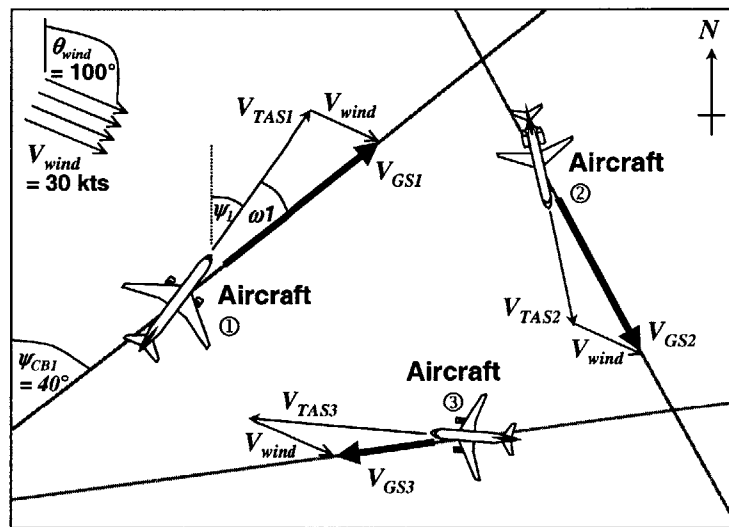


**Figure 7.10: Wind Field Estimation Example (3 Aircraft)**

**Table 7.1: Wind Field Parameter Estimation Results**

Aircraft	Assigned $V_{TAS}$	Assigned $\psi_{CB}$	Observed $V_{GS}$	Assigned $\omega$	Estimated $V_{wind}$	Estimated $\theta_{wind}$
①	350 kts	$40^\circ$	$360 \pm 5$ kts	$-5 \pm 2^\circ$	19-46 kts	$63-114^\circ$
②	300 kts	$140^\circ$	$320 \pm 5$ kts	$3 \pm 2^\circ$	16-37 kts	$95-120^\circ$
③	330 kts	$260^\circ$	$300 \pm 5$ kts	$2 \pm 2^\circ$	25-41 kts	$80-124^\circ$

By considering additional aircraft in the same wind field, the uncertainties in the possible wind parameters are reduced to within a 12 kt range in speed and a 20° range in direction defined by the strongest of the constraints for the three aircraft:

$$\begin{aligned} 25 \text{ kts} &\leq V_{wind} \leq 37 \text{ kts} \\ 95^\circ &\leq \theta_{wind} \leq 114^\circ \end{aligned} \quad \text{Equation 7.4}$$

By extension, an airspace with multiple aircraft in the wind field will allow further improvement in the estimate of the wind field parameters. The approach outlined above reduced the uncertainty in the wind field parameter estimate by considering multiple aircraft at the same time. An alternative approach is to consider a single aircraft over multiple updates of the surveillance system. One way to do this is to generate estimates of wind field parameters using weighted estimation equations similar to the  $\alpha$ - $\beta$  filtering equations employed in the HCS<sup>†</sup> [Brookner (1998)]:

$$\begin{aligned} \hat{V}_{wind_{n,n}} &= \hat{V}_{wind_{n,n-1}} + \beta_V (V_{wind_{obs}} - \hat{V}_{wind_{n,n-1}}) \\ \hat{\theta}_{wind_{n,n}} &= \hat{\theta}_{wind_{n,n-1}} + \beta_\theta (\theta_{wind_{obs}} - \hat{\theta}_{wind_{n,n-1}}) \end{aligned} \quad \text{Equations 7.5}$$

where  $\hat{x}_{wind_{n,n-1}}$  is the estimate of parameter  $x$  at update  $n$  based on measurement at update  $n-1$ ,  $\hat{x}_{wind_{n,n}}$  is the estimate at update  $n$  based on measurement at that update  $\hat{x}_{wind_{obs}}$  and  $\beta_x$  is the weighting parameter that acts on the difference between the observation and the previous parameter estimate. These equations are useful under more realistic conditions where there is noise in the measurements of the various surveilled properties so that noise effects can be filtered out over multiple updates. In order to illustrate this approach, assume the same general scenario as illustrated in Figure 7.9 but in which the following measurement uncertainties (assumed to be normally-distributed) now exist:

- Initial estimates  $V_{wind} = 19$  kts,  $\theta_{wind} = 63^\circ$  defined by low end of range identified above (Equations 7.3) with one aircraft.
- Surveilled aircraft heading,  $\psi_{obs} \sim N(36^\circ, 1^\circ)^*$ .
- Surveilled ground track angle  $\sim N(40^\circ, 1^\circ)$ .

<sup>†</sup> The  $\alpha$ - $\beta$  filtering equations are also known as  $g$ - $h$  filtering equations and are similar in form to those employed in the HCS to calculate the ground speed estimate of an aircraft from the radar returns.

\* Notation  $\sim N(\mu, \sigma)$  implies a measurement with Normal distribution defined by mean,  $\mu$  and standard deviation,  $\sigma$ .

- Surveilled ground speed,  $V_{GSobs} \sim N(364 \text{ kts}, 2 \text{ kts})$ .

These parameters can be used in Equations 7.1 to determine the observed wind speed and direction parameters for use in Equations 7.5. The resulting estimates for the wind speed and direction as a function of surveillance update for three different  $\beta$  values are presented in Figure 7.11. It can be seen that the higher  $\beta$  values are associated with more rapid convergence of the original estimate towards the true wind field parameter values (occurring within 10 surveillance updates), although there is significant variability in the steady-state estimate due to the relatively high influence of the noisy surveilled states. This is contrasted to the lower  $\beta$  values associated with slower convergence to the actual wind field parameters (taking approximately 50 surveillance updates for the lowest  $\beta$  value) but the steady-state estimate has considerably less variability. Implementation of this approach to estimate wind field parameters in actual ATC applications would require a trade study to define appropriate values for parameters such as the  $\beta$  value for convergence speed and steady-state variability.

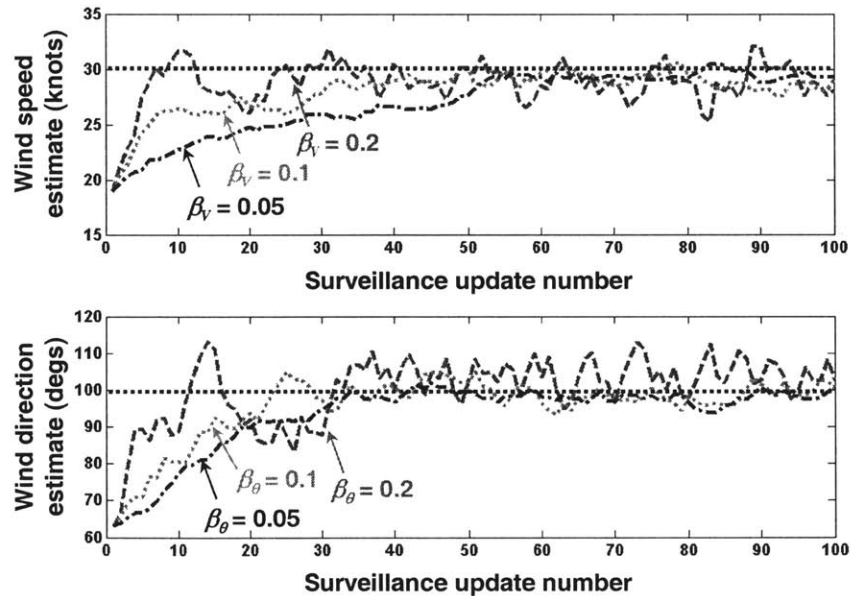


**Figure 7.11: Wind Field Estimation Using Filter Equations**

The advantages of the two approaches discussed above, both considering multiple aircraft at the same time and individual aircraft across multiple surveillance updates, can also be combined to improve the parameter estimation capability. This combined approach enables outlying data (e.g. due to a poorly calibrated sensor for one aircraft) to be diluted relative to other data points.

It should be noted that these studies have assumed a constant wind field existing in the environment being monitored: extensions to this application of the framework would need to consider more realistic environments in which the wind field is changing, both temporally and spatially and also the impact of meteorological effects such as gusts. Similar techniques to those demonstrated above could also be employed for estimating other environmental parameters that cannot or are not directly surveilled, but whose impacts can be observed from their effects on other states.

## 7.4 Summary

This Chapter has demonstrated two extended applications of the Conformance Monitoring Analysis Framework: intent inferencing and environmental parameter estimation.

In intent inferencing, parallels are drawn with the fault isolation task. Instead of employing classical fault isolation techniques with banks of system models, the intent inferencing task employs banks of Conformance Bases in the Conformance Monitoring Analysis Framework in an attempt to infer the Conformance Basis that an aircraft is following after it has been determined not to be following the default Conformance Basis. In this way, the “intent” of the aircraft is attempting to be inferred. The proposed approach was demonstrated using a simulated scenario of an aircraft transitioning 60 seconds late at a flight plan waypoint. Comparisons with a set of alternate trajectories was conducted by calculating the Conformance Residual relative to each and assigning highest likelihood of the “proper” trajectory to the one with the lowest residual. Although the intent inferencing example employed only a limited number of alternate trajectories in a simple non-conformance scenario, the approach holds significant promise for tasks such as ATC security analysis. For example, this approach could be used to determine if an aircraft is flying towards a high security target by carrying a direct path to that region as one of the alternate trajectories.

The environmental parameter estimation discussion has demonstrated how the Conformance Monitoring Analysis Framework can be employed to determine what environmental parameters must be existing (without direct surveillance of those parameters) if it is assumed that all the aircraft are conforming. These estimates can be used to assist in the development of appropriate Conformance Monitoring Models in the framework. The example of estimating wind speed and direction parameters using surveillance of multiple aircraft at one time and/or individual aircraft over multiple surveillance updates was used to demonstrate this extended application.

[This page intentionally left blank]

---

# CHAPTER 8: Conclusions, Contributions & Future Work

---

## 8.1 Conclusions

In order to maintain system safety, security and efficiency, conformance monitoring is conducted to ensure that aircraft adhere to their assigned clearances. New decision support tools (DSTs), coupled to advanced communication, navigation and surveillance technologies are being developed which may enable more effective conformance monitoring to be undertaken relative to today. However, there are currently no general analysis techniques to help identify fundamental conformance monitoring issues and more effective approaches that new DSTs should employ. These issues were discussed in detail in Chapters 1 and 2 of the thesis.

An approach to address the need for general conformance monitoring analysis techniques has been developed and presented in this work. It draws parallels between ATC conformance monitoring and general fault detection, allowing fault detection methods developed for other domains to be employed for this new application. The resulting Conformance Monitoring Analysis Framework provides a structure to describe and research conformance monitoring approaches. Detailed discussions have been presented in Chapter 3 for each element of the framework, specifically including:

- Conformance Basis
- Actual System Representation
- Conformance Monitoring Model
- Conformance Residual Generation Scheme
- Decision-Making Scheme

The Conformance Basis is a fundamental notion developed in this thesis to define the baseline against which observed aircraft behaviors are compared. The Actual System Representation includes the key elements involved in the execution of the Conformance Basis in the real world and involves a classical feedback control representation of the aircraft control system and dynamics, supplemented with upstream pilot and aircraft intent components to represent future behaviors. The intent components were

defined in this research according to current target, planned trajectory and destination states in the Surveillance State Vector in order to accurately mimic the way intent is communicated and executed in the ATC system. The resulting Actual System Representation allows potentially-surveillable states from various points in the control hierarchy to be visualized so that different surveillance environments can be described. The Conformance Monitoring Model (CMM) is used to generate expected state values. Different analytical and mental forms of CMM were discussed with a general trade-off of simplicity of design and implementation with a low fidelity model versus potential performance enhancements associated with employing higher model fidelity. A Conformance Residual generation scheme is then employed to quantify the difference between the observed states (from the surveillance systems) and the expected states (from the Conformance Monitoring Model). Different examples of Conformance Residual generation schemes employing different functions, weighting factors and scalar/vector forms were presented. The concept of using weighting factors on each state employed in the residual was proposed as a simple means of normalizing multiple states in a fashion analogous to concepts contained within the RNP-philosophy. The final stage in the framework involves a decision-making process from which a determination is made of whether the Conformance Residual behavior is characteristic of a conforming aircraft or not. The simple (and commonly-employed) threshold-based decision-making criterion was discussed whereby a Conformance Residual below some threshold value implies a conforming aircraft, while a Conformance Residual above the same threshold implies non-conformance.

Various figures of merit were proposed to assist in the development of implementations of the framework elements appropriate to different ATC environments. Those considered include the False Alarm (FA)/Time-To-Detection (TTD) measures and a Maximum Conformance Residual metric. The FA/TTD metric is useful under environments where a clear blunder initiation point can be defined and allows performance of the CMAF implementation to be compared to an ideal operating point. The Maximum Conformance Residual metric is more useful in environments where a blunder initiation point is harder to define and provides a predictive capability regarding the possible conformance behavior a short time into the future.

Example implementations of each of the framework elements and the suggested figures of merit have been demonstrated in Chapter 4 using GPS and databus data from a simple lateral non-conformance maneuver conducted with an experimental commercial flight test aircraft. Note that the element forms discussed are not intended to be exhaustive and part of the power of this framework is that future users can use the appropriate forms of each element most applicable to their situation.



The remainder of the document has contained a detailed set of analyses conducted with the CMAF to illustrate the application of the approach in realistic ATC scenarios. This involved simple forms of Conformance Monitoring Model, absolute function scalar residuals with weighting factors based on two standard deviation containment, threshold-based decision-making and False Alarm/Time-To-Detection figures of merit. These forms were chosen for their simplicity rather than any pre-conception of allowing superior performance. Analyses were conducted with operational ATC data from aircraft and ground-based systems during two test flights of a commercial aircraft in lateral, vertical and longitudinal domains in transitioning and non-transitioning flight regimes in Chapter 5. This provided a unique opportunity to compare and contrast the conformance monitoring capabilities in each operating domain and flight regime under traditional and potential future surveillance environments. The findings were supported and extended through the use of simulated ATC data in Chapter 6.

It was found that the CMAF approach allowed for effective comparisons to be made between the different surveillance environments. With even the simple forms of the CMAF elements employed here, more effective conformance monitoring could be conducted in the non-transitioning environments with the aircraft-derived data, with higher order dynamic states and/or with more sophisticated algorithms compared to what is possible with today's conformance monitoring decision support tools. These findings were contrasted with the greater conformance monitoring challenges during transitioning flight regimes. The challenges were especially with respect to Conformance Basis definition and the development of Conformance Monitoring Models at an appropriate fidelity to capture the key aircraft dynamics and autoflight timing issues in these transitioning environments. Many of these issues were demonstrated through the simulation studies of Chapter 6, especially with respect to the impacts of guidance mode, environmental disturbances, aerodynamic configuration and aircraft weight. The improvements with higher order dynamic states suggested in the non-transitioning environments are harder to realize in the transitioning case since the modeling challenges lead to errors in the higher order states that require larger thresholds be utilized in the decision-making scheme to achieve a given decision performance level. This is entirely consistent with the conformance monitoring approaches adopted by existing decision-support tools used in ATC described in Chapter 2. But the crucial difference is that the Conformance Monitoring Analysis Framework allows the relative benefits and disadvantages of different threshold placements (and other elements of the framework) to be analyzed to support specific conformance monitoring performance requirements. The CMAF approach allows consideration of intent states in addition to the traditional dynamic states. It was shown that the use of intent states can significantly improve conformance monitoring capability in the transitioning domain where the major challenges in conformance monitoring with traditional dynamic states exist.

These results have significant implications for future ATC system design, both technological and procedural. With even the simple forms of the CMAF elements employed (such as the low fidelity CMM), more effective conformance monitoring can be conducted in the non-transitioning environments with the aircraft-derived data, with higher order dynamic states and/or with more sophisticated algorithms compared to what is possible with today's tools. This suggests that the introduction of advanced surveillance systems such as ADS-B that can provide higher accuracy, update rate and content states to a monitoring tool hold significant potential for allowing improved conformance monitoring in future ATC environments in these non-transitioning domains. The improvements with higher order dynamic states suggested in the non-transitioning environments are harder to realize in the transitioning case. Medium or high fidelity CMMs are required to reduce the effects of modeling errors during transitioning domains. However, high fidelity models are not practical for most ATC operations and the more general medium fidelity models are often most appropriate. The modeling errors that then have to be accepted require larger thresholds be utilized in the decision-making scheme. These larger thresholds increase the time to detect a non-conformance for a given false alarm level. These findings imply that ATC procedures should generally not require rapid detection of non-conformances at transition points when only dynamic states are available. If rapid detection is essential to a particular ATC operation, more accurate modeling of the aircraft transition dynamics are needed, either through the development of sophisticated high fidelity modeling techniques or through strict proceduralization. Because the use of intent states can also significantly improve conformance monitoring capability in the transitioning domain, advanced surveillance systems that allow intent information to be surveilled also hold significant potential for allowing improved conformance monitoring in future ATC environments in the transitioning domains.

The fundamental importance of the Conformance Basis has also been discussed. Since inaccurate or incomplete Conformance Basis can limit automated conformance monitoring, future ATC environments in which DSTs are employed may need to focus as much on improved knowledge of the Conformance Basis as the more mainstream aircraft behavior states. Several enhancements to the current system that could be used to achieve higher Conformance Basis accuracy in future ATC systems have been discussed in terms of improved human-machine interfaces, communications systems that automatically record amended clearances and advanced surveillance systems that allow direct surveillance of active Conformance Bases on-board aircraft being monitored.

Finally, additional utility of the framework has been presented through two extended applications: methods for intent inferencing and environmental parameter estimation. The intent inferencing approach

uses parallels with traditional fault isolation tasks by employing banks of Conformance Bases in the Conformance Monitoring Analysis Framework to determine what alternate trajectory a non-conforming aircraft may be following. An example approach was presented in which Conformance Residuals for several alternate Conformance Basis trajectories were calculated and the most likely alternate was associated with the trajectory with the lowest residual. It is suggested that this approach holds significant promise for tasks such as ATC security analysis, for example to determine if an aircraft is flying towards a high security region by carrying a direct path to the region as one of the alternate trajectories. The environmental parameter estimation application demonstrated how the framework can be employed to determine what environmental parameters must be existing if it is assumed that all the aircraft are conforming. This can be used to assist in the development of appropriate Conformance Monitoring Models. The example of estimating wind speed and direction parameters using surveillance of multiple aircraft at one time and/or individual aircraft over multiple surveillance updates was used to demonstrate the approach.

## 8.2 Contributions

The specific contributions of the work described within this thesis are summarized below. Primary contributions are identified as a top-level bullet, while supporting contributions are contained as sub-bullets.

- Development of a novel Conformance Monitoring Analysis Framework (CMAF) based on fault detection techniques that provides a general structure for the identification and description of conformance monitoring issues and the development of conformance monitoring approaches for ATC applications.
  - CMAF approach enabled by the posing of an aircraft non-conformance as a fault within the ATC system needing to be detected.
- Identified key components required in a useful form of the Conformance Monitoring Analysis Framework.
  - Developed notion of a Conformance Basis for conformance monitoring tasks.
  - Developed Actual System Representation with intent formalization to accurately represent actual system process while allowing different surveillance environments to be described.

- Identified requirements for a Conformance Monitoring Model, Conformance Residual generation and Decision-making schemes with appropriate form and fidelity for chosen application.
- Identified use of various figures of merit as one way of designing CMAF elements to meet conformance monitoring performance requirements for different ATC applications.
- Demonstrated practicality of framework through various implementations of the individual CMAF elements with flight test and simulator data.
  - Developed sample Conformance Monitoring generation schemes with weighting factors to normalize states in a manner consistent with the RNP-philosophy.
  - Developed False Alarm/Time-To-Detection and Maximum Conformance Residual figures of merit to illustrate need to design CMAF elements to meet conformance monitoring performance requirements for different ATC applications.
- Identified important insights into conformance monitoring in ATC applications using Conformance Monitoring Analysis Framework with flight test and simulator data.
  - Identified importance of Conformance Basis knowledge.
  - Demonstrated the potential for improving conformance monitoring capability in non-transitioning lateral, vertical and longitudinal flight environments through the use of higher accuracy/update rate position states, as well as higher order dynamic states and more sophisticated DST algorithms compared to existing systems.
  - Illustrated significant challenges to performing accurate conformance monitoring in transitioning environments due to Conformance Basis uncertainty, as well as modeling the aircraft dynamics and autoflight logic.
  - Demonstrated use of higher fidelity Conformance Monitoring Models and intent states for improved conformance monitoring in the transitioning flight regimes.
  - Identified technical and procedural implications of findings for future ATC system design.
- Undertook detailed survey of Conformance Basis issues in current ATC environment observable in flight test data and identified specific approaches for improvement in future ATC systems.

- Demonstrated extended applications of the framework for intent inferencing and environmental parameter estimation.

### 8.3 Future Work

Specific recommendations to extend this research for future work include:

- Undertake more formal investigation to analyze appropriate CMAF element implementations to meet conformance monitoring performance requirements in various ATC environments.
  - Conformance Monitoring Model implementation options, e.g. through observer-based estimation techniques.
  - Different Conformance Residual generation strategies.
  - Determination of appropriate weighting factors, e.g. machine-learning techniques.
  - Determining appropriate targets on figures of merit in different applications.
- Undertake explicit consideration of needs and issues in aircraft-based (rather than ground-based) conformance monitoring where an aircraft is monitored by another aircraft (e.g. as required during pair-wise self-separation operations).
- Undertake formal assessment of Conformance Basis observability issues in the current ATC system and identification of technologies to mitigate issues in future ATC system.
- Extend intent inferencing study to assess potential for security and wider applied studies.
  - Avoidance of broad regions of restricted airspace, e.g. due to Special Use Airspace (SUA), Temporary Flow Restrictions (TFR) or convective weather regions.
  - Detection of “critical maneuvers”.
- Undertake more detailed investigation of environmental estimation algorithm techniques.
  - Applying more sophisticated filtering techniques.
  - Study of more realistic environmental conditions involving spatially and temporally-varying wind, temperature and pressure fields.
- Investigate application of approach to other domains.
  - Automobile/ship/patient conformance monitoring.

[This page intentionally left blank]

---

# References

---

- [Abbott (1996)] Abbott, D. J., “The Harrier/AV8B Engine Monitoring System Development and In-Service Experience”, *Aircraft Health and Usage Monitoring Systems (Selected Papers from Aerotech 95)*, IMechE Seminar Publication 1996-9, 1996.
- [ACARE (2002)] ACARE, “Strategic Research Agenda—Volume 2: Security of Navigation and ATM Infrastructure”, Advisory Council for Aeronautics Research in Europe, [www.acare4europe.com](http://www.acare4europe.com), 2002.
- [Airservices (2002)] Airservices Australia, “The Australian Advanced Air Traffic System (TAAATS)”, [www.airservices.gov.au](http://www.airservices.gov.au), 2002.
- [ARINC (2001)] ARINC, “ARINC 429 Digital Information Transfer System – Part 1: Functional Description, Electrical Interface, Label Assignments and Word Formats”, ARINC Report No. 429P1-16, Annapolis, MD, 2001.
- [Barhydt & Warren (2002)] Barhydt, R. & A. W. Warren, “Newly Enacted Intent Changes to ADS-B MASPS: Emphasis on Operations, Compatibility and Integrity”, AIAA Paper No. 2002-4932, *AIAA Guidance, Navigation and Control Conference*, Monterey, CA, August 2002.
- [Barkat (1991)] Barkat, M., *Signal Detection and Estimation*, Artech House, Boston, MA, 1991.
- [Billarant (2003)] Billarant, F., “Microsoft Flight Simulator Model Fidelity Analysis”, internal Massachusetts Institute of Technology technical report, 2003.
- [Boeing (1999)] Boeing, “ETOPS Maintenance on Non-ETOPS Airplanes”, *Boeing Aero Magazine*, No. 7, available online at [http://www.boeing.com/commercial/aeromagazine/aero\\_07/etops.html](http://www.boeing.com/commercial/aeromagazine/aero_07/etops.html), 1999.
- [Boeing (2000)] Boeing, “Required Navigation Performance (RNP) and Area Navigation (RNAV)”, Boeing document available at [www.boeing.com/commercial/caft/reference/documents/RNP082400S.pdf](http://www.boeing.com/commercial/caft/reference/documents/RNP082400S.pdf), 2000.
- [Boeing (2001)] Boeing, “Lateral and Vertical Navigation Deviation Displays”, *Boeing Aero Magazine*, No. 16, available online at [www.boeing.com/commercial/aeromagazine/aero\\_16/navigation.html](http://www.boeing.com/commercial/aeromagazine/aero_16/navigation.html), 2001.
- [Boeing (2003)] Boeing, “RNP Capability of FMC-Equipped 737, Generation 3”, Boeing Commercial Airplane Group, Document No. D6-39067-3, 2003.

- [Bornemann & Kelley (2000)] Bornemann, D. R. & W. E. Kelley, "The Future of Air Navigation", *Handbook of Airline Operations*, 1<sup>st</sup> ed., edited by G. F. Butler and M. R. Keller, The McGraw-Hill Companies, Inc., New York, 2000, Chap. 13, pp. 193-203.
- [Braff *et al.* (1996)] Braff, R., J. D. Powell & J. Dorfler, "Applications of the GPS to Air Traffic Control", *Global Positioning System: Theory and Applications Volume II*, edited by B. W. Parkinson and J. J. Spilker Jr., Vol. 164, Progress in Astronautics and Aeronautics, AIAA, Washington, D.C., 1996, Chap. 12, pp. 327-374.
- [Brookner (1998)] Brookner, E., *Tracking and Kalman Filtering Made Easy*, Wiley, New York, 1998.
- [Brown (1996)] Brown, R. G., "Receiver Autonomous Integrity Monitoring", *Global Positioning System: Theory and Applications Volume II*, B. W. Parkinson & J. J. Spilker Jr. (Eds.), Vol. 164, Progress in Astronautics and Aeronautics, AIAA, 1996, Chapter 5, pp. 143-165.
- [Celio *et al.* (2000)] Celio, J. C., K. C. Bowen, D. J. Winokur, K. S. Lindsay, E. G. Newberger & D. Sicenavage, "Free Flight Phase 1 Conflict Probe Operational Description", MITRE Technical Report MTR 0W00000100, McLean, VA, 2000.
- [Chen & Patton (1999)] Chen, J. & R. J. Patton, *Robust Model-Based Fault Diagnosis for Dynamic Systems*, Kluwer Academic Pub., Norwell, MA, 1999, pp. 19-64.
- [Davison (2003)] Davison, H. J., personal communication, 4 October 2003.
- [Davison & Hansman (2001)] Davison, H. J. & R. J. Hansman, "Identification of Communication and Coordination Issues in the US Air Traffic Control System", Master's Thesis submitted to the Department of Aeronautics and Astronautics (ICAT Report No. ICAT-2001-2), Massachusetts Institute of Technology, Cambridge, MA, 2001.
- [Davison & Hansman (2003a)] Davison, H. J. & R. J. Hansman, "Use of Structure as a Basis for Abstraction in Air Traffic Control", *12<sup>th</sup> International Symposium of Aviation Psychology*, Dayton, OH, April 2003.
- [Davison & Hansman (2003b)] Davison, H. J. & R. J. Hansman, "Supporting the Future Air Traffic Control Projection Process", *Human Factors of Decision Making in Complex Systems Conference*, Dunblane, Scotland, August 2003.
- [Denbigh (1998)] Denbigh, P., *Systems Analysis & Signal Processing with Emphasis on the Use of MATLAB*, Addison Wesley Longman Ltd., Harlow, England, 1998.
- [Dennis (2003)] Dennis, G. D., "TSAFE: Building a Trusted Computing Base for Air Traffic Control Software", Master's Thesis submitted to the Department of Electrical Engineering and Computer Science, Massachusetts Institute of Technology, Cambridge, MA, 2003.
- [Endsley & Rodgers (1994)] Endsley, M. & Rodgers, M., "Situational Awareness Requirements for En-route Air Traffic Control", DOT/FAA/AM-94/27, 1994.



- [Erzberger (2001)] Erzberger, H., "The Automated Airspace Concept", 4<sup>th</sup> *FAA/Eurocontrol Air Traffic Management Conference ATM2001*, Santa Fe, NM, December 2001.
- [Erzberger *et al.* (2001)] Erzberger, H., D. McNally & M. Foster, "Direct-To Tool for En Route Controllers", *New Concepts and Methods in Air Traffic Management*, L. Bianco, P. Dell'Olmo & A. R. Odoni (Eds.), Springer-Verlag, Berlin, 2001, pp. 179-198.
- [Erzberger & Paielli (2002)] Erzberger, H. & R. A. Paielli, "Concept for Next Generation Air Traffic Control System", *Air Traffic Control Quarterly*, 2002, Vol. 10, No.4.
- [FAA (1992)] FAA, "National Airspace System En-route Configuration Management Document – Computer Program Functional Specifications – Flight Plan Position and Beacon Code Assignment", NAS-MD-313, 1992.
- [FAA (1993)] FAA, "National Airspace System En-route Configuration Management Document – Computer Program Functional Specifications – Automatic Tracking", NAS-MD-321, 1993.
- [FAA (1995)] FAA, "National Airspace System En-route Configuration Management Document – Computer Program Functional Specifications – Introduction to Specification Series", NAS-MD-310, 1995.
- [FAA (1999)] FAA, "National Airspace System Architecture: Version 4.0", Washington, DC, 1999.
- [FAA (2000)] FAA, "Air Traffic Control", FAA Order 7110.65M, Washington, DC, 2000.
- [Frank (1992)] Frank, P. M., "Principles of Model-Based Fault Detection", *IFAC/IFIP/IMACS Symposium on Artificial Intelligence in Real-Time Control*, Delft, Netherlands, 1992, pp. 213-220.
- [Frank (1996)] Frank, P. M., "Analytical and Qualitative Model-Based Fault Diagnosis—A Survey and Some New Results", *European Journal of Control*, 1996, Vol. 2, No. 1, pp. 6-28.
- [Galotti (1997)] Galotti, Jr., V. P., *The Future Air Navigation System (FANS)*, Ashgate Publishing Limited, Aldershot, UK, 1997.
- [Gertler (1998)] Gertler, J., *Fault Detection and Diagnosis in Engineering Systems*, Marcel Dekker, New York, NY, 1998.
- [Green *et al.* (1998)] Green, S. M., R. A. Vivona & M. P. Grace, "Field Evaluation of Descent Advisor Trajectory Prediction Accuracy for En Route Clearance Advisories", AIAA Paper No. 98-4479, *AIAA Guidance, Navigation & Control Conference*, Boston, MA, 1998.
- [Green *et al.* (2000)] Green, S. M., K. D. Billimoria & M. G. Ballin, "Distributed Air Ground Traffic Management for En Route Flight Operations", AIAA Paper No. 2000-4064, *AIAA Guidance Navigation & Control Conference*, Denver, CO, August 2000.

- [Hoyhtya (1996)] Hoyhtya, A. K., "Intelligent Patient Monitoring: Detecting and Defining Significant Clinical Events", Master's Thesis submitted to the Department of Electrical Engineering and Computer Science, Massachusetts Institute of Technology, Cambridge, MA, 1996.
- [ICAO (1985)] ICAO, "ICAO Annex 10: Aeronautical Telecommunications", Vol. 1, 4<sup>th</sup> Edition, Montreal, Canada, 1985.
- [ICAO (1996)] ICAO, "Manual on Required Navigation Performance", ICAO Doc. 9613, Montreal, Canada, 1996.
- [Isermann (2000)] Isermann, R., "Integration of Fault Detection and Diagnosis Methods", *Issues of Fault Diagnosis for Dynamic Systems*, R. J. Patton, P. M. Frank & R. N. Clark (Eds.), Springer-Verlag, 2000, pp. 15-49.
- [Jain (1998)] Jain, L. C. (Ed.), *Knowledge-Based Intelligent Techniques in Industry*, CRC Press, Boca Raton, FL, 1998.
- [Jansen *et al.* (1998)] Jansen, R. B. H. J., G. J. Bakker & H. A. P. Blom, "Ground Supported Navigation and FPCM Detection Algorithms", NLR Memorandum VL-98-036, 1998.
- [Jansen *et al.* (1999)] Jansen, R. B. H. J., H. J. Kremer & W. C. Vertegaal, "PHARE Advanced Tools: Flight Path Monitor Final Report", Eurocontrol DOC 98-70-18/6, Brussels, Belgium, 1999.
- [Johnson (1995)] Johnson, E. N., "Multi-Agent Flight Simulation with Robust Situation Generation", Master's Thesis submitted to the Department of Aeronautics and Astronautics, Massachusetts Institute of Technology, Cambridge, MA, 1995.
- [Kayton & Fried (1997)] Kayton, M. & W. R. Fried, *Avionics Navigation Systems*, 2nd edition, John Wiley & Sons, Inc., New York NY, 1997.
- [Koslow & Fekkes (2002)] Koslow, S. & J. Fekkes, "NAV CANADA's GAATS: Effective Innovation for Oceanic Control", *Journal of Air Traffic Control*, 2002, Vol. 44, No. 4, pp. 3-6.
- [Kuchar (1996)] Kuchar, J. K., "Methodology for Alerting-System Performance Evaluation", *Journal of Guidance, Control & Dynamics*, 1996, Vol. 19, No. 2.
- [LaFrey (1989)] LaFrey, R. R., "Parallel Runway Monitor", *MIT Lincoln Laboratory Journal*, 1989, Vol. 2, No. 3, pp. 411-436.
- [Lee & Moray (1992)] Lee, J. & N. Moray, "Trust, Control Strategies and Allocation of Function in Human-Machine Systems", *Ergonomics*, 1992, Vol. 35, No. 10, pp. 1243-1270.
- [Lincoln (1998)] Lincoln Laboratory, "Air Traffic Control Overview: Kansas City ARTCC", MIT Lincoln Laboratory Group 41 Report, Lexington, MA, 1998.

- [Lindsay (2000a)] Lindsay, K. S., “Currency of Flight Intent Information and Impact on Trajectory Accuracy”, *FAA/Eurocontrol Technical Interchange Meeting on Shared Flight Intent Information*, Atlantic City, NJ, October 2000.
- [Lindsay (2000b)] Lindsay, K. S., “Results of a URET Operational Utility Experiment”, MITRE Working Note WN 99W0000081, McLean, VA, 2000.
- [Love *et al.* (2002)] Love, D., W. Horn & L. Fellman, “An Evaluation of the Use of the URET Prototype Tool at Indianapolis and Memphis Air Route Traffic Control Centers, Using Benefit Matrices”, *21<sup>st</sup> Digital Avionics Systems Conference*, Irvine, CA, October 2002.
- [Lozano (1998)] Lozano, P. C., “Dynamic Models for Liquid Rocket Engines with Health Monitoring Application”, Master’s Thesis submitted to the Department of Aeronautics and Astronautics (SERC Report # 7-98), Massachusetts Institute of Technology, Cambridge, MA, 1998.
- [McConkey & Bolz (2002)] McConkey, E. D. & E. H. Bolz, “Analysis of the Vertical Accuracy of the CTAS Trajectory Prediction Process”, report from Science Applications International Corporation, Arlington, VA for NASA Ames Research Center, 2002.
- [Moir & Seabridge (2003)] Moir, I. & A. Seabridge, *Civil Avionics Systems*, co-published by AIAA Education Series, Reston, VA and Professional Engineering Publishing Ltd., Bury St. Edmunds, UK, 2003.
- [Najm *et al.* (2001)] Najm, W. G., J. A. Koopmann & D. L. Smith, “Analysis of Crossing Path Crash Countermeasure Systems”, *17<sup>th</sup> International Technical Conference on the Enhanced Safety of Vehicles*, Paper No. 378, Amsterdam, Netherlands, 2001.
- [NavCanada (2001)] NavCanada, “Gander Automated Air Traffic System”, [www.navcanada.ca](http://www.navcanada.ca), 2001.
- [NLR (2002)] NLR, “NarSim Flight Position Monitor” website, [www.nlr.nl/public/narsim2/FPM.html](http://www.nlr.nl/public/narsim2/FPM.html), 2002.
- [Nolan (1999)] Nolan, M. S., *Fundamentals of Air Traffic Control*, Brooks/Cole Publishing Co., Pacific Grove, CA, 3<sup>rd</sup> edition, 1999.
- [NRC (1998)] NRC, *The Future of Air Traffic Control—Human Operators and Automation*, National Research Council, Washington, DC, 1998.
- [Owen (1993)] Owen, M. R., “The Memphis Precision Runway Monitor Program Instrument Landing System Final Approach Study”, DTIC Report No. DOT/FAA/NR-92/11, MIT LL Project Report ATC-194, Lexington, MA, 1993.
- [Oxborrow (2003)] Oxborrow, R. R., Boeing ATM Demonstration Team, personal communication, 23 April 2003.

- [Paglione *et al.* (2000)] Paglione, M. M., R. O. Oaks, H. F. Ryan & J. S. Summerill, "Description of Accuracy Scenarios for the Acceptance Testing of the User Request Evaluation Tool / Core Capability Limited Deployment", FAA William J. Hughes Technical Center Report, 2000.
- [Palmer *et al.* (1999)] Palmer, E., D. Williams, T. Prevot, S. Romahn, T. Goka, N. Smith & B. Crane, "An Operational Concept for Flying FMS Trajectories in Center and TRACON Airspace", *10<sup>th</sup> International Symposium on Aviation Psychology*, Columbus, OH, 1999.
- [Patton *et al.* (2000)] Patton, R. J., P. M. Frank and R. N. Clark (Eds.), *Issues of Fault Diagnosis for Dynamic Systems*, Springer-Verlag, New York, 2000.
- [Pawlak *et al.* (1996)] Pawlak, W. S., Brinton, C. R., Crouch, K. & Lancaster, K. M., "A Framework for the Evaluation of Air Traffic Control Complexity", *AIAA Guidance Navigation and Control Conference*, San Diego, CA, 1996.
- [Pelletier (2002)] Pelletier, G., Air Traffic Management Services, Raytheon Canada Ltd., personal communication, 17 December 2002.
- [Pollock (2003)] Pollock, J., "Using Microsoft Flight Simulator with MATLAB & Simulink", internal Massachusetts Institute of Technology technical report, 2003.
- [Post & Knorr (2003)] Post, J. & D. Knorr, "Free Flight Program Update", *5<sup>th</sup> FAA/Eurocontrol Air Traffic Management Conference ATM2003*, Budapest, Hungary, June 2003.
- [Raytheon (2000)] Raytheon, CAATS (Canadian Automated Air Traffic System) Product Sheet, Raytheon Systems Canada, Richmond, BC, Canada, 2000.
- [Reynolds & Hansman (2001)] Reynolds, T. G. & R. J. Hansman, "Analysis of Aircraft Separation Minima using a Surveillance State Vector Approach", *Air Transportation Systems Engineering*, G. L. Donohue & A. G. Zellweger (Eds.), Vol. 193, Progress in Astronautics and Aeronautics, AIAA, 2001, Chapter 34, pp. 563-582.
- [Reynolds *et al.* (2002)] Reynolds, T. G., J. M. Histon, H. J. Davison & R. J. Hansman, "Structure, Intent & Conformance Monitoring in ATC", *ATM2002 Workshop on ATM System Architectures and CNS Technologies*, Capri, Italy, 2002.
- [Robinson & Isaacson (2000)] Robinson, J. E. III & D. R. Isaacson, "A Concurrent Sequencing and Deconfliction Algorithm for Terminal Area Air Traffic Control", AIAA Paper No. 2000-4473, *AIAA Guidance, Navigation & Control Conference*, Denver, CO, 2000.
- [Roskam (1995)] Roskam, J., *Airplane Flight Dynamics and Automatic Flight Controls, Part I*, DARCorporation, Lawrence, KS, 1995.
- [RTCA (2000)] RTCA, "Minimum Aviation System Performance Standards: Required Navigation Performance for Area Navigation", RTCA/DO-236A, Washington, DC, 2000.

- [RTCA (2002)] RTCA, “Minimum Aviation System Performance Standards for Automatic Dependent Surveillance Broadcast (ADS-B)”, RTCA/DO-242A, Washington, DC, 2002.
- [Scott (2001)] Scott, W. B., “Technology is Key to Australia’s ATC”, *Aviation Week & Space Technology*, 22 October 2001, Vol. 155, No. 17, pp. 72-75.
- [Shank & Hollister (1994)] Shank, E. M. and Hollister, K. M., “Precision Runway Monitor”, *MIT Lincoln Laboratory Journal*, 1994, Vol. 7, No. 2, pp. 329-353.
- [Sheridan (1992)] Sheridan, T. B., *Telerobotics, Automation and Human Supervisory Control*, MIT Press, Cambridge, MA, 1992.
- [Slattery & Zhao (1997)] Slattery, R. & Y. Zhao, “Trajectory Synthesis for Air Traffic Automation”, *Journal of Guidance, Control & Dynamics*, 1997, Vol. 20, No. 2, pp. 232-238.
- [Spilker (1996)] Spilker, J. J., Jr., “Satellite Constellation and Geometric Dilution of Precision”, *Global Positioning System: Theory and Applications Volume I*, edited by B. W. Parkinson and J. J. Spilker Jr., Vol. 163, Progress in Astronautics and Aeronautics, AIAA, Washington, D.C., 1996, Chap. 5, pp. 177-208.
- [Troutman & Pelletier (2002)] Troutman, K. & G. Pelletier, “CAATS—New Generation ATM Automation”, *Journal of Air Traffic Control*, 2002, Vol. 44, No. 1, pp. 3-7.
- [Vakil (2000)] Vakil, S., “Analysis of Complexity Evolution Management and Human Performance Issues in Commercial Aircraft Automation Systems”, Doctoral Thesis submitted to the Department of Aeronautics and Astronautics, Massachusetts Institute of Technology, Cambridge, MA, 2000.
- [Walker *et al.* (2002)] Walker, R. S., F. W. Peters, B. Aldrin, E. M. Bolen, R. T. Buffenbarger, J. W. Douglass, T. K. Fowler, J. J. Hamre, W. Schneider Jr., R. J. Stevens, N. Tyson, H. R. Wood, “Final Report of the Commission on the Future of the United States Aerospace Industry”, Arlington, VA, 2002.
- [Wetherby *et al.* (1993)] Wetherby, B. C., J. C. Celio, S. M. Kidman & M. A. Stanley, “Full AERA Services Operational Description”, MITRE Technical Report MTR 0W00000100, McLean, VA, 1993.
- [Wilson (1996)] Wilson, I. A. B., “PHARE: Definition and Use of Tubes”, Eurocontrol DOC 96-70-18, Brussels, Belgium, 1996.
- [Winder & Kuchar (2001)] Winder, L. F. & J. K. Kuchar, “Generalized Philosophy of Alerting With Applications to Parallel Approach Collision Prevention”, AIAA Paper No. 2001-4052, *AIAA Guidance, Navigation & Control Conference*, Montreal, Canada, 2001.

[Yang *et al.* (2003)] Yang, L. C., J. H. Yang, E. Feron & V. Kulkarni, “Development of a Performance-Based Approach for a Rear-End Collision Warning and Avoidance System for Automobiles”, *IEEE Intelligent Vehicles Symposium*, Columbus, OH, 2003.

---

# Appendix A: Aircraft Navigation Issues

---

Many of the analyses of presented in this document have required a determination of cross-track position errors and target track angles for trajectory-following aircraft in the lateral domain. There are two general types of navigation often used to compute a path between one trajectory point and another:

- Rhumb line navigation
- Great circle navigation

Rhumb line navigation defines a path with constant true heading relative to the local meridians between the two points defining the current trajectory segment. This is illustrated in Figure A.1.

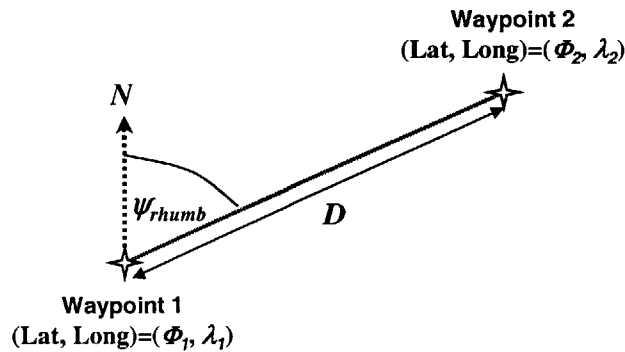


**Figure A.1: Rhumb Line Navigation**

Rhumb line navigation is often used for marine applications because the resulting path is a straight line on the commonly-used Mercator chart. The rhumb line heading between two waypoints,  $\psi_{rhumb}$  can be calculated from knowledge of the waypoint  $x, y$  co-ordinates on the Mercator chart according to:

$$\psi_{rhumb} = \text{atan} \frac{x_2 - x_1}{y_2 - y_1} \quad \text{Equation A.1}$$

The  $x, y$  co-ordinates in radians are related to the latitude, longitude ( $\Phi, \lambda$ ) co-ordinates according to:

$$\begin{aligned}
 x &= R(\lambda - \lambda_0) \\
 y &= \frac{R}{2} \ln \left[ \frac{1 + \sin \Phi}{1 - \sin \Phi} \right]
 \end{aligned}
 \tag{Equations A.2}$$

where  $\lambda_0$  is the longitude of the center of the chart and  $R$  is the radius of the Earth. Hence, the rhumb line heading can be calculated in terms of the  $\Phi, \lambda$  co-ordinates of the trajectory waypoints by substituting for  $x, y$  into Equation A.1:

$$\psi_{rhumb} = \text{atan} \left( \frac{2(\lambda_2 - \lambda_1)}{\ln \left[ \frac{(1 + \sin \Phi_2)(1 - \sin \Phi_1)}{(1 - \sin \Phi_2)(1 + \sin \Phi_1)} \right]} \right)
 \tag{Equation A.3}$$

Rhumb line navigation therefore involves a single calculation of a reference heading for each leg of the trajectory to be traversed. In addition to marine applications, it is also used in simple aircraft autopilots so that a constant heading reference can be used for that trajectory segment, and for straight line airway and VOR radial tracking tasks. Although simple, rhumb line navigation does not result in a trajectory of the shortest distance over a spherical surface. This is achieved through great circle routes that plot as straight lines on Gnomonic charts, although this is not a commonly used projection. A comparison of the rhumb line and great circle routes between Boston Logan Airport (BOS) and London Heathrow Airport (LHR) on a Mercator chart is shown in Figure A.2. The great circle route is seen to be 105 nm shorter than the direct rhumb line route.

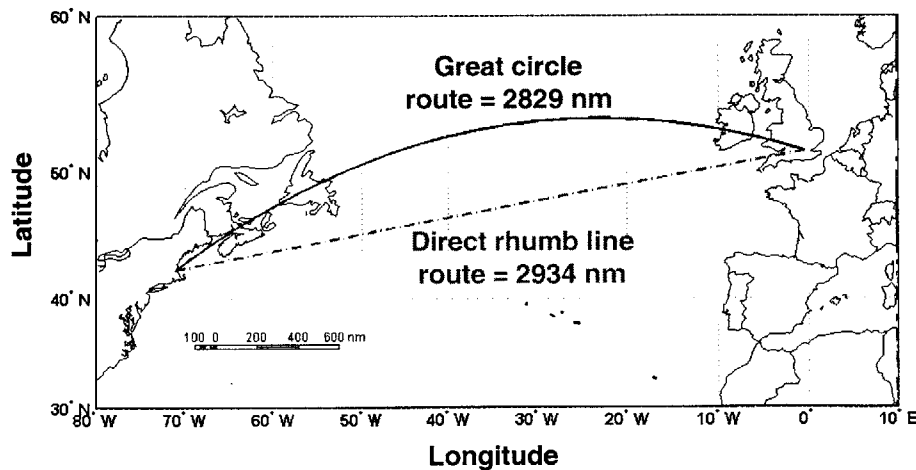


**Figure A.2: Comparison of Great Circle and Rhumb Line Routes Between BOS and LHR**



Although shorter, the great circle path results in a constantly-changing heading towards the next waypoint as the trajectory is traversed. The great circle heading,  $\psi_{GC}$  at each point on the trajectory can be calculated according to [Kayton & Fried (1997)]:

$$\psi_{GC} = \text{asin} \left[ \frac{\cos \Phi_2 \sin(\lambda_i - \lambda_2)}{\sin(D/R_G)} \right] \quad \text{Equation A.4}$$

where  $\Phi_i$ ,  $\lambda_i$  are the latitude and longitude of the intermediate point along the trajectory at which the heading is to be calculated,  $R_G$  is the Gaussian radius of curvature of the Earth (which can be approximated by the spherical radius of the Earth (3440.1 nm)) and  $D$  is the length of the trajectory segment, which is given by:

$$D = R_G \text{acos} \left[ \sin \Phi_i \sin \Phi_2 + \cos \Phi_i \cos \Phi_2 \cos(\lambda_i - \lambda_2) \right] \quad \text{Equation A.5}$$

Many modern flight management systems utilize the great circle equations to continuously calculate the heading target for the autopilot. An alternative technique involves dividing the great circle route into several rhumb line segments that can be flown at constant heading. An example three-segment approximation to the great circle route between Boston and London is shown in Figure A.3, resulting in a route only 12 nm longer than with the great circle.

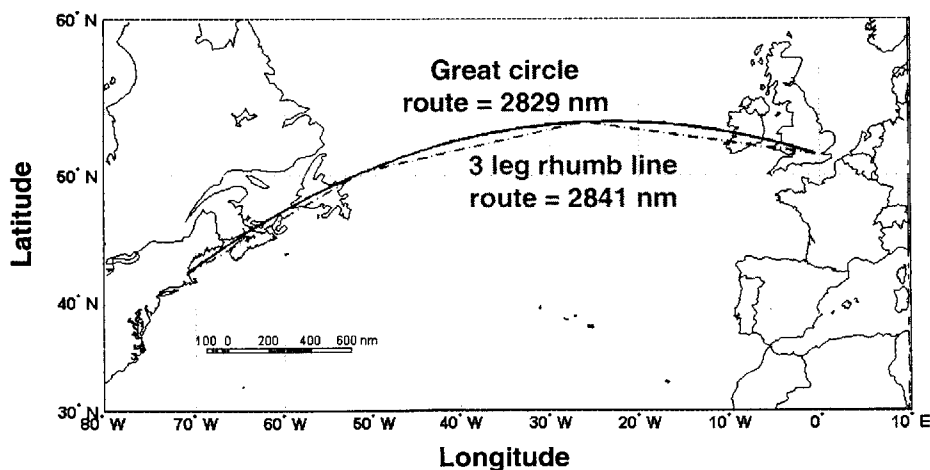


Figure A.3: Approximating Great Circle Route With Rhumb Line Segments

These navigation issues are relevant to conformance monitoring analyses since they affect how the cross-track position error and heading target states are calculated. For example, the FMS in the flight test aircraft was performing great circle navigation, and therefore the cross-track position errors had to be calculated relative to a great circle trajectory between the two appropriate waypoints of the flight plan. A rhumb line calculation would have resulted in comparison to an inappropriate reference trajectory (i.e. Conformance Basis) and the deviations would have been exaggerated as a result. Similarly, a rhumb line calculation would result in a constant expected heading along a given trajectory while a great circle calculation would have a constantly changing heading expectation.

The example analyses conducted in this document did use a great circle trajectory model for the cross-track position error calculations since a rhumb line calculation resulted in excessive errors (of the order of 1 nm) in the flight analysis. However, it was found that over the relatively short flight plan legs involved in the test flights, the differences between the constant expectation from a rhumb line calculation and the changing expectation from a great circle calculation were small. In order to generate a low fidelity Conformance Monitoring Model, a rhumb line calculation was therefore employed to determine heading expectations. Longer routes and higher fidelity Conformance Monitoring Models may need to explicitly model the actual navigation approach employed by the aircraft being monitored.